An analysis of high energy muons in extensive air showers

C. Adcock

AN ANALYSIS OF HIGH ENERGY MUONS IN EXTENSIVE AIR SHOWERS

by

C. Adcock, B.Sc.

A Thesis submitted to the
University of Durham for the
Degree of Doctor of Philosophy.

April, 1970.

A B S T R A C T

Calculations have been made to investigate the effects on high energy muon showers of varying some of the more important parameters of high energy nucleon-air nucleus collisions. The effects of different assumptions concerning the primary mass composition have also been investigated. The majority of the calculations have been designed to enable a comparison to be made with the experimental results of the Utah group on underground muons with threshold energies of the order of 1000 GeV, and above, and zenith angles in the region of 60°.

Assuming the primary composition to be similar to that found at primary energies ~10 GeV, it is concluded that if the multiplicity of secondary particles varies as $E_p^{\frac{1}{4}}$ then the value of the mean transverse momentum is 0.67 ± 0.1 GeV/c at primary energies $\sim 2\ 10^5$GeV, and if the multiplicity varies as $E_p^{\frac{1}{2}}$ a value of ~0.5 GeV/c is obtained at energies $\sim 4\ 10^5$GeV.

Using a value of 0.4 GeV/c for the mean transverse momentum, all the models predict significantly more muons than observed. An increase in the mean transverse momentum and/or the energy loss coefficient, b, are considered the most likely parameter changes to give better agreement.

The present work favours a multiplicity law varying as $E_p^{\frac{1}{4}}$ rather than one varying as $E_p^{\frac{1}{2}}$ but this cannot be regarded as conclusive.

As yet, due to lack of experimental data, no conclusions have been possible concerning the primary mass composition but there is no evidence for an increase in the proportion of heavy nuclei above 10^{12}eV as concluded by Grigorov et al. (1967).

The present work does not rule out the possibility of some muons in E.A.S. being produced by a process other than the decay of pions and kaons.

PREFACE

The work presented in this thesis was carried out while the author was a research student under the supervision of Professor A.W. Wolfendale in the Physics Department of the University of Durham, between September 1966 and September 1969. Since October 1969 the author has been employed as a Research Assistant in the same department.

The author has been a member of a small group working on problems associated with the theory of E.A.S. This group included Professor A.W. Wolfendale, Dr. H. Oda from Kobe University, Japan (for 12 months), Dr. J. Wdowczyk from the Institute of Nuclear Research, Lodz, Poland (for several months each year) and, since October, 1969, Dr. R.B. Coats. Inevitably some of the work has been done in collaboration with the above physicists but most of that reported here has been carried out by the author.

Early calculations (not reported in detail here) on fluctuations in E.A.S. and on the sensitivity of E.A.S. characteristics to model parameters have been reported in the Journal of Physics by Adcock et al. (1968a) and at the International Conference on Cosmic Rays, Calgary, by Adcock et al. (1968b) respectively. Interim reports on the present work have been given in the Journal of Physics by Adcock et al. (1969a) and at the International Conference on Cosmic Rays at Budapest by Adcock et al. (1969b).

CONTENTS

CHAPTER 1

THE SIGNIFICANCE OF COSMIC RAY STUDIES

1.1. Introduction

The primary cosmic rays falling onto the earth's atmosphere are now known to consist mainly of atomic nuclei with a small proportion of electrons and γ-rays. Their study is important in two main fields - astrophysics and high energy interactions. The former comes from a study of the energy spectrum of the primary particles, their chemical composition and their spatial anisotropy, and the latter from a study of the secondary particles produced when the primary particles interact with the nuclei of the atoms in the atmosphere.

1.2. The Characteristics of the Primary Radiation and their Astrophysical Significance.

1.2.1 The Energy Spectrum of Primary Cosmic Rays.

The energy spectrum of primary cosmic rays extends from an arbitrary limit less than a GeV to an hitherto undetected upper limit of greater than about 10^{20}eV. An integral primary spectrum deduced by Greisen (1966a) from the results of many workers is shown in figure 1.1. Although this does not agree in detail with those of other workers, the essential features are the same.

Thus the spectrum is seen to fall very rapidly with increasing energy, having an exponent of about -1.6 up to an energy of $\sim 10^{15}$eV after which it steepens in slope to about -2.1. This remains constant to an energy of about 3.10^{18}eV when the slope decreases to about -1.6 again.

Because of the very great energy range covered and the rapid fall in the flux with increasing energy no one method can be used to measure

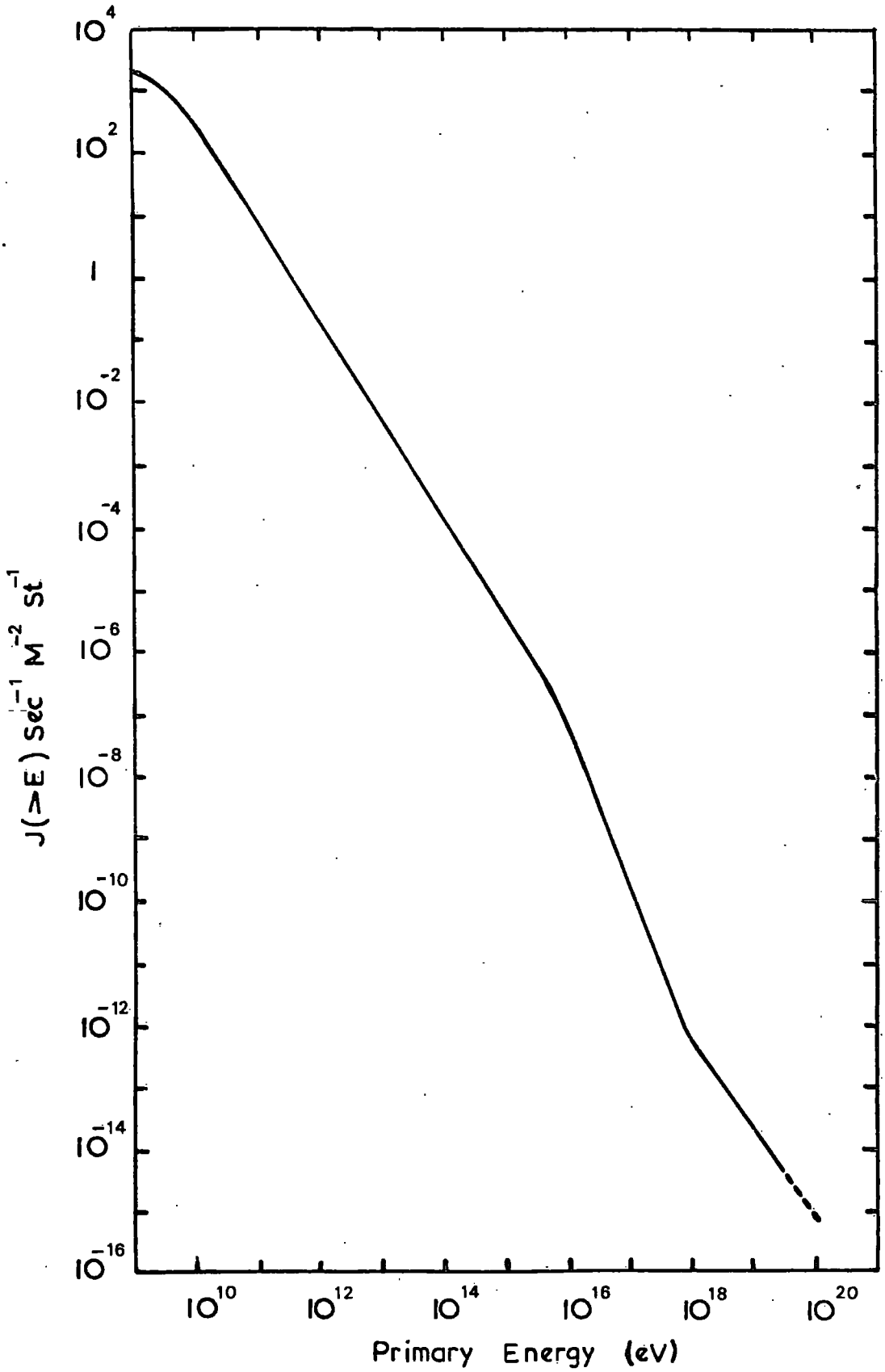

Fig. 1.1 Integral Primary Energy Spectrum
(after Greisen 1966a)

the spectrum over the whole energy range. At energies below about 10^{12}eV the flux is sufficiently large to enable it to be measured directly with detectors carried to the top of the atmosphere in balloons or in satellites. In the energy region 10^{12}-10^{14}eV the flux is so low that the primary spectrum has to be deduced from measurements on the secondaries of interactions of the primary nuclei with air nuclei, or rather their progeny (γ-rays and muons), although recently the flux has been measured in the energy range 10^{11} - 10^{14}eV by a satellite experiment (Grigorov et al., 1967).

Beyond about 10^{14}eV one has to rely on extensive air shower measurements for information (see section 1.4); in particular the measurements of shower size. In all of these indirect measurements a model of high energy interactions must be used. As a result when discrepancies occur about the nature of the primary spectrum deduced from different observations three possible explanations are suggested:- (i) unreliability of the data, arising from a lack of statistics, systematic errors and biases in the observations; (ii) a change in the slope of the primary spectrum with or without a change in composition; (iii) a change in the characteristics of high energy interactions at a suitable energy and in a suitable manner.

This has been the case for the two inflexions shown in the primary spectrum. They arose from changes in the slope of the shower size spectrum. The lower inflexion has now been definitely established in the size spectrum and according to Vernov and Khristiansen (1967) it is most unlikely to be due to a change in the characteristics of high energy interactions. Therefore it seems that the "kink" in the primary

spectrum is real and must be explained by astrophysical arguments, either in models of the origin of cosmic rays or in theories of their propagation or both.

The change in slope of the energy spectrum at energies ~ 10^{18}eV has also been fairly well established (Trumper, 1969) and the slope of the spectrum above the "kink" does seem to be about -1.6.

The discovery of an isotropic radiation of temperature approximately 3^{o}K (e.g. Roll and Wilkinson, 1967) has led to great interest in the extreme high energy end of the primary spectrum. The radiation has been postulated as being the remnant of the primeval fireball (Dicke et al., 1965) and according to Greisen (1966b) the transparency of space at the partinent wavelengths and the consistency of intensity from observations in numerous directions gives strong assurance that the radiation is universal.

The existence of a universal 3^{o}K radiation would have drastic consequences on the high energy end of the cosmic ray spectrum if the primaries were universal (Greisen, 1966b; Kuzmin and Zatsepin, 1966). The proton spectrum would terminate abruptly beyond a few times 10^{19}eV due to the onset of the photomeson interactions between the primary protons and the microwave photons. In the case of heavy primaries the break in terms of energy per nucleon would occur much earlier due to photo-disintegration processes for which the threshold energy is much lower. The relevant experimental observations are those of Linsley (1963a) and Andrews et al. (1969) who have detected showers with primary energies above the predicted cut-off. From these results it seemsthat if cosmic rays of high energy are extragalactic, then the 3^{o}K radiation cannot be universal or, alternatively, if the 3^{o}K radiation

is universal then the high energy cosmic rays cannot be so and are probably confined within the local super cluster (Sreekantan, 1968).

1.2.2. The Composition of the Primary Cosmic Rays.

The composition of cosmic rays is an essential feature in understanding their origin. At energies below ~10GeV the primary composition is known from direct measurements. It is approximately, with constant energy per nucleon, 93% protons and 6.3% alpha particles, the rest being heavier nuclei. At higher energies the composition is less well known because the rapidly falling intensity with increasing energy makes direct measurements very difficult and so indirect methods must be used. These are described fully in Chapter 2.

It is sufficient to say at this stage that up to energies ~ 10^{15}eV there is evidence that the composition is similar to that at lower energies. Above 10^{15}eV the evidence is very conflicting and it is one of the aims of this work to try to throw light on the composition at these energies. At energies of about 10^{17}eV Linsley and Scarsi (1962) have put forward some evidence that the composition is relatively pure and probably protonic in nature.

If one compares the composition of the low energy cosmic rays with the composition of the Universe in general one is struck by the relatively high proportion (a factor 10^5 times greater) in cosmic rays of the L-group of nuclei (Li, Be and B) and also a slightly greater proportion of heavy nuclei.

The latter excess points to the origin of cosmic rays in old stars which have a high proportion of heavy nuclei e.g. supernovae. The difference in the amounts of L-nuclei indicates that their

presence in the cosmic radiation is due largely to the fragmentation of heavier nuclei in penetrating ~ 3 g.cm^{-2} of matter on their way to the earth.

The origin of cosmic rays and the mechanism for accelerating them to energies ~10^{20}eV is still not known with certainty. The energy density of cosmic rays near the earth is the same order as that of starlight (1eV/cm^3) and so if the radiation were universal with a constant energy density the total energy involved in the cosmic radiation would be excessively great and this has led many workers to discount its being universal and suggest that it is a Galactic phenomenon, the particles being trapped in the Galaxy by Galactic magnetic fields. The value of the interstellar magnetic field is still in dispute and values from 10^{-5} - 10^{-7}gauss have been proposed. Evidence for the existence of such fields comes from a variety of measurements including the detection of magnetic bremsstrahlung radiation from relativistic electrons in the Galaxy.

Ginzburg and Syrovatskii (1964) favour the Galactic origin of cosmic rays from a single source, supernovae. These workers propose that acceleration takes place in the turbulent gas and magnetic fields by either of two processes:-

i) The Fermi process, which is a statistical process in which the charged particles collide with randomly moving magnetic fields. In a collision a particle may gain or lose energy; on the average it will gain since a head-on collision is more probable than an overtaking collision. The Fermi mechanism leads naturally to a power law energy spectrum.

ii) The second process is the interaction of charged particles with a slowly varying magnetic field (Betatron acceleration).

Zatsepin and Kuzmin (1968) have proposed that cosmic rays may originate in such stellar objects as quasars. If this is so then they state that above energies of about 10^{15}eV/nucleon heavy nuclei will be broken up into protons by the high energy photon field, and that protons will have increasing difficulty in escaping from the source thus accounting for the increase in the slope of the primary spectrum above this energy.

Colgate and White (1966) have considered the possibility that cosmic rays may be formed when a highly evolved star of mass ~10 times that of the sun collapses.

When the collapse has reached the stage that densities $\sim 10^{11}$g.cm^{-3} exist a neutron star may form. This stable configuration will halt the collapse and cause a shock wave to propagate outwards from the collapsed core carrying with it a portion of the star's mass. According to Kinsey (1968) the intense radiation field will quickly fragment the relativistic nuclei leading to a protons only spectrum above energies of $\sim 10^{3}$GeV/nucleon. However, some resynthesis of heavier elements may be possible behind the shock wave.

Hillas (1967,1968) has considered the effects of an evolving universe on cosmic rays assuming that the most energetic cosmic rays that have been detected are of extragalactic origin and that they originated in strong radio galaxies. Radio-astronomical evidence suggests that the output from such sources must have been much greater in the past than at present. If this is so, the importance of interactions between the 3°K radiation (assumed to be universal) and intergalactic

cosmic ray protons and heavier nuclei above 10^{15}eV is greatly increased because of "red-shifts" in the energies of the nuclei and the microwaves and changes in density so that the energy losses of the nuclei through pair production are greater than if a steady state model is considered.

Assuming that the output of these cosmic ray sources varies as $(\text{time})^{-3}$ and that the integral energy spectrum has a slope of -1.5 throughout, Hillas has shown that the energy loss would lead to the present day spectrum having a slope of -2.2 between primary energies $\sim 3 10^{15}$ - 10^{17}eV if production were assumed to start at 1.4 10^{8} years. An expected cut-off in the primary proton flux at $\sim 3 10^{19}$eV is still present as in Greisen's work, however, and this throws doubt on the theory.

A further explanation of the shape of the primary spectrum has been given by Linsley (1962) which is similar to a model by Peters (1961). This assumes that up to energies $\sim 10^{15}$eV the primary composition is similar to that found at lower primary energies and that the primary cosmic rays are all Galactic in origin. They are retained in the Galaxy by the Galactic magnetic fields. At these energies, however, the radius of the particles' trajectory approaches the extent of the field itself and so they are able to break away from the restraining influence of the magnetic field and leave the Galaxy. For a given magnetic rigidity the energy of a particle is proportional to its charge so that initially protons will escape followed by the heavier components in order of their charge (and hence mass), causing the primary energy spectrum to steepen. At energies $\sim 10^{18}$eV the Galactic field is unable to hold even the heaviest component of the primary cosmic radiation and the flux of

Galactic cosmic radiation falls below that entering the Galaxy from extra-galactic sources which are supposed to have a less steep energy spectrum, the same as that observed at energies $\gtrsim 10^{18}$eV in fact, and are believed to be composed almost entirely of protons due to any heavies being fragmented in collisions with inter-galactic matter. Obviously a good test of this theory is to see whether in fact the proportion of heavy primaries increases with energy above the first "kink" in the primary spectrum, and this is one of the main aims in extensive air shower work at present.

1.2.3 Spatial Anisotropies.

Anisotropies are usually quoted in terms of the parameter

$$\delta = \frac{I_{max} - I_{min}}{I_{max} + I_{min}} \qquad 1.1$$

where I_{max} and I_{min} are the maximum and minimum values of the observed intensity. This parameter has been measured in air showers up to the highest primary energies so far detected and within experimental errors the primary particles seem to be isotropically distributed.

The lack of directional anisotropies is not so much evidence for an isotropic distribution of sources as for the existance of inter-stellar magnetic fields which smear the original directions of the charged particles.

At sufficiently high energies particles may retain enough of their original direction to provide an observable anisotropy, but this depends on their source of origin.

Greisen (1966a) says that protons of energy $\sim 10^{21}$eV (if it is possible to detect them) should retain their original directions to within about 5° no matter how far away the sources may be, unless the

strength and organization of intergalactic fields are suprisingly great.

There are a number of directions in which a higher flux may be expected; these include the Galactic plane and the Galactic centre. It seems that the Galactic magnetic field is ordered along the spiral arms and so the spiral on which the solar system lies is another likely direction.

The absence of any such anisotropies is evidence that the particles travel through the interstellar gas primarily by diffusion with magnetized interstellar gas clouds as scattering centres. Hence more precise values of δ might be expected to provide information on the distribution and order of the magnetic fields in interstellar space.

1.3. High Energy Interactions.

The primary cosmic rays are useful in the study of high energy interactions because they provide a flux of very high energy particles with energies far exceeding those capable of being produced by present or even forseeable accelerators. The nuclei of the atmospheric atoms act as targets and studies on the secondary particles can give information on the characteristics of high energy interactions.

In the past these studies have led to the discovery of the π and μ - mesons and several of the strange particles, but at energies $\sim$ 30GeV accelerators are now better for investigating the characteristics of high energy interactions because of their greater flux. Thus the study of high energy interactions in cosmic rays is mainly concerned with energies above $\sim$ 100 GeV and in the next few years it should be possible for accelerators to produce energies of $\sim$ 300 GeV and maybe

higher so that interest in cosmic rays will have to be at energies above ~ 1000 GeV.

Already a lot of information has been obtained at and above these energies from experiments with nuclear emulsion stacks and from extensive air shower measurements which is summarized in Chapter 3.

Also postulated particles which have not been detected in accelerators presumably, if they exist, because their mass is too high are currently being looked for. Among these are the quark, a sub-nucleonic particle, and the intermediate vector boson which would show up in the apparent direct production of muons.

The Sydney group (e.g. McCusker and Cairns, 1969) have recently reported the detection of $2e/3$ quarks near to the cores of extensive air showers using a Wilson cloud chamber. However, these results cannot be regarded as conclusive and more experimental work is needed before any definite conclusions can be drawn.

Bergeson et al. (1967) have put forward some evidence for the production of muons by some new process, either by direct production or by the decay of some particle with a lifetime very much shorter than that of the pion or kaon. Again, however, the evidence cannot be regarded as conclusive at present.

1.4 Extensive Air Showers.

Extensive air showers are initiated by primary particles of very high energy. The particles in E.A.S. are divided into three principal components (a) the nuclear-active component which includes all kinds of particles that are strongly interacting, (b) the electromagnetic, or soft, component which consists of photons, electrons and positrons

and (c) the mu-meson component.

The genetic relations are believed to be well understood in general. The backbone of the shower consists of the nuclearactive component cascade, initiated by the interaction of a primary nucleus with an air nucleus and maintained by high energy secondary nucleons, antinucleons, mesons and hyperons. The decay of secondary K mesons and charged π mesons gives rise to the muon component, which is thereafter non-multiplying and is very slowly absorbed by ionization and beta-decay.

The decay of secondary π^0 mesons transfers energy repeatedly to photons each of which initiates an electromagnetic cascade. The overlapping photon-electron cascades rapidly grow to comprise the most numerous particles in the shower. The number of such particles can run into many millions and they are spread out over an area that can be as large as several square kilometres due to their being scattered by the atmosphere.

The great spread is one of the main advantages of extensive air showers. Thus the intensity of primary particles with an energy greater than 10^{18}eV on $1m^2$ is only ~ 1 per 3000 years. However, the extensive air shower produced by such primary particles contains $\sim 2\text{-}3\ 10^8$ particles at sea-level, spread out over a wide area and so they can be detected quite frequently with an array of well spaced detectors.

The individual electromagnetic cascades have a short range compared with the thickness of the atmosphere and the total soft component gradually dies away as the nuclearactive component becomes depleted in energy by further interactions. On average these occur every $80 g.cm^{-2}$ for nucleons and $120\ g.cm^{-2}$ for pions. If the path of the air shower in the atmosphere is sufficiently long the most numerous particles

remaining in the shower will be the muons because of their small interaction cross section.

However, most showers detected vertically consist mainly of electrons. For example in a shower of size 10^6 particles detected at sea-level, in the vertical direction, about 17 per cent are muons and the rest mainly electrons and photons. The muon component, however, carries far more energy in these showers than the electromagnetic one, the former carrying $\sim 9\ 10^{14}$eV, and the latter $\sim 1.6\ 10^{14}$eV. i.e. five or six times less than the muons. In showers of less than 10^6 particles the imbalance can be even larger.

This situation is a consequence of the long range of muons and the comparatively rapid absorption of the other components. In an average shower at sea-level the electromagnetic energy and that of the nuclear-active component are much depleted, while that of the muons has only been reduced by about one third through decay and ionization losses. At mountain altitudes, however, near the shower maxima the electrons are an order of magnitude more numerous than at sea-level and their average energy is also higher and so the energy balance is reversed.

The aim of the work in the field of extensive air showers is similar to that of cosmic rays in general i.e. to study the primary spectrum for astrophysical interest and to study the characteristics of high energy interactions.

There has been a significant increase in the accuracy of extensive air shower measurements in the past few years and this has led to greater interest being paid to the theory of shower development.

Increasing attention is being paid to more precise calculations of the various characteristics of E.A.S., electromagnetic, muonic and nuclear-active.

One of the main aims is to determine to what extent the E.A.S. characteristics are sensitive to the individual parameters of the elementary act and to select the characteristics depending on only a small number of parameters.

Initially it is important to compare the predictions of conservative models, with values of parameters obtained by extrapolating from the low energy region, with the experimental results, and by examining the direction in which the latter deviate from the former one should be able to tell, at least qualitatively, the required modifications needed to the parameters of the high energy interactions.

With the use of such models one should also be able to draw at least tentative conclusions on the primary mass and energy spectrum at very high energies.

1.5. The Significance of Muon Studies in E.A.S.

Muons in E.A.S. are the progeny of pions and kaons produced in high energy interactions. Their main characteristic is their extremely low probability of interacting with matter and so it should be possible to draw conclusions about nuclear interactions from all levels of the development of E.A.S. by studying muons of different energies at different distances from the core. The relativistic extension of the muon lifetime means that the majority of muons above a few GeV survive to sea-level. This means that fluctuations in the muon number are smaller than in the electron number and are less dependent on the

primary mass. Thus in theory a study of fluctuations in the electron number in E.A.S. containing a constant number of muons or alternatively a study of fluctuations in the muon number in E.A.S. of constant electron size could lead to information on the mass composition of the primary cosmic radiation. A number of workers have tried to obtain information in this way (De Beer et al., 1968 a; Adcock et al., 1968a) but the derivation of the muon number is very difficult, because of the need for many well shielded detectors over a large area in order to obtain the lateral distribution of the muons, and so far the experimental evidence is not sufficiently accurate to draw any definite conclusions. Such fluctuations can also give information on the model used in the calculations and hence indirectly on the parameters characterising high energy interactions (De Beer et al., 1968a).

The lateral spread of the muons about the core of extensive air showers results mainly from the transverse momentum imparted to the muon parent when it is created in high energy interactions. Thus studies of the shape of these lateral distributions should give information on the form of the transverse momentum distribution of these particles, on their mean value of transverse momentum, and on its variation with the interaction energy.

It may also be possible to draw conclusions on the primary mass spectrum from studies of the momentum spectra of energetic muons far from the core (Orford and Turver, 1969).

The sensitivity to the primary mass is due to the fact that high energy muons come from above ~10 kilometres (in the vertical direction) since at these heights the high energy pions produced have a greater

chance of decaying into muons before interacting than lower down in the atmosphere. Thus the muons reflect the first few interactions of the primary, whereas low energy muons near the core have been produced lower down in the atmosphere and the averaging effect of the many interactions that have occurred tends to mask the effects of different primaries. Some authors have pointed out that the fluctuations in the lateral distributions of high energy muons at large distances from the core are very large, however,(De Beer et al. 1968b) and this may have important consequences on the interpretation of the results.

Another way to study high energy muons is to look at muons at large zenith angles. In this case the first interaction of the primary will take place in less dense air than would be the case in the vertical direction and so the production of high energy muons would again be favoured. Also because of the large thickness of air traversed the low energy muons produced will have a tendency to undergo μ-e decay, since they will lose energy by ionization; this then will also tend to increase the average energy of the muons detected. Furthermore the large thickness of air will tend to filter out most of the electrons in the shower thus making the identification of the muons simpler. This method has been used by several workers and one of the groups (Rogers et al., 1969) has been able to draw conclusions on the mass composition of the primary particles above 10^{15}eV as well as on certain characteristics of high energy interactions. The main difficulty in this work seems to be the effect of geomagnetic deflection, but this is only true at large zenith angles ($> 60^{\circ}$).

Another feature of muons that can be measured is their heights

of origin. These are of great interest because they are dependent on the rate of energy dissipation in the E.A.S. and since this is sensitive to different models of extensive air shower development, the measurements can help to distinguish between different models. There are several methods of estimating this characteristic of E.A.S. It can be obtained from the geomagnetic distortion of the muon lateral distributions and the direction of motion of the muons in a shower relative to the shower axis (Earnshaw, 1968), from measurements on the radius of curvature of the shower front (Bennett et al., 1962) or by an analysis of the barometric attenuation of muons in air showers (Firkowski et al., 1967).

The relationship between the average number of muons in a shower and the average number of electrons can also be used, in principle, to obtain information about the primary mass spectrum (Adcock et al., 1968a). This arises from the fact that the relationship between the average electron number $\overline{N}_e$ and the average muon number $\overline{N}_\mu$ is

$$\overline{N}_\mu = K \overline{N}_e^{\alpha} \qquad 1.2$$

where α is approximately constant for all nuclei and K is a function of the mass of the primary nucleus. Equation 1.2 gives

$$\log \overline{N}_\mu = \alpha \log \overline{N}_e + \log K \qquad 1.3$$

and

$$\frac{d\log \overline{N}_\mu}{d\log \overline{N}_e} = \alpha \qquad 1.4$$

Thus a change in composition is reflected by a change in α

The measurements are possible for showers of fixed electron size or for fixed muon number. However, difficulties arise in obtaining good statistics since in order to see any change in α only small cells of shower size can be used.

In order to overcome the averaging effects in extensive air showers and study the effects from the first one or two nucleon interactions,

thereby also throwing light on the primary mass composition, one can study very high energy muons ($\gtrsim$1000 GeV) in extensive air showers.

This can be done by making the measurements deep underground where the electron and nuclear-active components of the air showers have been completely filtered out as have also the low energy muons. Thus the high energy muons can be regarded as the remnants of extensive air showers.

Such an experiment has been carried out at the University of Utah with a large detector situated under a mountain. The irregular contours of the mountain make it possible to study the frequency of muons, both single and multiple, with various threshold energies and at a variety of zenith angles. Also information has been gathered from the detector concerning the lateral distributions of these high energy muons.

Thus it seems that much valuable information may be gained on the primary mass composition and on the parameters of high energy interactions from a theoretical analysis of the preliminary results of this apparatus. Such an analysis forms the main theme of the present work.

Chapter 2 contains a survey of measurements done on the primary spectrum and its mass composition. Chapter 3 contains a survey of the characteristics of high energy interactions in order to get an idea of the parameters for a model of high energy interactions which is described in Chapter 4 along with the predictions of the model, with particular reference to the Utah detector. Chapter 5 gives a description of the Utah detector, the analysis of the data and

the final results. These are then compared to the theoretical predictions. Chapter 6 is a comparison between the results of other workers, both theoretical and experimental, and the present work. Chapter 7 contains the conclusions from the present work and proposed future work.

CHAPTER 2.

THE PRIMARY SPECTRUM AND ITS MASS COMPOSITION.

2.1. Introduction

As stated earlier, the underlying aim of the present work is to increase our knowledge on the mass composition of the primary cosmic rays responsible for creating E.A.S. and on the nature of nuclear interactions at energies unattainable by other means at present.

Because of the low intensities of primary rays at these energies it is not feasible to study them directly and so we are forced to draw conclusions about them from studies of the secondary components initiated by the high energy nuclear interactions of the primaries with air nuclei. This involves using theoretical models containing parameters whose values are uncertain and so our knowledge of the primary spectrum and of high energy interactions is closely related.

It is therefore important to make a survey of the present state of knowledge as regards the primary spectrum and its composition, and the characteristics of high energy nuclear interactions.

This chapter is concerned with the primary spectrum and the next with high energy interactions.

2.2. The Primary Spectrum in the Region $10^{11} - 10^{14}$eV.

Two main methods have been used in this energy region:- (i) studies of the π^0 component, which decays into gamma-rays and gives rise to electromagnetic cascades, and (ii) the muon component which arises from the decay of charged pions and kaons. These indirect methods must be used here because of the low intensity of the primary cosmic radiation in this energy region.

2.2.1 The Primary Spectrum from Cascade Measurements.

Malholtra et al. (1966a) used a tungsten-emulsion assembly of area 0.7 m^2 and 8 radiation lengths thickness. This was flown for 28 hours at an effective atmospheric depth of 22 $g.cm^{-2}$.

They were able to separate gamma-rays produced by the interaction of nuclear-active particles inside the apparatus from those produced externally, and used a photometric method to measure the energy of the cascades.

Figure 2.1. shows the spectrum of ΣE_γ and individual gamma-rays they observed.

The former is represented by

$$N(\geq \Sigma E_\gamma) \propto (\Sigma E_\gamma)^{-1.44 \pm 0.05} \qquad 2.1.$$

The primary energy spectrum was obtained from equation 2.1. under the following assumptions:-

i) The interaction lengths and fragmentation parameters of multiply charged nuclei are the same as at low energies. The interaction length of nucleons, λ_i, in graphite is 73 $g.cm^{-2}$.

ii) The attenuation length of nucleons in air is 125 $g.cm^{-2}$.

iii) The interaction length of nucleons in the detector was 176 $g.cm^{-2}$. An $A^{\frac{2}{3}}$ dependence was assumed when extrapolation was required. Checks on the depths of interaction in the detector confirmed this to within about 15%.

The charge composition of the primary particles was estimated in two ways:-

a) by observing the charge composition of the events in the emulsion, and

b) by assuming the primary composition to be the same as that measured at lower energies.

The two estimates were found to be in good agreement.

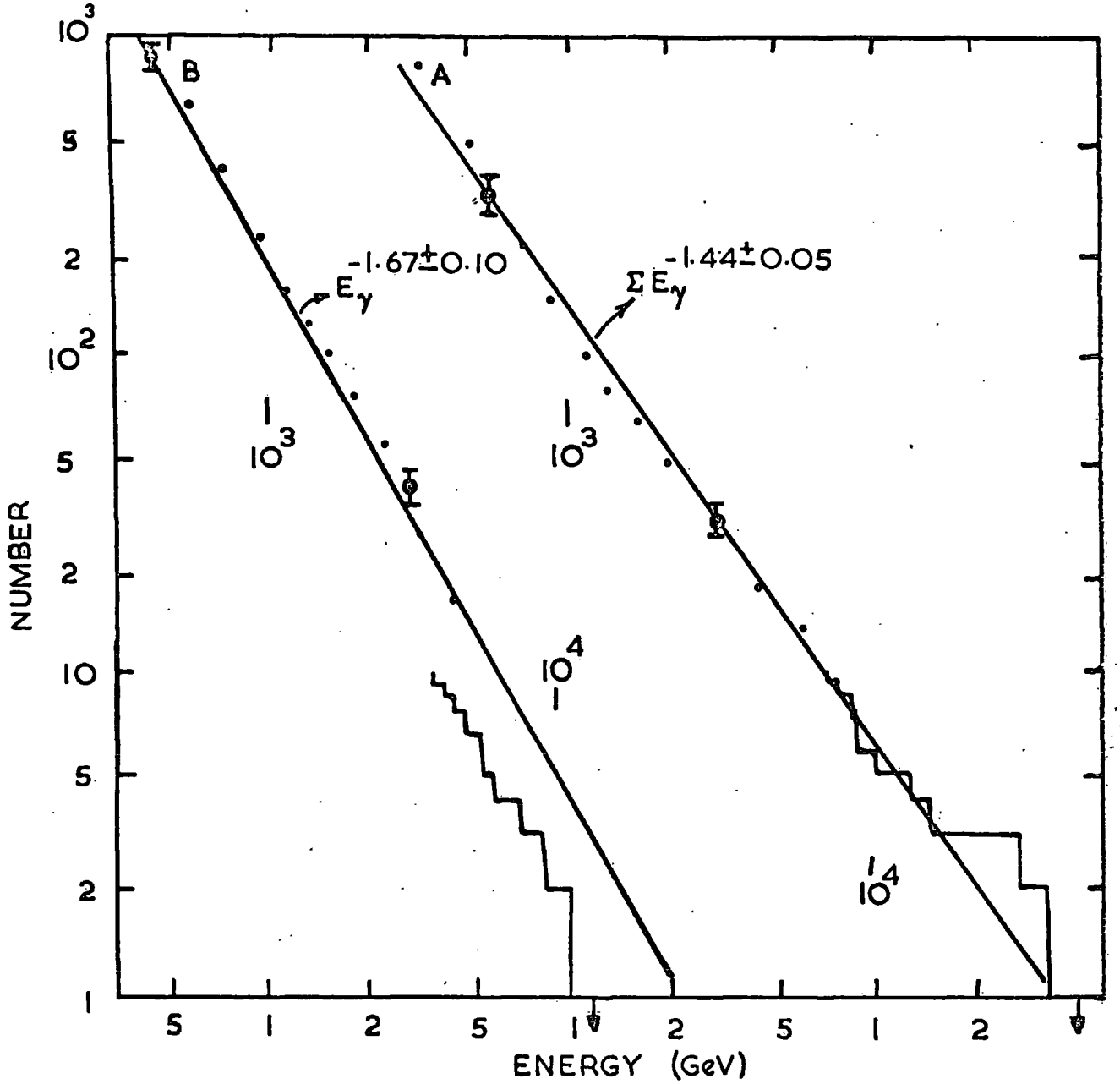

Fig.2.1

Integral Energy Spectra of Cascades Initiated by (A) Nuclear Particles Interacting in the Detector and (B) Single δ-rays or Electrons Obtained by Malholtra et al. (1966)

The primary energy, E_p, was obtained from the relation $E_p = (7.0 \pm 1.2)$ ΣE_γ, corresponding to $K_\pi = 0.43$ and $K_\gamma = K_\pi/3$. The pion elasticity was obtained from $\overline{K_\pi} = 0.35 \pm 0.05$ given by Dobrotin and Slavatinsky (1960) for an energy of 300 GeV, after allowing for the facts that the primary spectrum is a power law and that events were detected by their cascade energy. The rate of production of cascades of total energy greater than 370 GeV by protons at the top of the atmosphere was calculated to be $(1.2 \pm 0.3) \times 10^{-8}$ $sec^{-1}st^{-1}$ per gm of the detector. Multiplying this by the interaction length of protons in the detector, 176 ± 26 g. cm^{-2}, gives the primary proton flux to be

$$N_p(>E_p) = (1.6 \pm 0.5) \times 10^{12} \times E_p^{-1.44 \pm 0.05} cm^{-2} sec^{-1} st^{-1}. \quad 2.2$$

for $2.6\ 10^{12} < E_p < 2.6\ 10^{14}$ eV.

Assuming the composition to be the same as at low energies then the flux of all nuclei at the top of the atmosphere is given by

$$N(>E_p) = (3.2 \pm 1.0) \times 10^{12} E_p^{-1.44 \pm 0.05}\ cm^{-2} sec^{-1} st^{-1}. \quad 2.3$$

for $2.6\ 10^{12} < E_p < 2.6\ 10^{14}$ eV.

This integral primary spectrum is shown in figure 2.2.

Baradzei et al., (1962) have used an ionization calorimeter of area 0.2 m^2, flown at high altitudes, to measure the energy spectrum of single gamma-rays and of cascades initiated in the detector by nuclear-active particles. The cascades were formed by interactions in a carbon block above the apparatus. The nuclear-active particle spectrum was calculated from the cascade spectrum assuming the interaction length of nucleons in carbon to be 75 g. cm^{-2} and the average pion elasticity $\overline{K_\pi} = 0.32$.

Fluctuations in both parameters were considered because of the steepness of the primary spectrum. Charge symmetry was assumed among the pions formed in the interactions.

From the spectrum so obtained and assuming the absorption length of nucleons to be as given by Babetsky et al. (1960), they give the flux of all nucleons above a given energy per nucleon in the primary energy range $2\ 10^{11}$ - $2\ 10^{13}$eV as

$$N(>E_p) = (600 \pm 150)\left\{\frac{E_p}{10^{12}}\right\}^{-1.7\pm0.15} \quad hr^{-1}m^{-2}st^{-1} \qquad 2.4$$

Malhotra et al. (1966a) have combined all the data on cascade energy determinations and come to the conclusion that the flux of all nuclei is

$$N(>E_p) = (3.9^{+3.4}_{-1.8}) \times 10^{14} \times E_p^{-1.6\pm0.1}\ cm^{-2}sec^{-1}st^{-1} \qquad 2.5$$

in the energy range 10^{11} - $6\ 10^{14}$eV.

Figure 2.2 shows this spectrum compared with that of Malhotra et al(1966a) obtained as above, and that of Baradzei et al. increased by a factor 1.5 to convert it to the flux of all nuclei.

It should be pointed out that the measurements combined have been carried out at a variety of depths and show significant variations from each other.

2.2.2 <u>The Primary Spectrum from the Sea-Level Muon Spectrum.</u>

Brooke et al. (1964) have used measurements of the sea-level muon energy spectrum and proton spectrum, together with a "trial" primary nucleon spectrum, to derive values for the nucleon inelasticity K_t and the pion elasticity K_π in nucleon-air nucleus collisions. Using two models of interactions they showed that the values of K_t and K_π were almost model independent.

Using a value of K_t-K_π derived from other experiments they estimated the energy spectrum of primary nucleons in the energy range 10^{11}-10^{15}eV/nucleon.

The sea level spectrum used was that of Hayman et al. (1963) from which was obtained the pion production spectrum using the expression

$$P(E_\pi \pm)\ dE_\pi = N_\mu \left(\frac{E_\pi}{r}\right)\left\{1 + \frac{E_\pi}{rB}\right\} D\ (E_\pi)\ \frac{1}{r}\ dE_\pi \qquad 2.6$$

(Barrett et al., 1952). This assumes that all muons result from pion decay. $P(E_\pi \pm)$ is the production spectrum of charged pions, $N_\mu\ (E_\pi/r)$ is the sea-level muon spectrum, B = 90 GeV, $r = m_\pi/m_\mu = 1.32$ and $D(E_\pi)$ is a factor allowing for μ-e decay and energy loss by ionization in the atmosphere.

They then used two theoretical models to obtain a theoretical prediction of the pion production spectrum:-

i) The so-called constant-energy model in which all pions are assumed to be emitted with equal energy in the C-system, half in the backward direction and half in the forward direction, the former being assumed to have negligible energy in the L-system. This model was mainly used to find the sensitivity of the results to the model parameters.

ii) The so-called C.K.P. model which predicts that the energy spectrum of charged pions produced in nuclear interactions is

$$N(E_\pi \pm)\ dE_\pi = \frac{n_s}{3T}\ \exp\left\{-\frac{E_\pi}{T}\right\} dE_\pi \qquad 2.7$$

in the forward direction in the C-system where E_π is the pion energy in the L-system, n_s is the total multiplicity of all pions, T is the mean pion energy and charge symmetry is assumed. Half the pions are assumed to be emitted in the forward direction and half in the backward direction in the C-system, the latter being assumed to have negligible energy in the L-system.

The multiplicity was assumed to be given by $n_s = 2.7 \times E_p^{\frac{1}{4}}$ in both cases.

Assuming the primary nucleon spectrum to have the form $N_p(E_p)\ dE_p = B.E_p^{-\gamma} dE_p$ and neglecting the loss of pions due to decay and the formation of pions in pion-air nucleus collisions, it can be shown that for the

constant energy model

$$P(E_\pi \pm)\, dE_\pi = \frac{2}{1-(1-K_t)^{\gamma-1}} \left\{ \frac{Ba^u}{(1-\alpha)} \left(\frac{K_\pi}{3} \right)^V E_\pi^W \right\} dE_\pi \qquad 2.8$$

where $u = (2-\gamma)/(1-\alpha)$, $V = (\gamma-\alpha-1)/(1-\alpha)$, $W = (2\alpha-\gamma)/(1-\alpha)$ and α is given by $n_s = 2.7\, E_p^{\alpha}$.

The C.K.P. model gives similarly

$$P(E_\pi \pm)\, dE_\pi = \frac{2\, dE_\pi}{1-(1-K_t)^{\gamma-1}} \frac{3a^2 B}{K_\pi} \int_{3E_\pi}^{\infty} E_p^{-\gamma-\frac{1}{2}} \exp\left\{ \frac{-3aE_\pi}{K_\pi E_p^{\frac{1}{2}}} \right\} dE_p \qquad 2.9$$

where $a = 0.45$.

So by treating K_π as a variable it can be adjusted until agreement is obtained with equation 2.6.

The "trial" primary spectrum used was that given by Linsley et al. (1962) converted to intensities in terms of energy/nucleon assuming that below 10^4 GeV the primary flux consists, above constant rigidity, of 12.7% alpha particles, the remainder being protons, and that above 10^{15} eV the primary particles are all protons.

K_t was derived from the sea-level proton spectrum of Brooke and Wolfendale (1964) converted to the sea-level nucleon spectrum assuming the flux of neutrons and protons to be the same (which is justified if there is a high probability of charge exchange in nucleon-air nucleus collisions).

Assuming K_t to be constant over all energies the sea-level nucleon spectrum is given by

$$N_n(E)dE = \sum_{i=0}^{\infty} p(i) \frac{1}{(1-K_t)^i} N_p\left(\frac{E}{(1-K_t)^i} \right) dE \qquad 2.10$$

where $p(i)$ is the Poissonian probability of making i interactions. From the existing experimental data they took the interaction length of nucleons to be 80 g.cm^{-2} and obtained values of $K_t = 0.575$ at 10 GeV and 0.54 at a sea-level energy of 100 GeV.

They then obtained an estimate of the primary spectrum by assuming that K_t and K_π were independent of energy and that $K_t - K_\pi = 0.12$, the divergencies from these values found earlier being due to inaccuracies in the "trial" spectrum. This was then relaxed until consistency with the above assumptions and with the measured proton and pion production spectra was obtained. The resultant spectrum is given by

$$N(>E_p) = 0.87 \begin{matrix}+0.52 \\ -0.30\end{matrix} E_p^{-1.58} \quad cm^{-2}sec^{-1}st^{-1} \qquad 2.11$$

in the energy range $10^{10} < E_p < 3\ 10^{13}$eV/nucleon.

At higher energies the exponent increases reaching a value of about 2.1 in the region of 10^{15}eV.

Fluctuations were considered in the nucleon and pion inelasticities and found to have a negligible effect.

Kaons were neglected in the calculations. If they form a large fraction of the secondaries they will affect the results significantly at primary energies above $\sim 2\ 10^{12}$ eV/nucleon causing a lowering of the derived primary spectrum.

Also the accuracy of the muon and proton spectra used will affect the accuracy of the result. The muon spectrum used is a little lower than the currently accepted ones but up to a primary energy of $\sim 2\ 10^{13}$ eV/nucleon the underestimation should not cause a large error.

The spectrum is plotted in figure 2.2. in terms of energy per nucleus assuming that the primary composition is the same as at low energies.

2.2.3. Direct Measurement.

Recently a direct measurement has been made of the primary spectrum up to an energy of 10^{14}eV by Grigorov et al. (1967) using an ionization calorimeter in an artificial earth satellite.

Caption to Figure 2.2.

Integral Primary Energy Spectra as derived by the following authors.

A. Brooke et al. (1964).

B. Baradzei et al. (1962).

C. Malholtra et al. (1966a).

D. Limits to the primary intensity set by Malholtra et al. (1966a).

Fig. 2.2. Integral primary energy spectra derived by various authors.

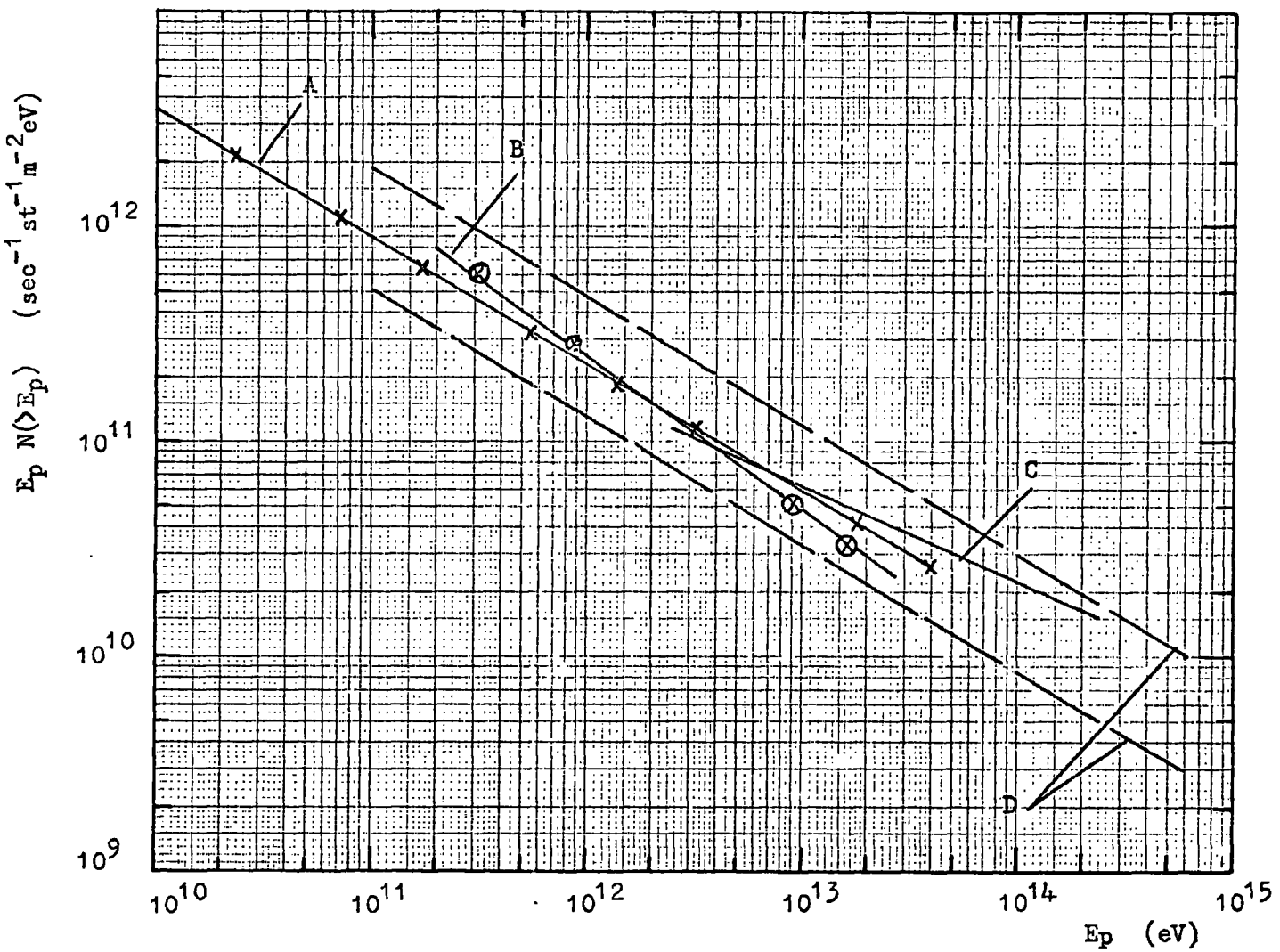

These workers found that the total primary spectrum has the form

$$N(>E_p) \propto E_p^{-1.74 \pm 0.06} \quad \text{for } 10^{11} < E_p < 10^{14} \text{eV} \qquad 2.12$$

somewhat steeper than has been concluded from other experiments.

They have also measured the proton spectrum and find that the slope is similar to that found for all particles up to 10^{12}eV but then the spectrum steepens and has a slope ~ -2.6. This would mean that at energies beyond 10^{12}eV heavy primaries start to be dominant in the primary cosmic radiation.

It is fairly obvious that these results disagree strongly with the indirect work and if they are borne out by further experiments it means that there is something seriously wrong with the assumptionsmade in the latter.

2.3. The Primary Spectrum from E.A.S.

The spectrum of cosmic rays above about 10^{14}eV can only be studied by the enhanced collecting power of extensive air showers because of the low primary cosmic ray intensities above this energy.

Extensive air shower arrays consist of a series of detectors spread over a fairly large area. These enable the density distributions of the showers to be measured and from these the total number of particles in the shower can be obtained.

This can only be related to the energy of the primary particle by means of a theoretical model and assumptions about the primary composition. However, for showers at their maximum of development most models seem to predict that the relationship between the shower size, N, and the primary energy E_p is

$$E_p \sim 2\,10^9\, N \text{ eV} \qquad 2.13$$

Thus, where possible, it is best to measure showers when they are at their maximum of development.

For this reason the results of the B.A.S.J.E. group (Bradt et al., 1966) are probably the most reliable in the energy range $8\ 10^{14}$ - $4\ 10^{17}$eV, since they have estimated the primary energy spectrum from the shower size spectrum of E.A.S. at Mt. Chacaltaya, 5200 metres above sea-level, an ideal depth for showers in the above energy range since they should be near their maximum of development.

By taking shower sizes with a fixed intensity over a range of zenith angles they were able to obtain shower development curves and from these they could estimate the number of particles in the shower at its maximum, and thus they obtained the integral intensity as a function of the shower size at the maximum in longitudinal development. They then assumed that

$$E_p = 2.0\ 10^9\ N_{max} \quad eV \qquad 2.14$$

where N_{max} is the number of particles in the shower at its maximum and thus obtained the primary integral energy spectrum.

To estimate the effect of fluctuations on this type of analysis they also carried out Monte-Carlo calculations of showers, using an assumed primary spectrum, and then derived the primary spectrum using the above method. They found that this type of analysis tended to steepen the spectrum slightly. Allowing for this fact they give the primary spectrum as

$$N(>E_p) = (2.0 \pm 0.4)\ 10^{-14} \left\{ \frac{E_p}{10^{17}} \right\}^{-2.2 \pm 0.15} \quad cm^{-2}sec^{-1}st^{-1}. \qquad 2.15$$

for $8\ 10^{14} < E_p < 4\ 10^{17}$ eV.

This spectrum is shown in figure 2.3.

In a later paper by this group (La Pointe et al., 1968) the results have been confirmed with better statistics and further Monte-Carlo calculations.

Vernov and Khristiansen (1967) have also derived a primary spectrum in the energy region above 10^{14}eV based on E.A.S. data. They conclude that the absolute value of the intensity is $1.7\ 10^{-10}$ $cm^{-2}sec^{-1}st^{-1}$ at a primary energy

of 10^{15}eV, which is determined to within a factor 2. The spectrum is shown in figure 2.3 and is seen to have two changes in exponent. The astrophysical importance of these has been outlined in Chapter 1.

Zatsepin et al. (1963) have estimated the energy carried by different components of extensive air showers with a size of 3.5 10^5 at mountain altitudes and have estimated the primary energy responsible for them as $(6\ ^{+1.8}_{-1.1}) \times 10^{14}$eV.

The different components are:-

i. Ionization loss above the observation level $(3.4 \pm 1) \times 10^{14}$eV.

ii. The energy carried by the nuclear-active particles at the observation level $(0.3\ ^{+0.3}_{-0.2}) \times 10^{14}$eV.

iii. The energy carried by the electron-photon component at the observation level $(0.75 \pm 0.16) \times 10^{14}$eV.

iv. The energy carried by the muon component at the observation level $(0.9^{+0.9}_{-0.2}) \times 10^{14}$eV.

v. The energy carried away by the neutrino component, which was obtained theoretically.

The intensity of showers with sizes above 3.5 10^5 at the same altitude is 1.9 10^{-2} h^{-1} $m^{-2}st^{-1}$. This point is plotted in figure 2.3.

Greisen (1966a) has given a primary energy spectrum based on the results of several groups. This is shown in figure 2.3.

The representation in the region of $\sim 10^{17}$eV and above conforms with the data of the Cornell group near sea-level and Linsley (1963b). There is considerable uncertainty in the energies quoted in this region because of the limited samplings of particle density and the lack of information on the lateral distribution close to the axis of very large showers (this is discussed further below). Also the data in this region are

very sparse and so the slope cannot be considered accurate, but Greisen (1966a) considers that the number of showers recorded does indicate that a change of slope has occurred.

Linsley (1963b) has measured the energy spectrum in the primary energy range 10^{17} - 3 10^{19}eV. In the range of overlap i.e. 10^{17} -10^{18}eV he gives a spectrum which is about 3 times lower than that obtained by the B.A.S.J.E. group (see Figure 2.3).

Linsley also finds evidence for a flattening in the primary spectrum at an energy of about 10^{18}eV. The exact value of the exponent above this energy has not been derived accurately but is in the region 1.6 - 2.0, the former being considered the more probable. Vernov and Khristiansen (1967) also find a similar flattening of the primary spectrum, but this is more gradual and starts at about 10^{17}eV. Other workers have also found this flattening e.g. Andrews et al.(1969), and so the change in slope of the primary spectrum in the energy range 10^{17} - 10^{18}eV seems to be confirmed.

The difference in the absolute intensity of Linsley and the B.A.S.J.E. group probably arises from either differences in the shower size determinations, or from the fact that the showers in the overlap range were not near enough to their maximum of development to warrant using the relation $E_p = 2N_{max}$ GeV in one of the experiments, or a combination of both factors. The B.A.S.J.E. group were in a better position to determine the shape of the structure function because of the more compact nature of their array. If this is the case it means Linsley has underestimated the size of his showers by about a factor 2.

Hillas (1969) has reanalysed the results of Linsley by working back from the quoted shower sizes, via the published structure function to find

the actual densities at radial distances of 300-500 metres. He has then joined the structure functions, at ~ 300 metres, to ones measured by the more compact Agassiz array out to ~ 300 metres after modifying these for differences in shower size and depth.

He considers that the uncertainty in density measured by smaller arrays at 300 metres is less serious than the uncertainty of extrapolating the data of the larger arrays e.g. Volcano Ranch in to 40 metres, the distance inside which most of the particles lie.

Using these composite lateral distributions he has re-estimated the shower sizes of Linsley and finds values about twice as large as those originally quoted.

He has then used an empirical, calorimetric, method to relate shower sizes to primary energy and finds that the primary spectra derived by this method using the Linsley results and those of the B.A.S.J.E. group come into good agreement. He also finds that the change in slope of the primary spectrum first found by Linsley (1963b) still exists with the revised data although it is less sharp than that found by Linsley.

From the above results it seems also that there is also a change of slope at ~ $3\ 10^{15}$eV in the primary spectrum. Adcock et al. (1968b) have considered the possibility that the change in slope of the shower size spectrum, from which the change in slope of the primary spectrum is inferred, may be due to a change in the characteristics of high energy interactions at ~ $3\ 10^{15}$eV. If this is the case they consider that the most likely change is an increase in the multiplicity of high energy interactions. Later calculations (unpublished) indicate that the necessary change in multiplicity is too great and so the explanation seems to be unlikely, although fluctuations in the interaction points of the

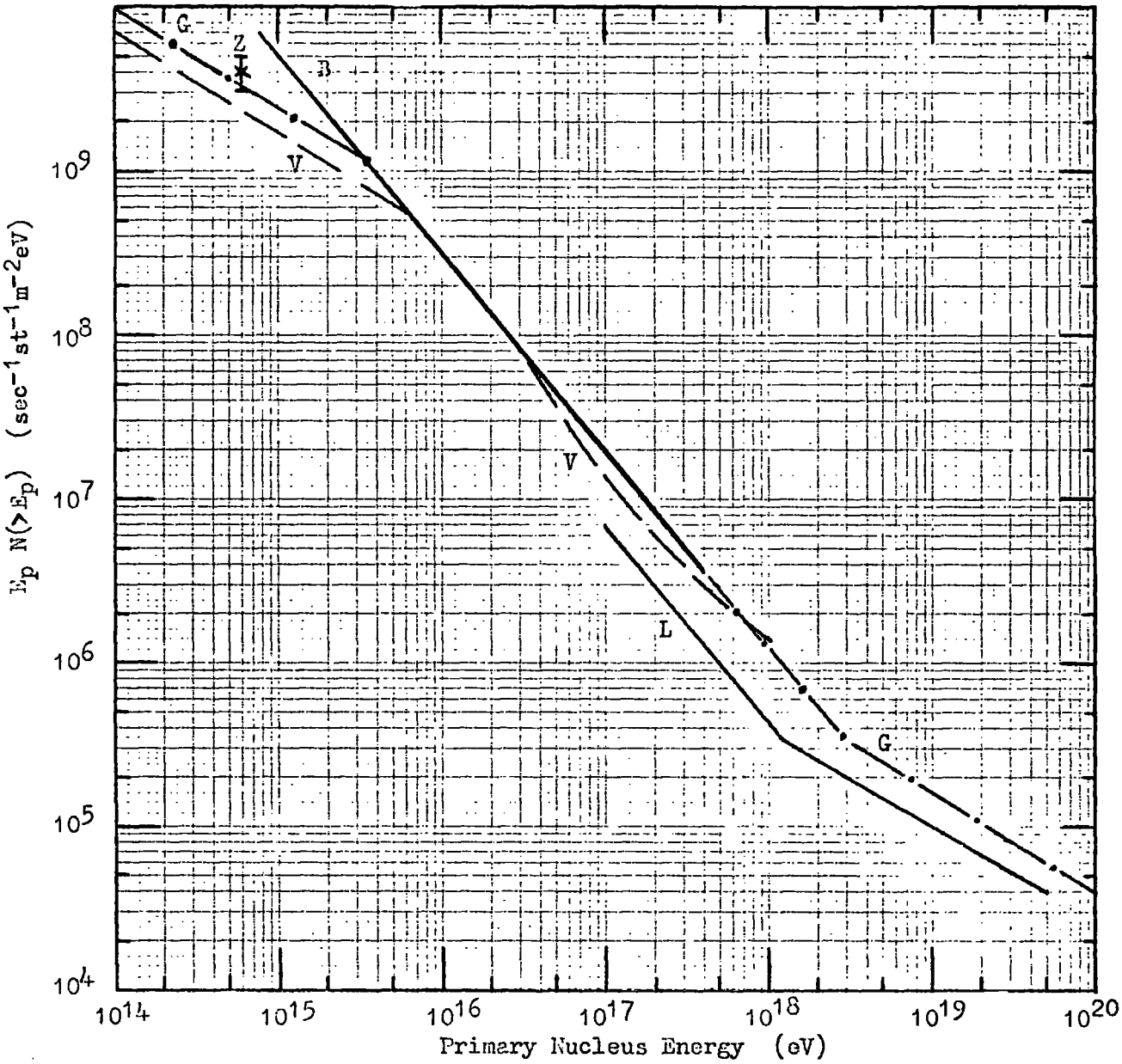

Fig. 2.3. Comparison of primary energy spectra derived from E.A.S. measurements. G, Greisen 1966a; V, Vernov and Khristiansen 1967; L, Linsley 1963b; B, Bradt et al. 1966; Z, Zatsepin et al. 1963.

leading nucleons have not been considered. This should have the effect of reducing the required change in multiplicity.

Vernov and Khristiansen (1967) have also considered the possibility of a change in the characteristics of high energy interactions. They conclude that it is difficult to reconcile all the experimental data with the necessary changes in the parameters of the elementary act.

Thus it seems that the change, at about 3 10^{15}eV, in the slope of the primary energy spectrum is genuine.

2.4. The Chemical Composition of Cosmic Rays.

2.4.1. Introduction

As pointed out in Chapter 1 a knowledge of the chemical composition of the primary cosmic radiation is important in understanding its origin and mode of propagation, and for studying some of the properties of interstellar space.

2.4.2. Direct Measurements.

The composition of the primary cosmic radiation has been measured by means of emulsion stacks or Cerenkov scintillator counters carried to high altitudes by balloons and satellites.

Absolute determinations of the fluxes for protons are particularly difficult because of the presence of singly charged "albedo" particles. These have two components, the "splash albedo" particles and the "re-entrant albedo". The former component is formed when the primary particles interact in the atmosphere and produce secondary particles, some of which travel upwards, out of the atmosphere, thus forming the "splash albedo" particles.

Some of the splash albedo particles are constrained by the geomagnetic field to re-enter the earth's atmosphere after having left it elsewhere. This is the "re-entrant albedo".

The use of Cerenkov detectors allows the effect of the splash albedo to be corrected for since these give the direction of motion of the detected particle, and the re-entrant albedo can be corrected for from a knowledge of the intensity of the splash albedo.

In determining the flux of nuclei heavier than protons from balloon measurements account must be taken of their probability of interacting with air nuclei above the detection apparatus. This causes them to fragment and so increases the proportion of lighter nuclei relative to the heavier nuclei. Allowance for this can be made from a knowledge of the fragmentation parameters of heavy nuclei.

The relative proportion of different groups of nuclei can also be determined as a function of the depth in the atmosphere and by extrapolation back to the top of the atmosphere the relative proportions of the groups in the primary radiation can be estimated.

Helium nuclei are, after the proton component, the most abundant component of the primary cosmic radiation and their behaviour in the radiation is understood the best. The reasons for this are that alpha particles are not commonly produced as fragmentation products in nuclear disintegrations initiated by singly charged particles and so the necessary corrections to the alpha particle flux due to albedo are small.

The total intensity of all nuclei heavier than helium is only $\sim 2\%$ of the total primary radiation above a given rigidity. Thus in order to permit the measurement of intensity values having meangingful statistical weight, it has become conventional to separate these nuclei into groups based on their charge. These groups are usually defined as:-

i. Lithium, Beryllium and Boron nuclei; $3 \leq Z \leq 5$, the so called L-nuclei.

ii. Carbon, Oxygen, Nitrogen and Fluorine nuclei; $6 \leq Z \leq 9$, the so called M-nuclei.

iii. Neon and heavier nuclei; $Z \geq 10$, the so called H-group.

As a result of the accumulation of data it has become possible to separate out a sub-group of the H-group, namely the VH-group containing nuclei with $Z \geq 20$.

Measurements on the proton and helium primary spectra extend out to well beyond 10 GeV, but the spectra of the L, M, H and VH groups are not very well known above energies of a few GeV.

Almost all workers, however, (e.g. Waddington, 1960 and Webber, 1967) agree that the spectra of the different charge groups are the same above energies of about 3 GeV/nucleon, and below this the primary composition is energy dependent.

Since the helium nuclei are probably the best known component, we shall consider the other groups in terms of this component where possible.

i. Protons.

The ratio P/He, in terms of energy/nucleon, rises from a value of ~3 at 200 MeV/nucleon to a value of ~18 at 5 GeV/nucleon, according to Webber (1967) from a survey of direct measurements, above which it is constant. This is confirmed by the results of Gloeckler and Jokipii (1967), as quoted in Fan et al., 1968, who find a ratio of ~15 at 10 GeV/nucleon. Ormes and Webber (1966) have measured the spectra of protons and helium nuclei, using a Cerenkov-scintillation counter, and find the P/He ratio rises from ~5 at 200 MeV/nucleon to ~20 at 5 GeV/nucleon.

ii. S-Nuclei.

The S-nuclei comprise the M and H groups. Webber (1967) gives the He/S ratio as 11.6 ± 0.2 above primary energies of 3 GeV/nucleon and concludes that above this energy the spectra have the same shape.

Anand et al. (1968) have measured the rigidity spectra of helium nuclei

at rigidities $\geq$ 12 GV using an orientated emulsion stack. They have also reanalysed the results of Danielson (1959) on S-nuclei and from these results and the results obtained from a survey of other measurements they conclude that the He/S ratio is not inconsistent with a constant value of $\sim$ 14 over the energy range $\sim$0.1 - 14 GeV. This would indicate that the helium nuclei and S-nuclei have the same spectral shape over this energy region.

Considering the individual groups of the S-nuclei, Webber (1967) gives the H/M ratio as 0.30 $\pm$ 0.02 above primary energies of 3 GeV/nucleon. This agrees well with the results of Durgaprasad et al. (1969), who measured the composition of the S-nuclei using a nuclear emulsion detector carried in the Gemini XI space-craft. This experiment is important because there are no fragmentation corrections to make. They conclude that there is no evidence for a significant change in the primary composition from $\sim$ 1-15 GeV/nucleon, and give the H/M ratio above 6 GeV/nucleon as 0.356 $\pm$ 0.066. Tamai et al. (1968) have measured the H/M ratio in the range 140 - 350 MeV/nucleon and find a value of 0.34 $\pm$ 0.13.

Webber (1966) finds some evidence for the H amd M nuclei having a primary spectrum with an exponent 0.1 $\pm$ 0.3 larger than that of the He spectrum above $\sim$800 GeV/nucleon but this cannot be regarded as conclusive yet until a higher statistical precision has been obtained and measurements made at higher energies.

Few measurements have been made on the VH-group and its spectrum is not known very well. There is some evidence that the spectrum has a similar shape to that of the M-nuclei (Webber, 1967), and that at energies above $\sim$800 MeV/nucleon the He/VH ratio is $\sim$200 (Webber, 1966).

iii. L-nuclei.

Webber (1967) has summarised measurements on the L/S ratio from

measurements on the integral spectra of these components and finds no evidence for a significant change in this ratio from ~ 1200 MeV/nucleon to ~8 GeV/nucleon and gives its value as 0.25 ± 0.02. This corresponds to a L/M ratio of ~0.33.

Fan et al. (1968) have measured the L/M ratio using a detector in an artificial earth satellite. At an energy of ~ 100 MeV/ nucleon they find L/M ~ 0.28.

Webber et al.(1966) have measured the L/M ratio from ~ 0.4 GeV/nucleon to ~ 5 GeV/nucleon and find a significant variation over this energy range, the value varying from ~ 0.6 at 0.4 GeV/nucleon to ~ 0.3 at 3 GeV/nucleon. They conclude that this indicates that the exponent of the L-nuclei spectrum is ~ 0.3 higher than that of the M-nuclei above primary energies of ~400 MeV/nucleon.

All these measurements are for very low primary energies, in most cases less than 10 GeV/nucleon. At higher energies evidence on the primary composition is very sparse from direct measurements.

Malholtra et al. (1966a) obtained 46 emulsion events of total energy above about 2. 10^{11}eV of which 34 were due to protons, 3 to neutral particles, presumeably neutrons, 6 to alpha particles and 3 to heavy nuclei.

In the Sydney 20 litre stack, 112 particles of energy >10^{12}eV were detected (McCusker, 1967). These comprised 52 protons, 18 alpha particles and 42 heavier than alpha particles.

In the Brawley and Bristol stacks a proton of energy 2 10^{14}eV was detected, an oxygen nucleus of energy 2 10^{14}eV and a calcium nucleus of energy 4 10^{14}eV.

2.4.3 Conclusions on the Primary Mass Composition from Direct Measurements.

From the above survey it seems that there are no strong objections to

assuming that the primary composition becomes constant above ~ 3 GeV/nucleon, except for the evidence that the spectrum of the L-nuclei is steeper than those of the other components.

The results seem to be adequately represented by the primary composition given by Ginzburg and Syrovatskii (1964) if one retains the assumption that above ~3 GeV/nucleon the composition remains constant, although data on the L and S components is still rather sparse at energies above ~ 10 GeV/nucleon. The composition given by these workers is shown in table 2.1.

Table 2.1.

Group of nuclei	Z	A	Relative content of nuclei with given energy/nucleon.
P	1	1	93%
He	2	4	6.3%
L	3 to 5	10	0.14%
M	6 to 9	14	0.42%
H	>10	31	0.14%
VH*	20	51	0.04%

*VH group is included in H group.

At energies > 10^{12} eV all one can say at present is that there is evidence for the presence of heavy nuclei up to energies of 4 10^{14}eV.

Thus at even higher energies indirect measurements must be made (except for the satellite results of Grigorov which have been considered in section 2.3.3).

2.4.4. γ-ray Measurements.

Since γ-rays detected high in the atmosphere come from neutral pions produced in the interactions of the primary particles they may

be expected to give information on the primary energy spectrum.

Yash Pal and Tandon (1966) have taken a model similar to that of Pal and Peters (1964) for nucleon propagation and meson production by cosmic rays.

Using a slope of the primary integral spectrum of -1.67 and a high energy per nucleon cut-off of 2 10^{14}eV they obtain quite good agreement with the gamma-ray spectrum measurements of Malholtra et al. (1965) and Bowler et al. (1962), which cover depths from about 20 - 250 g.cm^{-2}, if they use a primary chemical composition similar to that found at low primary energies.

In particular they can explain the observed change in slope of the γ-ray spectra and its energy variation with the depth of measurement.

These γ-ray spectra can be explained without invoking any contribution from a second component of the primary spectrum. However, a second component must exist on this model and its effect will be felt on the γ-ray spectrum at a few thousand GeV at low altitudes. Guided by E.A.S. data, this component was assumed to have a slope of -1.67, to consist of protons only and to have an intensity of 0.05 that of the first component. When compared with mountain altitude measurements of the γ-ray spectrum (Akashi et al., 1963) the fit is found to be quite good.

Yash Pal and Tandon normalised the γ-ray spectra from a simultaneous calculation of the sea-level muon spectrum which was normalised to the 100 GeV point of Menon and Ramana Murthy (1967). However, it should be noted that pions were considered as the only parents of muons and γ-rays and this may not be a valid assumption since there is evidence that kaon and hyperon production occurs in high energy interations, although Duthie et al. (1962) have shown that the simultaneous fitting of the γ-ray and muon intensities supports the view that pion production

remains dominant in the interactions of primaries of energy up to $\sim 10^{14}$eV/ nucleon.

These calculations then tend to support the model of a rigidity cut-off in the primary spectrum as postulated by Peters (1961), although a fuller analysis of E.A.S. characteristics using this model of the primary spectrum is needed and an explanation of the fact that some workers e.g. Baradzei et al. (1962) do not find a steepening of the γ-ray spectrum.

2.4.5. Fluctuation Studies in E.A.S.

A well known characteristic of E.A.S. is the wide fluctuations in shower size from primaries of a fixed energy, due mainly to fluctuations in the points of interaction of the primary particle. These fluctuations are greater for proton primaries than for heavy primaries because of the individual nucleons in the latter forming separate electromagnetic cascades in the main shower, thus reducing the effect of fluctuations in the interaction points. The fluctuations in muon numbers are very small, and so the number of muons can be considered as being related to a unique primary energy.

In order to attempt to use these facts De Beer et al. (1968a) have calculated $\sigma_{N_e}/\bar{N}_e$ as a function of $\bar{N}_e$ for a fixed muon size, N_μ, and $\sigma_{N_\mu}/\bar{N}_\mu$ as a function of shower size, $\bar{N}_e$, for fixed N_e using three primary mass spectra:-

i. Protons only.

ii. A constant composition throughout, consistent with that found at low energies.

iii. A modulated composition, assumed to be the same as (ii) at low energies, but with an enhanced contribution from heavy primaries above 10^{15}eV and the reappearance of protons from meta-galactic sources above 10^{17}eV.

The three spectra are chosen so as to give consistency with the measured sea-level size spectrum for vertical air showers. The calculations were done for two theoretical models:- the so-called C.E. model and the so-called C.K.P. model (see Brooke et al., 1964). The calculations indicate that to study the primary composition, measurements on the relative standard deviation of N_e (i.e. $\sigma N_e / \bar{N}_e$) for fixed N_μ are the most useful. Variations of the fluctuations of N_μ for fixed N_e being relatively insensitive to the primary mass composition, although they may be useful in deciding between models of interaction.

Adcock et al. (1968a) have compared $\sigma N_e / \bar{N}_e$ as a function of $\bar{N}_e$ for fixed N_μ, as calculated by De Beer et al. (1968a), with the experimental results of two groups: Tokyo (Hasegawa et al., 1963; Ogita, 1962) and Moscow (Khristiansen, 1967, private communication; Vernov et al., 1968) but found that the experimental errors were two large to be able to draw any definite conclusions about the primary mass composition. Similar considerations ruled out the possibility of drawing conclusions about the mass composition of the primary cosmic radiation when these workers compared the calculations of $\sigma N_\mu / \bar{N}_\mu$ as a function of $\bar{N}_e$ for fixed N_e with the experimental results of various groups.

Vernov and Khristiansen (1967) have published results of fluctuations in N_e as a function of $\bar{N}_e$ for fixed N_μ, but again the statistical errors are too large to draw any conclusions.

Thus this method of analysing the primary mass composition does not seem to offer much hope of success at present.

2.4.6. <u>The Variation of the Ratio of Muon to Electron Numbers with Shower Size.</u>

Another factor which De Beer et al. (1968a) show should be dependent on the primary mass is the exponent α in the relation $\bar{N}_\mu \propto \bar{N}_e^{\alpha}$ due to the

fact that heavy primaries are more efficient at producing muons but less efficient at producing electrons than are protons.

Adcock et al. (1968a) have compared the theoretical predictions of De Beer et al. with the experimental results of several workers but the width in shower size over which α was evaluated was so large in most cases that if any modulation effect was present it would tend to be averaged out. Thus no definite conclusions could be drawn about the mass composition.

The Lodz-Paris group (reported by Trumper, 1969) have presented evidence for a very rapid modulation effect at energies of about 10^{15}eV. This has been interpreted as a change from the normal composition to predominantly alpha particles in the region of energy ~ 3 10^{15}eV with a transition to a pure proton composition at higher energies.

An alternative explanation of these results is also possible (Wdowczyk 1970, private communication). This is that the primary composition changes from a mixture of alpha particles and protons to predominantly alpha particles followed by a transition to a pure proton composition at higher energies.

2.4.7. Horizontal Extensive Air Showers.

De Beer et al. (1969) have made a theoretical analysis of E.A.S. at very large zenith angles. They have considered two primary mass spectra:-

i. A modulated one with a composition similar to that found at low primary energies with a rigidity cut-off at 1.5 10^{15}eV for protons above which the exponent has been increased by 0.5 for each component. The slope below the kink is assumed to be -1.6 (integral).

ii. A spectrum identical to (i) below 10^{15}eV above which the spectrum is assumed to consist of protons only, with an integral slope of -2.1.

Both spectra are such as to give agreement with the measured sea-level size spectrum. Below 10^{15}eV the spectra are in quite good agreement with the composite spectrum given by Malhotra et al.(1966a). Above 10^{15}eV both spectra are slightly less steep than the one given by Bradt et al.(1966), which is probably the best estimate at present, but the slopes lie within the error limits of the latter. As regards intensities, (i) is higher than that quoted by Bradt et al. (1966) whilst (ii) is lower. At worst the difference in intensity as compared with Bradt et al. is a factor of ~ 2, but because of the steep slope of the spectra this only corresponds to a difference of ~40% in the energy of a given intensity. In view of the uncertainties in the factor used by Bradt et al. to convert from the shower size at the maximum of development to the corresponding primary energy this difference cannot be said to be significant.

Using the so-called C.K.P. model, De Beer et al. (1969) have derived density spectra for muons with energies above one GeV for a variety of zenith angles and mean transverse momenta of pions produced in high energy interactions for both of the primary spectra described above.

Rogers et al. (1969) have compared their results on the measurements of multiple muons at large zenith angles with the calculations of De Beer et al. (1969) and conclude that if the model is correct in every detail then the primary cosmic radiation in the energy region 10^{15}-10^{17}eV consists solely of protons or has a composition similar to that below 10^{15}eV.

These workers also compare the theoretical predictions with the results of Sekido et al. (1966), who have measured the angular distribution of multiple muons, and find quite good agreement up to zenith angles of about 60°. There is some discrepancy at 75° but since geomagnetic effects become large above 60° and are very difficult to correct for this discrepancy cannot necessarily be ascribed to a defect in the theory.

Parker (1967) has also measured the zenith angle distribution of multiple muons with an energy $\gtrsim 2$ GeV and in this case Rogers et al. (1969) find a discrepancy of about a factor 2 in absolute rates compared with the theoretical predictions, incorporating an estimate of the geomagnetic correction, although the shapes of the angular distributions are very similar. Rogers et al. state that there may be some uncertainty in the efficiency of the system due to its complex nature and perhaps, more importantly, there may be inaccuracies in their calculated rates using the predicted density spectra and the geometry of the system.

2.4.8. High Energy Muons at Large Radial Distances.

Earnshaw et al. (1967) have reported muon momentum spectra measurements using the Haverah Park Magnet Spectrograph, which consisted of a solid iron magnet with a mean induction of 14.6 Kg and four trays of neon flash tubes for track location. The spectrograph was located at the centre of an E.A.S. selection and recording complex comprising the large Haverah Park array which selected showers initiated by primaries of energy greater than $\sim 10^8$ GeV.

When the lateral distributions obtained from these results are compared with the theoretical predictions of De Beer et al. (1968b) and Hillas (1966) it is found that the theoretical distributions are much steeper at large radial distances, the discrepancy increasing with muon threshold energy, thus indicating a lack of high energy muons at these distances compared with experiment.

De Beer et al. (1968b) interpreted this as possibly due to a combination of experimental bias and an increase in the mean transverse momentum of the secondary pions produced in high energy interactions with increasing interaction energy.

Orford and Turver (1968) have also made calculations in order to explain the results of Earnshaw et al. (1967). They found that by assuming that the multiplicity of secondary pions varies with the interaction energy, E, as $E^{\frac{1}{4}}$ for $E < 3\ 10^3$ GeV and $E^{\frac{1}{2}}$ at energies above this, and that the mass of the primaries was > 10 then tolerable agreement could be obtained with the experimental results. Orford and Turver therefore concluded that the primary spectrum consists of particles with an average mass > 10 at $\sim 2\ 10^{17}$eV.

This conclusion, however, has been contested by Wdowczyk and Wolfendale (1969, private communication), who have verified the correctness of the above calculations, but contend that the results can be explained by primary protons if the exponent, X, in the multiplicity law E^X, is allowed to rise to a value slightly greater than 0.5, or, more likely, that the mean transverse momentum of pions produced in high energy interactions is allowed to increase with energy, reaching a value of 0.65 GeV/c at the energy responsible for the 100 GeV muons. If allowance is made for the selection bias, which they contend is present in the measurements, the necessary increase in $\langle p_t \rangle$ is even smaller. Such increases in X and $\langle p_t \rangle$ are possible, and measurements of $\langle p_t \rangle$ made at lower energies and extrapolated to the energies in question do suggest such values. Thus an alternative explanation to heavy primaries is possible at primary energies of $\sim 2\ 10^{17}$eV.

Orford and Turver (1969) have compared their theoretical predictions with the experimental momentum spectra of muons at large distances from the core reported by Machin et al. (1969). Andrews et al. (1969) have ascribed an energy of $1.7\ 10^{17}$eV to the primary particles responsible for the showers from which these data are derived assuming them to be

protons. Orford and Turver conclude that it is not possible to decide on the mass of these primaries from a consideration of the shape of the momentum spectra, but from a comparison of the primary energy estimated by Andrews et al. with that necessary to predict the observed absolute muon densities they conclude that the primaries are heavy.

Other evidence on the primary composition at these energies comes from the work of Linsley and Scarsi (1962). These workers measured showers of size $>10^7$ particles at an atmospheric depth of 820 g.cm^{-2}. From measurements of the fluctuations in the ratio of the number of muons to the number of electrons, they concluded that the primary cosmic rays in the primary energy region $\sim 10^{17}$eV and above consisted of purely protons or purely iron nuclei. Thus knowing that the primary composition was relatively pure they attributed any fluctuations in the ages of showers of the same size, measured at the same depth, to differences in their height of origin. They say that there should be a wider spread in the ages of proton induced showers than ones induced by iron nuclei because of the longer interaction length of the protons, and their results support the view that the primary particles consist of protons in the energy range $\sim 10^{17}$eV and above.

2.4.9. Density Spectrum Measurements.

Measurements of the density spectrum of E.A.S. show that it exhibits a steepening in slope at a density which increases with the altitude at which the measurements are made. The steepening at sea-level occurs at densities above $\sim$ 500 particles/m^2 (Prescott, 1956) and measurements by McCaughan et al. (1966) indicate a cut-off in the sea-level density spectrum at about 5000 particles/m^2.

Swinson and Prescott (1966) point out that this cut-off and its variation with altitude can be interpreted in terms of a limiting energy

per nucleon of the primaries, leading to an increase in the proportion of heavy primaries above $\sim 10^{15}$eV. They argue that the maximum observable density (the density in the core of the shower) is then limited in the case of proton induced showers by the cut-off in the proton energy and for a shower produced by a heavy particle, by the division of the energy among the individual, but associated cascades from the constituent nucleons of the fragmented nucleus. The cores in the subshowers are assumed to be sufficiently well separated that the maximum observable density is limited to the maximum in the sub-showers. This theory is based on a similar one of Bray et al. (1964) to explain their observations on multicores in E.A.S.. Other groups, however, who have observed multicores explain their results in terms of increased values of transverse momentum in high energy interactions or in terms of fluctuations in the development of the electromagnetic cascade (see section 2.4.10) and so the steepening in the density spectrum may not necessarily reflect the primary composition becoming heavy above $\sim 10^{15}$eV, although McCusker (1967) considers that the experimental results are decisively in favour of a cut-off in the energy per nucleon of the primary particles.

Swinson and Prescott (1968) note that the relative numerical values of the density scale-change for each altitude are very close to the mean energy fraction retained by a primary at the appropriate level in the atmosphere. They say this suggests a model in which the number of particles in a shower at any altitude and the density, in particles per square scattering length, are closely related to the energy available for the production of particles, at least for the showers that give rise to the largest observed densities. They say that the "gammanization" process proposed by Nikolskii (1967) would provide an effective means of linking the energy with the density for it allows the shower to develop very quickly.

The steepening of the density spectrum may then reflect partly the effect of the "gammanization" process and partly the steepening both of the number spectrum and the primary spectrum.

2.4.10. Multiple Core Measurements.

A number of groups have made observations of the lateral distributions of the electromagnetic component close to the core and have observed events in which more than one core was apparently present in the same shower, as well as events where only one core was present.

Bray et al. (1964,1966) and Bakich et al. (1968) using plastic scintillators, Geiger-Muller counters and several cloud chambers found that for air showers with sizes in the range 10^4-5 10^5 particles about 50% of the showers were multicored, while most of the showers with sizes greater than this were multicored. This was interpreted by Bray et al. (1964) as evidence for an increase in the proportion of heavy primaries above $\sim 10^{15}$eV.

McCusker et al. (1968) have shown that the results below shower sizes of $\sim 5\ 10^5$ can be understood in terms of a primary cosmic ray composition similar to that found at $\sim 10^{11}$eV, using a variety of models with conservative parameters. They say that the choice of model is relatively unimportant, whereas the choice of primary particle is very important. As yet they have done no calculations at larger shower sizes, but Bakich et al. (1968) conclude that to explain their results in the shower size range $10^6 < N < 10^8$ very large values of transverse momentum are needed even if the results are interpreted in terms of heavy primaries.

Ogita et al. (1968) have made three dimensional Monte-Carlo calculations on E.A.S. using proton primaries and a mean transverse momentum, $\langle p_t \rangle$, of 2.5 GeV/c for nucleons and 1 GeV/c for pions. They conclude that

to explain the results of Bray et al. at the larger sizes a large increase in $\langle p_t \rangle$ must be assumed even for very heavy primary nuclei.

Thielheim and Beiersdorf (1970) have also made calculations on multicore structure and find that the effect of the mass of the primary particle is small compared with the effects of fluctuations in the development of the electromagnetic cascade or from fluctuations connected with the detection of the particles. They therefore conclude that under conventional assumptions about nuclear interaction parameters it is not possible to infer the primary cosmic ray composition from observed multicore structures in the electromagnetic component of vertical E.A.S. at sea-level.

Miyake et al. (1968) have also observed multicores using 48 plastic scintillators covering an area of 12 m^2 above and below a water tank 2m. in depth. The frequency of these events increases only slowly over the shower size range 10^4-5 10^5 particles, and comprise about 25% of the total events observed. They conclude that since the multicore E.A.S. have no special age parameter or distribution of core density to distinguish them, their formation is not dependent on the composition of the primary cosmic radiation but rather on the nature of high energy interactions.

Matano et al. (1968) have used a 20 m^2 spark chamber array and find that only 3% of the showers with size greater than 10^5 particles show multicore effects. They attribute these to events with high values of transverse momentum.

Bohm et al. (1968) have used a 32 m^2 neon hodoscope comprising about 180,000 neon tubes of 1 cm diameter. Thus they are able to obtain very good spatial resolution. They found that about 0.7% of their events exhibited double core structure and all these events were clustered around

shower sizes of 10^5 particles. Initially they interpreted these as due to primary alpha particles, but according to a later paper (Samorski et al., 1970) they can now be understood in terms of Poissonian fluctuations.

It seems then that most of the evidence on multicores, both theoretical and experimental, indicates that no measure of the primary mass can be obtained from them. Rather it seems that they may be due to fluctuations in the electromagnetic cascade process, from fluctuations connected with their detection, or to events with large values of transverse momentum.

2.4.11 Conclusions on the Mass Composition of Primary Cosmic Rays.

At energies of about 10 GeV the mass composition is known reasonably well and is approximately as given in table 2.1.

Above 10^{12}eV the evidence is very conflicting. There is some evidence for a rigidity cut-off in the primary spectrum from γ-ray spectra and density spectra measurements but this is far from being conclusive, and furthermore the actual energy at which the cut-off occurs differs in the two cases.

The evidence for an increase in the proportion of heavy primaries above 10^{15}eV from multicore measurements must now be treated with caution in view of the Kiel results.

The studies of muons at large zenith angles indicate either a pure proton flux, or a composition similar to that found at lower energies, in the energy region 10^{15}-10^{17}eV.

The work of Linsley and Scarsi indicates a predominantly proton flux at energies above $\sim 10^{17}$eV, while there is some evidence from the measurements of the momentum spectra of high energy muons far from the shower core that the primaries at $\sim 2\ 10^{17}$eV are heavy.

Fluctuation studies are inconclusive except for those of the Lodz-Paris group which indicate a rapid modulation at primary energies ~3 10^{15} eV above which there is a transition to proton primaries.

Thus the whole picture is very confused and no definite conclusions can be drawn about the primary composition above 10^{15} eV.

CHAPTER 3.

CHARACTERISTICS OF HIGH ENERGY INTERACTIONS.

3.1. Introduction

As stated previously the ultimate aim of this work is to infer, from a comparison of the predictions of the theoretical model and the experimental results on very high energy muons at large zenith angles, the nature of the primary cosmic radiation and the characteristics of ultra high energy interactions beyond the energies attainable by modern accelerators.

At the relevant energies direct experimental data on the characteristics of these interactions is almost negligible; thus it seems that the most sensible course to adopt is to initially use values of the parameters measured at lower energies, or if the indications are that they are energy dependent to extrapolate them from lower energies to the relevant ones. If disagreement is found between experiment and theory an indication of how to change these parameters may be obtained. Any change, however, must be such as not to disagree with known experimental facts.

Thus it is necessary to survey the known experimental facts on high energy interactions both in order to find suitable values for model parameters and also to find the limits on the range of possible alternative values that can be used in the model.

Seven parameters are the most important in this survey:- the multiplicity of secondary mesons, the energy spectrum of secondary mesons, the fraction of energy initially carried by the primary which appears as mesons and their energy after an interaction, the transverse momentum distribution of the secondary mesons and the mean value of the transverse

momentum, and the inelastic interaction lengths for nucleon-air nucleus and pion-air nucleus collisions.

3.2. Interaction Length and Inelasticity.

3.2.1. Nucleon-Air Nucleus Collisions.

The interaction length and inelasticity for nucleon-air nucleus collisions are very closely related for cosmic ray nucleons. Assuming the differential primary spectrum to have an exponent γ it can be shown that

$$\frac{\lambda_i}{\lambda_a} = 1 - (1 - K_t)^{\gamma - 1} \qquad 3.1.$$

where λ_i is the interaction length for inelastic collisions and λ_a is the attenuation length of nucleons in air. K_t is the inelasticity i.e. the fraction of its initial energy lost by the nucleon in its interaction.

Direct measurements on λ_i have not been made at high energies but it is thought that it will approach its geometric value asymptotically. There seems to be some evidence for this. Williams (1960) has worked out a relation between σ_{nn} i.e. the nucleon-nucleon cross section and the interaction length in air. He concludes that $\lambda_i \sim 106 g.cm^{-2}$ at about 10 GeV. Cocconi (1961) gives σ_{nn} as 32 mb at 24 GeV, which corresponds to $\lambda_i \sim 93 g.cm^{-2}$. Bozoki et al. (1968) give $\sigma_{np} = 27.0 \pm 5.5$ mb at 60 GeV and $\sigma_{pp} = 36.3 \pm 8.9$ mb from studies of the attenuation of penetrating shower-producing cosmic ray neutrons in paraffin and graphite. The cross sections correspond to interaction lengths of $\sim 98 g.cm^{-2}$ and $\sim 92 g.cm^{-2}$ in air respectively.

Grigorov et al. (1967) using a carbon target and an ionization calorimeter in the "Proton 1" and "Proton 2" artificial earth satellites estimate λ_i as $97 g.cm^{-2}$ at 20 GeV and $83 g.cm^{-2}$ at 500 GeV.

Cocconi (1966) states that at energies of about 10^{13}eV the cross section for proton - proton interactions remains at about 40 mb which corresponds to $\lambda_i \sim 85$ g.cm^{-2}.

Thus at these energies the interaction cross section appears to be reaching its asymptotic limit of about 43 mb which corresponds to $\lambda_i = 80$ g.cm^{-2}.

This seems to be supported by the work of Matano et al. (1963) who, from an analysis of extensive air showers, estimate $\lambda_i = 80 \pm 10$ g.cm^{-2} for the primary cosmic ray particles. This work corresponds to energies of 10^5 - 10^8GeV. However, these workers assume that the most important factor causing fluctuations in extensive air showers are fluctuations in the point of the first interaction, which is not necessarily so, and perhaps more importantly they do not know the nature of the primary particles.

Thus although there is some disagreement on the exact value of λ_i a value of 80 g.cm^{-2} seems reasonable at very high energies.

Measurements on λ_a indicate that its value lies between 110-125g. cm^{-2}. Taking $\lambda_i = 80$ g.cm^{-2}, $\lambda_a = 120$ g.cm^{-2} and $\gamma = 2.58$ and substituting in equation 3.1 gives $K_t = 0.509$. This agrees well with most experimental work. Brooke et al. (1964) using the assumption that K_t and K_π remain constant over all energies (where K_π is the fraction of the primary energy carried off by the secondary pions) conclude that $\langle K_t \rangle = 0.47$.

Eremenko et al. (1968), using an installation consisting of an ionization calorimeter and a cloud chamber, give $\langle K_t \rangle$ as 0.55 ± 0.25 from an analysis of 50 jets at an energy of about 350 GeV. This may be an overestimate since it is possible that some of the events with large

K_t correspond to jets initiated by primary pions.

Koshiba et al. (1968) from an analysis of interactions caused by high energy heavy nuclei and by their fragmentation products in a block of large nuclear emulsion sheets, give $\langle K_t \rangle$ as 0.54 ± 0.13 at an energy of 1000 GeV.

Thus the inelasticity K_t seems to vary very little with energy. This is also supported by the studies of Abraham et al. (1967) and Yamada and Koshiba (1967).

Imaeda (1962) has reported a decrease in $\langle K_t \rangle$ with increasing interaction energy but Murzin (1966) has shown that this can be explained by inaccuracies in the energy determination.

Thus it is assumed that $\langle K_t \rangle$ is constant with energy and lies in the range 0.4 - 0.6. The average value used by most authors of 0.5 is reasonable.

The inelasticity distribution is also uncertain. Brooke et al. (1964) have fitted a form

$$P_1(f_1)\, df_1 = -(1+\alpha)^2 f_1^{\alpha} \ln f_1 \, df_1 \qquad 3.2$$

to the elasticity distribution of Dodd et al. (1961), where f_1 is the elasticity. They find that the best value of α is 1.43. However, the new mean elasticity is 0.53 as compared to 0.50 without fluctuations and so the effect of these does not seem too important.

It is important to differentiate between K_t and K_π. The former is the fraction of the primary energy given to all secondary particles, whereas the latter is the fraction of the primary energy given to the secondary pions. Brooke et al. (1964) give a value 0.35 for K_π under the same assumptions made in estimating K_t. Because of the difficulty in identifying pions among the secondaries of high energy interactions the only way to measure K_π experimentally is to estimate K_{π^0} from cascade measurements

and assume equipartition of charge. Perkins (1960) in a summary of cosmic ray jet interactions gives $K_{\pi} \simeq 0.3$ and concludes that 80% of the secondaries are pions in the energy range 10^3 - 10^5GeV, on the assumption that the mean transverse momentum is independent of energy.

Evidence on the fluctuations of the elasticity K_{π} is also sparse. Brooke et al.(1964) have used the form

$$F(K_{\pi})\, dK_{\pi} = -(1+\alpha)^2 (1+K_{\pi})^{\alpha} \ln(1-K_{\pi})\, dK_{\pi} \qquad 3.3$$

where $\alpha = 3.6$. This agrees fairly well with the distribution found by Guseva et al. (1962) for proton-LiH collisions at an energy ~ 250 GeV. They also find that the effect of fluctuations on the effective mean value of K_{π} is very small, the fluctuations decreasing the value of K_{π} from 0.35 to 0.33.

3.2.2. Pion-Air Nucleus Collisions.

The uncertainties in the pion-air nucleus interaction length and inelasticity are even greater than those in nucleon-air nucleus collisions. The assumed interaction length varies considerably in theoretical models; Dedenko (1964) takes a value of $\lambda_{\pi} = 80$ g.cm^{-2}, Hillas (1966) 100g.cm^{-2}, Cowsik (1966) 120 g.cm^{-2} and De Beer et al. (1966) 120 g.cm^{-2}. McCusker et al. (1968b) have measured the pion-nucleon inelastic cross-section, $\sigma_{inel}(\pi N)$, as about 26 mb at an energy of about 450 GeV from proton primary jets in emulsions. This would correspond to an interaction length in air of ~100 g.cm^{-2}. Alakoz et al. (1968) give $\sigma_{inel}(\pi N)$ as (19.0^{+5}_{-3}) mb at about 100 GeV from measurements in carbon and lead. This corresponds to an interaction length in air of approximately 125 g.cm^{-2}.

Most authors usually take pion-air nucleus interactions to be totally

inelastic. This is justified by the lack of knowledge on the inelasticity coefficient in these interactions. The main reason for this is the difficulty in identifying the leading pion in the secondaries of such interactions. However, McCusker et al. (1968b) find that one pion usually carries off about 40% of the incident energy at primary energies of about 4.5 10^2GeV, while Gierula et al. (see De Beer et al., 1968b) state that there is some evidence for a pion inelasticity of about 0.5.

3.2.3. Heavy Nucleus - Air Nucleus Interactions.

The interaction length decreases with the increasing mass number of the primary particle. Peters (1952) gives the relationship

$$\lambda_A = \frac{205}{(0.6+A^{\frac{1}{3}})^2} \quad g.cm^{-2} \qquad 3.4$$

for the interaction length of a primary of mass A in air.

Observations on heavy nuclei are very sparse but Bradt and Rappaport (1967) conclude from a brief survey that the heavy nuclei typically survive several interactions without complete disintegration into single nucleons. In their calculations they assume that each interaction of the residual nucleus (atomic weight A, and energy E_i) causes approximately half the mass to be detached in the form of alpha-particles, each having an energy $4E_i/A$. At the subsequent interaction of each alpha particle, four nucleons are released and these in turn proceed to produce pions in their subsequent interactions. They state, however, that their results on the energy spectra and lateral distributions of nuclear-active particles and muons are relatively insensitive to the break-up model assumed.

Thus the usual assumption made by most authors, that a shower initiated by a heavy nucleus of mass A with an energy E_p can be represented

Caption for Figure 3.1.

The number of charged secondaries as a function of the incident particle energy as reported by the following authors.

1. von Lindern (1961).
2. Lal et al. (1962).
3. Dobrotin et al. (1962).
4. Lohrman et al. (1961).
5. Abraham et al. (1963).
6. I.C.E.F. (1963).
7. Malholtra et al. (1966b).
8. Aly et al. (1960).
9. Abraham et al. (1967).

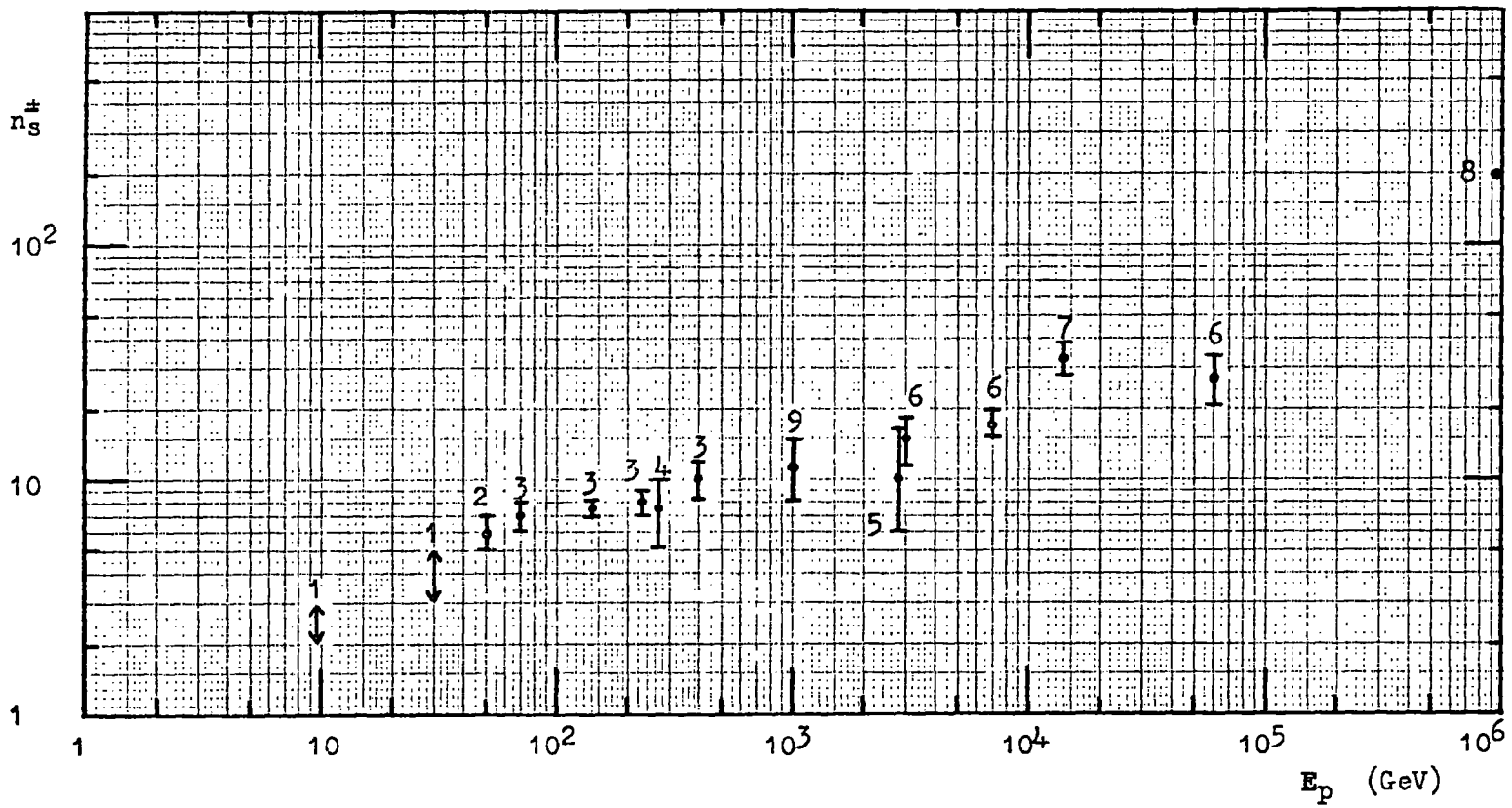

Fig. 3.1.

by a superposition of A showers initiated by primary protons of energy E_p/A seems reasonably valid.

Abraham et al. (1967) say that the collisions of nuclei can be understood in terms of a superposition of nucleon-nucleon collisions.

Orford (1968) has made calculations on the lateral distributions of high energy muons at large distances from the core for different fragmentation probabilities. He finds some sensitivity to the amount of fragmentation but concludes that for fragmentation probabilities greater than 0.1 the effect is small.

3.3. The Multiplicity of Secondary Particles.

Figure 3.1. shows a survey of experimental results on the variation of the mean multiplicity of charged secondaries with primary energy. The lower energy events come mainly from experiments using accelerators, while the higher energy ones come from cosmic ray emulsion measurements.

Many multiplicity laws have been quoted which give objective fits to the experimental results but these depend strongly on the actual contents of a survey. Some examples are:-

i) Wdowczyk I (1966)

$$n_s^{\pm} = 1.8\ E_p^{\frac{1}{4}} \qquad 3.5$$

ii) Hillas (1966)

$$n_s^{\pm} = 1.8\ E_p^{\frac{1}{4}} \text{ for } Ep < 3 10^3 \text{GeV}$$

$$n_s^{\pm} \propto E_p^{\frac{1}{2}} \quad \text{for } E_p > 3\ 10^3 \text{GeV} \qquad 3.6$$

iii) Wdowczyk II (1966)

$$n_s^{\pm} = 1.0\ \ln\ (E_p + 2) \qquad 3.7$$

iv) Malholtra (1964)

$$n_s^{\pm} = 1.6 \ \ln\left\{\frac{E_p}{2.7}\right\} \qquad 3.8$$

In the above equations E_p is the primary energy and $n_s^{\pm}$ is the number of charged secondaries.

Some workers have also proposed forms for the multiplicity law on semi-empirical grounds.

Yash Pal and Peters (1964) have done calculations using a combined fireball-isobar model. The model requires a multiplicity law of the form

$$n_s = 2S n_s^{1} + n_s^{2} E_p^{\epsilon} \qquad 3.9$$

where S is the probability of baryon excitation, n_s^{1} the average number of pions emitted in their decay, and $n_s^{2} E_p^{\epsilon}$ represents the creation of pions in the pionization process. They conclude that to fit the experimental data the simplest expression is

$$n_s = 4.75 + \frac{E_p^{\frac{1}{2}}}{4} \quad (E_p \text{ is in GeV}) \qquad 3.10$$

for nucleon-nucleon collisions.

In contrast to this, in the treatment due to Fermi (1950) it is assumed that as soon as the discs overlap the whole of the energy is distributed among the secondaries. The collision volume is treated as a black body at high temperature and the multiplicity of the secondaries is given by

$$n_s \propto E_p^{\frac{1}{4}} \qquad 3.11$$

However, there are many discrepancies between the predictions of the Fermi model and experimental results.

Frautschi (1963) has produced a model which gives

$$n_s \propto \ln E_p \qquad 3.12$$

He assumes the secondaries are grouped in "clumps". The number of fireballs formed rises as the logarithm of the laboratory energy and each one decays into about six pions. Thus the multiplicity of particles varies essentially as a logarithmic law.

All these multiplicity laws agree within the statistics up to an energy of $\sim 5\ 10^{12}$eV, but above this energy the results are somewhat contradictory and it is impossible to choose any particular one because of the paucity of the experimental data.

McCusker and Peak (1963) have measured the multiplicity of nucleon-nucleon interactions at an energy of 280 GeV and find that these results combined with the mean multiplicity of secondaries measured by Hansen and Fretter (1960) and Dobrotin and Slavatinsky (1960) give a best fit to the multiplicity law of

$$n_s^{\pm} = 4.1 \frac{\log E_p}{\log 16} \qquad 3.13$$

McCusker and Peak (1963) consider this to be not only superior to an $E_p^{\frac{1}{4}}$ law but find that it fits the experimental results from 16-2800 GeV.

Peak and Woolcott (1966) using an energy evaluation method which is model dependent find very good agreement with McCusker and Peak (1963) and find their results compatible with a logarithmic type multiplicity law up to an interaction energy of $\sim 10^{13}$eV.

Dobrotin and Slavatinsky (1967) have also measured the mean multiplicity variation with energy, using an ionization chamber, and find that

their results are compatible with either a logarithmic type multiplicity law or a power law varying as $E_p^{\frac{1}{4}}$ up to an energy of about 10^{12}eV.

The results of McCusker and Peak and Dobrotin and Slavatinsky agree quite well within the experimental errors.

These results refer only to energies less than about 5.10^{12}eV, however, where the choice between a power law or a logarithmic type law is not important for model calculations, since it is only at somewhat higher energies that the difference in the predictions between the two types of law becomes serious.

Pinkau (1966) has concluded from studies of the variation of the height of the maximum of development of E.A.S. that a logarithmic type law is most probable up to energies of about 10^{10}GeV, but the magnitude of the errors is very large.

Bowler et al. (1962) and Fowler and Perkins (1964) suggest that at $E_p \simeq 10^{14}$eV there is evidence for a change in the nature of collisions, leading to a saturation in the mean c.m.s. energy of the secondaries. This would lead to an $E_p^{\frac{1}{2}}$ type multiplicity law.

This is supported by the work of Orford and Turver (1968) who postulate a law

$$n_s \propto E_p^{\frac{1}{4}} \quad \text{for } E_p < 3\ 10^3\text{GeV}$$
$$n_s \propto E_p^{\frac{1}{2}} \quad \text{for } E_p \geq 3\ 10^3\text{GeV} \qquad 3.14$$

to explain their results on high energy muons at large radial distances from the core.

Thus there is a wide range of alternatives for the multiplicity law above about 5.10^{12}eV and it is one of the aims of this work to establish it in the very high energy region.

Fluctuations in the multiplicity of high energy interactions can be quite large. Imaeda (1968) has given the formula

$$P(n_s)dn_s = C\, n_s^{\beta-1} \exp\left\{-\frac{n_s}{\alpha}\right\} dn_s \qquad 3.15$$

where $C = (\alpha^{\beta}\ \Gamma(\beta))^{-1}$.

For nucleon-nucleon collisions Imaeda finds $\beta = 3$ and $\alpha = \bar{n}_s/\beta = \bar{n}_s/3$, where $\bar{n}_s$ is the mean multiplicity.

This expression agrees very well with the experimental distribution given by Abraham et al. (1965) for the frequency distribution of the multiplicity of cosmic ray jets.

So far we have been considering only interactions by nucleons. The information on interactions initiated by pions is even less, and most authors assume that the same multiplicity law applies.

McCusker et al. (1968b) find a logarithmic increase in the multiplicity with interaction energy. This is similar to their results for nucleon initiated interactions and gives some justification to the above assumption.

De Beer et al. (1966) assumed a relation

$$n_s = 2.7 \times 2^{\frac{1}{4}} (K E_p)^{\frac{1}{4}} \qquad 3.16$$

for all interactions, where K is the inelasticity coefficient, but the effects of the difference in the multiplicity for pions and nucleons due to their different values of K should not affect the very high energy muon component seriously.

Imaeda (1968) states that fluctuations in the multiplicity of π-N collisions can be described by a similar expression to equation 3.15 with $\beta \simeq 3\text{-}4$.

Caption for Figure 3.2.

The mean transverse momentum as a function of the incident particle energy as reported by the following authors.

1. Goldsack et al. (1962).
2. Peters (1962).
3. Hansen and Fretter (1960).
4. Guseva et al. (1962).
5. Edwards et al. (1958)
6. Minakawa et al. (1959).
7. Akashi et al. (1962).
8. Malholtra et al. (1966b).
9. From review by Fowler and Perkins (1964).
10. From review by Fowler and Perkins (1964).

• Measurements on charged secondaries.

■ Measurements on neutral secondaries which give rise to electromagnetic cascades.

Fig. 3.2.

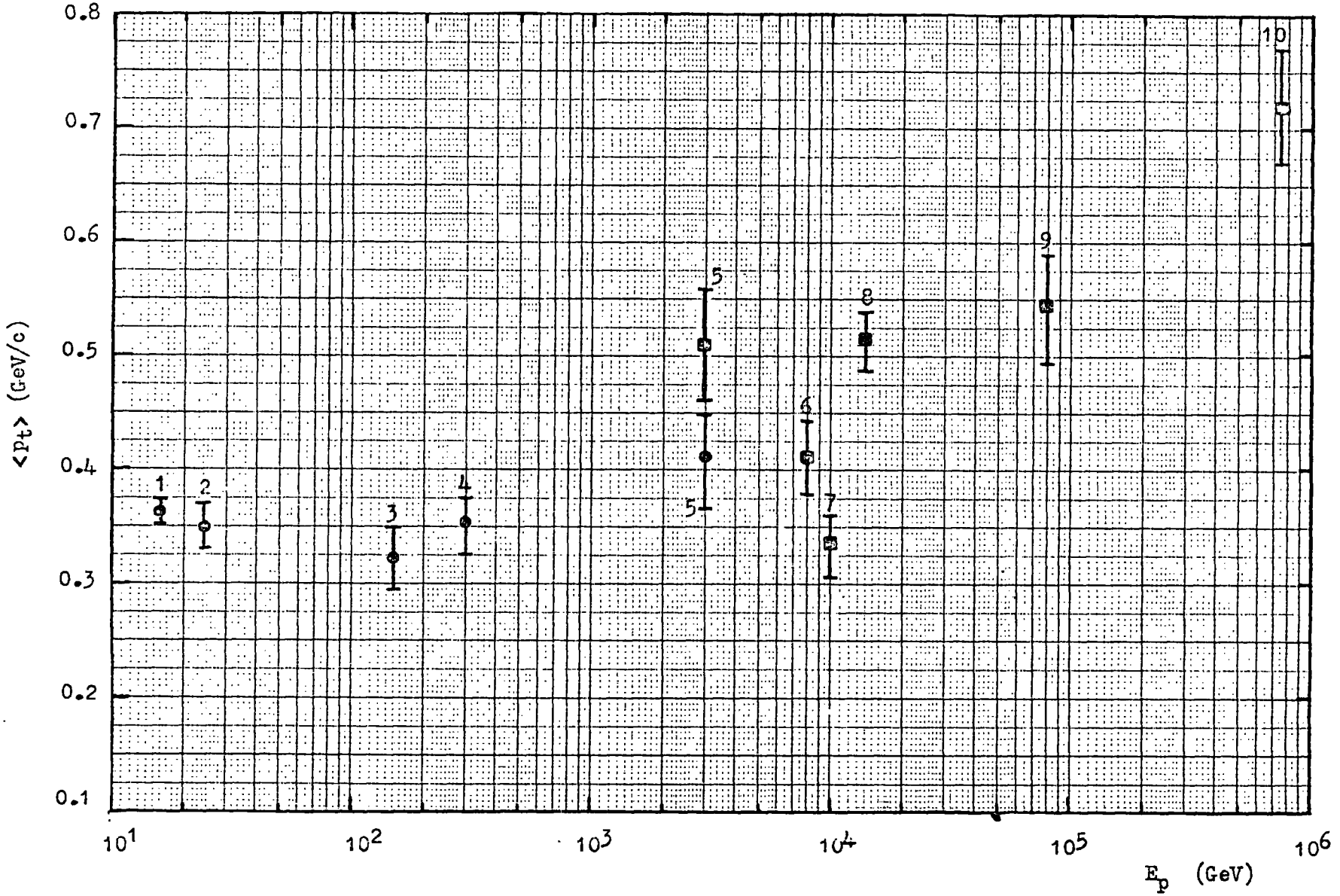
0.8
0.7
0.6
0.5
0.4
0.3
0.2
0.1
<pt> (GeV/c)
1
2
3
4
5
5
6
7
8
9
10
10^1
10^2
10^3
10^4
10^5
10^6
Ep (GeV)

3.4. Transverse Momentum.

Figure 3.2 shows a survey of the mean transverse momentum, $\langle p_t \rangle$, dependence on primary energy, E_p, of secondary pions produced in high energy interactions based on surveys by Fowler and Perkins (1964), and De Beer et al.(1968b). Although this does not represent all measurements, the tendency for $\langle p_t \rangle$ to increase slowly with interaction energy seems to be fairly well established.

A number of forms have been suggested for the transverse momentum distribution of secondary pions. These may be expressed mathematically as follows:-

i) C.K.P.

$$N(p_t)\, dp_t = \frac{p_t}{p_o^2} \exp\left\{-\frac{p_t}{p_o}\right\} dp_t \qquad 3.17$$

where $\langle p_t \rangle = 2\, p_o$ GeV/c.

ii) Aly et al. (1964)

$$N(p_t)\, dp_t = \frac{2p_t}{p_o} \exp\left\{-\frac{p_t^2}{p_o}\right\} dp_t \qquad 3.18$$

where $\langle p_t \rangle = 0.8862\, p_o^{\frac{1}{2}}$ GeV/c.

iii) Nikolskii (1963)

$$N(p_t)\, dp_t = \frac{p_t^2}{2p_o^3} \exp\left\{-\frac{p_t}{p_o}\right\} dp_t \qquad 3.19$$

where $\langle p_t \rangle = 3\, p_o$ GeV/c.

iv) Elbert et al. (1968)

$$N(p_t)\, dp_t = \frac{1}{1.33 p_o}\left\{\frac{p_t}{p_o}\right\}^{3/2} \exp\left\{-\frac{p_t}{p_o}\right\} dp_t \qquad 3.20$$

where $\langle p_t \rangle = 2.5\, p_o$ GeV/c.

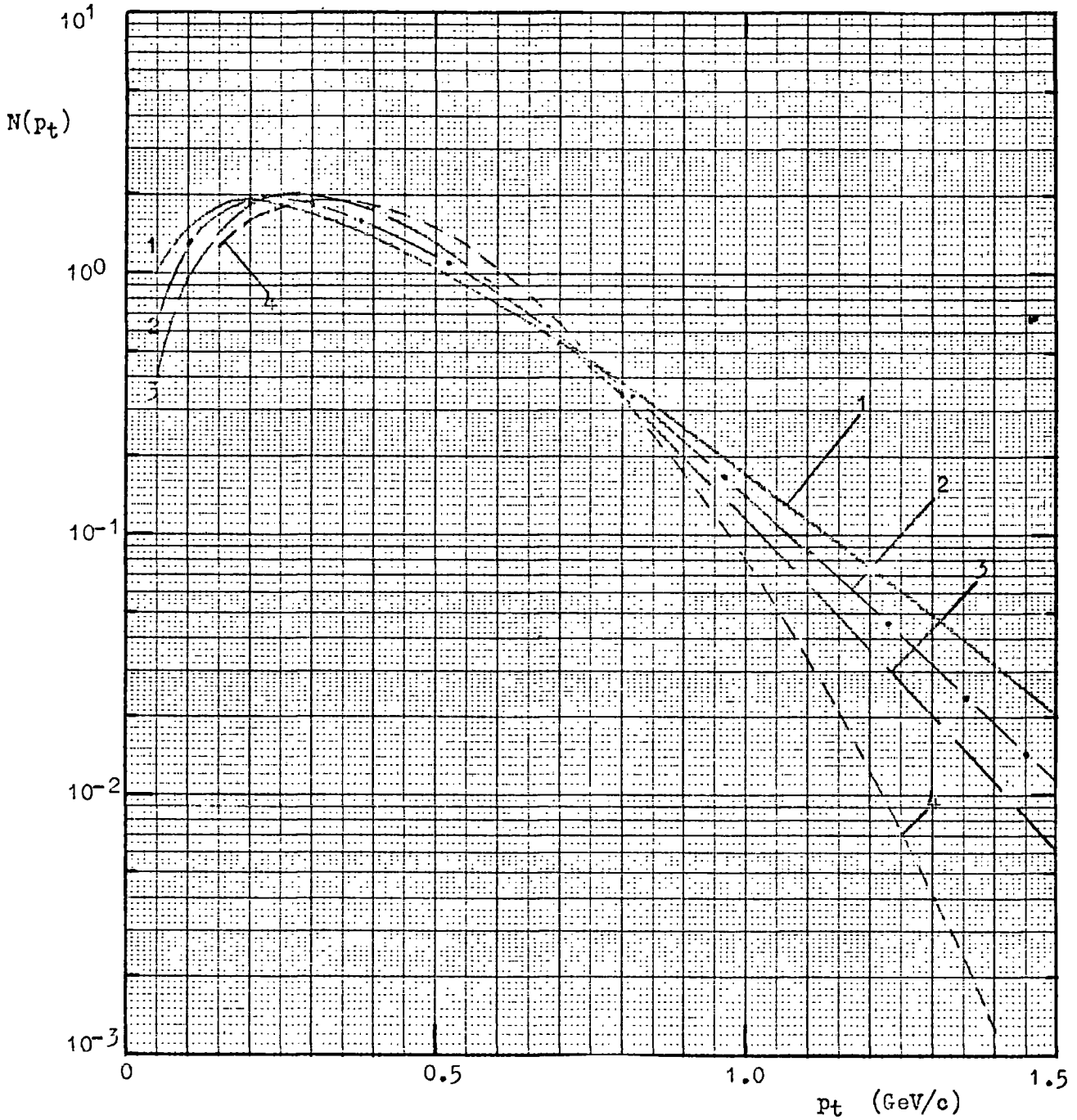

Fig. 3.3. Comparison of transverse momentum distributions proposed by various authors ($\langle p_t \rangle$ =0.4 GeV/c).
1, C.K.P.; 2, Elbert et al. (1968); 3, Nikolskii (1963);
4, Aly et al. (1964).

These distributions are shown in figure 3.3 for $\langle p_t \rangle = 0.4$ GeV/c.

Support for the C.K.P. type of distribution comes from the results of Guseva et al. (1962) using a magnetic cloud chamber at interaction energies of ~300 GeV, Hansen and Fretter (1960) using a magnetic cloud chamber at 150 GeV and C.E.R.N. using a hydrogen bubble chamber for 24 GeV proton-proton interactions (as quoted in Fowler and Perkins, 1964).

These results pertain to $p_t > 0.2$ GeV/c. There is some evidence that this distribution may not be valid for $p_t \lesssim 0.2$ GeV/c. For example when used to calculate the lateral distributions of muons it is found that the theoretical predictions of the lateral distributions tend to be higher than the experimental ones close to the shower axis indicating that the distribution tends to overestimate the number of pions with low values of transverse momentum (De Beer et al., 1966)

Tomaszewski et al. (1966) have also found a deficiency of low transverse momentum secondaries using nuclear emulsions. There are also a number of theoretical arguments supporting this view. As has been pointed out by von Dardel (1962, C.E.R.N Internal Report NP62-17) the C.K.P. distribution predicts a cusp at the origin, a physically unreasonable result. This wdrker suggests using a Gaussian distribution which would be flatter near the origin. Lindenbaum and Sternheimer (1962) suggest that on general theoretical grounds there should be a lower limit to the transverse momentum in the range 0.15 - 0.28 GeV/c. Also the C.K.P. distribution comes from the work of Cocconi et al. (1961) and refers to proton-C, Be and B nucleus collisions and a degree of confirmatory data from p-p collisions. In proton-air nucleus collisions, which are relevant to E.A.S., the probability of a pion being scattered

inside the nucleus after production is greater and this would give rise to a reduction in the probability of small transverse momenta.

Ratner et al. (1967) have measured the transverse momentum of secondaries in proton-proton collisions at 24 GeV using an accelerator. Their results pertain to $p_t^2 > 0.1$ $(GeV/c)^2$ and suggest a Gaussian distribution

$$N(p_t)\, dp_t \propto \exp(-Ap_t^2)\, dp_t \qquad 3.21$$

where $A = 3.5$ $(GeV/c)^{-2}$.

This important question of the transverse momentum distribution will be examined later.

Finally we consider the evidence for the existence of very high values of transverse momentum.

As mentioned previously the lateral distributions measured by Earnshaw et al. (1967) indicate an excess of high energy muons at large distances from the core when compared with the theoretical predictions of several workers. De Beer et al. (1968b) say that the results of Earnshaw et al. are probably subject to some detection bias (due to the preferential selection of flat showers) but even so, if they are interpreted in terms of an increase in value of the mean transverse momentum, $\langle p_t \rangle$, then assuming the C.K.P. transverse momentum distribution, De Beer et al. (1968b) say that they imply $\langle p_t \rangle = 1.0 \pm 0.3$ GeV/c at an interaction energy of $\sim 4\ 10^3$ GeV.

However, other explanations have been put forward e.g. by Orford and Turver (1968) and so the explanation in terms of an increase in $\langle p_t \rangle$ is not necessarily the correct one.

Evidence for high values of p_t has also come from multicore studies. Matano et al. (1968), from their results on the fine structure of air shower cores for sizes $>10^5$ particles, if interpreted in terms of transverse

momentum, find that the transverse momentum distribution above 5 GeV/c is well represented by a power law $f(>p_t) \propto p_t^{-1.7 \pm 0.2}$. They find that the fraction of the secondaries with high values of p_t account for $\sim 3\ 10^{-4}$ of the total compared to $\sim 10^{-8}$ expected for the C.K.P. distribution with a mean transverse momentum of 0.4 GeV/c. The maximum observed transverse momentum was ~50 GeV/c.

Bakich et al. (1968) state that to explain their results above shower sizes of 10^6 particles seems to necessitate high values of transverse momentum even if heavy primaries are assumed.

This is confirmed by the calculations of Ogita et al. (1968) who state that to explain the separation of the multi cores found in a number of experiments, mean transverse momenta of about 10 GeV/c are required for forward going particles.

Miyake et al. (1968) have also come to the conclusion that high values of transverse momentum are needed to explain their observations of shower cores.

3.5. The Energy Distribution of the Secondary Particles.

3.5.1 Introduction

As yet there is no comprehensive theory of high energy interactions and although a number of models have been put forward none of these satisfactorially explains all the observed facts.

These models may be roughly divided into so-called "one-centre" and "multi-centre" models.

Examples of the former are the models of Fermi (1950), Landau (1953) and Heisenberg (1952). In these models the nucleon-nucleon interaction is treated as a single system during the emission of mesons. As a result

of the collision, field energy is liberated in a strongly localised volume, and the way in which the energy is subsequently dissipated depends on some statistical model. In the Fermi and Landau theories, the original nucleons themselves are included in the statistical distribution of energy, whereas in the Heisenberg theory, the nucleons are generally considered to have escaped from the interaction volume before the final state is achieved.

Lewis et al. (1948), Kraushaar and Marks (1954) and Bhabha (1953) have suggested that, as in the "one-centre" models, the result of the collision is to leave each nucleon in a highly excited state at the expense of the kinetic energy of the colliding particles. But contrary to the "one-centre" theory, they consider that the lifetime of these excited states is sufficiently long for each nucleon to escape from the region of their mutual interaction before decaying by the emission of mesons. In Kraushaar and Marks' model, the distribution of energy among the various particles (including the nucleons) in each "centre" is obtained by postulating a Fermi type thermodynamical equilibrium. Takagi (1952), Cocconi (1958) and Ciok et al. (1958) have suggested a variant of the "two-centre" models based on a phenomenological interpretation of the experimental data. They propose that after the collision the original energy is sub-divided into four distinct regions viz. the two recoiling nucleons, and two meson clouds, or "fireballs" , which trail after the nucleons and subsequently evaporate by meson emission. These are the so-called "fireball" models.

3.5.2. The C.K.P. Distribution.

Because of the unsatisfactory state of the high energy models Cocconi et al. (1961) made calculations according to a set of empirical rules suggested by experimental data.

These workers took a transverse momentum distribution for pions following approximately the Boltzmann law

$$N(p_t)\,dp_t = \frac{p_t}{p_o^2}\exp\left\{-\frac{p_t}{p_o}\right\}dp_t \qquad 3.22.$$

where $2p_o = \langle p_t \rangle = 0.4$ GeV/c and is independent of energy and θ, the angle of emission.

They assumed a multiplicity law $n_s = 2.7E_p^{\frac{1}{4}}$ and that the energy content of the pions was fairly constant and in the range of ~0.3 -0.5 of the energy of the incident nucleon.

They also assumed a distribution in energy for the secondary pions emitted in the forward direction in the C.M.S. of the form

$$N(E_\pi)dE_\pi = \frac{n_{seff}}{T}\exp\left\{-\frac{E_\pi}{T}\right\}dE_\pi \qquad 3.23.$$

where T is the mean energy of the secondary pions and $n_{s_{eff}}$ is the effective multiplicity i.e. the number of pions emitted in the forward direction in the C.M.S. and is taken to be half the total multiplicity. The backward moving pions are considered to contribute very little due to their low energy in the laboratory system. Thus

$$n_{s_{eff}}\,T = K_\pi E_p \qquad 3.24$$

where E_p is the primary energy and K_π is the fraction of E_p given to the pions.

They found that these assumptions gave good agreement with experimental results above primary energies of about 25 GeV.

They say that the formula will tend to underestimate the flux at very low energies ($\lesssim$ 1 GeV). Evidently the formula does not seem to hold for energies greater than two-thirds of the primary energy at machine energies, but they feel that these shortcomings will be less

at higher primary energies.

Thus the final energy distribution for pion secondaries of all charges is

$$N(E_\pi)\, dE_\pi = \frac{n_s}{2T} \exp\left\{-\frac{E_\pi}{T}\right\} dE_\pi \qquad 3.25.$$

There is some support for this type of distribution from cosmic ray measurements on the production of γ-rays resulting from collisions in carbon targets which produce π^0 mesons. However, these represent results over many collisions, and they only extend to pion energies of about a tenth of the primary energy.

Despite this they do suggest that the average form of the pion energy distribution is the same over a large primary energy range.

Aly et al. (1964), however, suggest that the C.K.P. distribution underestimates the number of pions of energy $\lesssim 2$ GeV and overestimates the number in the energy range above this.

3.5.3. Isobar Model.

Some workers e.g. Peters (1962) have suggested that at very high energies the leading particles in a collision may frequently be a pair of nucleon isobars carrying the bulk of the C.M.S. energy. Peters (1966) says that the forward isobar carries away about 80 % of the incident energy. The colliding baryons usually emerge in an excited state and decay on average into three mesons, each of which receives about 10% of the primary energy. The great bulk of the pions formed come from fireballs and the average energy given to these fireballs is about 20% of the primary energy. The transverse momentum distribution of the fireball products and of the decay products of the excited baryon states are similar and the angular distributions in their respective mass systems

are essentially isotropic.

Yash Pal and Peters (1964) and Cowsik (1966,1968) have used this model as the basis of their calculations and a comparison between the predictions of Cowsik's model and those of the C.K.P. model will be made, for high energy muons, in Chapter 6.

It should be noted that at low energies the major contribution to the muon component comes from the pionization process, while at higher muon energies the muons come from the isobar process.

Fowler and Perkins (1964) have criticised this model on the basis that at very high energies the differential γ -ray spectrum and the integral muon spectrum should both follow the differential primary spectrum, whereas they are found to be significantly steeper. However Yash Pal and Tandon (1966) have used the model to predict the γ -ray spectra at various altitudes and find that by making certain assumptions about the primary chemical composition it is possible to get agreement with experiment (see Chapter 2).

Grigorov et al. (1966) have concluded that there is no evidence for isobar decay into pions at energies $\sim 5\ 10^3$GeV from their ionization calorimeter measurements.

Thus the evidence on the isobar model is contradictory at present and no definite conclusions can be drawn as to whether they exist or not.

3.5.4. The Two-Fireball Model.

Huggett (1966) has compared the predictions of the symmetrical two-fireball model of ultra-high energy interactions with those of the C.K.P model, which is essentially a one-centre model.

He constructed artificial jets, according to each model, using a Monte Carlo method. These jets corresponded to 3000 GeV nucleon-nucleon

interactions.

Huggett finds that the integral energy spectra, in the laboratory system, predicted by both models are very similar, but that at secondary energies above ~ 600 GeV the two-fireball model spectrum has a tail which is very much higher than that predicted by the C.K.P. model.

The effect of this would be to increase the number of very high energy muons produced in extensive air showers.

3.6. The K/π Ratio.

When considering very high energy muons it is important to know the fraction of secondary particles formed which are kaons, since these are more efficient at producing high energy muons than are pions.

Fowler and Perkins (1964) give the ratio of the number of kaons to the number of pions as ~10% in interactions of primary energy 20-30 GeV, and less than 20% for interaction energies between 100-10^4 GeV.

Osborne and Wolfendale (1964) have derived the K/π ratio from electromagnetic cascade measurements and find that the K/π ratio varies from $20 \pm 20\%$ at $2\ 10^4$ GeV, through 10^{+15}_{-10} % at $7\ 10^4$ GeV to $40 \pm 30\%$ at $6\ 10^5$ GeV.

Orford et al. (1968) find that the charge ratio is not significantly different from unity for muons in E.A.S., indicating that the great majority of muon parents in E.A.S. are pions.

These workers found some evidence for the production of secondaries, most probably kaons, with a large charge asymmetry in extremely high energy interactions. This evidence came from the charge ratio of muons at large distances from the core. However, in a later paper, Machin et al. (1969), better statistics have been obtained and these workers conclude

that there is no significant evidence for a positive excess for distant high energy muons.

3.7. Conclusions

From this analysis it seems that as the basis of an initial model one should assume that the interaction length of nucleons in air is about 80 $g.cm^{-2}$ and that the inelasticity of nucleon-air nucleus collisions is about 0.5. For pions an interaction length of 120 $g.cm^{-2}$ and an inelasticity of 1.0 seem to be good approximations.

The C.K.P. energy spectrum does not seem to strongly contradict any experimental data and neither does the C.K.P. transverse momentum distribution. The average value of the transverse momentum is somewhat uncertain and calculations should allow for the possible variation of its value with the interaction energy.

The form of the multiplicity law of secondary particles is also uncertain above interaction energies of $\sim 3\ 10^{3}$ GeV and this is also a parameter which should be allowed to vary in any calculations.

CHAPTER 4.

THE CALCULATION OF THE CHARACTERISTICS OF HIGH ENERGY MUON SHOWERS AT LARGE ZENITH ANGLES.

4.1. The Adopted Model Parameters.

As a result of the survey of the characteristics of high-energy interactions the following parameters are assumed as the initial basis of the model used to make predictions on the characteristics of high energy muons:-

i) High energy nucleons lose 50% of their initial energy in each collision and have an interaction length of 80 $g.cm^{-2}$, both quantities being energy independent.

ii) All secondary particles produced in high energy nuclear interactions are assumed to be pions, there being equal numbers of each charge.

iii) The secondary pions are assumed to have an energy distribution in the laboratory system given by the C.K.P relationship i.e.

$$N(E_\pi)\, dE_\pi = \frac{n_s}{2T} \exp\left\{-\frac{E_\pi}{T}\right\} dE_\pi \qquad 4.1.$$

where n_s is the total multiplicity of all pions produced in the interaction and T is the average energy of the pions in the forward cone in the laboratory system. Pions in the backward cone are neglected because they will have a very low energy in the laboratory system, and this work is concerned only with very high energy muons.

iv) Two multiplicity laws are considered. The first is taken to be

$$n_s = 2.7\, E_p^{\frac{1}{4}} \qquad 4.2$$

where n_s is the number of pions produced by the interaction of a nucleon of energy E_p GeV. This will be termed the "$E^{\frac{1}{4}}$ model". The

second multiplicity law used is

$$n_s = 2.7\ E_p^{\frac{1}{4}} \qquad E_p \leq 3\ 10^3 \text{ GeV}$$
$$n_s = 0.36\ E_p^{\frac{1}{2}} \qquad E_p \geq 3\ 10^3 \text{ GeV} \qquad 4.3$$

with the symbols having the same meaning as before. This is termed the "$E^{\frac{1}{2}}$ model".

v) The transverse momentum distribution adopted is that suggested by Cocconi et al. (1961) :-

$$N(p_t)\ dp_t = \frac{p_t}{p_o^2} \exp\left\{-\frac{p_t}{p_o}\right\} dp_t \qquad 4.4$$

Initially the mean transverse momentum is taken to be 0.4 GeV/c and independent of energy although other values are considered.

vi) Pion-induced interactions are considered to be totally inelastic, the interaction length of such interactions being 120 g. cm^{-2}. The secondaries are again considered to be all pions and all other parameters are assumed to be the same as in nucleon induced interactions.

vii) The energy distribution of the muon in π-μ decay is, in the laboratory system,

$$N(\epsilon)\, d\epsilon = \frac{d\epsilon}{E_\pi\ (1-r^2)} \qquad r^2 E_\pi \leq \epsilon \leq E_\pi \qquad 4.5$$

ϵ being the energy of the muon produced by the decay of a pion of energy E_π, and r is the ratio of the mass of the muon to that of the pion. The value of r is taken to be 0.76. This distribution arises because in two body $\pi \rightarrow \mu + \nu_\mu$ decay the muon has a unique energy in the C.M.S. and an isotropic angular distribution.

4.2. The Method of Computation.

The method of computation is based on the following diffusion equation

$$\frac{\partial \pi(E,x)}{\partial x} = -\left\{1 + \frac{B}{E(x+x_o)}\right\}\pi(E,x) + \int_E^\infty S(E',E)\pi(E',x)dE' \qquad 4.6$$

which describes the pion energy spectrum at a depth x due to the interaction of a primary nucleon at a depth x_o, where depths are measured in units of pion interaction lengths i.e. 120 g. cm^{-2}.

The first term in brackets on the right hand side of equation 4.6 describes the loss of pions due to interaction and the second term dsecribes the loss of pions due to π-μ decay. The integral describes the formation of pions of energy E due to the interaction of pions of energy E' at a depth x.

Equation 4.6 is solved by the method of succesive generations assuming that the loss of pions by decay is negligible. This latter assumption is valid because we are only interested in very high energy muons (> 600 GeV). It is also assumed in calculating the muon numbers and lateral distributions that the energy loss of muons in travelling through the atmosphere is negligible compared to the muon energy since at a zenith angle of 60^o it should only be ~4 GeV. Also neglected is the loss of muons by μ-e decay since at the energies and zenith angles we are interested in the survival probability of muons is almost unity.

The decay constant, B, is given by

$$B = \frac{m_\pi c\, h_o}{\tau_\pi} \qquad 4.7.$$

in the vertical direction, where m_π is the mass of the charged pion, c is the velocity of light, h_o is the atmospheric scale-height and τ_π is the mean charged pion lifetime.

For zenith angles up to $\sim 70^{\circ}$ it is valid to take the flat-earth approximation (Ashton and Wolfendale, 1963) and in this case

$$B_{\theta} = B \sec \theta \qquad 4.8,$$

where B_{θ} is the decay constant at a zenith angle θ. Since we are interested in zenith angles less than $\sim 70^{\circ}$ this approximation has been made. Putting in the values of the constants in equation 4.8, one obtains

$$B_{\theta} \simeq 140 \sec \theta \text{ GeV} \qquad 4.9.$$

In the basic calculations geomagnetic deflection is also ignored. The displacement, δ, due to this is given by

$$\delta = \frac{150 H h^2}{pc} \qquad 4.10$$

H being the appropriate component of the earth's magnetic field, h is the height of pion formation and pc the momentum in eV/c. Putting in typical values of the parameters in equation 4.10 indicates that this effect will increase the mean radius of the lateral distribution of muons of energy greater than 1000 GeV by less than 10% at a zenith angle of 60°.

Multiple Coulomb scattering is also ignored, simple calculations showing its effect to be much less than that of geomagnetic deflection.

The solution of the diffusion equation and the method of calculation are described in appendix A.

From the basic programme used in the calculations one obtains, for one nucleon interaction at different values of x_o, the mean number of muons and the first five moments of the lateral distribution for a fixed transverse momentum of 0.2 GeV/c as a function of primary energy and

muon threshold energy.

The lateral distributions are reconstructed from the moments, calculated as described previously. For a C.K.P. type transverse momentum distribution of mean 0.4 GeV/c, it can be shown that the lateral distributionsare given by

$$\rho_\mu(r) = \frac{1}{2\pi} \int_0^\infty \frac{f(r_o)}{r_o^2} \exp\left\{-\frac{r}{r_o}\right\} dr_o \qquad 4.11$$

where $f(r_o)$ is the radial distribution of the muons for a fixed p_t of 0.2 GeV/c.

The distribution $f(r_o)$ is obtained from the moments calculated as above and is found to be well described by the expression

$$f(r_o)\ dr_o \quad \propto \quad r_o^{\alpha}\ e^{-\beta r_o^2}\ dr_o \qquad 4.12$$

In fact $\rho_\mu(r)$ is relatively insensitive to the form of $f(r_o)$ and almost indentical results are obtained if it is approximated by a gamma-function.

The advantage of calculating the moments of the lateral distribution is that equation 4.11 can easily be adjusted to give the lateral distributions for other transverse momentum distributions which one may wish to investigate.

4.3. The Muon Number as a Function of Multiplicity.

Figure 4.1. shows the muon number as a function of the multiplicity of pions produced in the interaction of the leading particle for four interaction depths. The curves are for a primary energy of $2\ 10^5$ GeV, a muon threshold energy of 10^3 GeV, and a zenith angle of 60^o ($2\ 10^5$ GeV is about the median primary energy of "doubles" in the Utah detector, as will be seen later, for the "$E^{\frac{1}{4}}$ model"). It is seen that

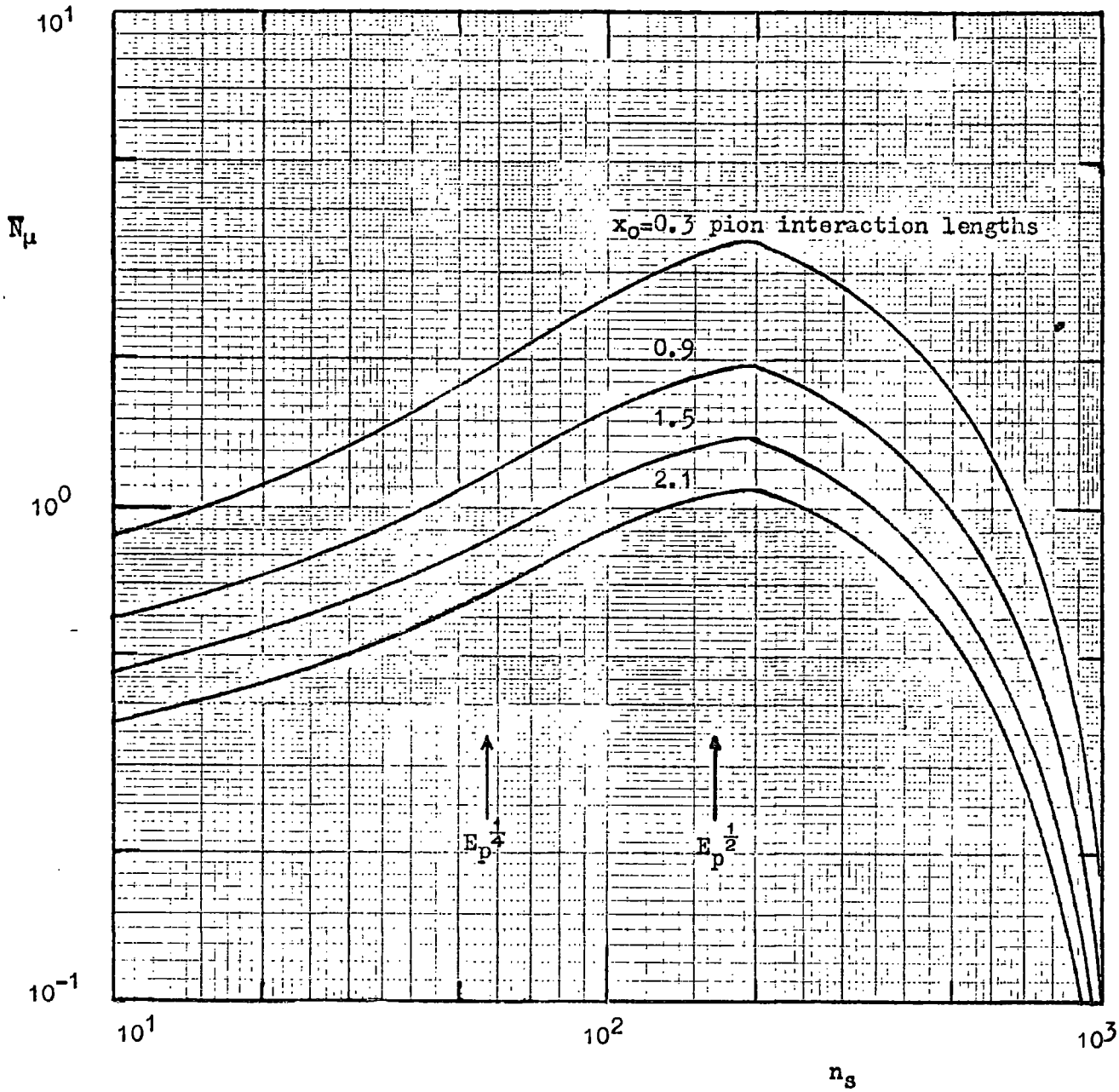

Fig. 4.1. Mean muon number as a function of the number of pions produced in the first interaction of the leading nucleon for one such interaction at various atmospheric depths. E_μ>1000 GeV, θ=60°. $E_0 = 2 \cdot 10^5$ GeV

there is a slow rise in muon number until about a multiplicity of 200 is reached and then the number of muons predicted falls. The reason for this is that as the multiplicity increases the mean energy of the pions formed falls and so the chance of pions decaying increases. This coupled with the increased number of pions leads to an increase in the muon number. This process continues until the point where so many pions are produced in the nucleon interaction that their mean energy becomes lower than the threshold energy of the muons. Above this point although the number of pions is high their mean energy is low and they are unable to produce efficiently muons with an energy above the threshold.

Thus one would expect a maximum in the curve at about the multiplicity which gives a mean pion energy slightly above the muon threshold energy. This is seen to be the case here where the maximum occurs at multiplicities just below 200, the multiplicity required to make the mean pion energy in the first pion generation equal to 1000 GeV.

The multiplicity at which the maximum number of muons is formed is seen to be independent of the depth of the interaction, as would be expected from the above considerations.

Similar curves for other primary energies show the same phenomena, with the maximum number of muons being produced at the multiplicity required to make the mean pion energy about equal to the threshold energy.

The multiplicities given by the "$E^{\frac{1}{4}}$ model" and the "$E^{\frac{1}{2}}$ model" for an interaction energy of 2.10^5 GeV are marked in the figure 4.1.

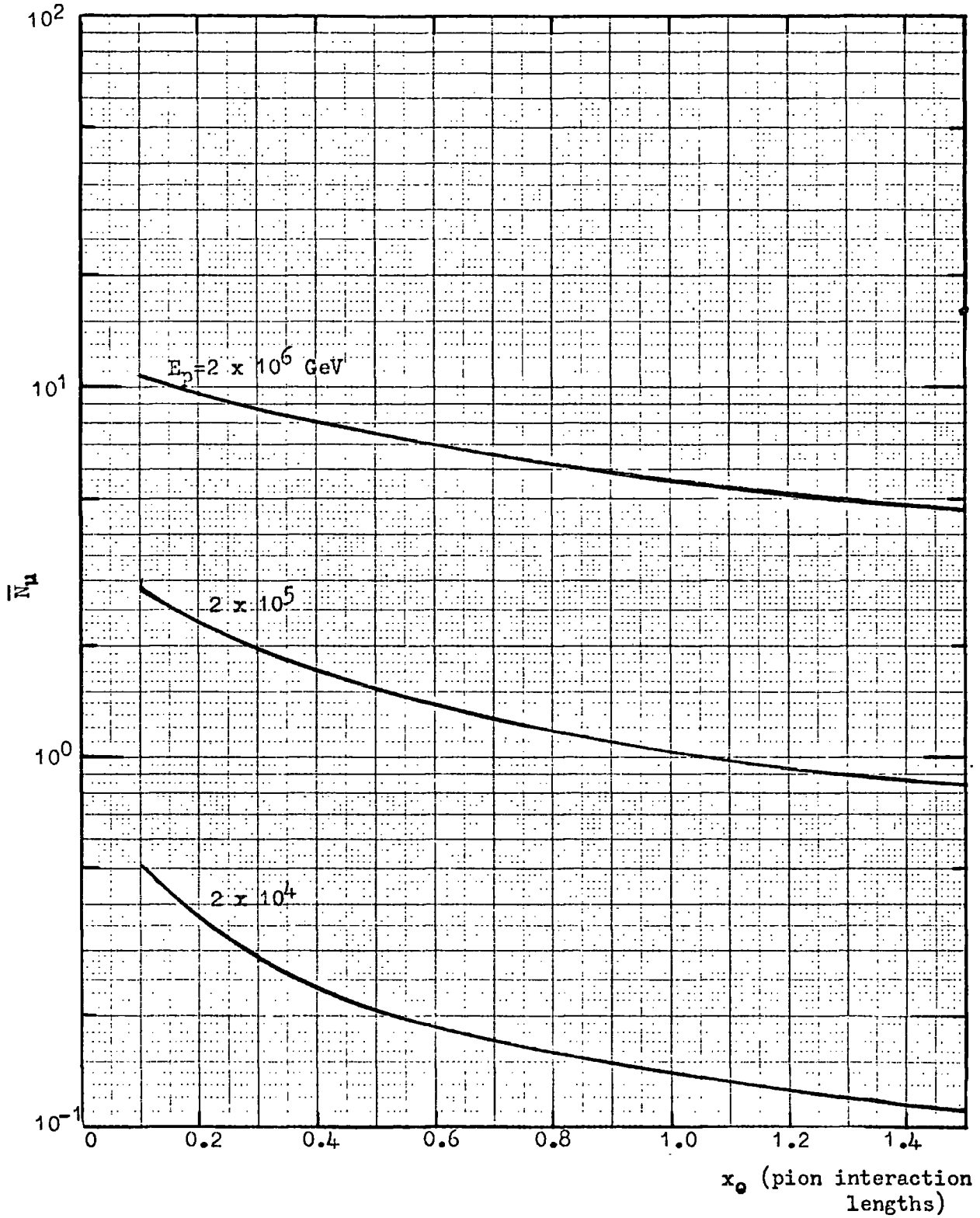

Fig. 4.2. Mean muon number as a function of the depth of interaction of the leading nucleon for one such interaction. E_μ>1000 GeV, θ=60°, "$E^{1/4}$ model" and π's only.

4.4. Muon Number as a Function of the Depth of Interaction of the Leading Particle.

Figure 4.2 shows the variation of the mean muon numbers for muons of energy greater than 1000 GeV for one interaction of the leading nucleon at different depths in the atmosphere (measured in pion interaction lengths) for a variety of primary energies at a zenith angle of 60^{o} and for the "$E^{\frac{1}{4}}$ model".

It is seen that at interaction depths greater than 0.3 pion interaction lengths in the atmosphere the number is only slightly sensitive to the depth of interaction.

The results for the "$E^{\frac{1}{2}}$ model" are similar and also for other threshold energies.

4.5. The Mean Shower Radius as a Function of the Depth of Interaction of the Leading Nucleon.

The mean radii of showers, for one nucleon interaction, as a function of the depth of interaction of the leading nucleon are shown in figure 4.3 for the "$E^{\frac{1}{4}}$ model" and "$E^{\frac{1}{2}}$ model". The curves refer to several primary energies and are for a zenith angle of 60^{o} and a threshold energy of 1000 GeV. The mean radius is seen to be fairly insensitive to the depth of interaction and it is seen that the mean radii of showers predicted by the "$E^{\frac{1}{2}}$ model" are greater than those predicted by the "$E^{\frac{1}{4}}$ model".

This is a consequence of the more rapid degradation of energy in the former model leading to the muons coming from the decay of pions higher up in the atmosphere.

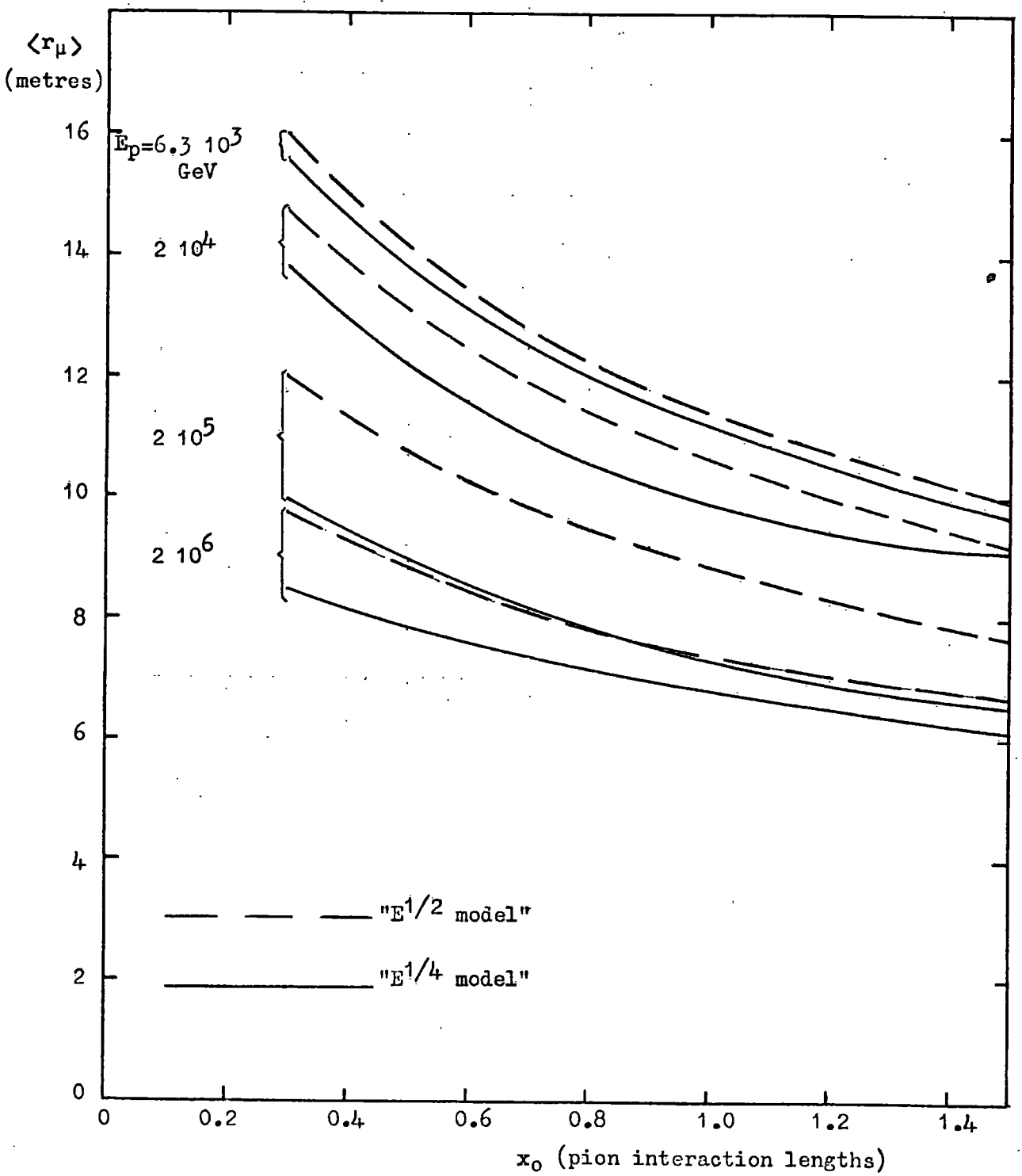

Fig. 4.3. Mean radii of muon showers produced by one interaction of the leading nucleon as a function of the depth of this interaction. $E_\mu > 1000$ GeV, $\theta = 60^\circ$, π's only, $\langle p_t \rangle = 0.4$ GeV/c.

The results are similar for other threshold energies.

4.6. Effective Depth of Interaction.

To obtain accurate values of $\overline{N}_\mu$ and the lateral distribution, either semi-Monte Carlo calculations should be carried out i.e. the position of the interaction point of the leading nucleon should have been allowed to fluctuate according to Poissonian statistics and the average values of N_μ and the lateral distributions found, or the same results could have been obtained by calculating the muon numbers and lateral distributions for a set of values of the interaction depth, x_o, and integrating them over x_o, after weighting them with the appropriate Poissonian interaction probabilities. However, in order to save computational time an "effective" value of x_o is found using the relation

$$\langle r_{eff} \rangle = \frac{\int_0^\infty e^{-1.5x_o} \langle r(x_o) \rangle \overline{N}_\mu (x_o)\, dx_o}{\int_0^\infty \overline{N}_\mu (x_o)\, e^{-1.5 x_o}\, dx_o} \qquad 4.13$$

where $\langle r(x_o) \rangle$ is the mean radius of a shower formed by a nucleon interacting at a depth x_o, and $\overline{N}_\mu (x_o)$ is the mean number of muons in that shower.

The calculated values of $\langle r_{eff} \rangle$ are looked up on the appropriate graph of $r(x_o)$ vs. x_o and so an effective value of x_o is obtained for the first interaction of the leading nucleon. This is denoted by $x_{o_{eff}}$. This method is approximate because the effective value of x_o varies across the shower, decreasing with increasing radial distance. However, for the determination of the density spectra for a detector of large area, for which these particular calculations are to be used, it is the values of the mean radii of the showers which are important, and as has been shown previously the muon numbers and mean radii are not

very sensitive to x_o.

The contribution from the second interaction of the leading particle is obtained by assuming that the interaction occurs at a depth $x_{o_{eff}}$ + 0.667 pion interaction lengths. The neglect of fluctuations in this interaction point is justified by the insensitivity of $\overline{N_\mu}$ and $\langle r \rangle$ to x_o at large values of the latter, which is the case here. Also the contribution from the second interaction is smaller than that from the first due to the leading nucleon having less energy and the depth of interaction being greater.

The contribution from further nucleon interactions is neglected.

4.7. Muon Number as a Function of Primary Proton Energy.

Figure 4.4. shows the dependence of the mean muon number on the energy of the primary nucleon for three threshold energies, at a zenith angle of 60^o, for the "$E^{\frac{1}{4}}$" and "$E^{\frac{1}{2}}$" models.

It is seen that the "$E^{\frac{1}{4}}$ model" gives rise to more muons at lower primary energies than the "$E^{\frac{1}{2}}$ model". This is because of the fact noted earlier, that the greatest contribution to the muon number comes when the mean energy of the pions in the first generation is about equal to the muon threshold energy. At low primary energies, however, the mean energy of the pions is well below the threshold energy in the "$E^{\frac{1}{2}}$ model" case and so fewer muons are formed than in the "$E^{\frac{1}{4}}$ model" where the mean energy is higher, despite more secondary pions being produced in the former. At higher primary energies the "$E^{\frac{1}{2}}$ model" predicts more muons because the pions responsible for these are formed higher in the atmosphere than in the case of the "$E^{\frac{1}{4}}$ model" and so they have a greater chance of decaying before interacting.

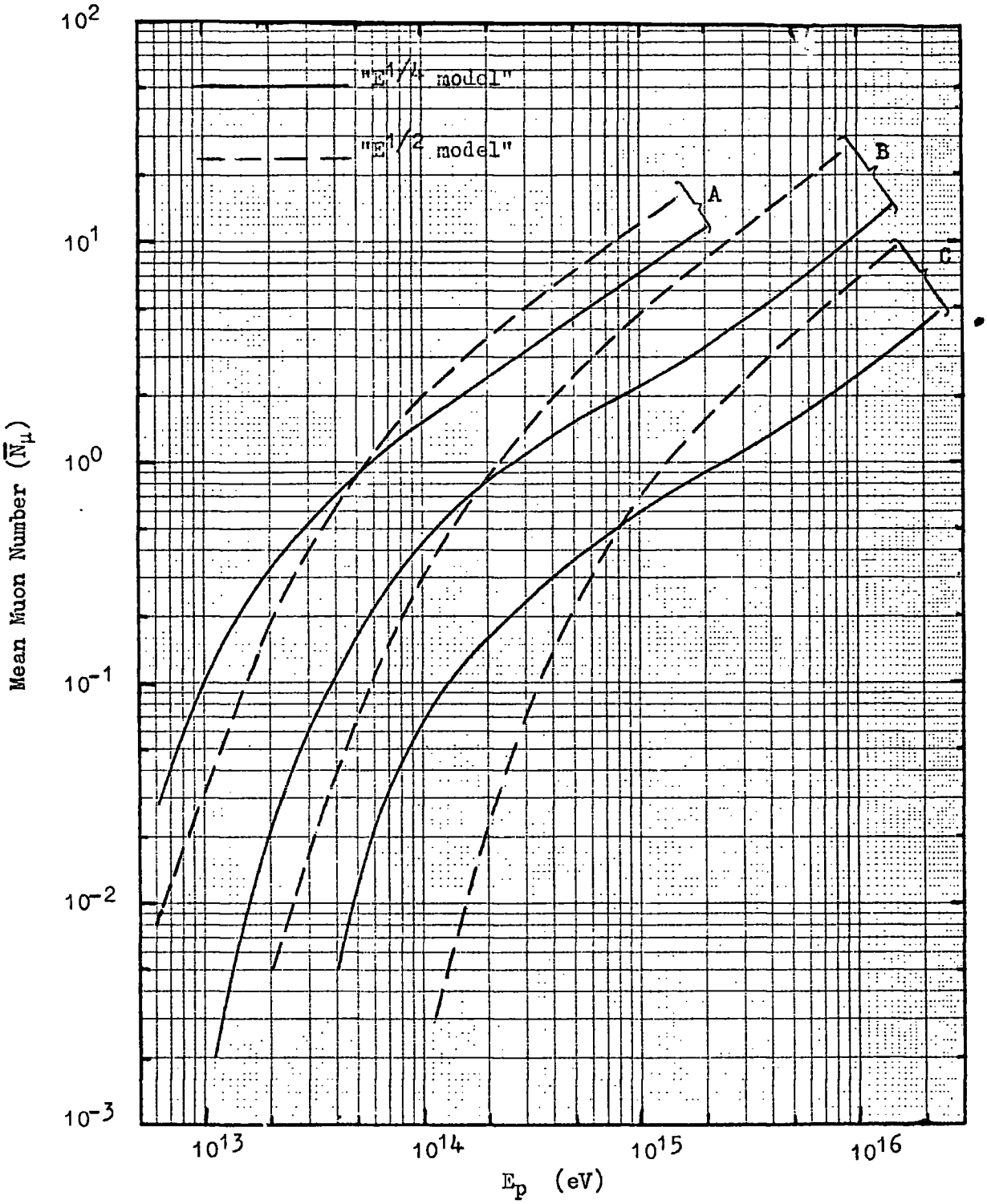

Fig. 4.4. Mean muon number as a function of primary nucleon energy for $\theta=60^\circ$, π's only and various threshold energies.
A, $E_\mu>1000$ GeV; B, $E_\mu>2000$ GeV; C, $E_\mu>5000$ GeV.

Taking the curves for a threshold energy of 1000 GeV as an example it can be seen that above a certain primary energy, in this case $\sim 3\ 10^{13}$eV, the curves are almost linear on a log-log plot. Below this the mean number of muons produced falls rapidly with decreasing primary energy. This fall is due to the mean energy of the secondary pions formed falling with decreasing primary energy until it becomes so low that the probability of producing muons above the threshold energy is very small.

4.8. Lateral Distributions for Proton Primaries.

The calculated lateral distributions for muon threshold energies of 1000 GeV and 2000 GeV, for the "$E^{-\frac{1}{4}}$" and "$E^{-\frac{1}{2}}$" models, are shown in figures 4.5, 4.6, 4.7 and 4.8 respectively for a zenith angle of 60^{o}.

It is seen that the shapes, for a given threshold energy, E_{μ}, are dependent on the primary energy, the distributions becoming narrower with increasing primary energy. This is because at the higher primary energies the later pion generations are becoming important, and thus the pion parents of the muons are formed lower down in the atmosphere.

Also it is seen that the "$E^{-\frac{1}{2}}$ model" gives wider curves than the "$E^{-\frac{1}{4}}$ model", the reason being that the energy is degraded more rapidly in the former which leads to the muons being formed higher up in the atmosphere.

The behaviour of the curves in figure 4.4 is seen to be reflected in the lateral distributions for the two models i.e. the intensities due to the "$E^{-\frac{1}{2}}$ model" are lower at low primary and higher at high primary energies.

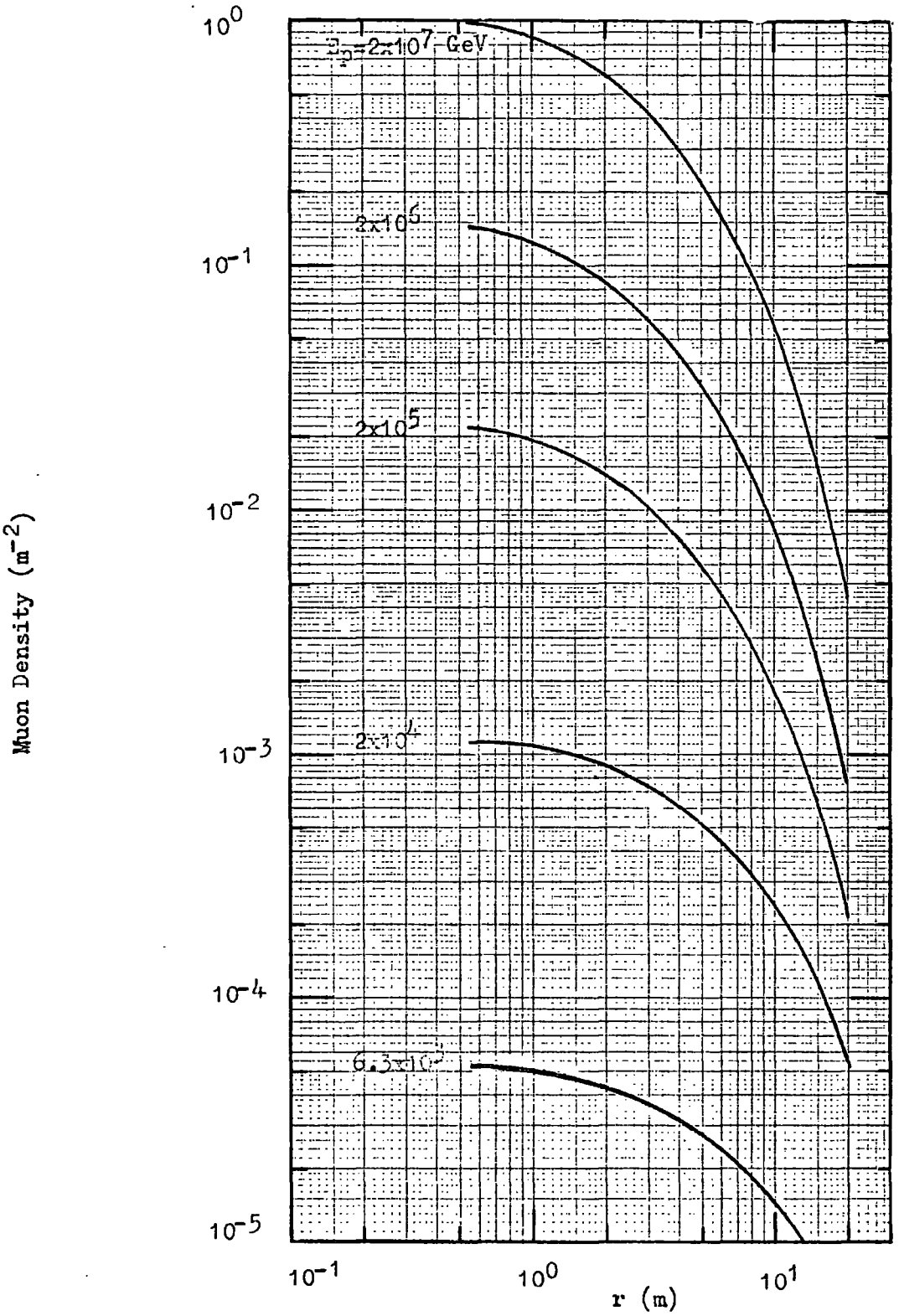

Fig. 4.5. Muon lateral distributions for E_μ>1000 GeV, θ=60°, π's only, $\langle p_t \rangle$ =0.4 GeV/c, "$E^{1/4}$ model".

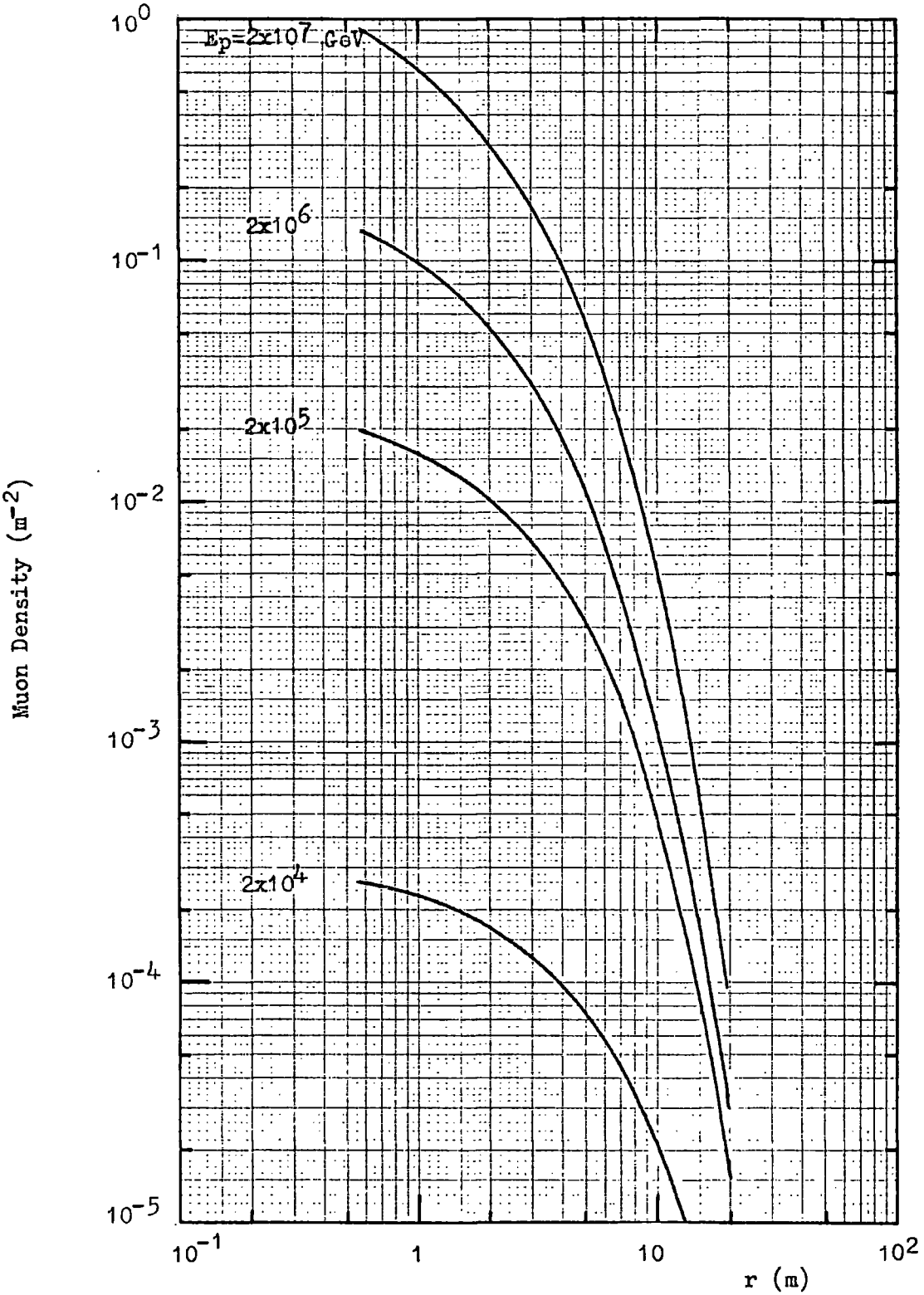

Fig. 4.6. Muon lateral distributions for E_μ>2000 GeV, θ=60°, π's only, $\langle p_t \rangle$=0.4 GeV/c, "$E^{1/4}$ model".

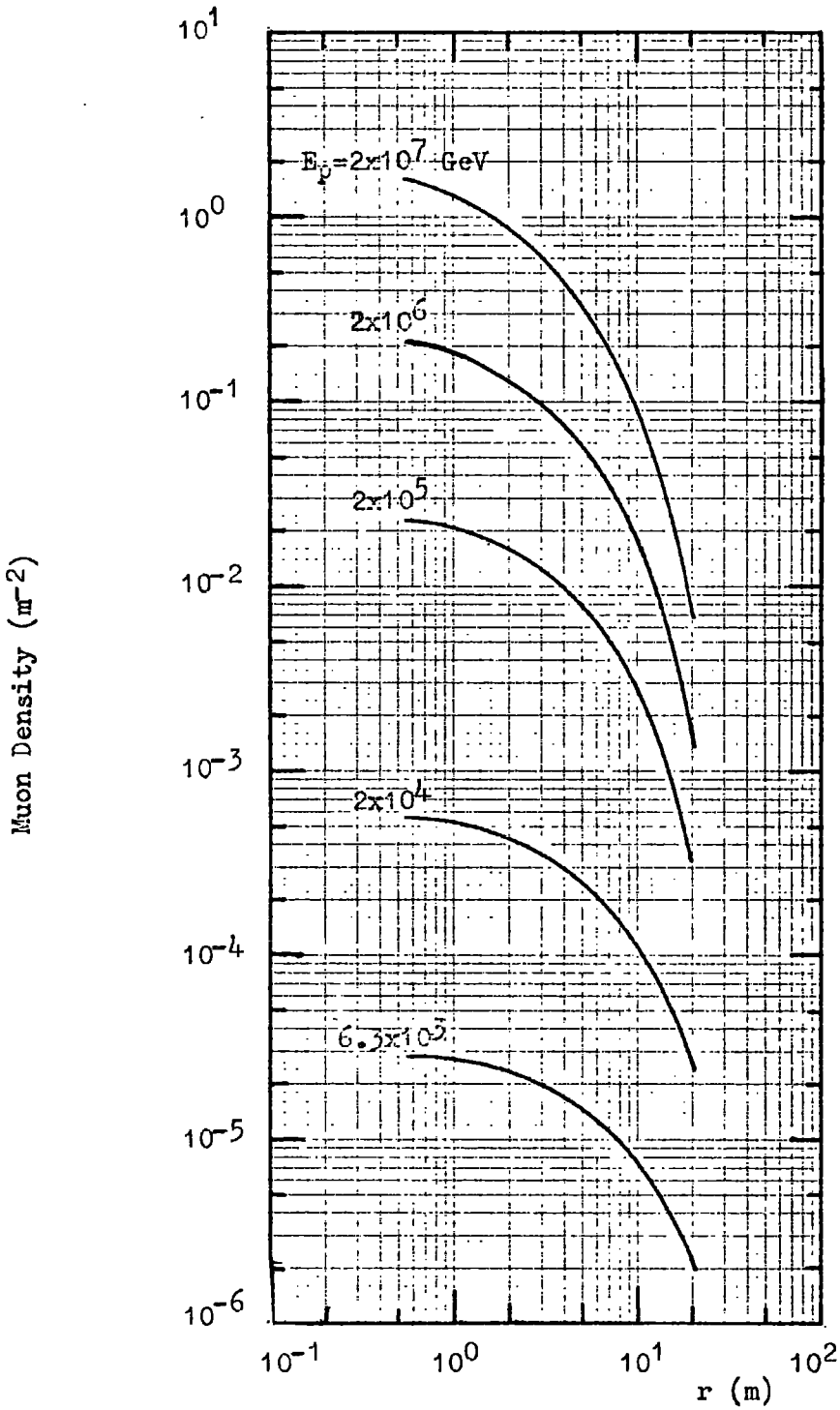

Fig. 4.7. Muon lateral distributions for E_μ>1000 GeV, θ=60°, π's only, $\langle p_t \rangle$=0.4 GeV/c, "E $^{1/2}$ model".

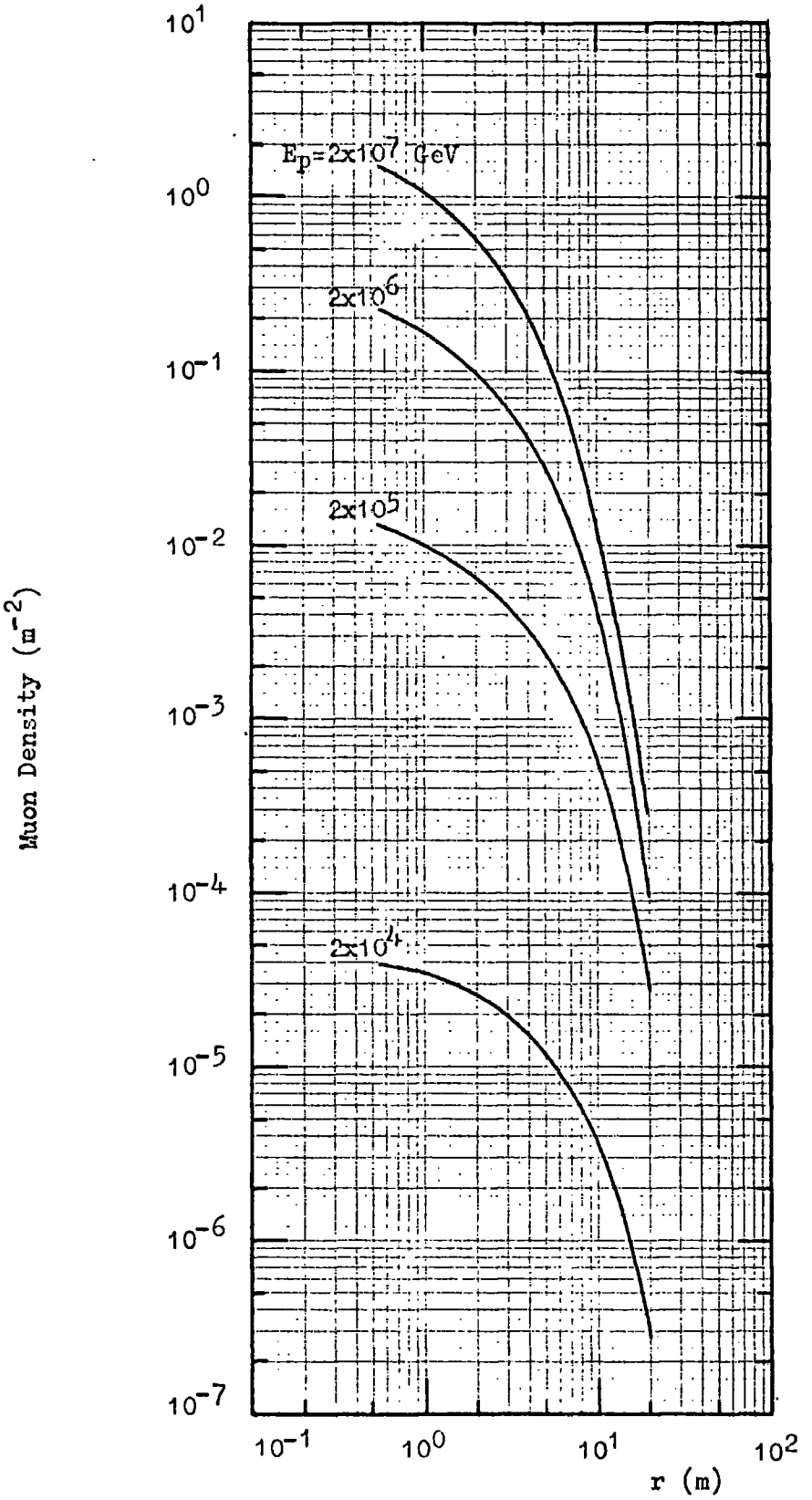

Fig. 4.8. Muon lateral distributions for $E_\mu > 2000$ GeV, $\theta = 60^\circ$, π's only, $\langle p_t \rangle = 0.4$ GeV/c, "$E^{1/2}$ model".

Over the range of radial distances $2 < r < 15$ m the lateral distributions can be approximately represented by a relation of the form $\rho_\mu(r) \propto \exp - (r/r_o)$, where r_o is a slowly varying function of the primary energy and a more rapidly varying function of zenith angle and muon threshold energy. Confining attention to showers which give two detected particles and the "$E^{\frac{1}{4}}$ model" with $\langle p_t \rangle = 0.4$ GeV/c, we find that the relationship is, for $1000 < E_\mu < 2000$ GeV

$$r_o \propto \sec^{1.3} \theta \quad \text{for} \quad 45^o < \theta < 60^o \qquad 4.14.$$

and for the same angular range

$$r_o \propto E_\mu^{-0.8} \quad \text{for} \quad 700 < E_\mu < 3000 \text{ GeV} \qquad 4.15$$

All the curves shown so far refer to a mean transverse momentum of 0.4 GeV/c. Assuming the same form of transverse momentum distribution it can easily be shown that for a mean transverse momentum of 0.4 f GeV/c, where f is a constant, the required lateral distributions are obtained from those given by dividing the original density by f^2 and multiplying the corresponding radial distance by f.

The experimental results on the transverse momentum distribution surveyed in Chapter 3 and also the work of De Beer et al. (1966), using approximately the same model as that used here, indicated that the C.K.P. distribution may overestimate the number of particles with low values of transverse momentum. To investigate the effects of this on the previous results, calculations have been made for a C.K.P. type distribution with all particles having a transverse momentum less than 0.1 GeV/c being suppressed. Under this assumption equation 4.11 becomes

$$\rho_\mu(r) \propto \int_o^{10\, r p_o} \frac{f(r_o)}{r_o^2} \exp\left\{-\frac{r}{r_o}\right\} dr_o \qquad 4.16$$

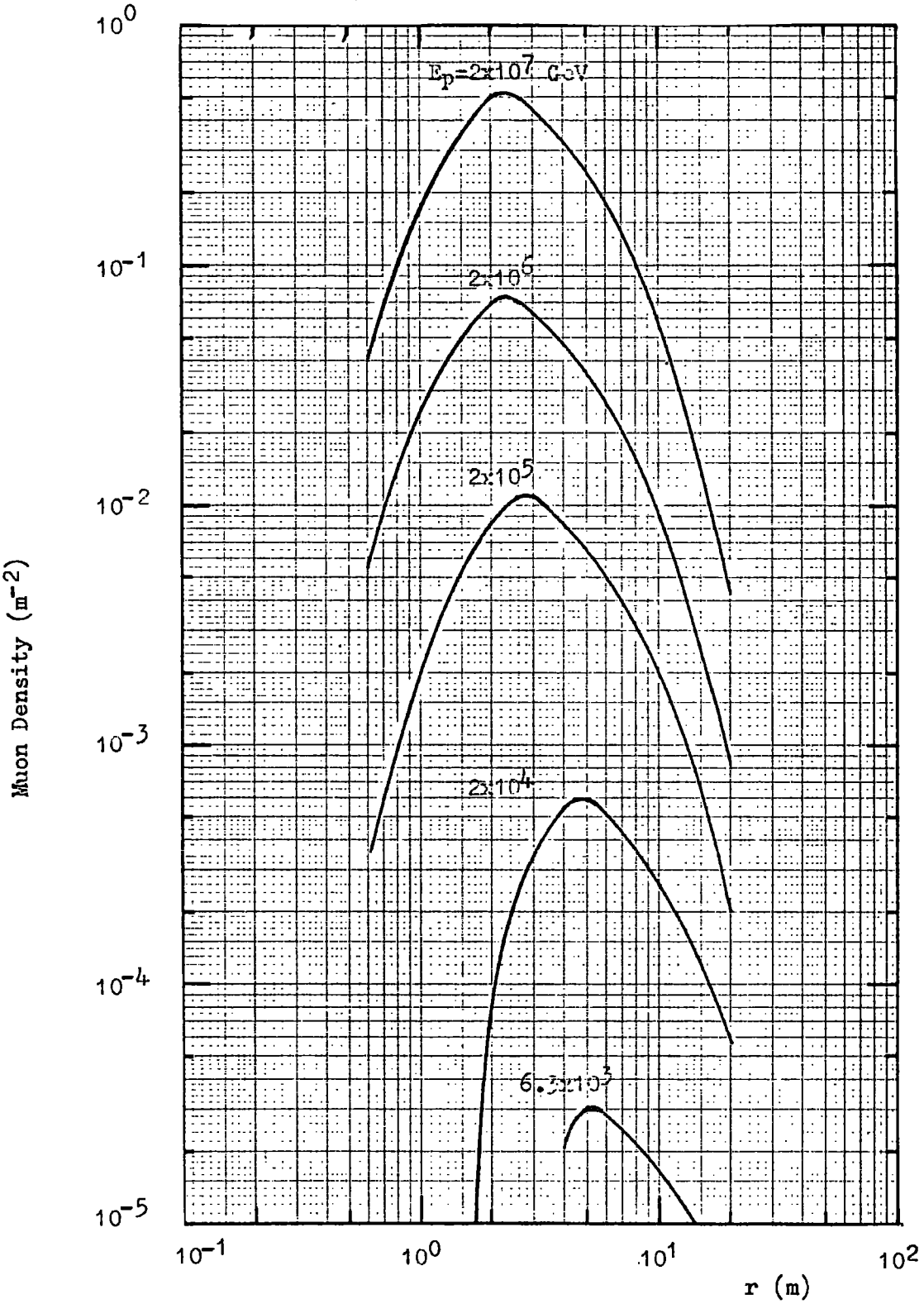

Fig. 4.9. Muon lateral distributions for E_μ>1000 GeV, θ=60°, π's only, $\langle p_t \rangle$=0.4 GeV/c, "$E^{1/4}$ model", and no π's with a value of p_t<0.1 GeV/c.

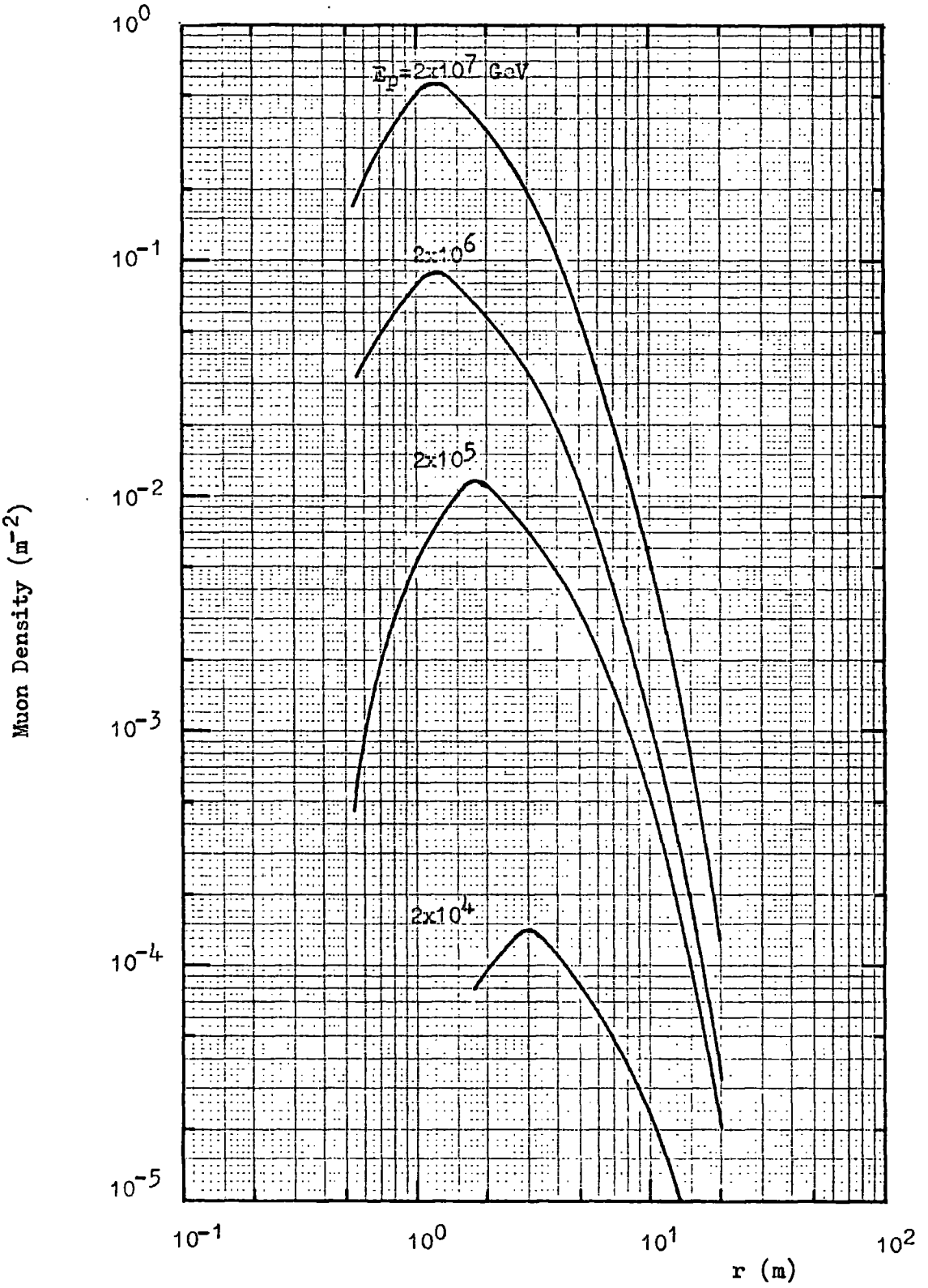

Fig 4.10. Muon lateral distributions for $E_\mu > 2000$ GeV, $\theta = 60^\circ$, π's only, $\langle p_t \rangle = 0.4$ GeV/c, "$E^{1/4}$ model", and no π's with a value of $p_t < 0.1$ GeV/c.

where $\langle p_t \rangle = 2\ p_o = 0.4$ GeV/c.

The results are shown in figures 4.9 and 4.10 for threshold energies of 1000 and 2000 GeV respectively using the "$E^{\frac{1}{4}}$ model" at a zenith angle of 60^o.

It is seen that at distances near to the axis the lateral distributions are changed significantly, the density in this case falling very rapidly. However, as will be seen later, the effect is much reduced for a large detector.

4.9. The Effect of the Detector Area on the Lateral Distributions for Proton Primaries.

The above results are ultimately intended to be used to make predictions which can be compared with the experimental results of Porter and Stenerson (1969) obtained with the Utah detector.

These workers give their results in the form of empirical density spectra. In using the density spectra to obtain rates of events one assumes that the density across the detector is uniform. However, the area of the Utah detector is effectively $2 \times 10\ m^2$ (Stenerson, private communication) which is not negligible compared to the area of the showers detected. Therefore calculations have been made to allow for the effects of this area in order to obtain "effective" lateral distributions, which can be used to calculate density spectra appropriate to the Utah detector area.

Using the lateral distributions already calculated, the average number of muons falling on the detector area from one shower is obtained as a function of the distance of the axis of the shower from the centre of the array. Dividing this average muon number by the area of the array then gives the lateral distribution of the shower

if it is assumed that the density does not vary across the detector area. These lateral distributions can then be used to calculate "effective" density spectra for an area of 20 m^2.

The mean number of muons falling on the detector as a function of the distance (r) of the shower axis from the centre of the detector is obtained by considering the shower axis to fall at different positions on the circumference of a circle of radius r, whose centre is the centre of the detector. For each of these points the lateral distribution is numerically integrated over the area of the detector and hence the number of muons falling on the detector for each point is obtained. The muon numbers so obtained are then averaged appropriately.

The resultant distributions are shown in figures 4.11 and 4.12 for the "$E^{-\frac{1}{4}}$ model" and two muon threshold energies. It is seen that the main effect of the large detector area is to lower the lateral distribution near to the axis of the shower the effect being greater for the showers of smaller radius because the relative area of detector to that of the shower is greater.

The same procedure has been applied to the lateral distributions where a p_t cut-off has been assumed for p_t less than 0.1 GeV/c. The results are shown in figures 4.13 and 4.14 for the "$E^{-\frac{1}{4}}$ model" with threshold energies of 10^3 and 2.10^3 GeV respectively. It is seen that the effect is to bring the lateral distributions into better agreement with those obtained with no transverse momentum cut-off, although the densities at small radial distances are a little lower. Thus the effect of the p_t cut-off on the density spectra will be to lower them slightly at the larger densities although the effect should be small.

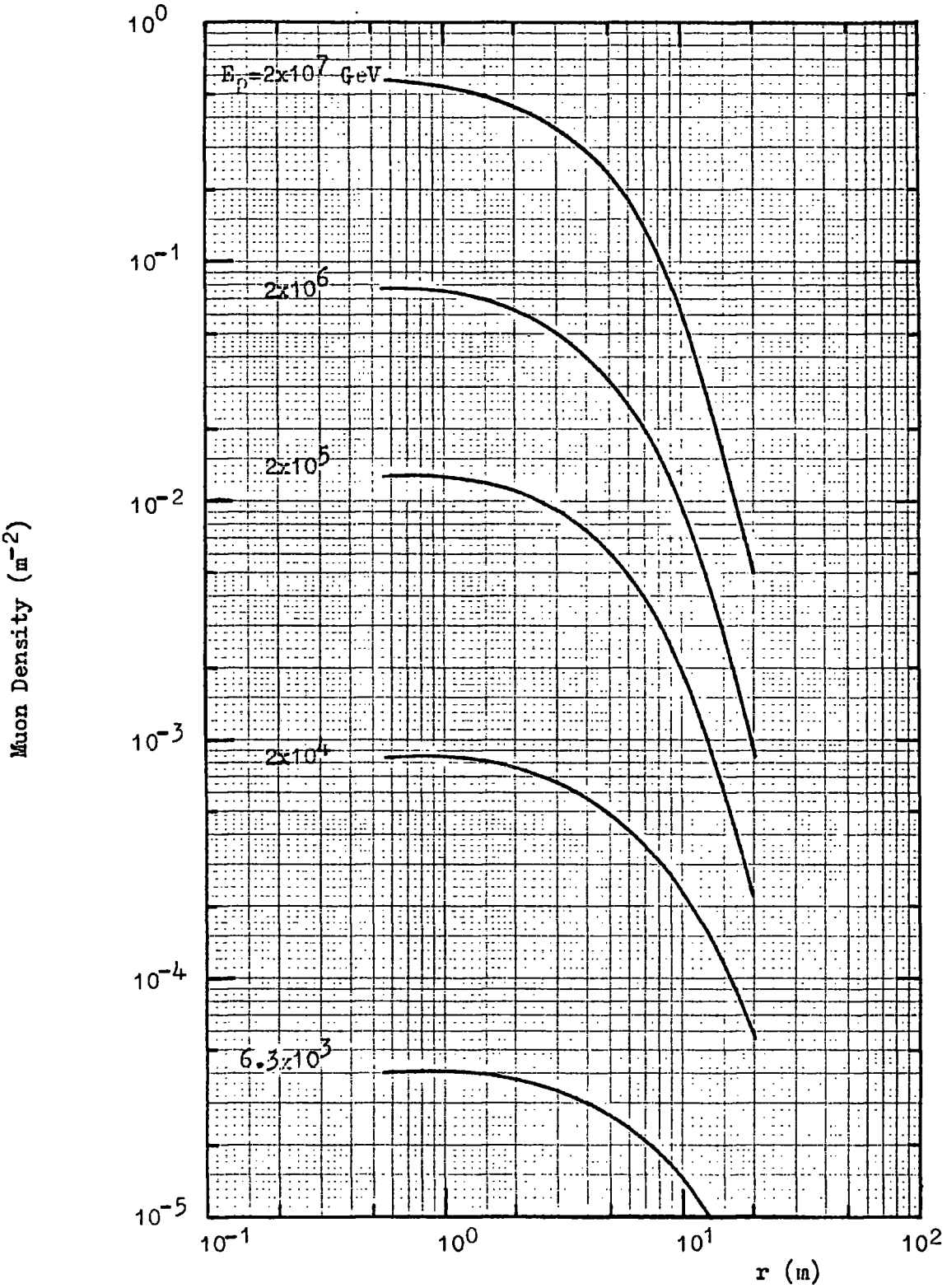

Fig. 4.11. "Effective" muon lateral distributions for a detector area of 20 m^2. E_μ>1000 GeV, θ=60°, π's only, $\langle p_t \rangle$=0.4 GeV/c, "E $^{1/4}$ model".

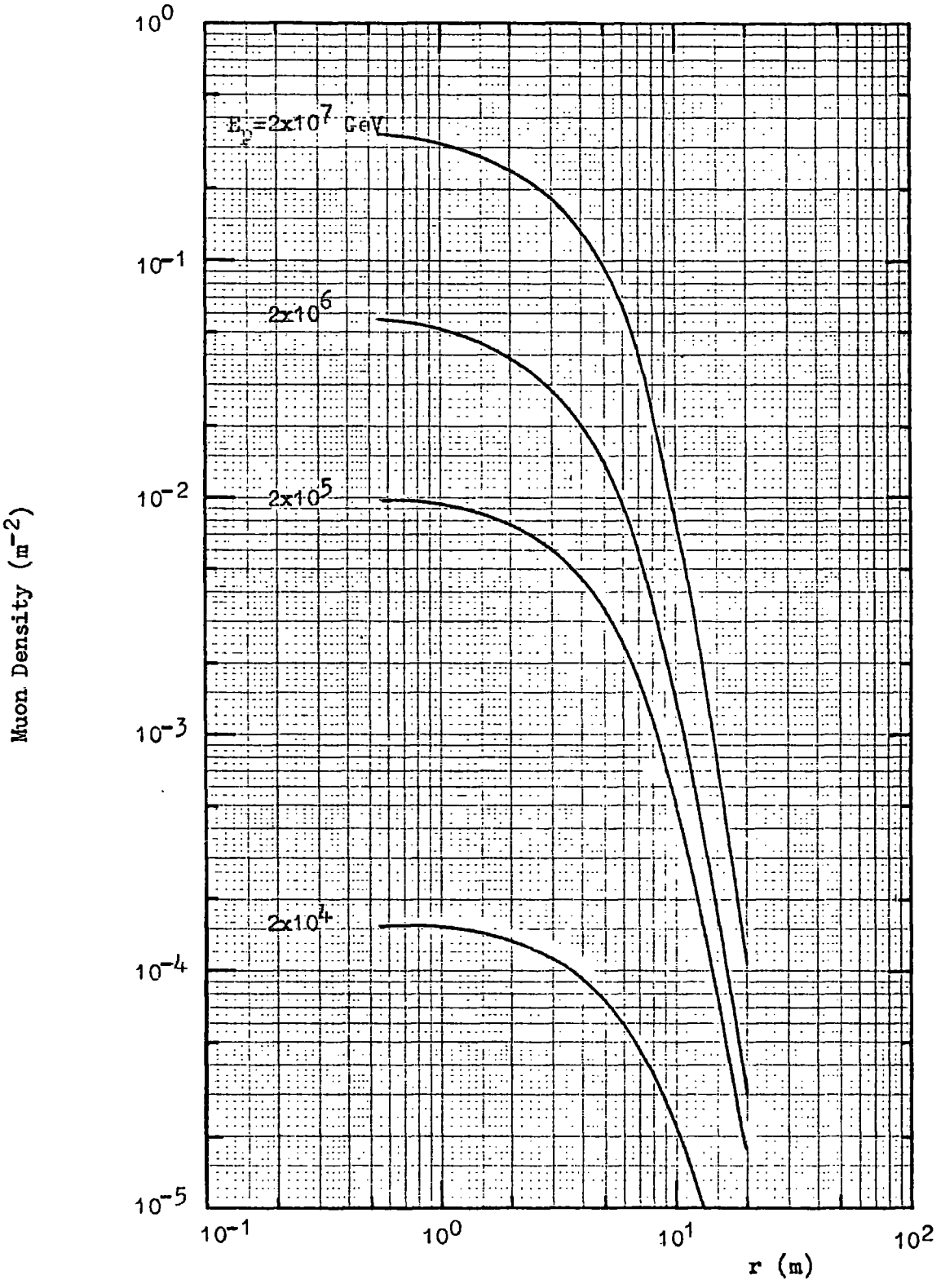

Fig. 4.12. "Effective" muon lateral distributions for a detector area of 20 m^2. $E_\mu > 2000$ GeV, $\theta = 60^\circ$, π's only, $\langle p_t \rangle = 0.4$ GeV/c, "$E^{1/4}$ model".

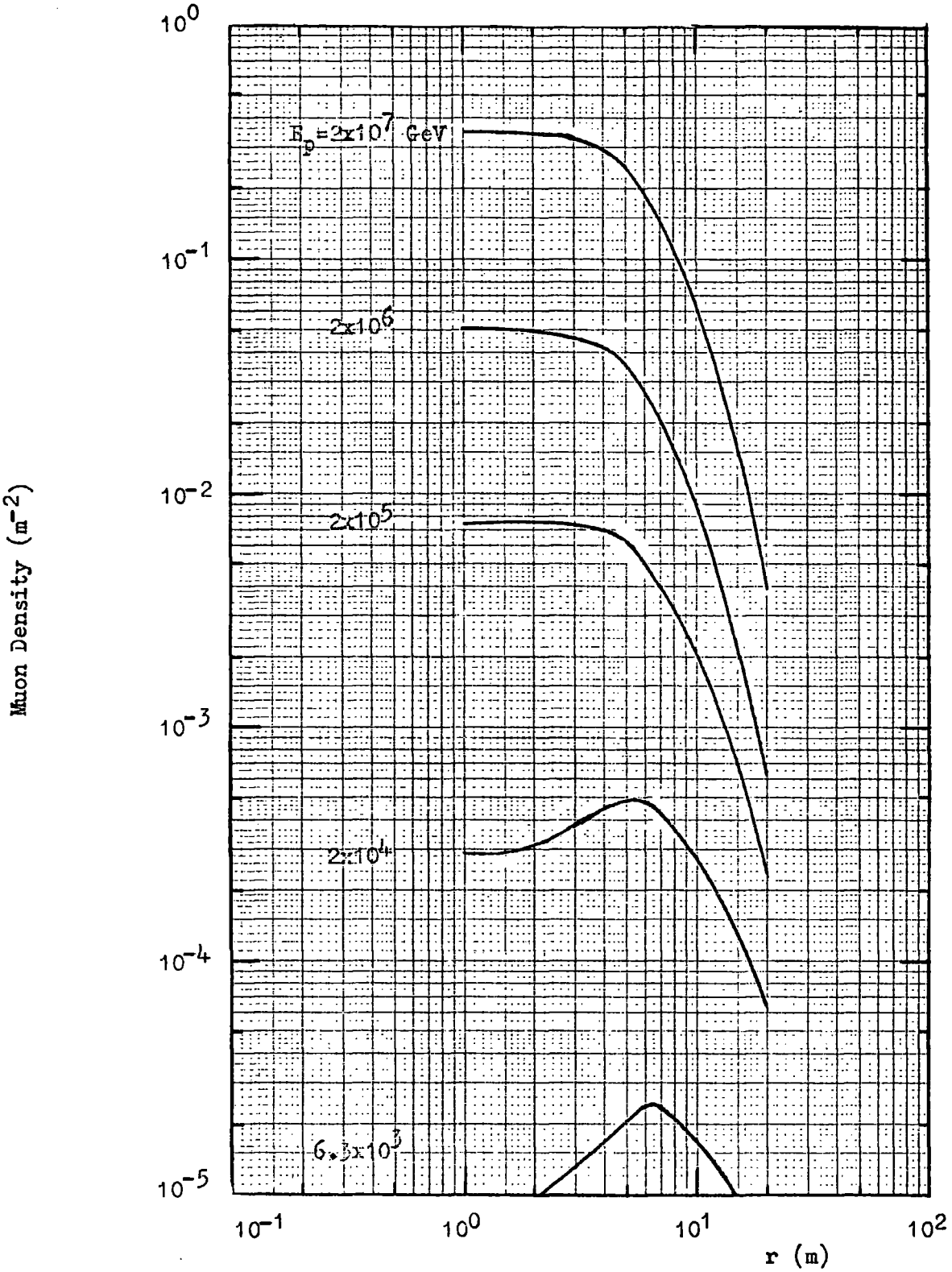

Fig. 4.13. "Effective" muon lateral distributions for a detector area of 20 m^2. $E_\mu > 1000$ GeV, $\theta = 60^\circ$, π's only, $\langle p_t \rangle = 0.4$ GeV/c, "$E^{1/4}$ model, and no π's with a value of $p_t < 0.1$ GeV/c.

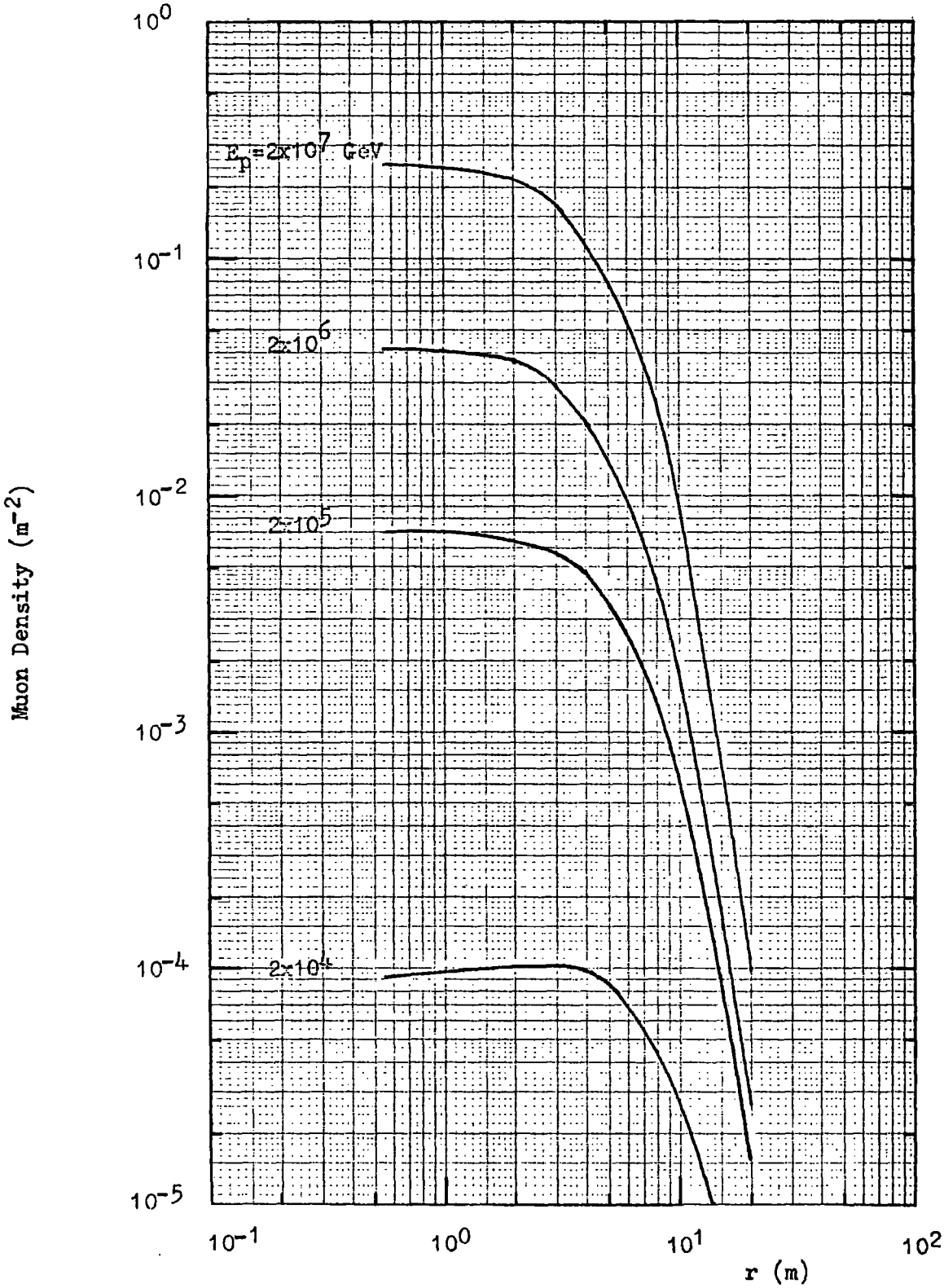

Fig. 4.14. "Effective" muon lateral distributions for a detector area of 20 m^2. $E_\mu > 2000$ GeV, $\theta = 60^\circ$, π's only, $\langle p_t \rangle = 0.4$ GeV/c, "$E^{-1/4}$ model", and no π's with a value of $p_t < 0.1$ GeV/c.

Qualitatively it can be seen that the effect of having a large detector area is to decrease the density spectra at large densities compared to what would be obtained for a small area, since these densities come mainly from high energy showers near to the detector.

4.10 The Primary Spectra Adopted.

In order to predict density spectra and single muon energy spectra it is necessary to adopt a primary spectrum. Since one of the aims of the present work is to determine the mass composition in the energy region above 10^{15}eV, two spectra have been chosen, namely those given by De Beer et al. (1969) for the "$E^{\frac{1}{4}}$ model". The reason for this is that they were calculated from E.A.S. data using a model similar to the one used in the present work.

Below 10^{15}eV both spectra are identical and when expressed in terms of energy per nucleon the spectra are given by

$$j(E_p) = 8.4\ 10^3\ E_p^{-2.6}\ \ m^{-2}sec^{-1}st^{-1}\ GeV^{-1} \qquad 4.17$$

for E_p less than 10^{15}eV.

The composition in this region is based on that given by Ginzburg and Syrovatskii (1964) from a survey of direct measurements of the primary composition at low primary energies. Above primary energies of 10^{15}eV two compositions have been assumed:-

i) Protons only. This spectrum is shown in figure 4.15 and is denoted by A. This is termed "Spectrum A".

ii) A modulated spectrum with each mass component having a differential exponent of -3.1 above a constant rigidity. For protons this rigidity corresponds to a primary energy of $1.5\ 10^{15}$eV. This spectrum is shown in figure 4.15 and is denoted by B. This is

Figure 4.15. Comparison of Spectrum A and Spectrum B with the composite one of Malholtra et al. (1966a).

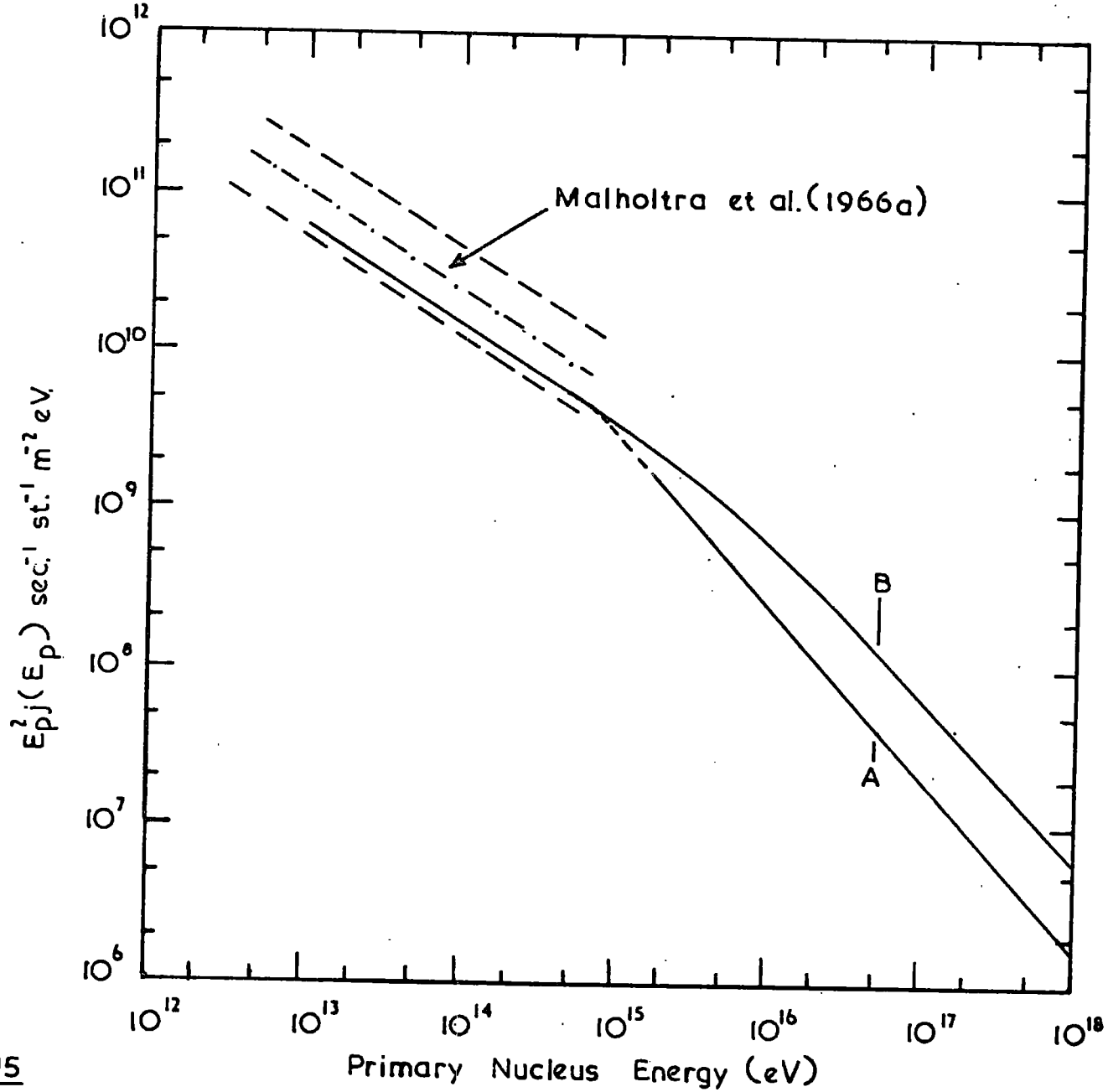
Malholtra et al.(1966a)
B
A
$E_{pj}^2(\epsilon_p)$ sec.$^{-1}$ st.$^{-1}$ m^{-2} eV
Primary Nucleus Energy (eV)
10^{12}
10^{11}
10^{10}
10^{9}
10^{8}
10^{7}
10^{6}
10^{12}
10^{13}
10^{14}
10^{15}
10^{16}
10^{17}
10^{18}

Fig. 4.15

termed "Spectrum B".

Also shown in figure 4.15 is the composite primary spectrum due to Malholtra et al. (1966a) for comparison. Figure 4.16 shows the primary spectra of the individual mass components of the two adopted spectra for the "$E^{\frac{1}{4}}$ model".

When using the "$E^{\frac{1}{2}}$ model" the intensity of the adopted primary spectra must be raised somewhat to preserve agreement with the measured sea-level size spectrum. This is because the more rapid degradation of energy in this model means that a fixed size of shower, measured by an extensive air shower array, corresponds on average to a higher primary energy (De Beer et al., 1966). The primary spectrum of each mass component has been raised by a factor 2.6 at 10^{15} eV to allow for this and made to coincide with the corresponding spectrum for the "$E^{\frac{1}{4}}$ model" below $3\ 10^{12}$eV since the models are identical here.

It is necessary to note that the adopted intensities in the energy region of 10^{10}eV are below those measured directly by about a factor 2. They are similarly below the energy per nucleon spectrum of Brooke et al. (1964), which was based on the sea-level muon and proton spectra using a model similar to that used here. This apparent inconsistency is due to the fact that in the work of Brooke et al. (1964) allowance was made for the difference in the total inelasticity K_t and the fraction of energy passed on to the pion component, K_π, in nucleon-air nucleus collisions. The difference $K_t - K_\pi$ was taken to be 0.12. In De Beer et al. (1969), however, it was assumed that $K_t - K_\pi = 0$, thus accounting for the difference in the primary spectra of the two groups.

In fact there is experimental evidence that secondary particles

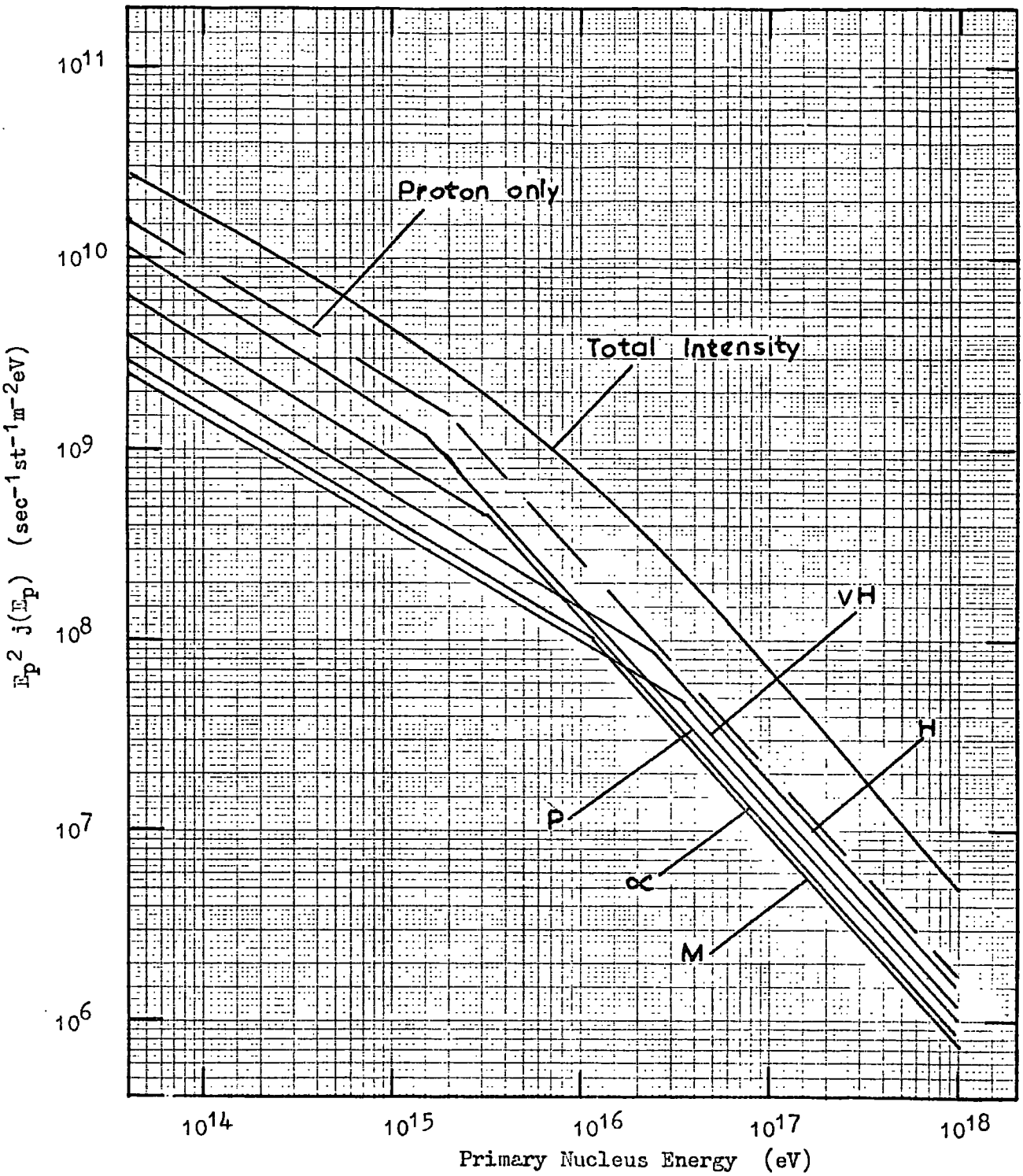

Fig. 4.16. The form of the primary flux for the adopted primary spectra.

other than pions are formed. These include K-mesons, nucleon-antinucleon pairs and hyperons.

In the work of Brooke et al. the kaons did not contribute greatly to the low energy muon flux (at primary energies below $\sim 10^{12}$eV) and the nucleon-antinucleon pairs should not contribute at all. Thus the assumption made by these authors that only pions were responsible for the low energy muon flux and their neglect of the energy resulting from the difference in K_t and K_π seems reasonable.

The assumption made by De Beer et al. (1969) that all the energy released in high energy interactions goes into the pion component is less well justified and it may be that the spectra estimated by them are somewhat underestimated. However, the higher fraction of the energy released in high energy interactions going into the pion component will increase the number of muons formed and thus tend to compensate for the lower intensity of the primary spectrum in their case.

4.11. Sea-Level Muon Energy Spectrum.

The integral sea-level muon energy spectrum is obtained by evaluating the integral

$$\int_{E_{min}}^{\infty} j(E_p) \cdot \exp\left(-\bar{N}_\mu(E_p)\right) \left\{ \bar{N}_\mu(E_p) + \frac{2\bar{N}_\mu(E_p)^2}{2!} + \frac{3\bar{N}_\mu(E_p)^3}{3!} \cdots \right\} dE_p \qquad 4.18.$$

for each threshold energy, where $\bar{N}_\mu(E_p)$ is the average number of muons above the threshold energy due to a primary of energy E_p, $j(E_p)$ is the primary differential energy spectrum expressed in terms of energy/nucleon, and E_{min} is the primary energy below which no muons with energy above the given threshold energy are produced.

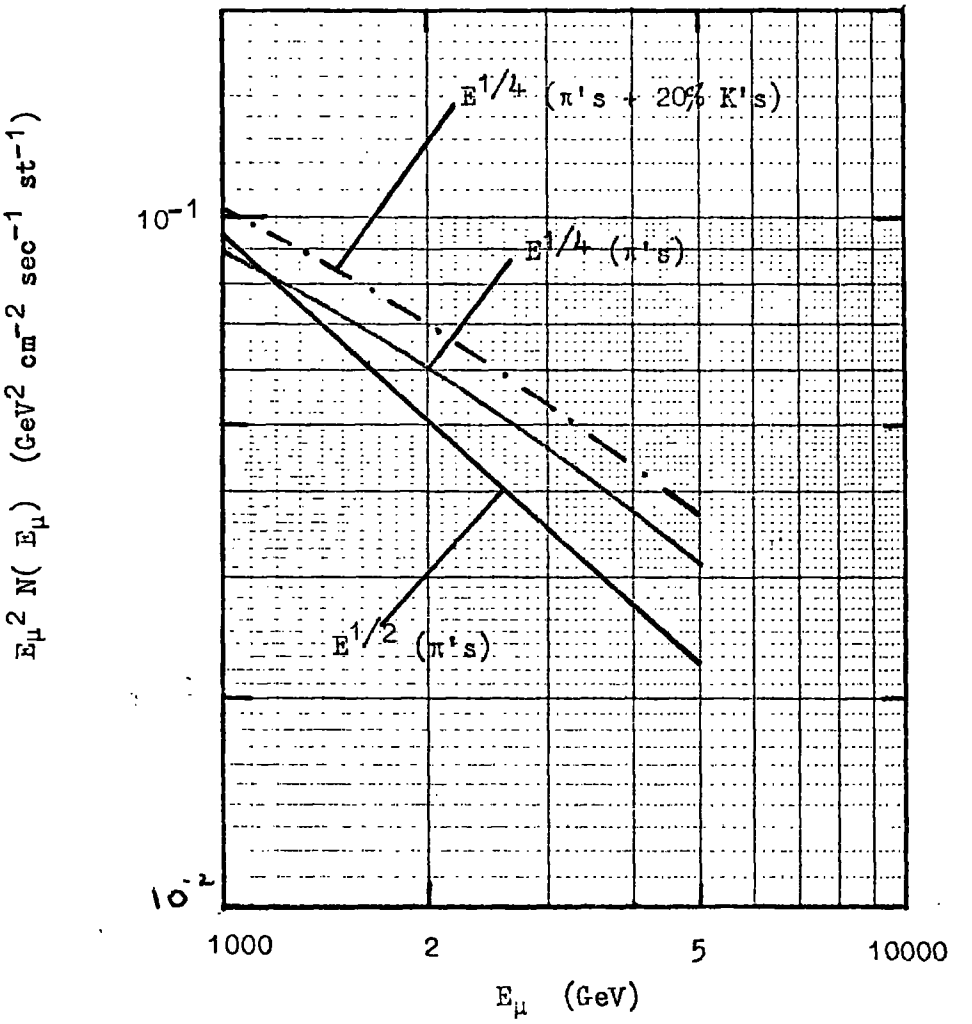

Fig. 4.17. Single muon spectra for $\theta=60^\circ$.

Equation 4.18 reduces to

$$\int_{E_{min}}^{\infty} j(E_p)\ \bar{N}_\mu(E_p)\ dE_p \qquad 4.19$$

i.e. one simply folds in the primary spectrum with the curves of $\bar{N}_\mu$ as a function of E_p given in figure 4.4. This is approximately equal to the single muon energy spectrum.

The resultant spectra are shown in figure 4.17 for the "$E^{-\frac{1}{4}}$" and "$E^{-\frac{1}{2}}$" models for a zenith angle of 60^0. Also shown is the "$E^{-\frac{1}{4}}$ model" with 20% kaons over and above the full pion component. In adding these only muons formed via the K_{μ_2} mode were considered since this mode contributes most to the high energy muons produced by kaon decay. This procedure is equivalent to taking a slightly higher primary spectrum which compensates to a certain extent the neglect of the difference between the values of K_t and K_π by De Beer et al. (1969) in deriving their primary spectra.

The "$E^{-\frac{1}{2}}$ model" spectrum is seen to be steeper than that for the "$E^{-\frac{1}{4}}$ model" and kaons are seen to increase the predicted muon number.

4.12. The Density Spectra of High Energy Muons.

The lateral distributions have been folded in with the two primary spectra to give the expected integral density spectra for various threshold energies. The details of the calculations are as follows. Using the relevant lateral distributions the radial distribution, $r(\Delta, E_p)$, has been found as a function of primary energy, E_p, for a variety of values of density Δ.

The integral density spectrum follows immediately as

$$N(>\Delta) = \int_{E_{min}}^{\infty} \pi\ [\, r(\Delta, E_p)\,]^2\ j(E_p)\ dE_p \qquad 4.20$$

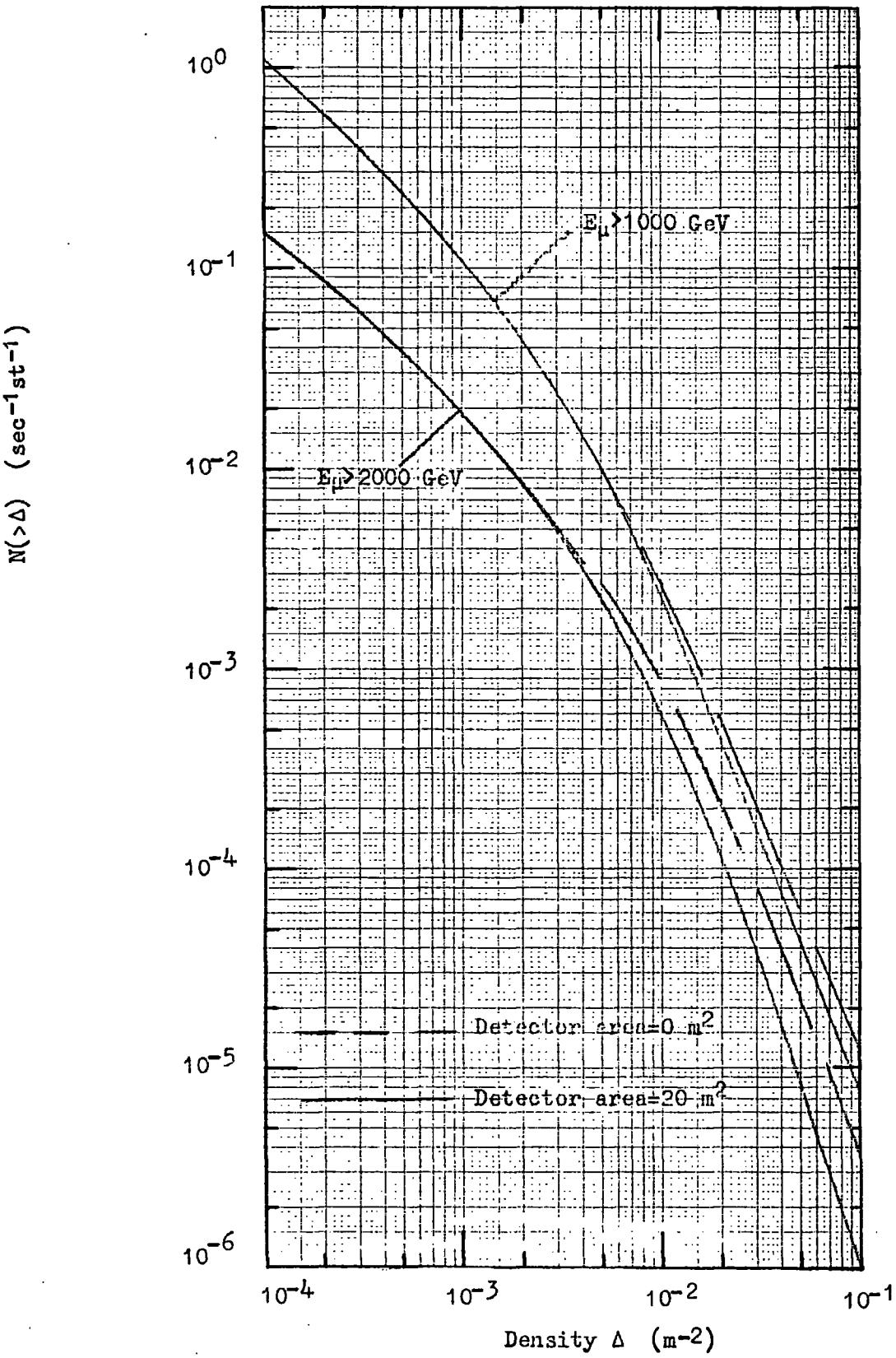

Fig. 4.18. Integral density spectra for Spectrum A, π's only, $\theta=60^{\circ}$, $\langle p_t \rangle=0.4$ GeV/c, "$E^{1/4}$ model".

where E_{min} is the energy below which a primary particle cannot produce a shower having a density Δ at the axis and $j(E_p)$ is the differential primary intensity.

Figure 4.18 shows the density spectra predicted by the "$E^{\frac{1}{4}}$ model" for two threshold energies, 1000 and 2000 GeV, at a zenith angle of 60° using Spectrum A and assuming a mean transverse momentum of 0.4 GeV/c.

The density spectra are indicated both for the case of a point detector and a detector having an area of 20 m^2 normal to the shower axis.

As can be seen the effect in this case of the finite detector area is quite large at high densities, and increases with increasing threshold energy. This is due to muons with a higher threshold energy having narrower lateral distributions and hence a more rapid variation of density across the detector.

The decreasing slope of the curves at the lower densities is a reflection of the rapid fall in the mean muon number with decreasing primary energy, as shown in figure 4.4, at the lower primary energies.

Figure 4.19 shows the density spectra predicted for a detector of area 20 m^2 using the "$E^{\frac{1}{2}}$ model" and the modified version of spectrum A. The fact that the curves are higher at large densities compared to those of the "$E^{\frac{1}{4}}$ model" is due to the greater efficiency of the model for producting high energy muons at higher primary energies, and the increased primary spectrum. These factors off-set the greater width of the showers in this model which would otherwise tend to decrease the density spectra, although the effect of the

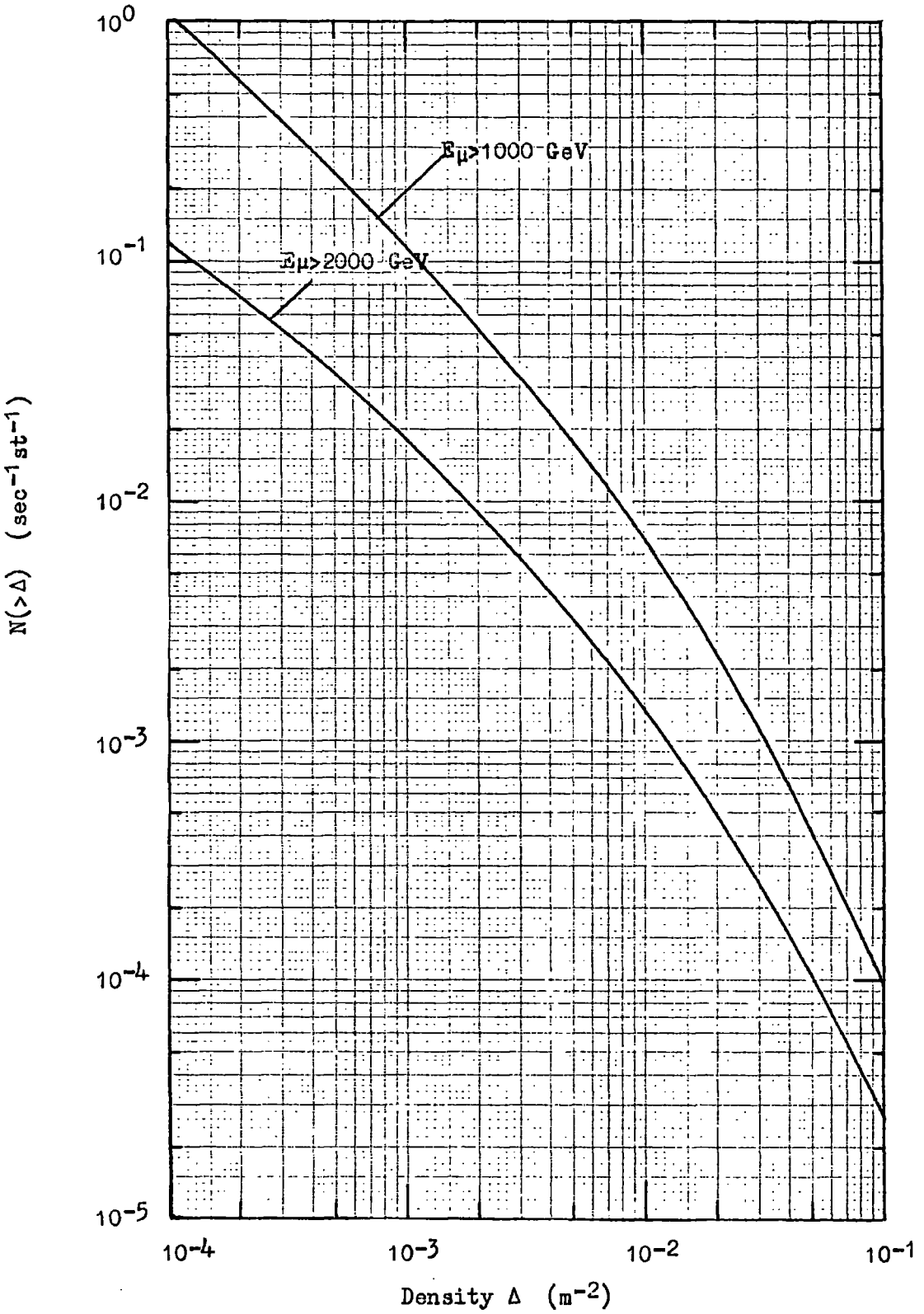

Fig. 4.19. Integral density spectra for Spectrum A, θ=60°,π's only, $\langle p_t \rangle$=0.4 GeV/c, "$E^{1/2}$ model", detector area=20 m^2.

detector area would be expected to compensate for the greater shower width.

Figure 4.20 shows the predicted density spectra for the "$E^{\frac{1}{2}}$ model" with the same basic parameters as used previously but with the modulated primary spectrum folded in i.e. Spectrum B. The curves refer to a detector area of 20 m^2. The curves are similar to the corresponding ones for Spectrum A up to densities $\sim 10^{-2}$ m^{-2} and to be higher after that. The reason for this increase is that at these densities the contribution from heavy primaries is becoming very important because of their greater efficiency of producing muons at the primary energies responsible for producing these densities although, as in the case for the "$E^{\frac{1}{2}}$ model" , see above, the lateral distributions of heavy nuclei for a given primary energy are wider than in the case for proton primaries. The consequences of this latter fact are the same as dsecribed for the "$E^{\frac{1}{2}}$ model". The greater width of the lateral distributions for heavy primaries arises from the fact that in these calculations a shower initiated by a heavy nucleus of mass A and primary energy E_p is considered to be a superposition of A showers of primary energy E_p/A, and the mean radius of a shower increases somewhat with decreasing primary energy.

Figure 4.21 shows the corresponding density spectra for the "$E^{\frac{1}{2}}$ model". They are again seen to be higher than those for the "$E^{\frac{1}{2}}$ model", the reasons being the same as those given for Spectrum A.

4.13. <u>The Calculation of Rates of Events and their Sensitivity to Detector Area</u>.

Although rates can be calculated directly from the differential

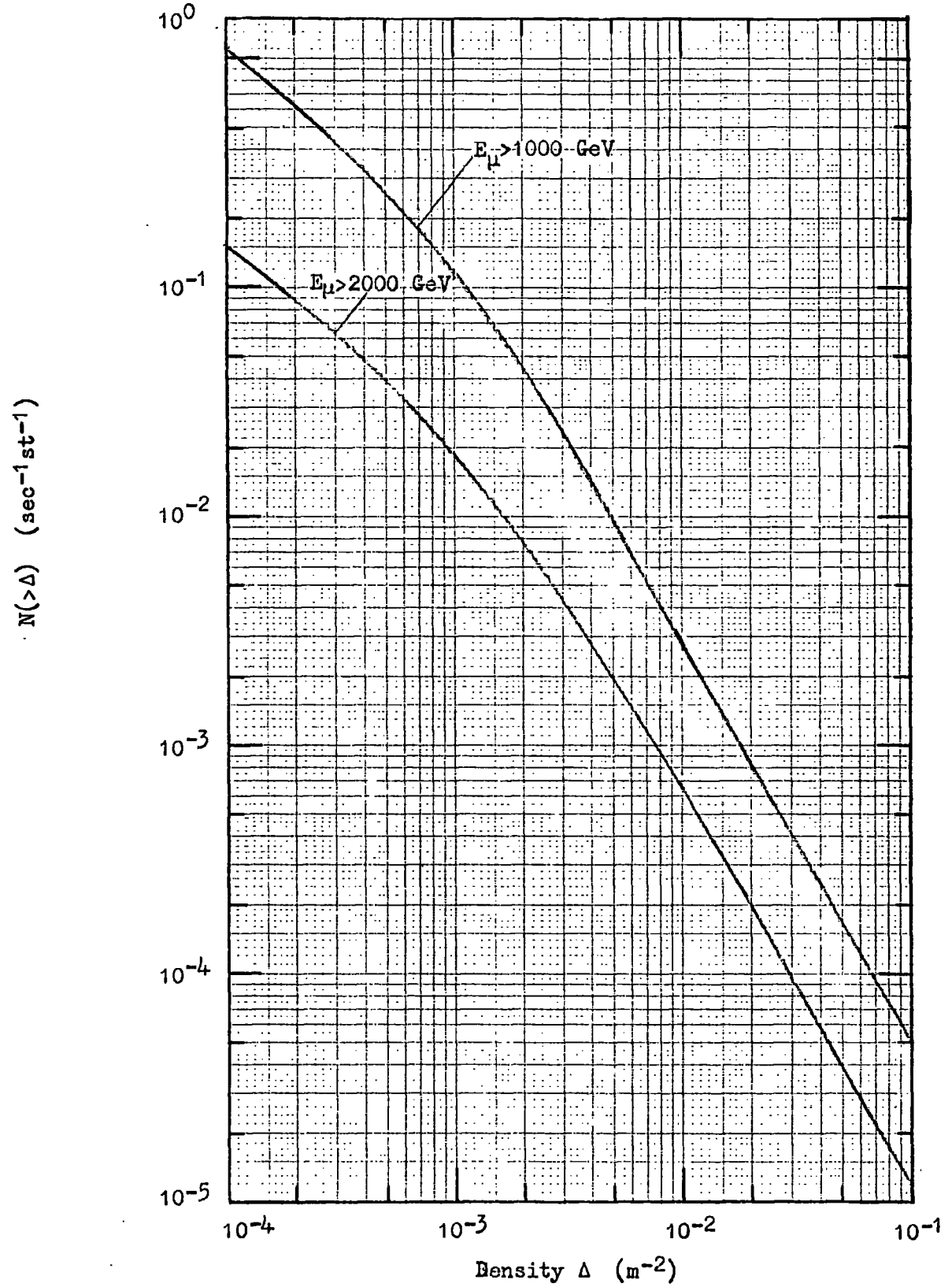

Fig 4.20. Integral density spectra for Spectrum B, $\theta=60^o$, π's only, $\langle p_t \rangle$=0.4 GeV/c, "$E^{1/4}$ model", detector area=20 m^2.

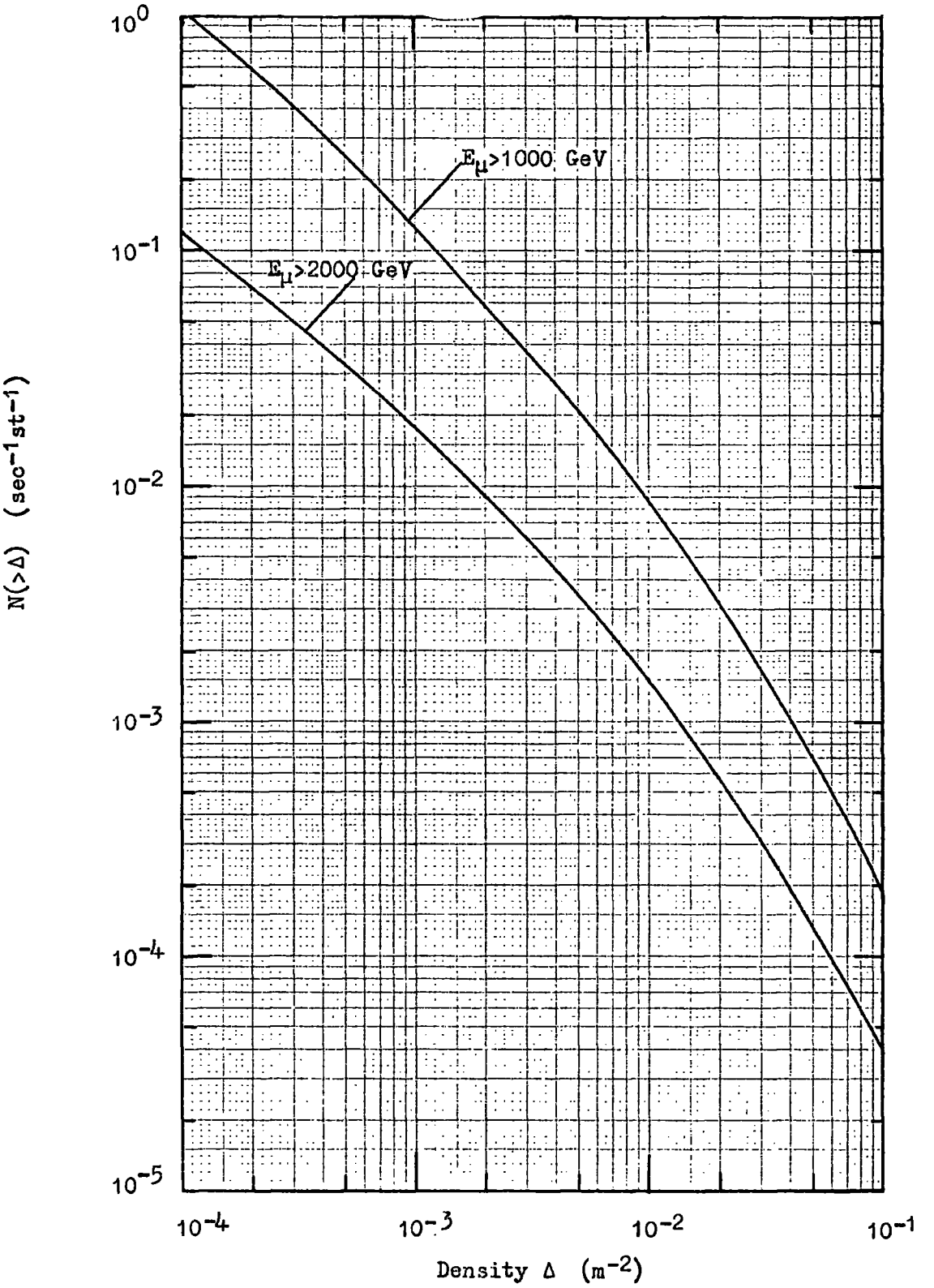

Fig. 4.21. Integral density spectra for Spectrum B, $\theta=60^o$, π's only, $\langle p_t \rangle$=0.4 GeV/c, "$E^{1/2}$ model", detector area=20 m^2.

density spectra, modified for the finite area of the detector, it is also possible, and in some cases more convenient, to calculate the expected rates of events of different multiplicities without the use of density spectra.

The calculations in this work have been specifically designed for comparison with the results of Porter and Stenerson (1969) who give their results in the form of empirically derived density spectra as described in the following chapter. Thus it is useful to predict density spectra since it enables a direct comparison with these results to be made. It is perhaps unreasonable to expect to get exact agreement with the shape of the Utah density spectra because of their semi-empirical nature, but from a direct comparison with the theoretically predicted ones it should be possible to see where the differences lie and which particular model is likely to give the best agreement. In the final analysis, however, it is the comparison of the predicted and observed rates that is important.

The variation of detector area on the predicted rates of events can also be studied. This is important because although the effective area of the Utah detector is quoted as 20 m^2 the area is somewhat sensitive to zenith and azimuthal angle variations and it is important to know if these changes in area will affect the results significantly.

The method of calculating the rates is as follows:- if $X(r)$ is the average number of muons falling on the detector from a shower of primary energy E_p whose axis is a distance r from the centre of the detector the probability, $P_n(r)$, of detecting n muons is given by the Poissonian probability $X(r)^n \exp - (X(r)) / n !$.

The total rate of detecting n particles from showers of primary energy E_p is then given by

$$R_n(E_p) = 2\pi \int_0^\infty r\, P_n(r)\, dr \quad j(E_p) \qquad 4.21$$

where $j(E_p)$ is the differential primary energy spectrum.

The total frequency of detecting n particles is then given by

$$R_n = \int_{E_{min}}^\infty R_n(E_p)\, dE_p \qquad 4.22$$

Figures 4.22 and 4.23 show the functions $P_2(r)$ and $P_3(r)$ respectively as a function of r and E_p for the "$E^{-\frac{1}{2}}$ model" assuming a detector area of 20 m^2, a threshold energy of 1000 GeV, a zenith angle of 60° and proton primaries. From these curves it can be seen that doubles tend to come from showers falling further away from the detector than is the case for triples and that the contributions from showers falling further than 20 metres from the detector are very small for these multiplicities.

For higher threshold energies the relevant distances will be even less due to the showers being less wide. The shape of the curves for a primary energy of $2\ 10^7$GeV is due to the fact that if the axis of such a shower falls on or near the detector, the average number of muons falling on the detector is so great that the probability of detecting 2 or even 3 muons is very small for this threshold energy.

Calculations have been made to investigate the effect of changing the detector area. These calculations have been made assuming a primary composition consisting of protons alone, the spectrum being represented by

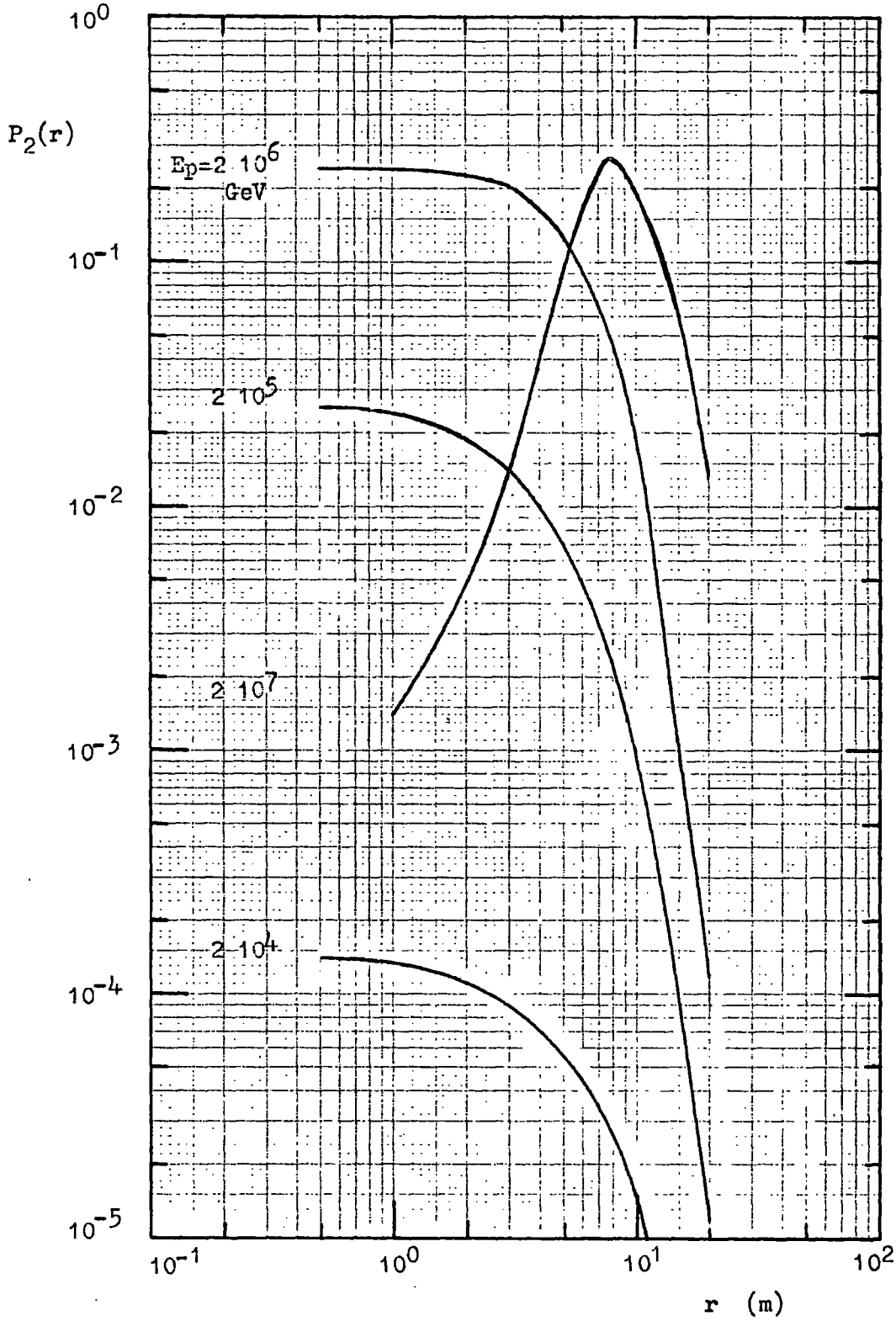

Fig. 4.22. The function $P_2(r)$ versus r for a detector of area 20 m^2 and various primary nucleon energies (see text for explanation). $\theta=60^o$, $\langle p_t \rangle$=0.4 GeV/c, π's only, "$E^{1/4}$ model", E_μ>1000 GeV.

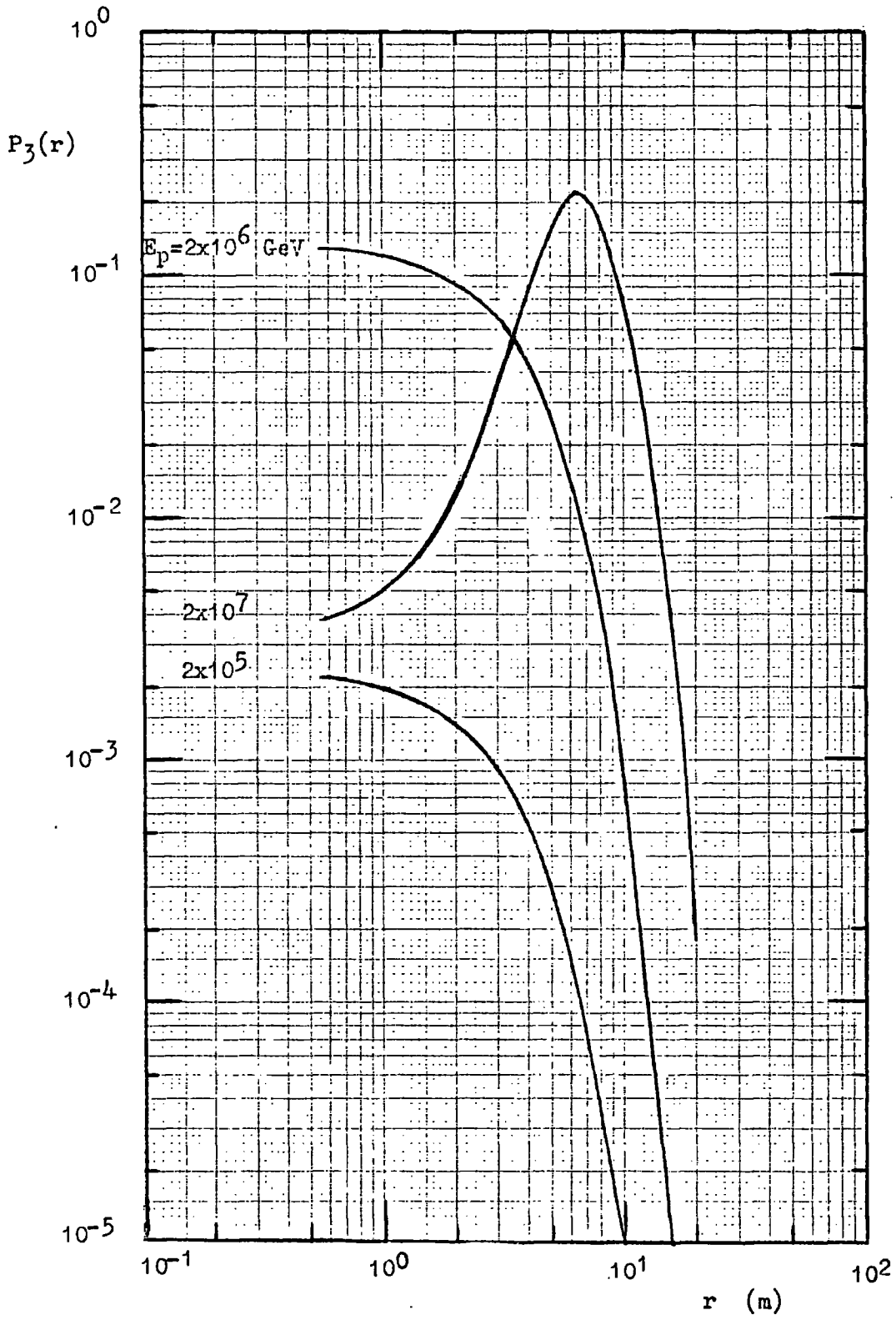

Fig. 4.23. The function $P_3(r)$ versus r for a detector of area 20 m^2 and various primary nucleon energies (see text for explanation). $\theta=60$, $\langle p_t \rangle=0.4$ GeV/c, π's only, "$E^{1/4}$ model", $E_\mu>1000$ GeV.

$$j(E_p) = 0.9E_p^{-2.6} \text{ cm}^2\text{sec}^{-1}\text{st}^{-1}\text{GeV}^{-1} \text{ for } E_p < 2\ 10^6 \text{ GeV}$$

$$j(E_p) = 1.3\ 10^3\ E_p^{-3.1} \text{ cm}^2\text{sec}^{-1}\text{st}^{-1}\text{GeV}^{-1} \text{ for } E_p > 2 10^6 \text{GeV} \qquad 4.23.$$

This spectrum is consistent with the sea-level size spectrum if the "$E^{-\frac{1}{2}}$ model" is used. It will be denoted by "Spectrum C".

The results of the calculations for "doubles" are shown in figure 4.24, using the "$E^{-\frac{1}{2}}$ model", where the ratio of the frequency of doubles to the square of the detector area S, all divided by the equivalent factor for a point detector, K^1, is plotted as a function of S for a threshold energy of 1000 GeV and a zenith angle of 60^0.

The curve can be understood as follows. For small areas the density across the detector will be almost constant and so equation 4.21 becomes

$$R_2(E_p) \simeq S^2 \quad \frac{2\pi}{2!} \int_0^\infty r\ [\ \Delta\ (r, E_p)\ ]^2\ dr\ \ j(E_p) \qquad 4.24.$$

since $S\,\Delta\ (r, E_p) \simeq 0$; where $\Delta(r, E_p)$ is the density at a distance r from the axis due to a shower of primary energy E_p. Therefore $R_2 \propto S^2$.

For very large areas, when the whole of the shower is contained in the detector area, equation 4.21 can be written as

$$R_2(E_p) \simeq S.\ \frac{\bar{N}_\mu (E_p)^2}{2!} \quad \exp\ (-\ \bar{N}_\mu\ (E_p))\ j\ (E_p) \qquad 4.25.$$

where $\bar{N}_\mu\ (E_p)$ is the mean number of muons in a shower of primary energy E_p. Therefore $R_2 \propto S$.

It can be seen that at areas of about 20 m^2 the rates of doubles is fairly insensitive to small changes in area.

Figure 4.25 shows the rate of triples through an area S divided

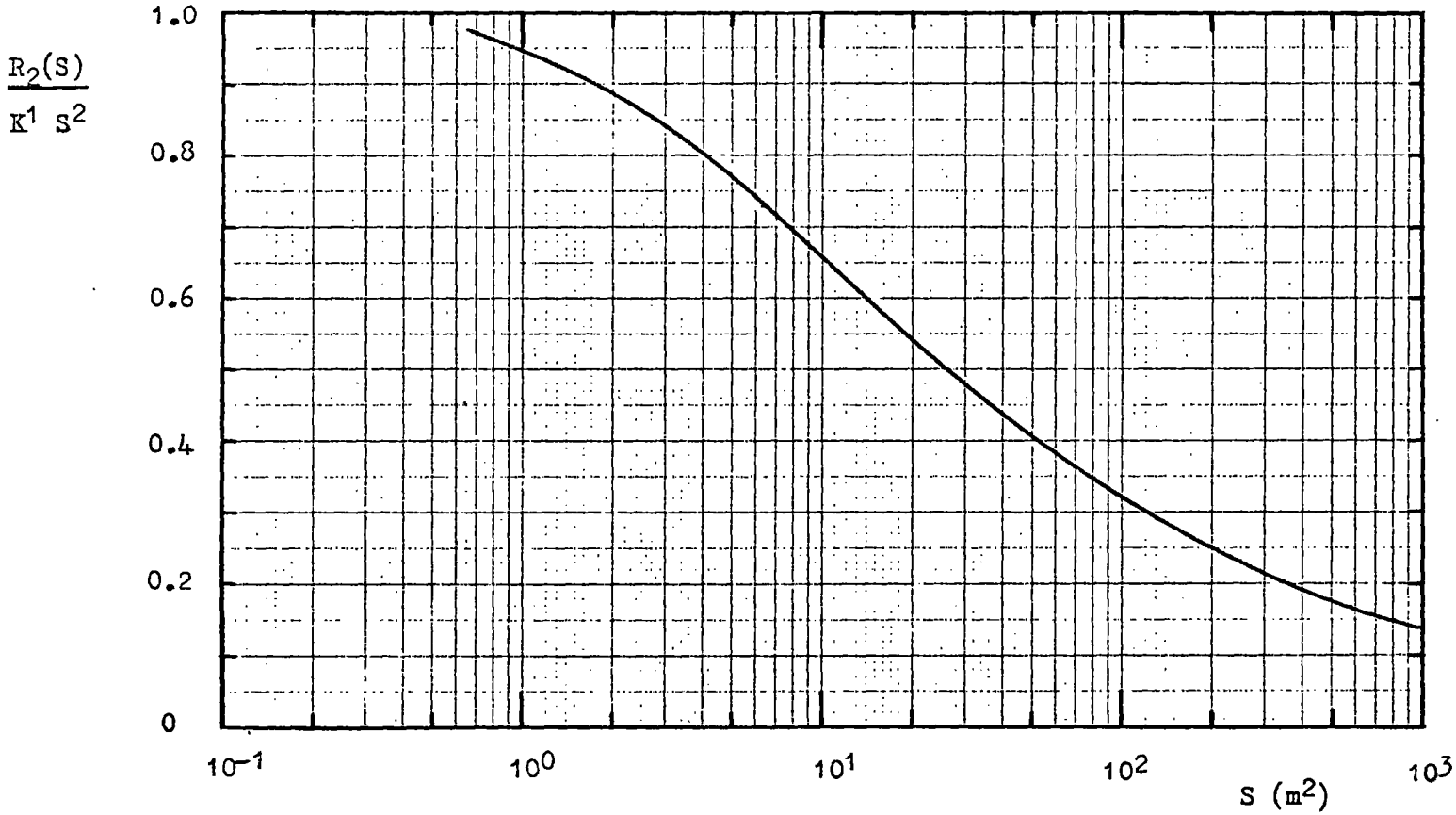

Fig. 4.24 Variation of the rate of detection of "doubles" with detector area. E_μ>1000 GeV, $\theta=60^o$, primary protons, $\langle p_t \rangle$ = 0.4 GeV/c, "$E^{1/4}$ model".

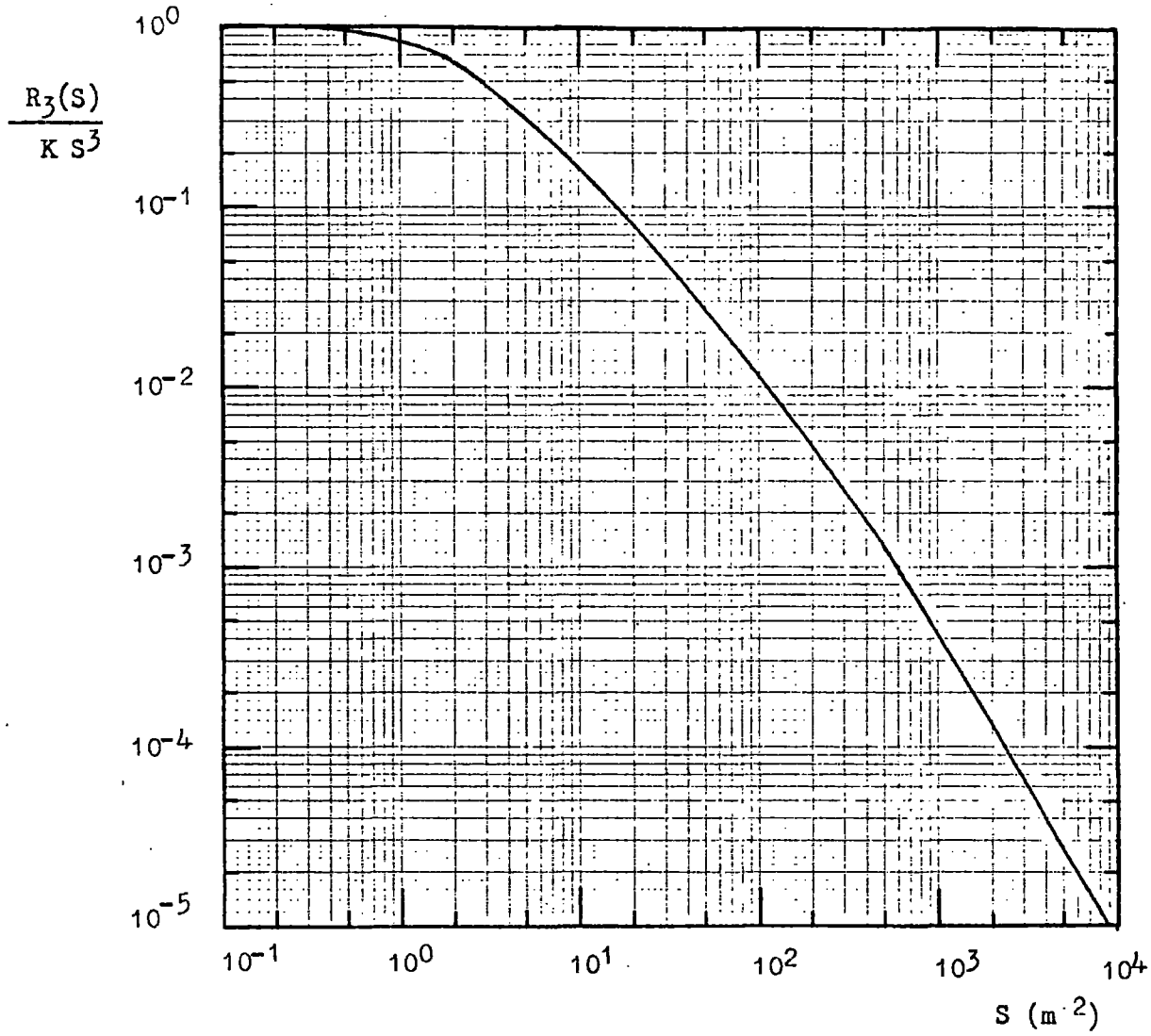

Fig. 4.25. Variation of the rate of detection of "triples" with detector area. E_μ>1000 GeV, θ=60°, primary protons, $\langle p_t \rangle$=0.4 GeV/c, "$E^{1/4}$ model".

by S^3, all divided by the equivalent factor for a point detector, K, plotted as a function of S for a threshold energy of 1000 GeV and a zenith angle of 60^o. It is seen that the rate of triples is more sensitive to the detector area than the rate of doubles. This is reflected in figure 4.18, which shows the predicted density spectra using the primary spectrum containing protons only above a primary energy of 10^{15}eV, for a detector of area 20 m^2 and a point detector. It is seen that the effect of the finite area increases with increasing density. At higher threshold energies and greater detected multiplicities the effect will be larger for the reasons already mentioned.

Predictions of the expected frequencies of detection of different muon multiplicities as a function of muon threshold energy are shown in figure 4.26 for a detector of area 20 m^2, a zenith angle of 60^o and the "$E^{\frac{1}{4}}$ model" folded in with the primary spectrum given by equation 4.23 i.e Spectrum C. Also shown are more approximate predictions using the "$E^{\frac{1}{2}}$ model" and a suitably modified version of Spectrum C.

The "$E^{\frac{1}{2}}$ model" is seen to predict higher frequencies of multiple events. This is partly due to the higher primary spectrum used and partly due to the greater efficiency of the model for producing muons at higher primary energies.

Figure 4.27 shows the approximate median primary energies for producing different detected multiplicities as a function of threshold energy at a zenith angle of 60^o and an area of detection of 20 m^2, for both the "$E^{\frac{1}{4}}$" and "$E^{\frac{1}{2}}$" models. In both cases the primary spectrum assumed was that given by equation 4.23. The

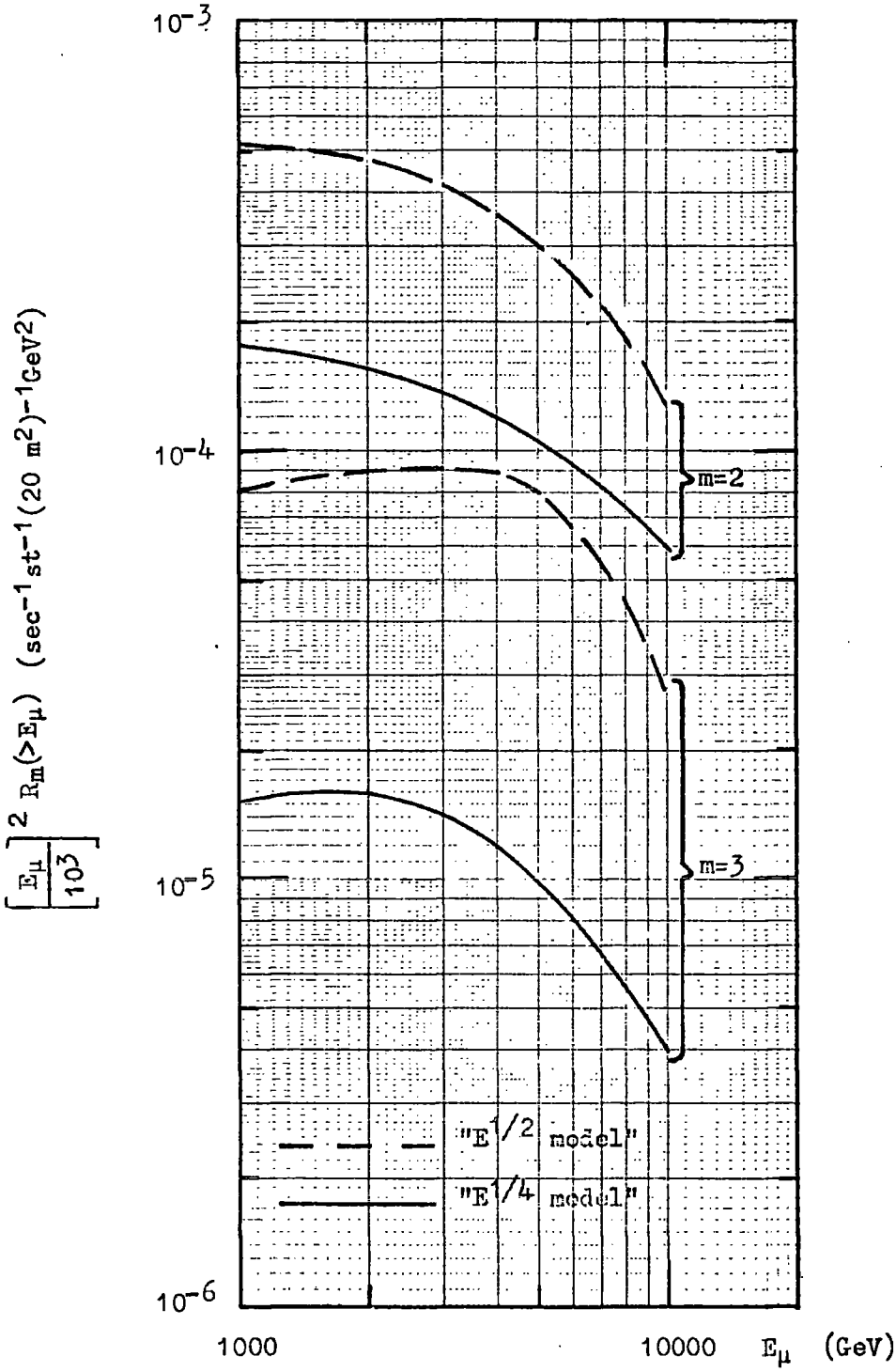

Fig. 4.26. Expected frequency of detecting m muons in 20 m^2 area at 60° as a function of muon threshold energy. Primary protons, $\langle p_t \rangle$ =0.4 GeV/c.

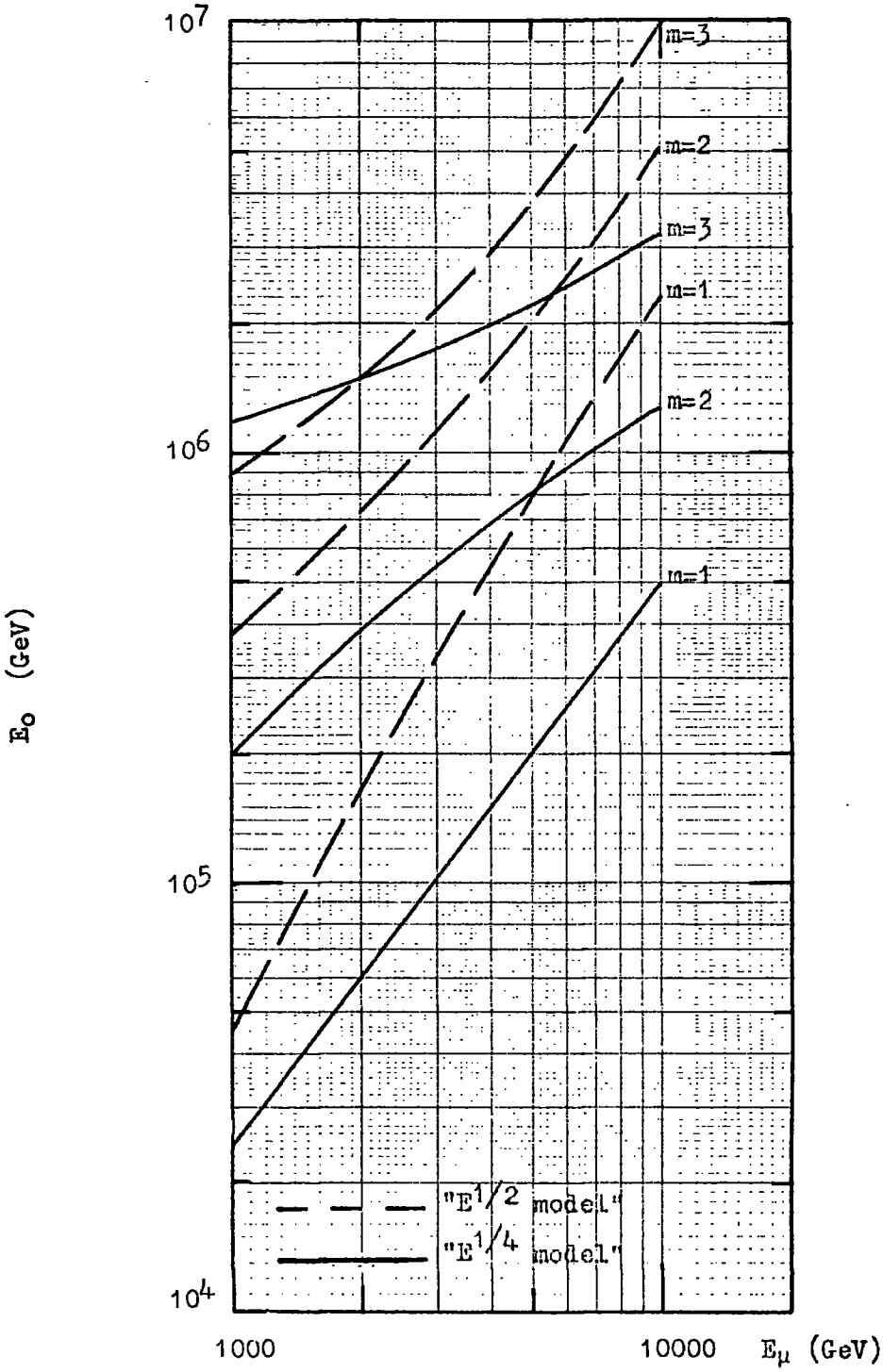

Fig. 4.27. Median primary energy, E_o, as a function of muon threshold energy for various multiplicities, m, of detected muons at 60°. Primary protons, $\langle p_t \rangle$ =0.4 GeV/c.

convergence of the curves above about 10^6 GeV arises from the increased slope of the primary spectrum above this energy and the fact that as the detected multiplicity increases the effect of fluctuations becomes less and the energy spectrum responsible for the multiplicity sharpens up and the means become closer.

The results shown in figures 4.24, 4.25, 4.26 and 4.27 have been obtained using a different method of calculation to that described in section 4.2, but using the same model parameters.

The adopted mean transverse momentum is 0.4 GeV/c in the above calculations.

4.14 The Lateral Distributions of Muons at Large Radial Distances.

The study of the lateral distributions of muons at large distances is important because it gives us information on the form of the p_t-distribution at large transverse momenta and, when combined with the results at smaller distances, on the value of $\langle p_t \rangle$.

Recently Coats et al. (1969) published results showing the measured decoherence curve of high energy muons out to large separations, and in order to compare this with theoretical predictions one must calculate accurate values of the lateral distributions of high energy muons out to large radial distances.

As stated previously the lateral distributions calculated earlier are not accurate out to large distances because of the neglect of the variation of the effective height of interaction with radial distance. At large distances the lateral distributions are very sensitive to the height of interaction and calculations have therefore been made to allow for its variation with radial distance, thus giving lateral

distributions accurate out to large radial distances. The result for the C.K.P. transverse momentum distribution is shown in figure 4.28 for a primary energy of 2.10^5 GeV (the approximate median energy for doubles in the Utah detector) using the "$E^{\frac{1}{2}}$ model", a threshold energy of 1000 GeV and a zenith angle of 45°. On this lateral distribution the median transverse momentum of the detected muon parents, denoted by '$p_{t_{med}}$', is given for various radial distances. These have been calculated from a knowledge of the median height of interaction, h, and the median energy of the parent pions, $E_{\pi_{med}}$, obtained from the muon energy spectra at a given radial distance r, under the assumption that $E_{\pi_{med}} = 1.3\ E_{\mu_{med}}$. Thus one obtains

$$p_{t_{med}} = \frac{r}{h}\ E_{\pi_{med}} \qquad 4.26.$$

It will be noticed that measurements around r = 30 - 40 m, which probably represents the limit beyond which precise experimental data will not be available, are sensitive in the region of 1.0 GeV/c (for the C.K.P. distribution).

In order to investigate the sensitivity to the form of the p_t - distribution calculations have also been made using the relationship suggested by Aly et al. (1964):-

$$N(P_t)\ dp_t = 2\alpha\ p_t \exp(-\alpha\ p_t^2)\ dp_t \qquad 4.27$$

where $\langle p_t \rangle = \alpha^{-\frac{1}{2}}\ \Gamma(1.5)$ GeV/c;

and that of Elbert et al. (1968):-

$$N(p_t)\ dp_t = \frac{1}{1.33 p_c} \left\{\frac{p_t}{p_o}\right\}^{3/2} \exp\left\{-\frac{p_t}{p_o}\right\} \qquad 4.28$$

where $\langle p_t \rangle = 2.5\ p_o$ GeV/c;

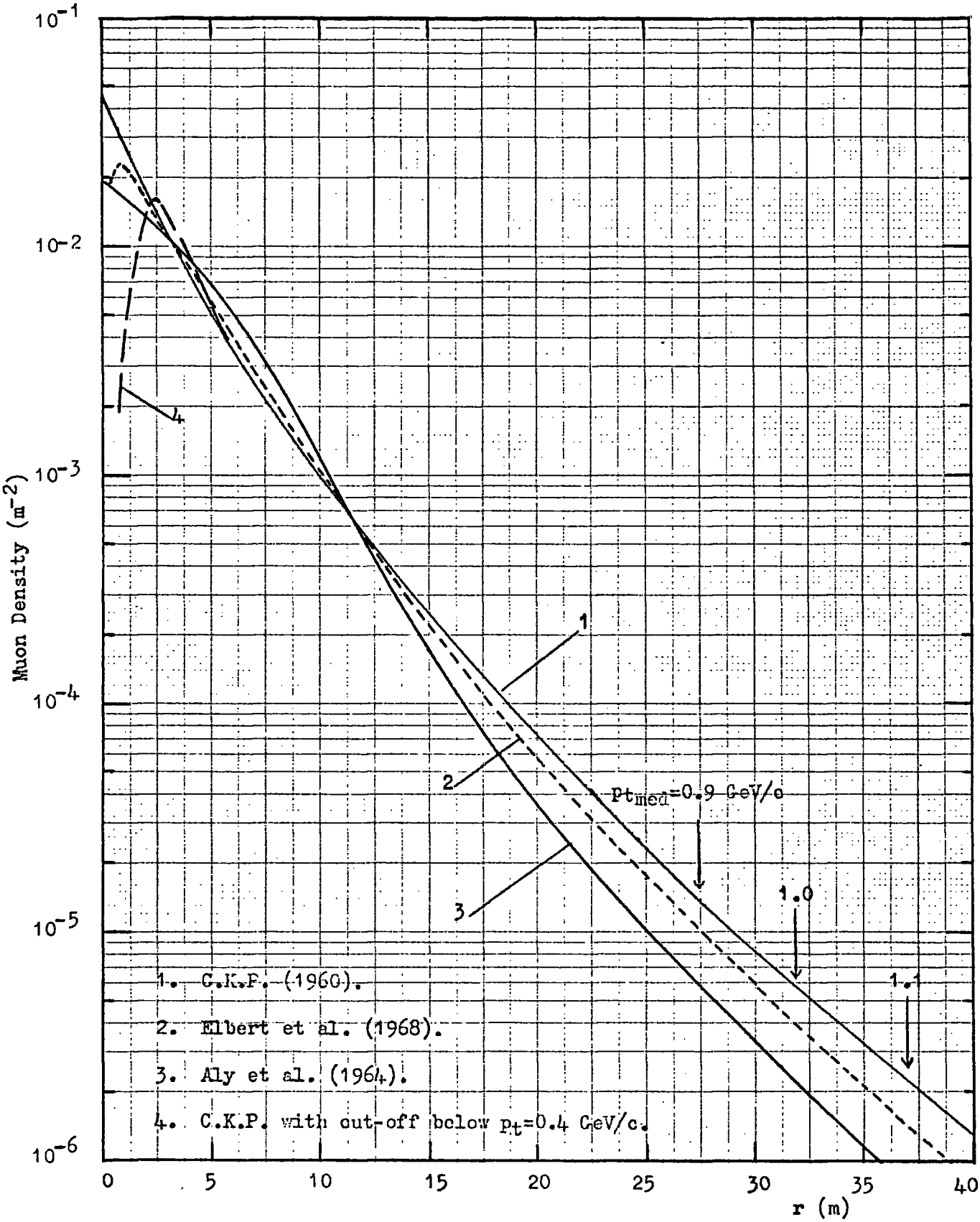

Fig. 4.28. Muon lateral distributions for various transverse momentum distributions. $E_p=2x10^5$ GeV, $\theta=45^o$, $\langle p_t \rangle=0.4$ GeV/c, "$E^{1/4}$ model" and $E_\mu>1000$ GeV.

both for $\langle p_t \rangle$ = 0.4 GeV/c. The results shown in figure 4.28 indicate that there is some sensitivity to the form of the p_t - distribution chosen particularly between the C.K.P. and Aly distributions, the two extreme cases, especially at large radial distances.

The shape of the lateral distribution for the C.K.P. model can be approximately understood from a consideration of the shape expected from a simplified model, where the height of origin of the pions is considered constant. From these assumptions one obtains for the lateral distribution of muons with energy above E/1.3 (see Appendix B)

$$\rho_\mu(r) \propto \frac{1}{h^2 p_o^2 T} \left\{ \frac{E}{\alpha} + \frac{1}{\alpha^2} \right\} \exp(-\alpha E) \qquad 4.29$$

where $\alpha = r/hp_o + 1/T$. 4.30

Here h is the height of formation of the pions, T the mean energy of the pions in the forward cone, $2p_o$ is the mean transverse momentum and r is the radial distance.

At large distances one obtains

$$\rho_\mu(r) \propto \frac{1}{r} \exp\left\{ -\frac{r}{r_o} \right\} \qquad 4.31$$

where $r_o = hp_o/E$. 4.32.

Factors which might affect the curves given so far when applied to the results from the Utah group are:-

i) Multiple Coulomb scattering in the rock.

ii) Geomagnetic deflection of the muons when traversing the atmosphere.

iii) The possibility that the C.K.P. relation overestimates the frequency of p_t - values below about 0.1 GeV/c.

Approximate calculations show that multiple Coulomb scattering contributes a displacement of less than about 3 metres even at large

distances and so should not be important.

Geomagnetic deflection on the other hand can have larger effects, particularly at large radial distances, since the inclined heights of production at these distances are very large and the mean energy of the muons falls with increasing r. Using equation 4.10 with the appropriate values of the parameters it can be shown that for the Utah experiment, for a zenith angle of 45° and radial distance ~40 metres the displacement in the plane of the detector is ~12 metres for muons incident in the vertical plane of the spark counters (see Chapter 5). At smaller radial distances the displacement is less because the effective heights of production are less and the mean muon energies higher. Thus the deflection is ~3 metres at a radial distance of 10 metres and approaches zero near the shower axis. The overall effect is to cause r_0 to increase a little more rapidly than given in figure 4.28.

The effect of cutting-off p_t - values below 0.1 GeV/c has been studied and the result is shown in figure 4.28.

4.15 The Decoherence Curve of High Energy Muons.

Because the detectors used by Coats et al. (1969) were of rather small area, the axes of the showers detected could not be located and so the lateral distributions could not be studied directly. Instead the frequency of events in which two muons cross two separate areas, each of $1m^2$, was studied as a function of the distance apart of the detectors, and this can be compared with theoretical predictions.

Consider two areas of $1m^2$ each, separated by a distance x. Let a shower of primary energy E_p fall on a small area, da, at a distance

r_1 from one detector and r_2 from the other. Then the probability that the two detectors are hit, $F^1(x)$, is given by

$$F^1(x) = [1 - \exp(-\rho_\mu(r_1, E_p))][1 - \exp(-\rho_\mu(r_2, E_p))] \qquad 4.33.$$

where $\rho_\mu(r, E_p)$ represents the density at a distance r. Assuming that the probability of getting more than one particle through a detector is small, equation 4.33 reduces to

$$F^1(x) \simeq \rho_\mu(r_1, E_p)\,\rho_\mu(r_2, E_p) \qquad 4.34.$$

Integrating this over the area of the whole plane containing the detectors, and all primary energies gives the total rate of detecting two particles separated by a distance x, $F(x)$ as

$$F(x) = \iint \rho_\mu(r_1, E_p)\,\rho_\mu(r_2, E_p)\,da\; j(E_p)\,dE_p \qquad 4.35$$

The integral over the area can be solved analytically for certain forms of the lateral distributions e.g. Gaussian and exponential forms, but in the case of the above lateral distributions the integration has been performed numerically.

The lateral distribution for a primary energy of 2.10^5 GeV is taken as the basis of the calculation, since this corresponds to the approximate median energy of detected two's. Thus a decoherence curve is obtained assuming that all lateral distributions have the same shape as that shown in figure 4.28. The primary radiation is assumed to consist only of protons and to have the same form as that given by equation 4.23. However, the lateral distribution used so far is a "mean" one and the effective height of shower production varies with the radial distance from the axis. This is not the case when one is considering the frequency of two particles passing through detectors,

since the particles must have come from the same shower. To estimate the effect of this "coherent" production on the decoherence curve already calculated, the difference between the decoherence curve calculated allowing for the "coherence" effect and that calculated using the "mean" lateral distribution has been found using the "constant height" model (see Appendix B). This is approximate because the lateral distributions obtained using the latter are somewhat different to the more accurately calculated ones, but since one is taking the ratio of the two predictions the approximation should be reasonable. It is found that the coherence effect tends to raise the decoherence curve calculated from the "mean" lateral distribution, particularly at large separations.

The enchancement factor, F, is given in table 4.1. as a function of detector separation x.

Table 4.1.

x (m)	6	12	18	24	30	36	42	48
F	1.14	1.6	2.02	2.28	2.6	2.65	2.65	2.65

The decoherence curves obtained using a C.K.P. type transverse momentum distribution for muons of threshold energy 10^3 GeV and zenith angle of 45° are shown in figure 4.29 for several values of the mean transverse momentum. If one has a decoherence curve for $\langle p_t \rangle$ = 0.4 GeV/; it can be shown that the curve for $\langle p_t \rangle$ = 0.4 f GeV/c is obtained by multiplying the separation of the detectors by f and decreasing the corresponding frequency by f^2.

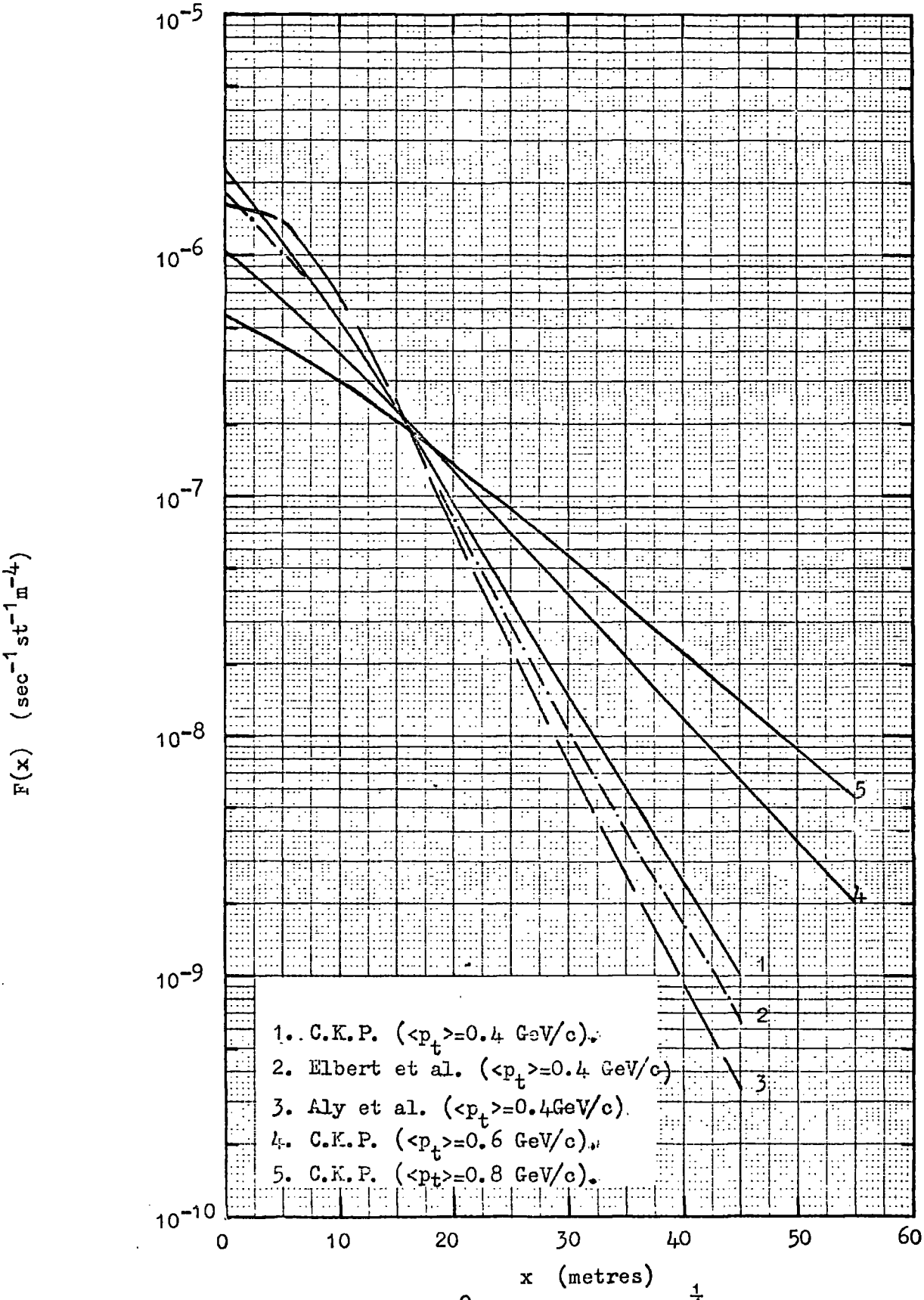

Fig. 4.29. Decoherence curves for $\Theta=45^{\circ}$, $E\mu>1000$ GeV, "$E^{\frac{1}{4}}$ model", and various transverse momentum distributions.

Figure 4.29 shows the decoherence curves obtained for the Elbert et al. (1968) and the Aly et al. (1964) transverse momentum distributions under the same assumptions as used in obtaining the curves for the C.K.P. distribution. Although there are differences in the shapes it is unlikely that a choice can be made between the curves since small changes in $\langle p_t \rangle$ can probably be made in order to make the curves similar.

These curves should not be regarded as final because of the approximations made. Also other factors have not been included in their calculation , notably the effect of heavy primaries, multiple Coulomb scattering, geomagnetic deflection and fluctuations in the multiplicity of the nuclear interactions.

CHAPTER 5.

THE UTAH EXPERIMENT

5.1. Introduction

The University of Utah neutrino detector has been used to study high energy muon showers, with threshold energies ranging from 500 - 5000 GeV, which have penetrated to great depths underground. The particular features which have been studied are the frequency of different multiplicities of muons, over the given threshold energy range and a zenith angle range of 30° - 75°, and the lateral distributions of these showers. Although more data were collected in this experiment than had previously been obtained from all preceeding experiments the statistics at particular depths and zenith angles are still not yet good enough for a complete analysis of the results and so *a priori* assumptions about the general character of the showers have been made and these are tested for consistency with the data.

The end product of the analysis, enabling the results to be compared with the theoretical predictions of the last chapter, are a set of density spectra for different muon threshold energies and zenith angles, estimates of the mean shower radii and a decoherence curve i.e. the rate of detecting muons in two $1m^2$ detectors as a function of the separation of the detectors, enabling information about the lateral distributions to be obtained.

5.2.1. The Apparatus.

The detector is located in a chamber 1850 feet below the surface of a mountain, the contours of which are shown in figure 5.1. The

Figure 5.1. Terrain above the Utah detector.

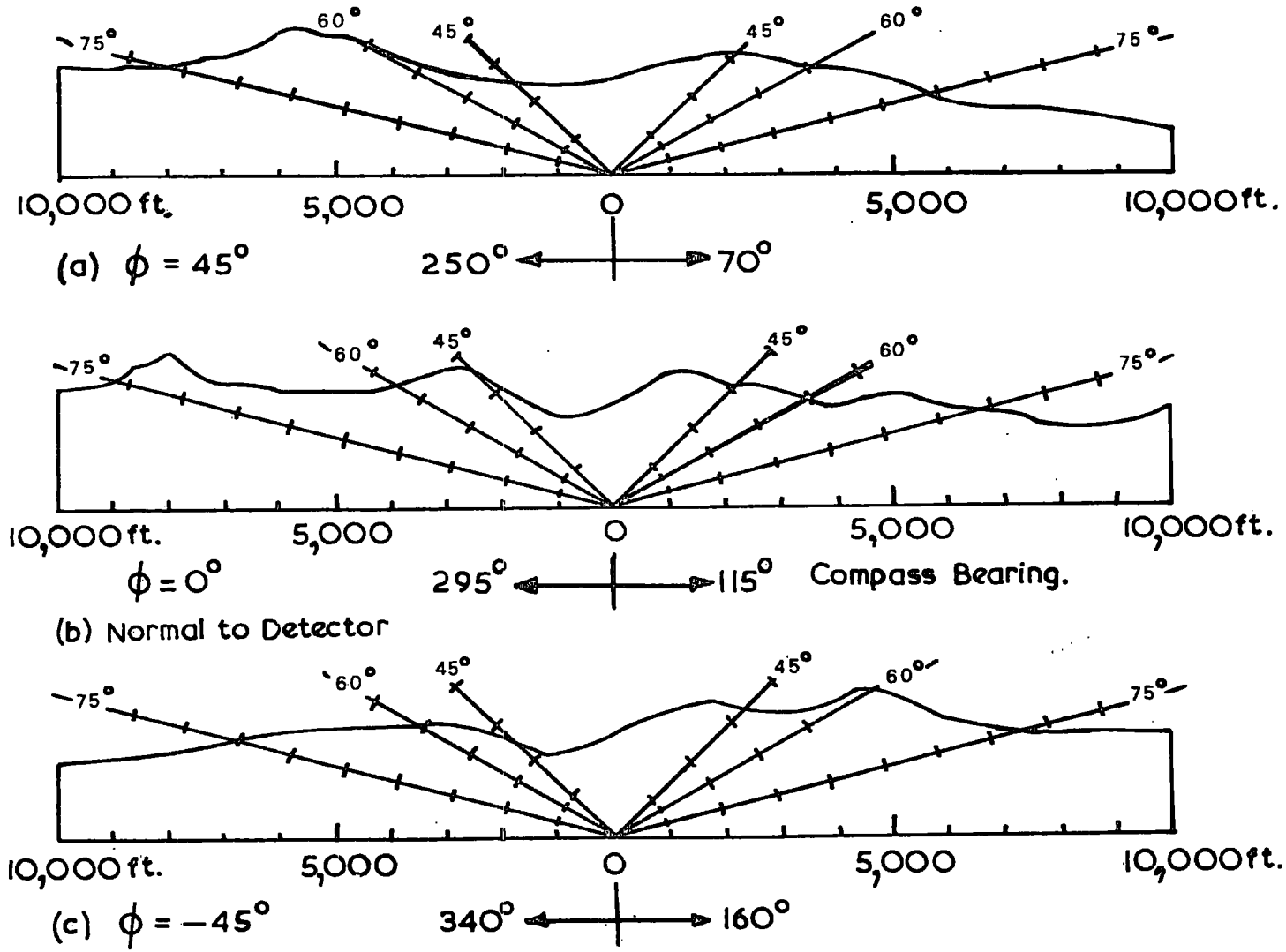
75°
60°
45°
45°
60°
75°
10,000 ft.
5,000
0
5,000
10,000ft.
(a) $\phi = 45°$
250°
70°
75°
60°
45°
45°
60°
75°
10,000ft.
5,000
0
5,000
10,000ft.
$\phi = 0°$
295°
115°
Compass Bearing.
(b) Normal to Detector
75°
60°
45°
45°
60°
75°
10,000ft.
5,000
0
5,000
10,000ft.
(c) $\phi = -45°$
340°
160°

Figure 5. 1.

geographical co-ordinates of the site are 40.623 degrees north latitude, 111.537 degrees west longitude. Slant depths are measured from the U.S. Geological Survey and the error is estimated to be ± 20 feet.

A rock survey indicated that the mean density of the rock is 2.61 $g.cm^{-3}$ and the mean Z^2/A value is 5.65. This latter value is slightly higher than that for standard rock (5.5) but since this difference is less than the uncertainty in the density (3%) and other experimental measurements no correction is made for it in determining the rock depths in $hg.cm^{-2}$.

The irregular terrain gives the possibility of making measurements at a variety of inclined depths and zenith angles and these measurements indicate that the variations in density are small over the range used.

5.2.2. The Detector

The complete detector, which was essentially designed to detect neutrino-induced muons, is shown in figure 5.2 and consists basically of four directional Cerenkov counters, an array of 600 cylindrical spark counters (CSC's) and two 16-kilogauss solid iron magnets. The dimensions are 21 x 11 x 6 metres in height.

The passage of a particle through the detector causes the generation of a 'trigger' pulse by the Cerenkov counters, and the cylindrical spark counters and data gathering electronics are activated.

The localized nature of the discharges in the CSC's makes it possible to detect several discharges in one CSC, which makes them very suitable for detecting multiple muons. The sparks are detected

by a sonic ranging technique to an accuracy of about 3m.m., thus enabling the trajectories of individual muons passing through the detector to be reconstructed.

A more detailed account of this system has been given by Hilton et al. (1967), Keuffel and Parker (1967), and Bergeson and Wolfson (1967).

During the collection of most of the data discussed in this chapter, only the Cerenkov tanks C and D, the magnet between them, and the nine rightmost columns of CSC's were operational.

The efficiency of the Cerenkov tanks was measured to be 86% for each tank where a muon passed no closer than one foot to the edge of a wall. This result was independent of the zenith and azimuthal angles of the triggering muon, although only muons with zenith angles greater than 50° could be used in these tests and so it had to be assumed that the efficiency was the same at smaller zenith angles. Determinations of the CSC and scanning efficiencies were also made and the results corrected accordingly.

The efficiency of finding muon pairs, where one of the muons passes through only one CSC group is thought to be not much greater than 72%. (Group I consisted of columns 7,8 and 9; Group II of columns 10 and 11; Group III of columns 12 and 13; and Group IV of columns 14 and 15). However, the requirement that each of at least two triggering muons passes through at least two CSC groups increases their probability of detection to 95% in the worst case. Higher multiplicity events would have been detected with an even higher efficiency.

Figure 5.2. The Utah Detector.

In the front view (XZ plane) the CSC's are seen end on as circles stacked in columns 40 high on either side of the water-filled Cerenkov counter tanks labelled A, B, C and D. The dark dotted areas between A and B and between C and D are the solid iron magnets. The light dotted areas between B and C are concrete. In the top view (XY plane), columns of CSC's appear as lines labelled 1 to 15, and the light collecting walls of the Cerenkov tanks are labelled 1 to 8.

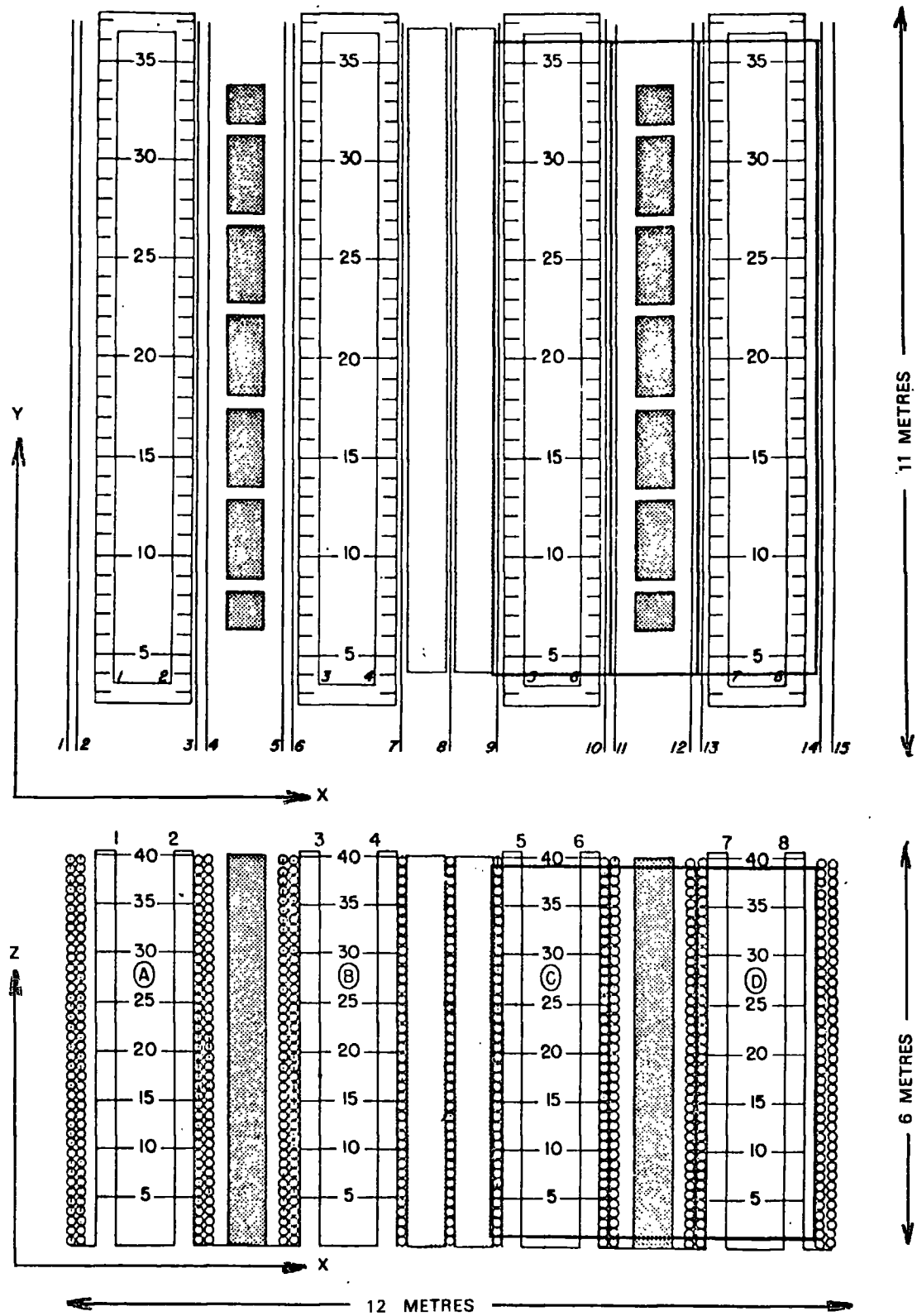

FIGURE 5.2.

In the later experiment, to study the lateral distributions at large radial distances, performed by Coats et al. (1969), the whole of the main detector was used and in addition three separate detectors positioned as shown in figure 5.3 where they are labelled α , β and γ. These detectors each consisted of three trays of cylindrical spark counters and had dimensions 22.5 x 4 x 2 feet in height. They were activated when one or more particles triggered the main array. In order to be accepted in the ensuing analysis each muon in the main detector had to pass through two forward Cerenkov walls and three CSC groups, and the muons in the outer detectors had to pass through the three groups of CSC's.

The range of muon separations capable of being measured with each detector is shown in figure 5.3 for the first run. In a second run the outer detectors were moved so that muon separations up to ~60 metres could be measured.

5.3.1. Data Analysis and Results.

The multiple muon events analysed were distributed in two 18 x 26 angular cells, one for westward-going and one for eastward-going muons. The eighteen 2.5° zenith angle intervals extended from 30° to 75°, and the twenty six 5° azimuthal intervals extended from -65° to + 65° with respect to the x-axis of the detector (see figure 5.2).

An effective depth was associated with each cell and was calculated assuming a linear variation of depth from edge to edge across the bin and weighting the depths over the bin with a world-wide vertical depth intensity curve (WWDI curve) compiled by Larson (1968).

The estimates of the projected zenith angle were accurate to about

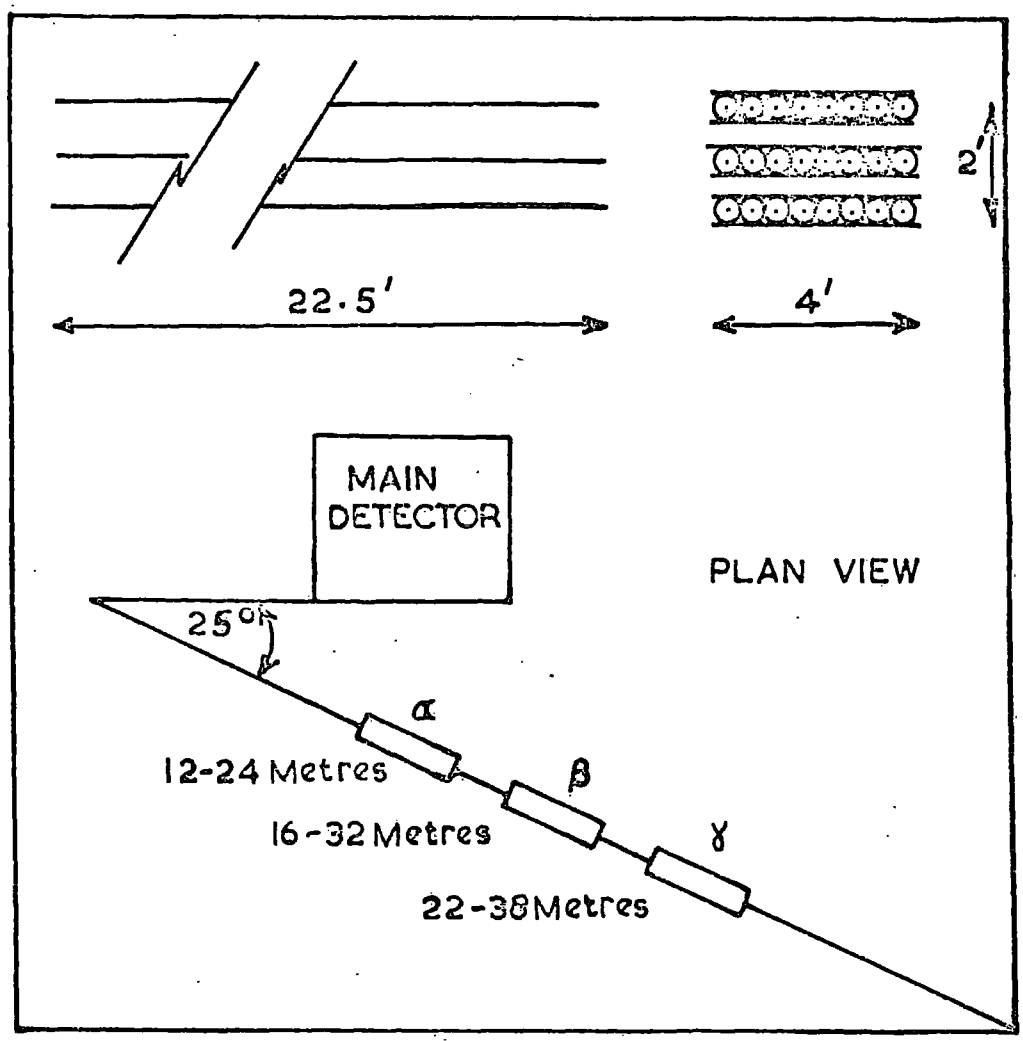

Fig. 5.3. The Outrigger Layout.

1°, and better than 0.5° in azimuth.

Events were accepted if the muons in the event were parallel to within 5°, and in fact more than 66% of the pairs were parallel to within 1°. The most frequently observed spatial separation was about 4 metres and so if the showers were formed in the rock they would have to be formed at distances greater than about 200 metres away from the apparatus to achieve this degree of parallelism. Range-energy relation calculations show that muons of this range must have an energy of at least about 150 GeV and so the parent pions, whose energy must be at least as great as this, have very little chance of decaying before they interact in rock. The cross section for pair production of muons at this energy by energetic muons is far too small to account for the observed number of events and so it appears that the only reasonable origin of these muons is as the remnants of muons produced in E.A.S.

5.3.2. The Derivation of the Empirical Density Spectra.

Because of the complexity of the aperture for multiple muon events, the wide variation in zenith and azimuthal angle and depth, Porter and Stenerson decided to derive empirical density spectra to enable their results to be compared with the results of other experiments and with theoretical productions.

The method adopted was as follows: - a trial differential density spectrum of the form

$$n(h,\theta,\Delta)\, d\Delta = G(h)\, F(\theta)\, H(\Delta)\, d\Delta \qquad 5.1.$$

was adopted.

$H(\Delta)$ was taken to be of the form

$$H(\Delta) = K_\beta \Delta^{-\beta} \quad \text{for} \quad \Delta > \Delta_o$$
$$= K_\alpha \Delta^{-\alpha} \quad \text{for} \quad \Delta < \Delta_o \qquad 5.2$$

where $K_\beta \Delta_o^{-\beta} = K_\alpha \Delta_o^{-\alpha}$ The reason for taking this form was that in the experiments of Barrett et al. (1952) and Chatterjee et al. (1966) it was found that the number of underground muons was related to the size of the original air shower by a power law. Since the size spectrum is approximately given by a power law in N, the density spectrum for underground showers would be expected to be a power law in density, Δ. They explain the change in slope as being due to the sharp cut-off which would occur in the density spectrum when only one muon is present in the shower and say that a sharp cut-off is unphysical (as it is, due to the effect of fluctuations) and that a change in slope is the more likely effect at this point.

In fact one would tend to expect spectra whose slope at low densities is increasing with increasing density, due to the rapid increase of muons with increasing primary energy at the lowest energies capable of producing muons above a given threshold energy, followed by a fairly constant slope as the number of muons becomes almost a power law function of the primary energy and then a further increase in slope due to the "kink" in the primary spectrum, although if the "kink" is due to a rigidity cut-off the change in slope of the density spectra will not be so marked due to the increasing porportion of heavy nuclei which are more efficient at producing muons at the relevant energies. A further factor causing a steepening of the density spectra will be the large area of the detector which will tend to increase the slope at high densities. Thus a two power

law is likely to be a reasonable approximation over a range of densities but not over the entire range.

The choice of the function G(h) where h is the depth, was determined by the decision to try and construct density spectra which could predict the rates of single as well as multiple muons. Because of this it is argued that G(h) must have the same dependence on depth as the vertical depth intensity curve. It was assumed that the integral sea-level energy sepctrum of muons can be represented by a power law $I(>E) \propto E^{-\gamma}$. An approximate range-energy relation (see Barrett et al., 1952; Kobayakawa, 1967) was then used to predict the depth intensity relation

$$I(h) \propto \frac{a'}{b} \left\{ \exp(b\,h) - 1 \right\}^{-\gamma} \qquad 5.3$$

The factor a'/b varies slowly with energy but was assumed to be constant in this case. Both b and γ increase slowly with energy but it was found that a good fit could be obtained by fixing b and letting γ increase with depth. Thus by this hypothesis

$$G(h) = C\,(\exp(bh)-1)^{-\gamma} \qquad 5.4$$

where C is a constant, $b = 3.5\ 10^{-4}$ hg.$^{-1}$cm^2 and $\gamma = 2.4 + 0.25$ ln $(h/10^3$ hg).

The justification for this procedure is that it gives agreement with the world-wide depth intensity curve of Larson when C is put equal to 1.55×10^{-7} sec^{-1}st^{-1}cm^{-2}. Thus the procedure is justified for singles but it is not necessarily justified for events of higher multiplicity since according to the theoretical calculations the shape of the spectra of doubles and triples passing through 20m^2

is different to that of singles. This is to be expected since these depend on factors which are not important in the case of singles e.g. the mean radius of the lateral distributions and the size of the detector. Thus the factor γ in equation 5.4 will be different, giving rise to a different depth intensity relation if the value of b is unchanged.

Also no account has been taken of fluctuations in the muon energy loss. One would expect the effect of this to be that the effective range of multiples will be less than that of singles and so when a depth is converted back to a threshold energy using the average range energy curve of Kobayakawa (1967) the corresponding energy for singles should be slightly different to that for multiples. However, this effect should only be important at large depths, where the statistics are poor, and should not affect the conclusions.

The justification for the method must be that it gives agreement with the experimental measurements. It may be that with better statistics the assumptions made will have to be modified.

In the calculations of the final density spectra C was included in the normalization factor K_β.

The number of events of various multiplicities in each 2.5° x 5° angular bin was known, and the trial density spectrum was used to calculate the expected numbers in each bin up to a multiplicity of 3, allowing for the variations in aperture and efficiency of detection with the type of event. K_β, the normalization factor, was chosen to give exact agreement with the observed and expected number of two

muon events. In these calculations the value of the effective depth ($\bar{h}$), calculated as described previously, was used in the function G(h). The calculation of $\bar{h}$ is open to the same criticsm as G(h) for multiple events.

A sum over the azimuthal angles was then carried out for both the predicted and observed rates, thus collecting the two sets of numbers into 18 zenith angle bins from 30° to 75°, corresponding to slant depths ranging from 1500 to 6000 hg.cm^{-2}.

Using the parameters α, β and Δ_o as variables a χ^2-test was carried out on the fit between the observed and predicted number of events in each bin and an attempt was made to find the form of the function $F(\theta)$.

No simple form could be found for $F(\theta)$, but calculations indicated that the point of discontinuity in the slope of the density spectra was a function of zenith angle. Therefore a new trial density spectrum of the form

$$n(h,\theta,\Delta)\, d\Delta = G(h)\, H(\Delta,\theta)\, d\Delta \qquad 5.5$$

was taken. $H(\Delta,\theta)$ had the same dependence on Δ as taken previously, but the point of intersection of the two power laws in density was given by

$$\Delta_o = (D + E \cos\theta)\ m^{-2} \qquad 5.6$$

Qualitatively this variation can be explained by the mean radius of the showers being more sensitive to changes in zenith angle than is the total number of muons in the shower. Thus at smaller zenith angles the primary energy responsible for a certain density is smaller

than at larger zenith angles. Thus the "kink" in the density spectra, which is interpreted as being due to the rapid fall in mean muon number with decreasing primary energy at low primary energies (see figure 4.4) will occur at higher density values for smaller zenith angles.

Using this form for the density spectra with α, β, D and E as variables fits could be obtained near the 30% confidence level for singles and triples and even better fits for the doubles using the χ^2-test.

No unique set of parameters was obtained, but several sets gave almost equally good fits and these are given in table 5.1.

Table 5.1.

	β	α	D	E	Normalization Factor.
(a)	2.75	1.8475	.0006	.0015	$192.89\ 10^{-8}$
(b)	2.86	1.8975	.002	.002	$130.93\ 10^{-8}$
(c)	3.2	1.9210	.004	.004	$35.11\ 10^{-8}$

Figure 5.4 shows the difference in shape of the density spectra depending on the set of parameters used for two different threshold energies (depths were converted to energies using Kobayakawa's range-energy curves). In the density range 10^{-3}-10^{-2} m^{-2} the curves do not differ very much in shape and amplitude and so they can be compared with theoretical predictions in this region but at very small and very large densities the slopes and amplitudes show wide differences.

Porter and Stenerson decided to use the "set a" parameters because the fits for doubles and triples improve somewhat as β

Figure 5.4. Empirical integral density spectra for two threshold energies and three parameter sets. (after Porter and Stenerson, 1969).

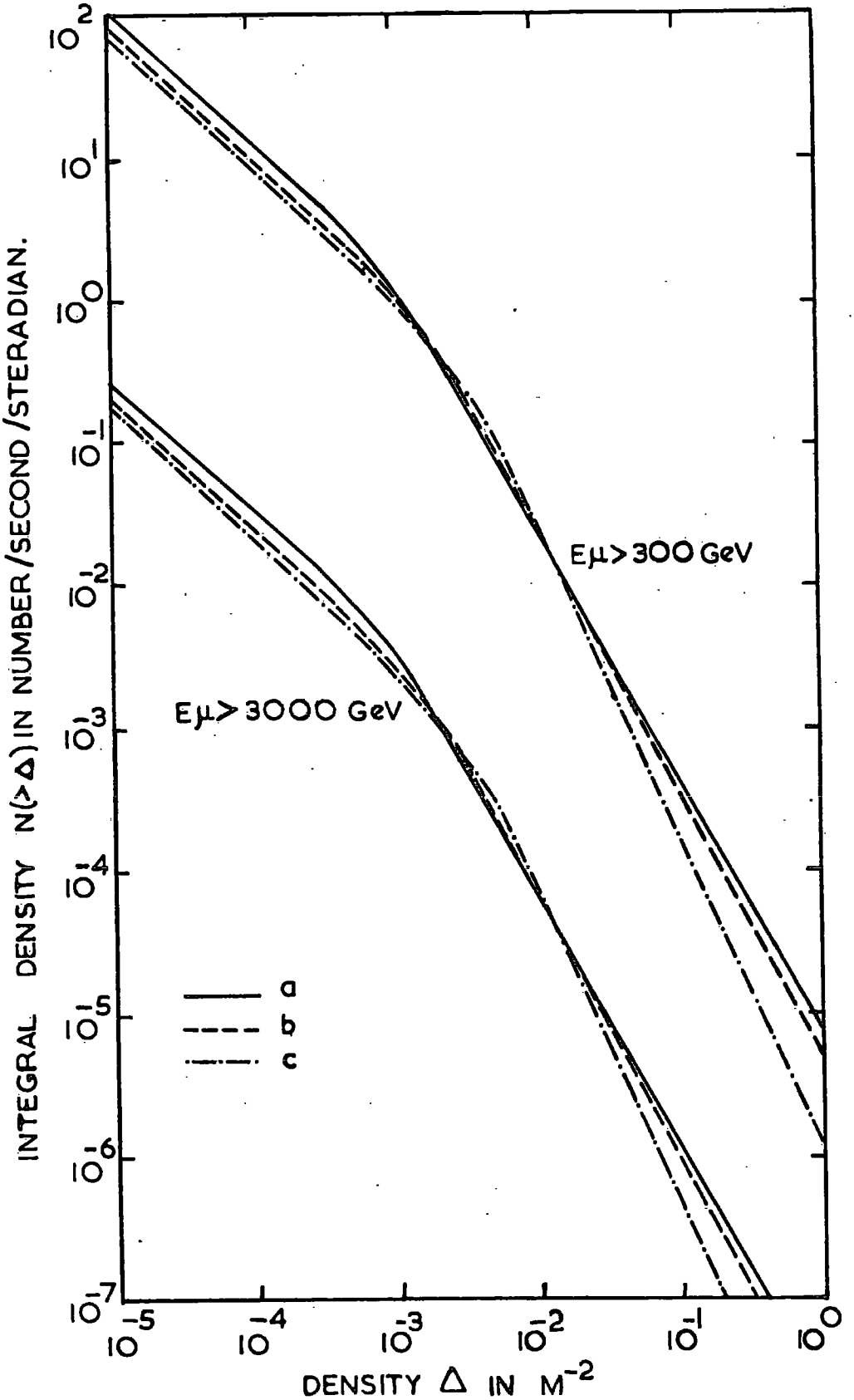
INTEGRAL DENSITY N(>Δ) IN NUMBER/SECOND/STERADIAN.
DENSITY Δ IN M^{-2}
Eμ> 300 GeV
Eμ> 3000 GeV
a
b
c

Figure 5.4

increases.

The final set of curves for varying muon threshold energy and zenith angle are shown in figure 5.5

Several checks were made on these curves. Figure 5.6 shows the predicted and observed numbers of events in each of the 18 zenith angle bins. This serves as a check on the zenith angle distribution used.

Figure 5.7. shows the predicted and observed number of events in 200 hg.cm^{-2} intervals. This serves as a check on the depth dependent factor in the density spectra.

In order to provide a breakdown of the observed data according to both depth and zenith angle, the data were summed in 10^{0} zenith angle and 500 hg.cm^{-2} depth intervals. The results are shown in table 5.2.

Unfortunately the statistics were not sufficiently good to break down the results into smaller depth and zenith angle intervals, and the results of further runs must be awaited before it is profitable to do this.

5.3.3. Decoherence Curves.

Because of the relatively large area of the muon showers compared to the size of the detector it was not possible to locate the shower cores unambiguously and this precluded a direct study of the lateral distributions of the showers. These are of particular interest because of their relevance to the mean transverse momentum and the form of the transverse momentum distribution of secondary particles produced in high energy interactions.

TABLE 5.2

Distribution of Multiple Muons in Utah Experiment (after Porter and Stenerson, 1969)

Zenith angle (deg)	Depth range (m.w.e)	Approx. E_μ (GeV) (threshold)	Multiplicity 1	2	3	4	4
40 - 50	1400 - 1900	540	18	27	3	4	0
	1900 - 2400	800	1831	153	40	5	9
	2400 - 2900	1100	2465	157	35	10	10
	2900 - 3400	1500	281	14	0	1	1
50 - 60	1900 - 2400	800	48	14	0	0	0
	2400 - 2900	1100	2315	107	17	4	6
	2900 - 3400	1500	1756	86	12	3	0
	3400 - 3900	1800	629	31	2	3	0
	3900 - 4400	2300	39	2	1	0	0
60 - 70	2400 - 2900	1100	19	1	0	0	0
	2900 - 3400	1500	834	25	3	1	1
	3400 - 3900	1800	1074	32	9	0	0
	3900 - 4400	2300	471	18	2	0	0
	4400 - 4900	2900	215	11	0	1	0
	4900 - 5400	3600	35	4	0	0	0
	5400 - 5900	4500	21	0	0	0	0
70 - 75	3900 - 4400	2300	99	1	0	1	0
	4400 - 4900	2900	138	4	1	0	0
	4900 - 5400	3600	107	3	0	0	0
	5400 - 5900	4500	25	1	0	0	0
	5900 - 6400	5500	9	0	0	0	0
	6400 - 6900	6700	11	1	0	0	0

Figure 5.5. Empirical integral density spectra from the Utah experiment (after Porter and Stenerson, 1969).

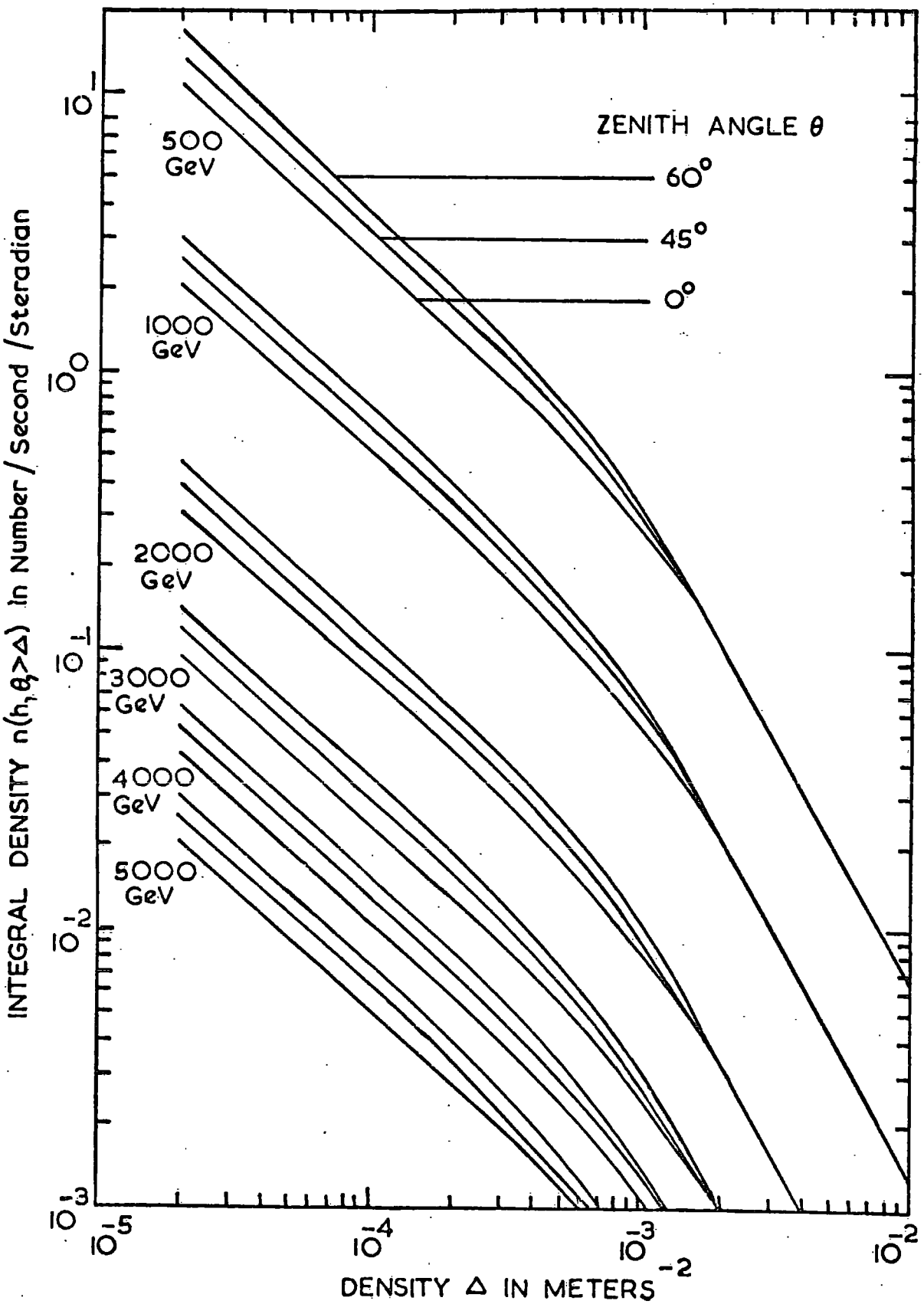
ZENITH ANGLE θ
60°
45°
0°
500 GeV
1000 GeV
2000 GeV
3000 GeV
4000 GeV
5000 GeV
INTEGRAL DENSITY n(h, θ>Δ) in Number / Second / Steradian
DENSITY Δ IN METERS
10^-1
10^0
10^-1
10^-2
10^-3
10^-5
10^-4
10^-3
10^-2

FIG. 5.5

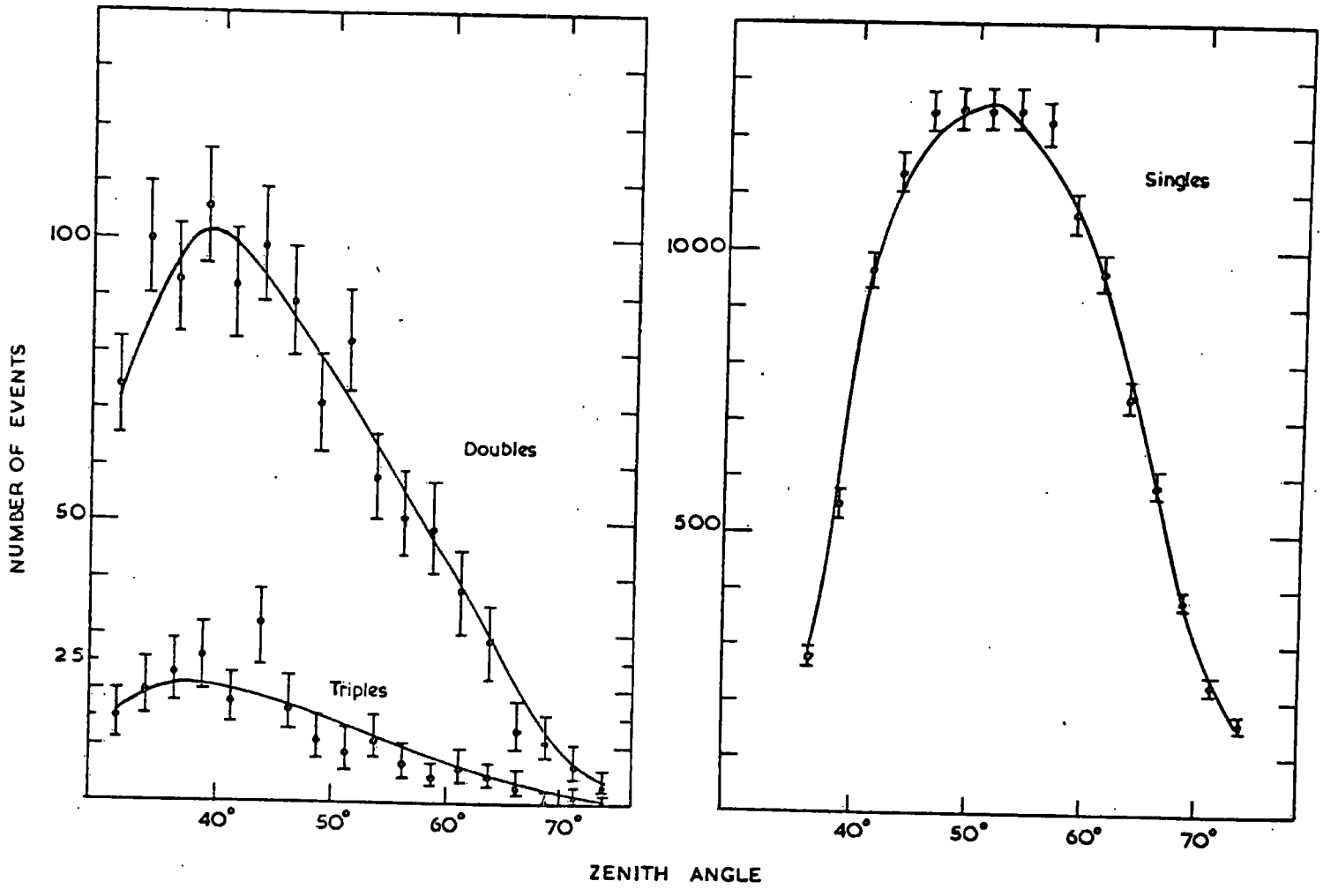

Fig. 5.6. Measured angular dependence of singles, doubles, and triples compared with the predictions of the empirical density spectrum (after Porter and Stenerson 1969).

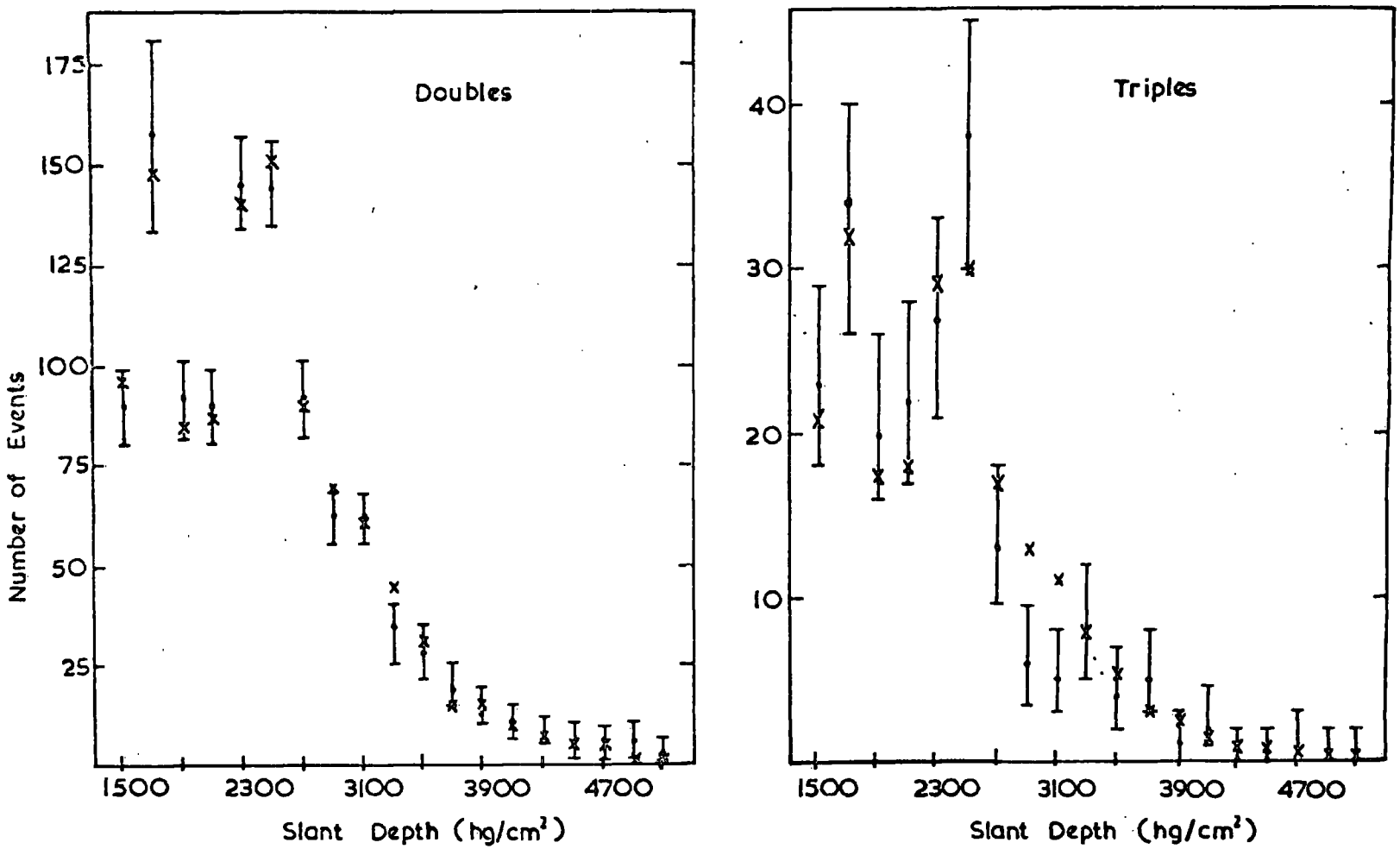

Fig. 5.7. Measured depth dependence of singles, doubles, and triples compared with the predictions of the empirical density spectrum (after Porter and Stenerson 1969).

The work of the Utah group can be split into two parts on this particular topic; that done before the additon of the "wing" trays i.e. the work of Porter and Stenerson (1969) which provides some information on the radial extent of the muon showers; and the subsequent work of Coats et al. (1969) in which a study of the lateral distributions was made out to radial distances of the order 50m from the core.

Considering the work of Porter and Stenerson first, then following Barrett et al. (1952) the number of coincidences observed between two small detectors of areas A_1 and A_2 separated by a distance x due to muon showers is given by

$$C_{12}(x) = A_1 A_2 \sum_{M=1}^{\infty} M(M-1) F(M) \int \phi(M,r_1) \cdot \phi(M,r_2)\, da \qquad 5.7$$

where F(M) is the number of showers containing M muons whose axes fall on a small area da at distances r_1 and r_2 from the detectors A_1 and A_2, $A\,\phi(M,r)$ is the probability that a given muon, in a shower of size M, falls on an area A at a distance r from the axis. The integral is carried out over the plane containing the detectors. The equation assumes that the probability of getting two muons in either detector is small.

The integral was carried out for two assumed forms of the lateral distributions, a flat distribution of radius σ and Gaussian distribution with a r.m.s. radius of σ.

The function $C_{12}(x)$ was found for each of the angular bins (allowance being made for the strong dependence of the sensitive area on the zenith and azimuthal angles).

Because of the poor statistics the experimental data and the predicted numbers were put into 10^0 zenith angle bins and 500 hg. cm^{-2} bins. χ^2 - tests were then applied to the predicted and observed numbers in each of these bins for values of σ from 5 to 20 metres. $\Sigma M(M-1) F(M)$ was determined in each case by finding the minimum value of χ^2 for each value of σ . This procedure neglects the variation of the mean radii of the showers with zenith angle and depth and this combined with the uncertainty in the lateral distribution means that only a reasonable estimate of σ can be obtained.

The results are shown in figure 5.8 for three combinations of zenith angle and depth. The coarseness of the calculations is immediately apparent. For the zenith angle range 40^0 - 50^0 it is found that showers penetrating to a depth 1900-2400 hg.cm^{-2} (i.e. a muon threshold energy of about 800 GeV) have a smaller average radius than showers penetrating to 2400-2900 hg.cm^{-2} (i.e. a muon threshold energy of about 1100 GeV). This is in contradiction with theoretical results which show that for a given zenith angle the mean radius of a shower decreases with increasing threshold energy. The results also show that for a given depth the mean radius of a shower increases with decreasing zenith angle. This is also in contradiction with theory since muons at larger zenith angles have travelled a longer distance, h, through the atmosphere and the radial distance from the axis is proportional to h for muons of a certain fixed energy.

These discrepancies are perhaps due to the functions taken for the shape of the lateral distributions being inaccurate although the mean radii seem almost independent of the function used. For the square

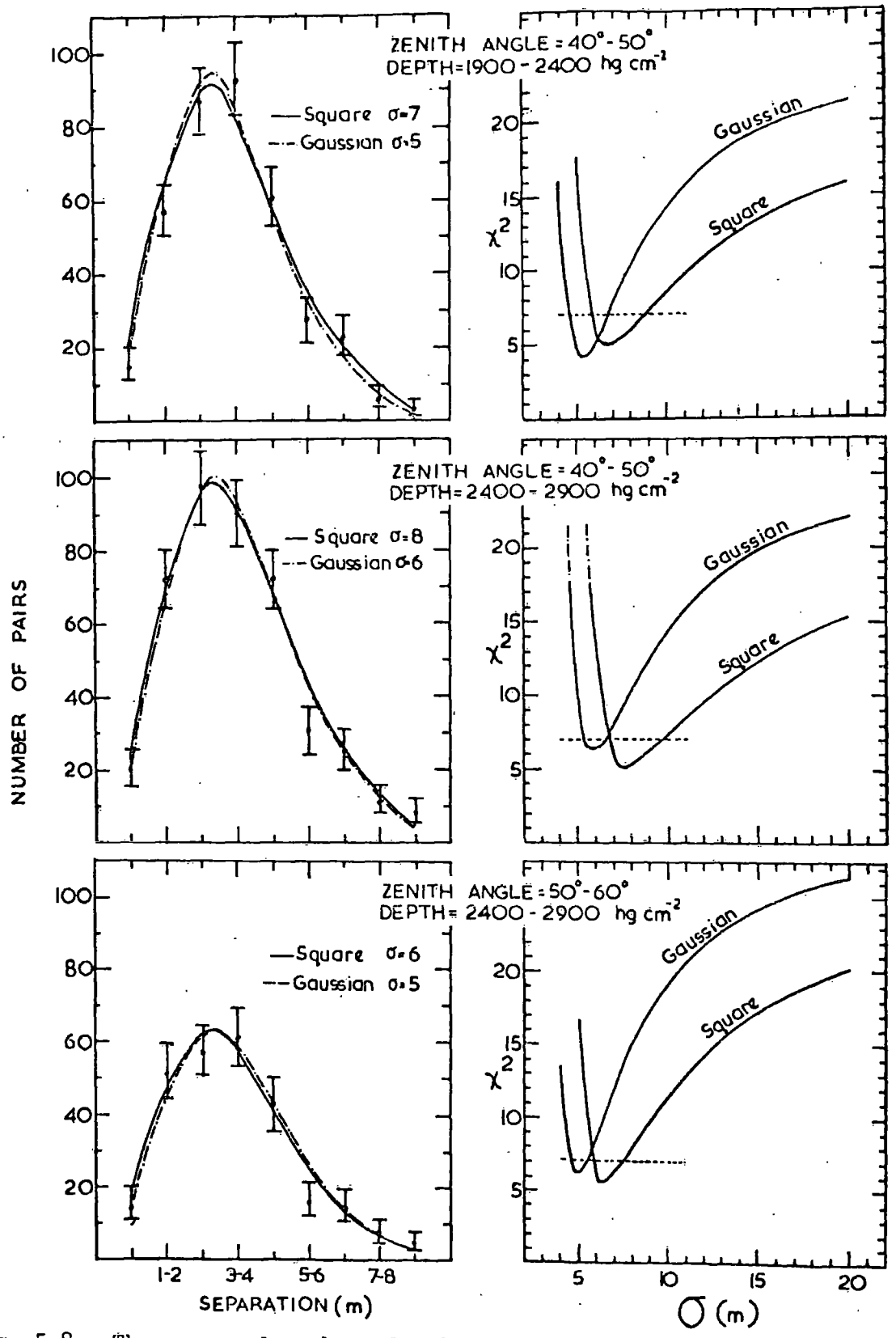

Fig. 5.8. The measured number of pairs as a function of the separation together with the predictions assuming a square and a Gaussian radial distribution (after Porter and Stenerson 1969).

lateral distributions the mean radius, $\langle r \rangle$, is given by $0.667\,\sigma$ while that for the Gaussian type lateral distribution is given by $\langle r \rangle = 0.886\,\sigma$. Also relevant is the fact that it was necessary to combine bins at several depths and zenith angles.

Porter and Stenerson consider that the mean radii of the detected showers lie in the range 6 - 10 metres.

An estimate of the mean number of muons in these showers can also be obtained from the above results. From equation 5.7. it can be shown that

$$\frac{I_o \langle M(M-1) \rangle}{I_o \langle M \rangle} = \frac{\langle M^2 \rangle}{\langle M \rangle} - 1 \qquad 5.8$$

$$= \int \frac{2\pi x \; C_{12}(x)\, dx}{A_2 \, N_1} \qquad 5.9$$

where N_1 is the number of single muons detected in the detector of area A_1, $\langle M(M-1) \rangle$ is the average value of $M(M-1)$, $\langle M \rangle$ is the average value of M and I_o is the total number of showers per unit area. $I_o \langle M(M-1) \rangle$ was computed for three of the large bins corresponding to the range of σ's which gave a fit within the 33% confidence limit when a χ^2 - test was carried out. $I_o \langle M \rangle$ was obtained from the data on single muon events. Thus $\langle M(M-1) \rangle / \langle M \rangle$ could be calculated. These results together with the ranges of σ are shown in table 5.3.

Since $1 < \langle M \rangle < \langle M^2 \rangle^{\frac{1}{2}}$ they were able to infer the inequality $1.37 < \langle M^2 \rangle < 4.4$ covering the three sets of results. This shows that the average underground shower contains very few muons. Also, under the assumption that the number spectrum of muons follows

a power law, $M^{-\delta}$, they were able to obtain estimates of δ from the ratio $\langle M^2 \rangle / \langle M \rangle$ for the three bins considered. These results are also shown in table 5.3.

Table 5.3.

Zenith Range (degrees)	Depth Range ($hg.cm^{-2}$)	σ_+ σ_o σ_- (m)	$\frac{\langle M^2 \rangle}{\langle M \rangle}$	δ
40 - 50	1900-2400	10	2.11	3.40
		7	1.52	3.70
		6	1.41	3.90
40 - 50	2400-2900	11	2.10	3.40
		8	1.70	3.60
		7	1.58	3.70
50-60	2400-2900	8	1.56	3.70
		6	1.37	3.95
		6	1.37	3.95.

The work of Coats et al. (1969) has extended the range of muon separations studied up to ~ 50 metres and also improved the statistical accuracy considerably. 3385 pairs of parallel muons were detected in the accepted range of depths and zenith angles i.e. 1900 -3000 hg. cm^{-2} and 40° - 60°. This depth range corresponds to muon threshold energies of 700 - 1500 GeV assuming that the energy loss coefficient $b = 4.0\ 10^{-6}\ g.cm^{-2}$. Despite the improved statistics they are still not yet good enough for a comparison to be made separately for each zenith angle and depth cell and so the data has been converted to a mean zenith angle of 45° and a depth of 2500 $hg.cm^{-2}$ i.e. a muon

threshold energy of ~1050 GeV. This of course means that certain theoretical assumptions had to be made in combining the data.

The mean radius of showers at a zenith angle θ is assumed to be related to that at 45° by the equation

$$\bar{r}_{45^\circ} = \bar{r}_{\theta} \left\{ \frac{\sec 45^\circ}{\sec \theta} \right\} \qquad 5.10$$

This comes from assuming that the vertical height of formation of the parent pions is independent of zenith angle. The theoretical calculations in Chapter 4, for showers contributing mainly to doubles, indicated the relation

$$\bar{r}_{45^\circ} = \bar{r}_{\theta} \left\{ \frac{\sec 45^\circ}{\sec \theta} \right\}^{1.3} \qquad 45^\circ \leq \theta < 60^\circ \qquad 5.11$$

It is assumed in the conversion from a threshold energy E_μ to the standard threshold that the mean radii of the showers are connected by the relation

$$\bar{r}_{1050} = \left\{ \frac{E_\mu}{1050} \right\} \bar{r}_{E_\mu} \qquad 5.12.$$

while the theoretical calculations indicate that

$$\bar{r}_{1050} = \left\{ \frac{E_\mu}{1050} \right\}^{0.8} \bar{r}_{E_\mu} \qquad 700 < E_\mu < 3000 \text{ GeV.} \quad 5.13.$$

However, over the energy and zenith angle range covered these differences should not be important.

The variation in depth is scaled according to the single muon depth intensity curve, this being consistent with the experimental results.

The final decoherence curve is shown in figure 5.9.

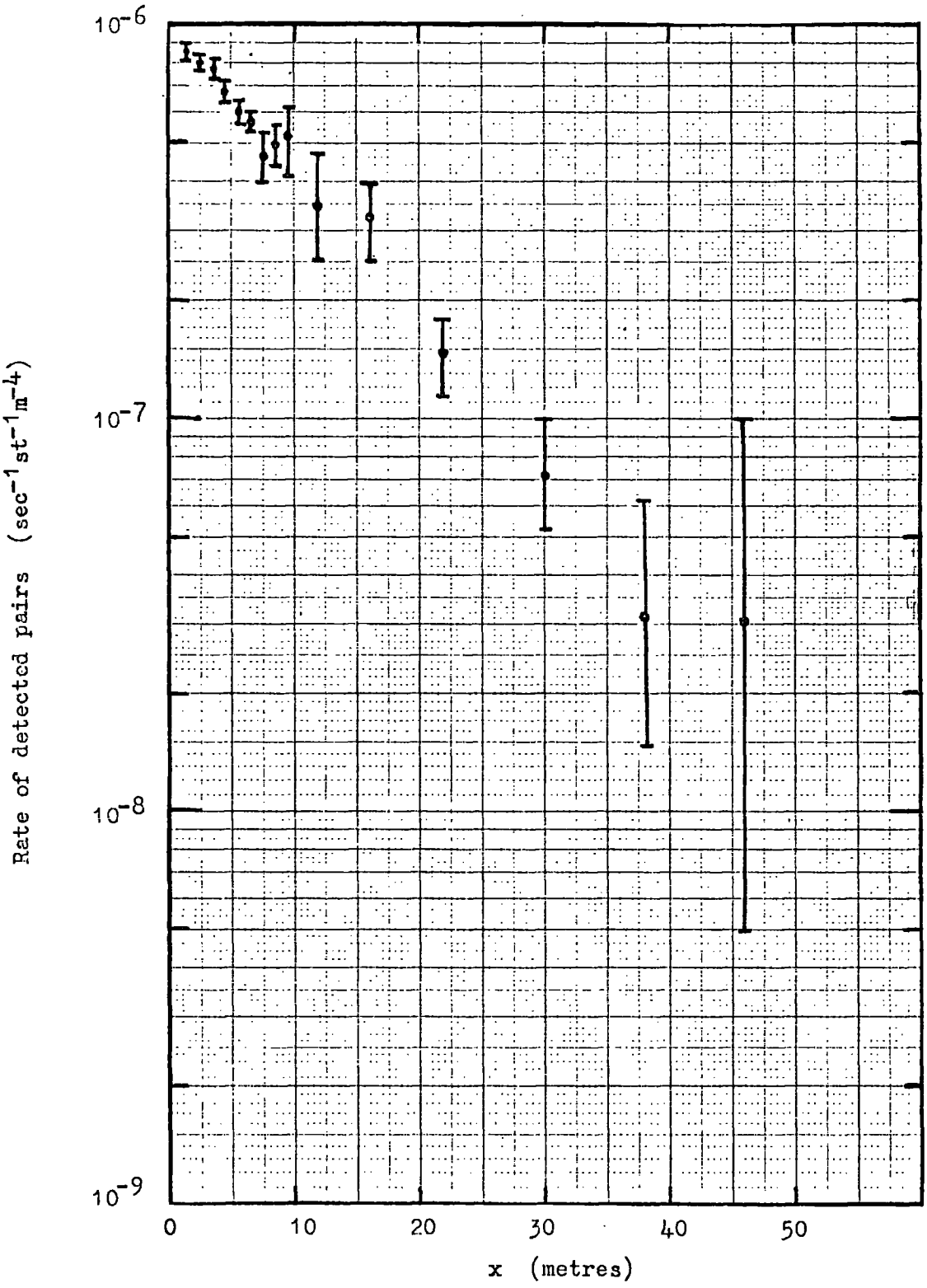

Fig. 5.9. Measured decoherence curve at a mean zenith angle of 45° and a threshold energy of 1000 GeV.

5.4. Comparison of Experimental and Theoretical Results.

5.4.1. Single Muon Energy Spectrum.

Difficulty arises in comparing the theoretical predictions with those obtained at Utah because two spectra have been quoted. Both these spectra are derived from the same set of experimental data and the difference is due to the different manner in which the data have been treated.

The first spectrum is due to Bergeson et al.(1968) and is derived purely from measurements of single muons. These authors found that the enhancement in the intensity of single muons with increasing zenith angle was less than the sec θ increase which would be expected if the detected muons were, as is usually thought, the progeny of pions or kaons. They have suggested that in addition to the normal pion and kaon produced components there is a further process which produces muons - the so-called "direct production" process. The intensity of this component required to fit their observations on the angular distribution of high energy muons is about 2% relative to the pion and kaon component, and this only becomes important at very high muon energies (> 1000 GeV) where the probability of pion or kaon decay is very small. A consequence of this process is that the vertical sea-level single muon spectrum is both higher and flatter than that derived previously from the measured vertical depth intensity curve. Thus in order to maintain agreement with depth intensity measurements it is necessary to make a further postulate that the rate of energy loss of muons above 1000 GeV increases with energy at a much faster rate than previously thought. This is

attributed, at present, to a rise in the photo-nuclear cross section.

At a zenith angle of 60° the spectrum predicted is as shown in figure 5.10 where it is seen that it is flatter and also still higher than the conventional one of Aurela and Wolfendale (1967), which has been enhanced by a factor sec 60° to convert it from the vertical, despite the weaker dependence on zenith angle of the intensity.

The density spectra of Porter and Stenerson can be used to obtain the single muon energy spectrum. For a zenith angle of 60° we get

$$F_{60^{\circ}} (> E_{\mu}) = \int_{0}^{\infty} N_{60^{\circ}} (\Delta , E > E_{\mu}) \quad \Delta \, d\Delta \qquad 5.14$$

where $N(\Delta , E > E_{\mu})$ is the differential density spectrum of muons with energies above E_{μ} for a zenith angle of 60°.

As would be expected from the results of Bergeson et al. (1968) the predicted curve is lower than that of Aurela and Wolfendale since Porter and Stenerson used a b value of $3.5\ 10^{-6}\ g^{-1}.cm^{2}$ to convert their measured depths to energies in accordance with the calculations of Kobayakawa (1967). It also appears that they have neglected the effect of fluctuations in the energy lost by the muons, which tends to become important at higher energies. This effect will tend to steepen their predicted energy spectrum somewhat.

Since we use the spectra of Porter and Stenerson for comparison with our predictions for multiple events we adopt their single muon energy spectrum for an initial comparison with the present work. From figure 5.10 we see that the experimentally derived spectrum is lower than all the theoretical ones.

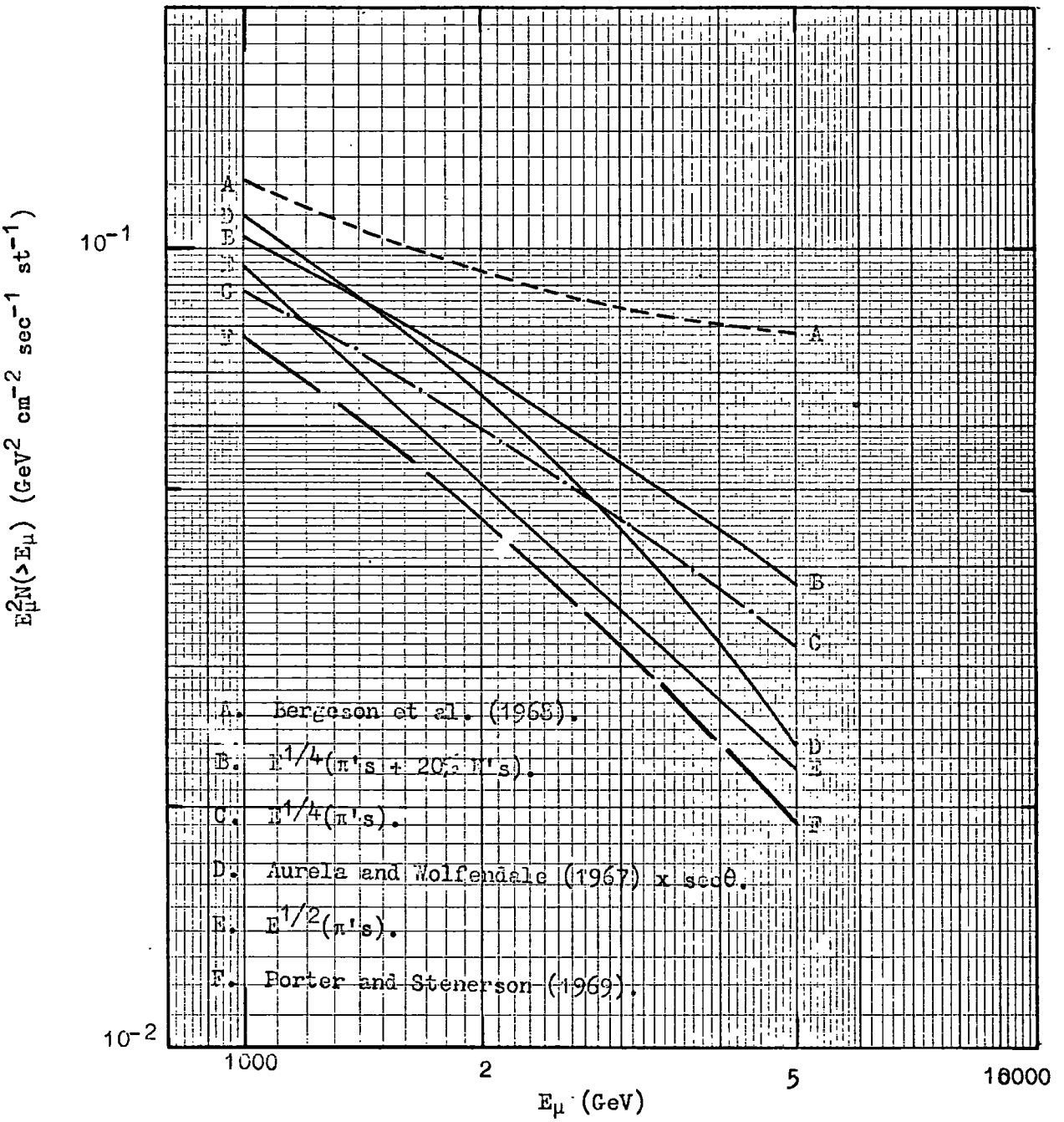

Fig. 5.10 Single muon spectra for θ=60°.

Taking the "$E^{-\frac{1}{2}}$ model" it is seen that the predicted spectrum is less steep than the Utah one, having an exponent ~ 2.7 if it is approximated by a power law, although it may be slightly steeper than this as the point at $5\ 10^3$ GeV is not very accurate ($\sim 20\%$) and is probably an upper limit. The addition of 20% kaons over and above the pion component is seen to worsen the fit as regards absolute magnitude.

The spectrum predicted by the "$E^{-\frac{1}{2}}$ model" is seen to agree better at high energies but worse at low energies as regards absolute magnitude, compared to the "$E^{-\frac{1}{2}}$ model", and to be in better agreement as regards shape.

In order to find the effect of fluctuations in the energy losses of muons on the comparison, the Utah single muon energy spectrum has been converted to a depth intensity curve using the average range energy relationship of Kobayakawa for $b = 3.5\ 10^{-6}$ g.$^{-1}$cm^2. The theoretical spectra have also been converted to depth intensity curves using the same b value but taking into account the effect of fluctuations as calculated by Kobayakawa. These results are shown in figure 5.11. Also shown is a world wide depth intensity curve compiled by Larson (1968) which has been enhanced by sec 60°.

As would be expected, the effect of fluctuations is to make the fit between experiment and theory worse, especially at large depths.

Considering the "$E^{-\frac{1}{2}}$ model" it is seen that it agrees to within $\sim 20\%$ at 2600 hg.cm^{-2} but due to it being less steep the fit deteriorates with increasing depth.

The "$E^{\frac{1}{2}}$ model" agrees somewhat better in shape with the Utah curve but again the fit deteriorates with increasing depth, although it is better than for the "$E^{\frac{1}{4}}$ model".

Furthermore the intensity of the single muon energy spectrum derived from the empirical density spectra does not have the same angular dependence as would be expected for the theoretical curves. This can be clearly seen from a comparison of the observed depth intensity curve of Porter and Stenerson and that due to Larson enhanced by sec 60° in figure 5.11. Although no single events were detected below a zenith angle of 35° the assumed angular dependence built into the empirical density spectra enables a prediction to be made of the vertical depth intensity curve. The results obtained agree with the world wide vertical depth intensity curve of Larson within the statistical errors of the curve of Porter and Stenerson and the estimated accuracy (10%) of the curve due to Larson. At a zenith angle of 60°, however, it is seen from figure 5.11 that the curve due to Larson, enhanced by sec 60°, is higher than that predicted by the empirical density spectra. The enhancement factor obtained by Porter and Stenerson is ~ 1.5 compared to the factor ~ 2 expected if the observed muons are the progeny of pions or kaons.

It must be concluded therefore that the results, if correct, cannot be explained by either of the models, and that possibly some new process is needed. As has been pointed out earlier in this section such a process has been postulated already by Bergeson et al. (1968).

Better agreement can be obtained between the depth intensity curve of Porter and Stenerson and the theoretically predicted ones

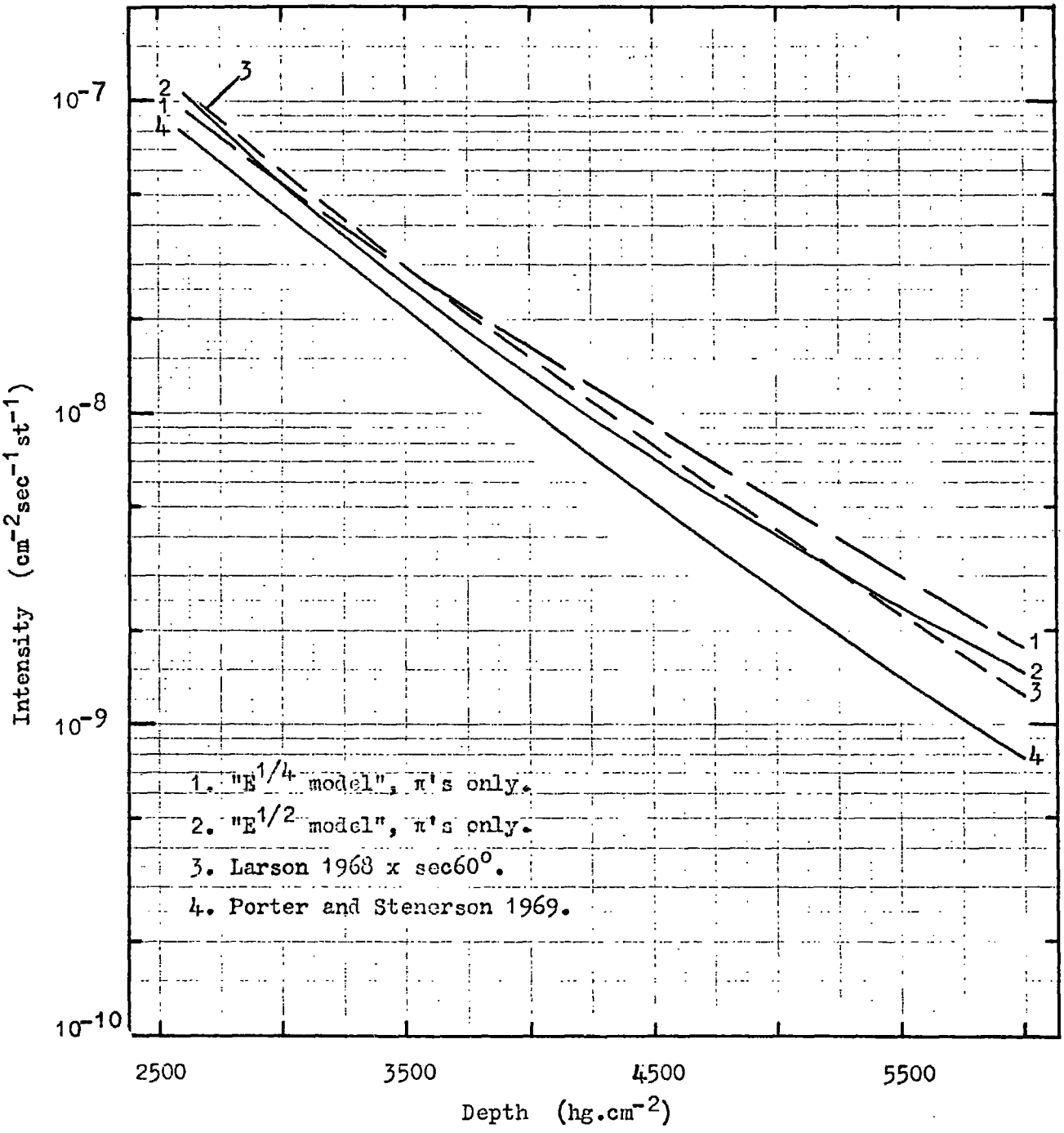

Fig. 5.11. Depth intensity curves for θ=60°.

if a different b value is chosen e.g. at a zenith angle of 60° the "$E^{\frac{1}{4}}$ model" gives an approximate fit if a b value of $4.0\ 10^{-6}\ g^{-1}\ cm^2$ is assumed, and in fact there is evidence for values higher than $3.5\ 10^{-6} g^{-1} cm^2$ (see section 5.4.5d). However, this will destroy the fit with the measured vertical depth intensity curve and will still not give agreement with the angular variation of the single muons found by Porter and Stenerson.

5.4.2 Comparison of the Experimental and Theoretical Decoherence Curves of High Energy Muons.

As previously mentioned two sets of results have been published concerning the decoherence curve of high energy muons obtained from the Utah detector, those of Porter and Stenerson and the later ones of Coats et al.(1969) which extend the decoherence curve out to muon separations of about 50 metres.

The former results have already been shown to be internally inconsistent and so only a brief comparison will be made. Considering the mean radius of detected showers Porter and Stenerson find a value of $\sim$ 4 - 5 metres in the zenith angle range 50° - 60° and depth range 2400 - 2900 $gm.cm^{-2}$, this latter corresponding to a muon threshold energy of $\sim$1100 GeV (for b = $3.5\ 10^{-6}\ gm^{-1}cm^2$). This is to be compared to a mean radius of $\sim$9 metres expected from the "$E^{\frac{1}{4}}$ model" and an even bigger value from the "$E^{\frac{1}{2}}$ model". For the same depth bin in the angular range 40° - 50° the experimental value of the mean radius is $\sim$ 5 - 7 metres and this is to be compared with an expected value of $\sim$ 7 metres from the "$E^{\frac{1}{4}}$ model" and a somewhat bigger value from the "$E^{\frac{1}{2}}$" one.

Porter and Stenerson have also quoted a value of $3.4 < \delta < 4.0$ for the exponent of the muon number spectrum if it is assumed that it can be represented by a power law. Figure 5.12 shows the number spectra of muons, predicted by the "$E^{\frac{1}{4}}$" and "$E^{\frac{1}{2}}$" models, of energies greater than 1000 GeV at a zenith angle of 60° assuming the primary spectrum given by equation 4.23. The same spectrum has been used for each model since we are only interested in the approximate slopes of the spectra. The spectra only go up to showers containing 10 muons but this covers the range of showers which contribute to the singles and doubles in the Utah detector in the relevant energy and zenith angle ranges. Thus for the "$E^{\frac{1}{4}}$ model" doubles come typically from showers containing about 5 muons, singles from showers containing 1 to 2 muons and triples from showers containing about 10 muons. The corresponding values for the "$E^{\frac{1}{2}}$ model" being a little larger due to the relatively wider showers given by this model.

It is seen that in the range of muon sizes covered a power law is a fairly good approximation for both models. For the "$E^{\frac{1}{4}}$ model" the slope of the spectrum, δ, is ~ 3.5, while for the "$E^{\frac{1}{2}}$ model" $\delta \simeq 3.0 - 3.2$. The reason for the latter curve being less steep is the greater efficiency of the model for producing high energy muons at high primary energies. For the same reason heavy primaries would also cause a flattening of the spectra. Comparing the above values of δ with the experimental value of $3.4 - 4.0$ it seems that the "$E^{\frac{1}{4}}$ model" gives the best fit but obviously no definite conclusions can be drawn because of the approximate nature

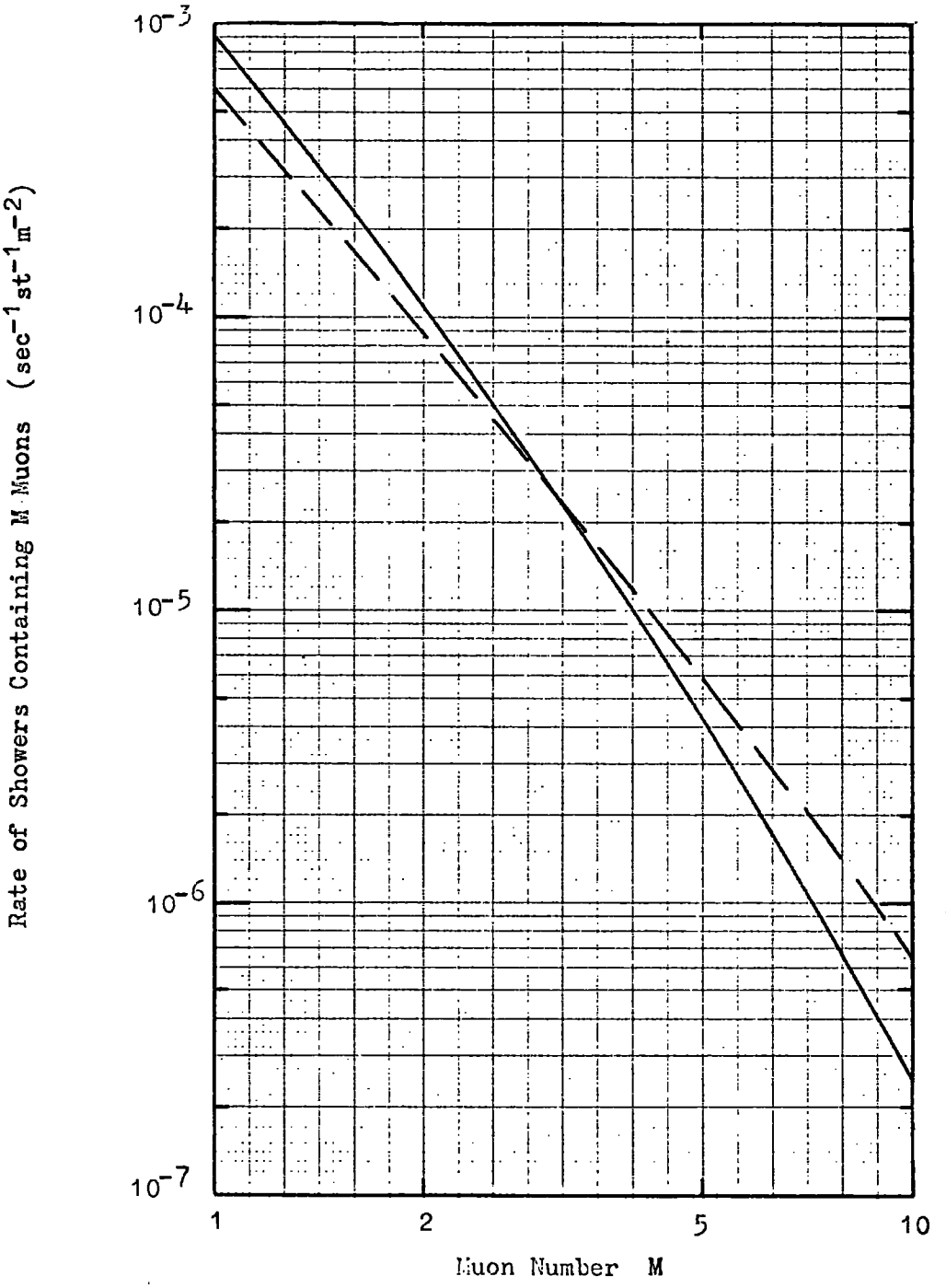

Fig. 5.12. Muon multiplicity spectrum predicted by the "$E^{1/2}$ model" (dashed line) and the "$E^{1/4}$ model" (full line) for $\theta=60^{o}$, π's only, $E_{\mu}>1000$ GeV and Spectrum C.

of the Utah results. However, the experimental and theoretical results can be seen not to strongly contradict each other.

Coats et al. (1969) have measured the decoherence curve of muons out to about 50 metres and have given a decoherence curve corresponding to a mean zenith angle of 45° and a threshold energy of 1000 GeV. The method of analysis is given in section 5.3.3. A comparison is now made with the expected curves based on a variety of assumptions about the value of the mean transverse momentum and the form of the transverse momentum distribution. These calculations have been described in Chapter 4.

It has been seen already that the difference in the decoherence curves due to the different p_t-distributions is significant. However, the data so far obtained experimentally are not great enough to allow a distinction to be made between them. Consequently an attempt has been made to try and estimate the value of $\langle p_t \rangle$ using the C.K.P. distribution.

Figure 5.13 shows the decoherence curves so obtained for four different values of $\langle p_t \rangle$ each curve being normalized to the total number of observed pairs, compared with the experimental points. A χ^2-test gives a best fit value of $\langle p_t \rangle = 0.72 \pm 0.08$ GeV/c.

Since the majority of the experimental data come from muon separations of less than about 25 metres, where the decoherence curve is not very sensitive to the shape of the transverse momentum distribution, the mean transverse momentum of the other distributions must also be close to 0.72 GeV/c.

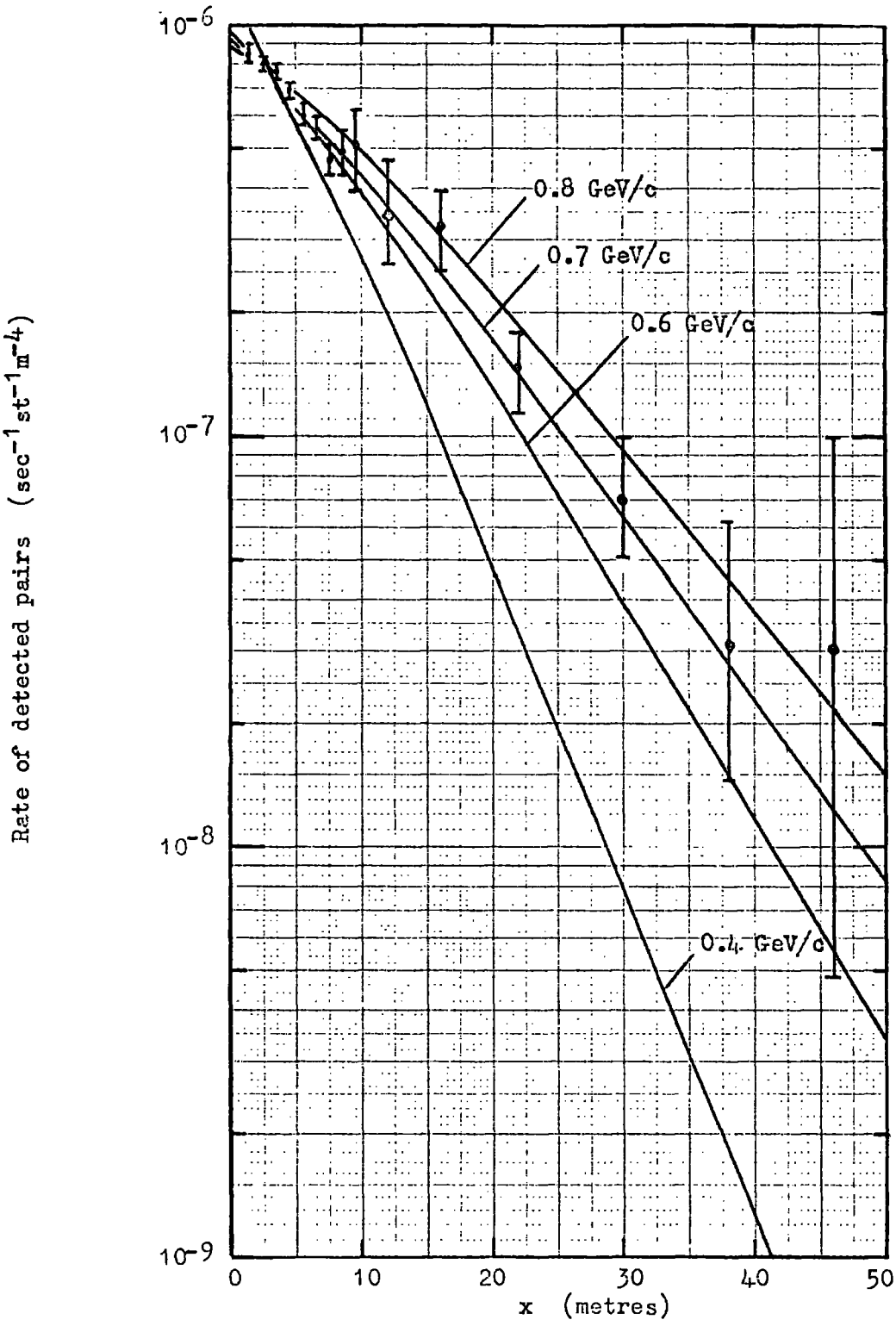

Fig. 5.13. Comparison of the measured decoherence curve with the theoretical curves obtained using the C.K.P. p_t-distribution and different values of $\langle p_t \rangle$. $\theta=45^{\circ}$, $E_\mu>1000$ GeV, "$E^{1/4}$ model".

It should be noted that the theoretical curves calculated refer to the "$E^{\frac{1}{4}}$ model". Calculations for the "$E^{\frac{1}{2}}$ model" give a mean transverse momentum ~ 0.2 GeV/c less than the above value.

The mean value obtained above is only valid under the assumptions made. It has been assumed that the primary cosmic rays consist only of protons. If heavies are present to the extent considered in the two spectra given by De Beer et al. (1969) below 10^{15}eV then some flattening should occur in the decoherence curves and a smaller value of $< p_t >$ would be obtained. Approximate calculations have been made for this composition and it is estimated that the mean transverse momentum will be reduced by the order of 0.05 GeV/c (although it is conceivable that the effect will be larger).

Fluctuations in the multiplicity have also been considered using the distribution suggested by Imaeda (1962)

$$f(n_s)\, dn_s \propto n_s^2 \exp\left(-\frac{3n_s}{\bar{n}_s}\right) d n_s \qquad 5.15$$

where $\bar{n}_s$ is the mean multiplicity. These approximate calculations indicate that the effects on the decoherence curve are very small.

Another effect that may be important are correlations of n_s and p_t e.g. Elbert et al. (1968) have found that in 25 GeV/c $\pi^- p$ collisions $< p_t >$ is inversely related to the multiplicity of the secondaries. In view of the lack of information about the likely magnitude of the correlations at the very high energies involved, however, no calculations have been carried out.

It should be noted that the effects of geomagnetic deflection and Coulomb scattering have been neglected. The former will be the most important here and the effect of both will be to reduce

the mean value of transverse momentum found.

Also the Utah data is a combination of the results from the main detector and from the out-riggers. If any systematic difference exists between these results the value of $< p_t >$ obtained will be affected, although there is no apparent reason why such a difference should exist.

One further point should be made that the analysis is based on the assumption that the mean energy for all separations of muons is $\sim 2\ 10^5$ GeV and the lateral distributions have been assumed to have the shape corresponding to this irrespective of energy. In practice this will not be the case. One would expect that the mean energy contributing to each separation will vary. Since the lower energy showers have wider lateral distributions and because of the steepness of the primary spectrum one would expect the mean energy contributing to decrease with increasing muon separations. This would mean that the average radius of the showers detected was a function of the separation of the muons. The effect of this would probably lead to a flattening of the decoherence curve. If one assumed that $< p_t >$ was independent of energy this would lead to a reduction in its value.

Assuming that heavy primaries are present in the primary cosmic radiation to the extent assumed in Section 4.10 leads to a value of the mean transverse momentum of 0.67 ± 0.1 GeV/c for the "$E^{\frac{1}{4}}$ model" and a value of ~ 0.5 GeV/c for the "$E^{\frac{1}{2}}$ model" under the approximations considered above.

5.4.3. Comparison of the Experimental and Theoretical Density Spectra of High Energy Muons.

As mentioned in Chapter 4 calculations have been made on the density spectra of high energy muons at a zenith angle of 60° under different assumptions about the primary mass composition and the multiplicity law of the secondary particles produced in high energy interactions. To allow for the large area of the Utah detector the calculations were made for a detector area of 20 m^2 which is about the effective area of the Utah array at 60°. However, the sensitive area is a function of azimuthal angle and the multiplicity of detected muons and no allowance has been made for this in the calculations.

Turning to the density spectra of Porter and Stenerson, no fit was obtained for the shape of the spectra which was significantly better than several others. The shape in the density region 10^{-3} - 10^{-2} m^{-2} seems to be fairly independent of the parameters used but in other density regions wide variations in shape seem possible while still fitting the experimental data.

Despite these facts a comparison of the predicted and empirical density spectra is useful because it enables one to see which models are most likely to fit the experimental data and what modifications to the models are necessary to bring about agreement.

Figure 5.14 shows a direct comparison between the preferred Utah curves for threshold energies of 1000 and 2000 GeV and the predictions of the "$E^{\frac{1}{4}}$ model", $\langle p_t \rangle$ = 0.4 GeV/c, folded in with the modulated

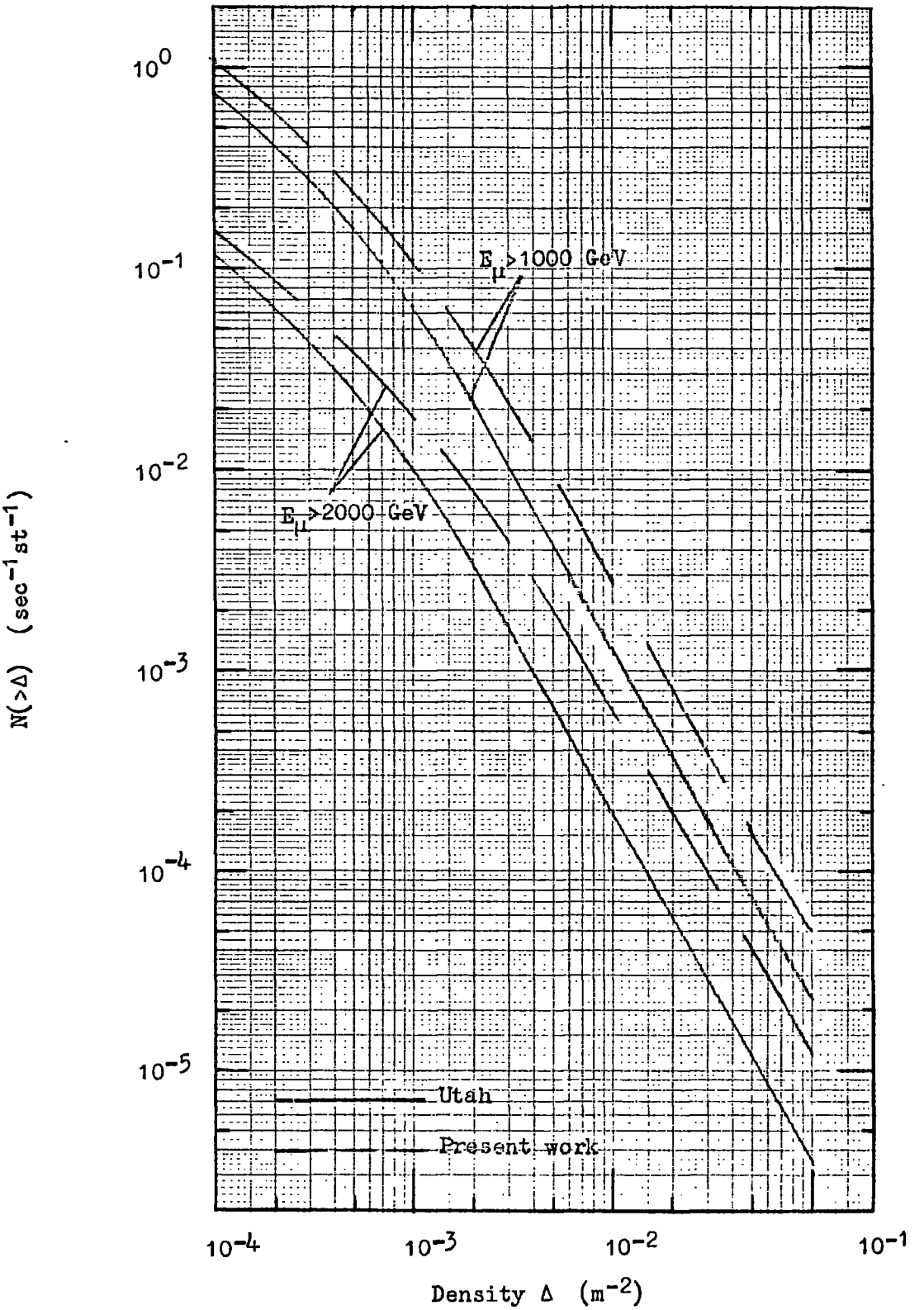

Fig. 5.14. Integral density spectra - comparison with the Utah empirical spectra. Modulated spectrum, π's only, $<p_t>$=0.4 GeV/c, '$E^{1/4}$ model", θ=60°.

primary spectrum i.e. Spectrum B (see Chapter 4).

Figure 5.15 (a) gives the ratio, R, of the calculated density spectra to the corresponding preferred Utah density spectra plotted as a function of density, Δ , for various models and two threshold energies, assuming the modulated primary spectrum. Also shown are the approximate median energies corresponding to the given densities for the "$E^{\frac{1}{4}}$ model".

Considering the "$E^{\frac{1}{4}}$ model" first one sees that over the density range covered, which corresponds to the range contributing mainly to doubles and triples, the theoretical curves are higher than the empirical ones everywhere, thus predicting more multiple muon events than were observed. In order to try and get a better fit a slow increase in $< p_t >$ with increasing interaction energy has been considered as suggested by De Beer et al. (1968b). This has some justification from the comparison between the predicted and measured decoherence curve which indicated a value of $< p_t > = 0.67 \pm 0.1$ GeV/c at primary energies of $\sim 2\ 10^5$ GeV (see section 5.4.2). This is to be compared with a value of $< p_t > = 0.5$ GeV/c, at the same energy, given by De Beer et al.

It can be seen that although there is some reduction in the predicted density spectra it is not big enough to bring about agreement particularly at the 2000 GeV energy threshold.

When 20% kaons are added to the secondary component the fit becomes worse, particularly at high densities (see figure 5.15(b)). This is because of the greater efficiency of kaons in producing high energy muons. It should be noted that the mean transverse

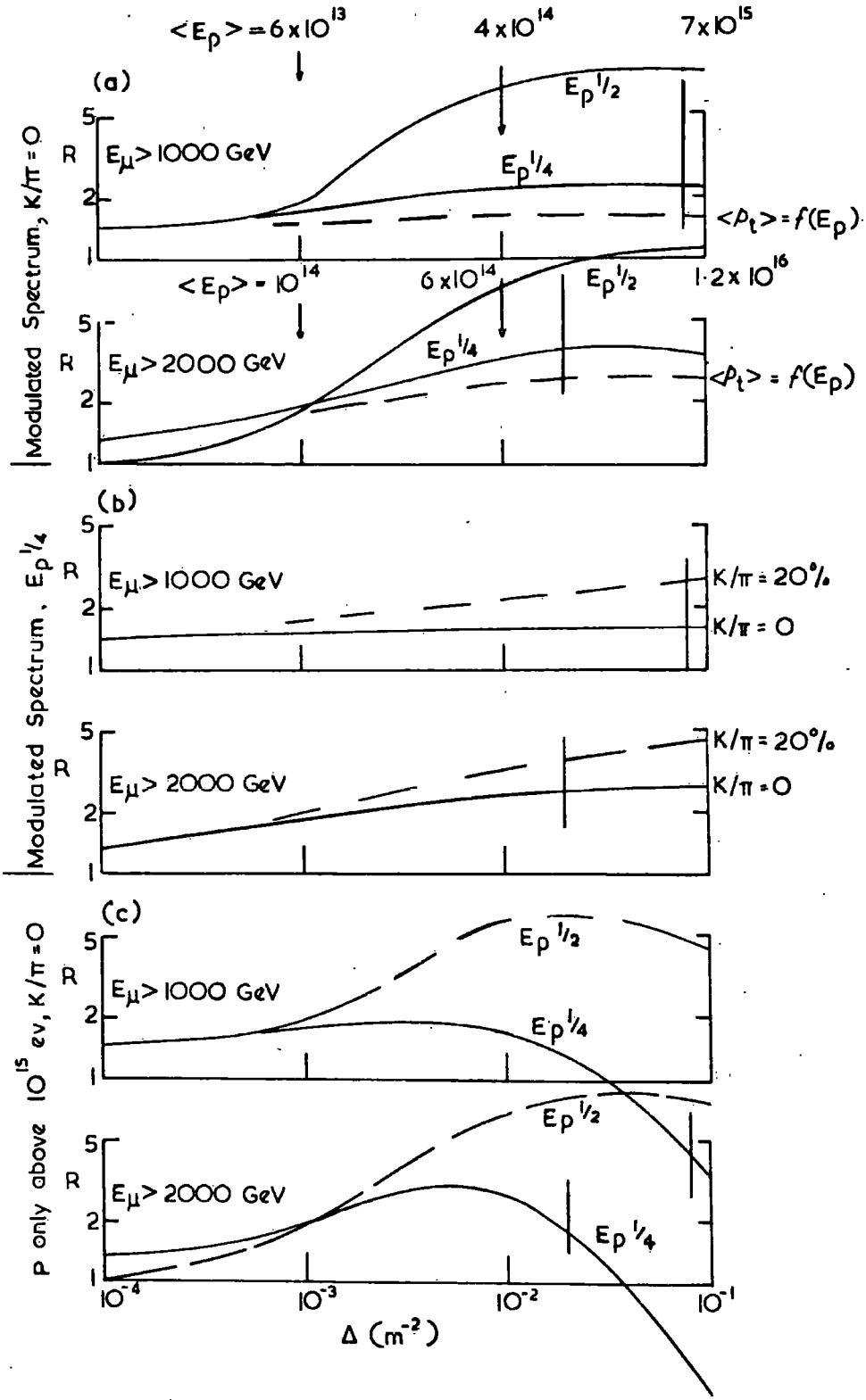

Fig. 5.15 Ratio R of calculated integral density spectrum to Utah empirical spectrum. (The short vertical lines mark the end of the region of good statistical accuracy.)

momentum has been assumed to be the same as that for the pions in this calculation. There is some evidence, however, that this is not the case (Bigi et al. 1962) and that the value for kaons is higher. Thus the contributions indicated are upper limits to the intensity.

Taking the primary spectrum to consist only of protons above $\sim 10^{15}$ eV i.e. Spectrum A, results in the density spectra falling much more rapidly than previously at densities above 10^{-2} m^{-2}. This is clearly seen in figure 5.15 (c) for a mean transverse momentum of 0.4 GeV/c. In fact the fall is so rapid that the predicted density spectra fall below the preferred Utah ones at high densities. However, if instead of taking the preferred Utah curves we take those corresponding to the set c parameters (see section 5.3.2) then the fit at the higher densities is improved although it is made worse at the lower densities and in the density region 10^{-2} - 10^{-3} m^{-2} it is not greatly changed the predicted curves still being higher than the empirical ones in this latter region, the discrepancy increasing with threshold energy.

The fit in this region can be improved if instead of taking heavy primaries to be present the primary spectrum is considered to contain only protons and to have the form given by equation 4.23 i.e. Spectrum C. The discrepancy still increases with increasing threshold energy, however, and the fit at low densities becomes worse, see Figure 5.16.

Considering the "$E^{\frac{1}{2}}$ model" and the modulated primary spectrum, figure 5.15 a, one sees that the fit is much worse than that obtained for the "$E^{\frac{1}{4}}$ model", the density spectra of the former being much

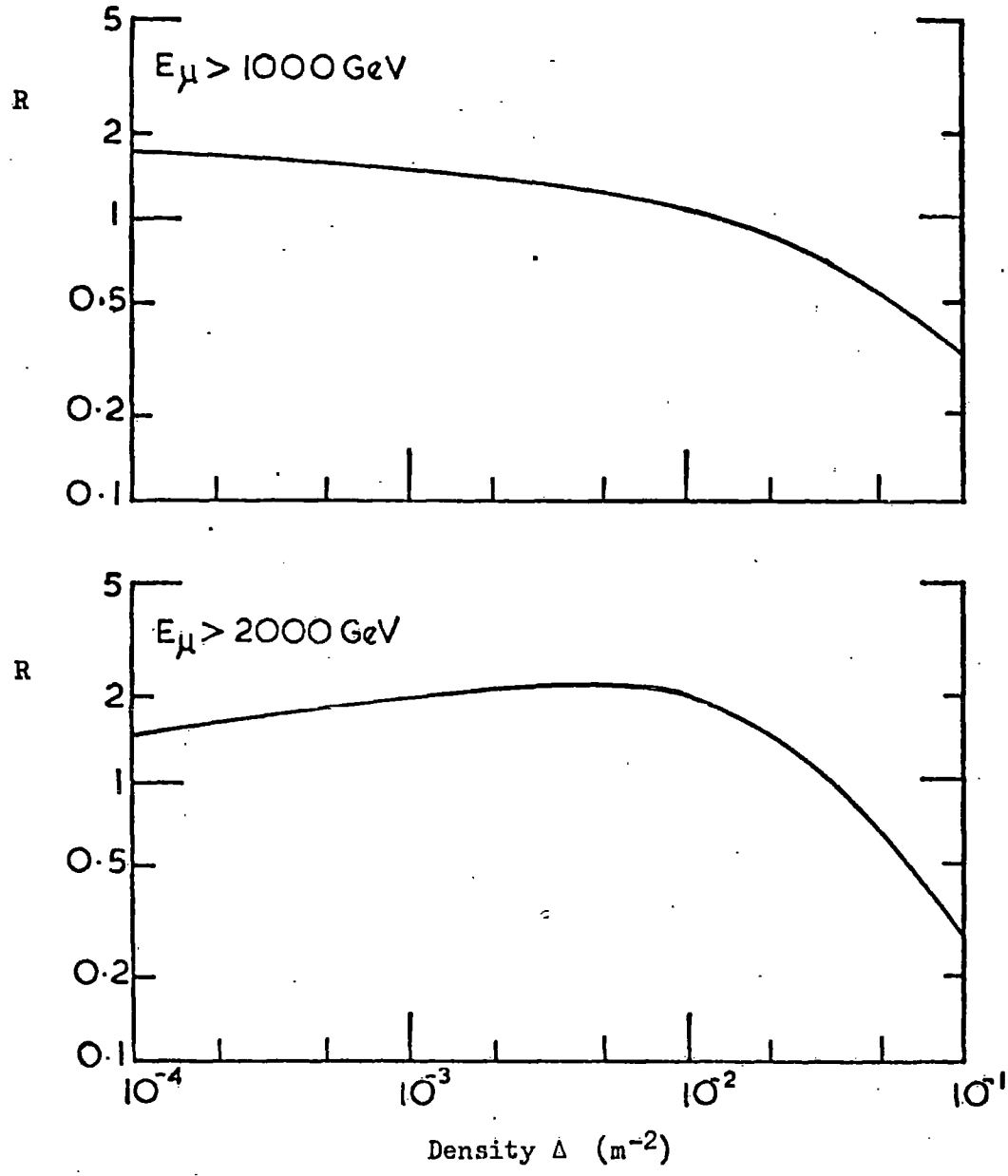

Fig. 5.16. Ratio R of calculated integral density spectrum to Utah empirical spectrum. "Protons only" primary spectrum, π's only, $\langle p_t \rangle = 0.4$ GeV/c, "E1/4 model", $\theta = 60^\circ$.

higher than those of the latter at high densities for the reasons already given in Chapter 4.

When the model is folded in with the spectrum containing only protons above 10^{15}eV i.e. Spectrum A the fit is improved slightly at the higher densities but is still very poor, see figure 5.15c.

From the above comparison one must conclude that none of the models used gives a good fit to the shape of the preferred Utah spectra. This is not altogether unexpected because of the semi-empirical nature of the latter. However, the above comparison enables us to eliminate those models which cannot be expected to give agreement with the observed rates of Porter and Stenerson.

Thus it seems that the "$E^{\frac{1}{2}}$ model" predicts too many multiple events irrespective of the primary spectra which have been considered. The "$E^{\frac{1}{4}}$ model" also predicts too many events when folded in with the modulated spectrum even when a slow rise in $\langle p_t \rangle$ with interaction energy is allowed.

The cases when the "$E^{\frac{1}{4}}$ model" is folded in with a primary spectrum containing only protons above 10^{15}eV and one consisting only of protons are not so clear-cut, since the predicted density spectra cross-over the Utah spectra, and so it is not possible without further calculations to say whether the predicted and observed rates of multiples agree.

5.4.4. A Comparison of the Predicted and Measured Rates of Multiple High Energy Muons.

In determing the empirical density spectra the predictions are summed over a variety of zenith angles and depths according to the assumptions made concerning these variations and compared with the

experimental results. The parameters which give a fit using a χ^2 - test at the 30% confidence level are then found. This is to improve the statistical accuracy of the results and to make them more easily comparable with other experimental results and with theoretical predictions. However, this makes it very difficult to estimate the experimental errors since the errors on the parameters of the density spectra are not given.

The rates of doubles and triples through 20 m^2 have been calculated as a function of threshold energy from the preferred Utah density spectra for a zenith angle of 60°. These are shown in figure 5.17.

In order to make an estimate of the errors on the rates of doubles the statistical errors on the number of events detected between zenith angles 50° - 70° have been evaluated using the figures given in table 5.2. except for the last point which has had an error of $\pm$ 25% imposed on it since the errors for doubles should not be larger than for triples. Obviously this does not give the true errors because the assumed function for the density spectra should tend to make the real errors smaller than those given, and so these should be regarded as upper limits.

In the case of triples the rates calculated from the density spectra based on the parameter sets a and c have been compared, i.e. the two most widely differing sets of curves, and found to differ by ~25%, being lower in the case of the set c parameters. Thus since both sets of curves fit the experimental data it seems reasonable to assume an error of ~ $\pm$ 25% on the rates of triples, and this has

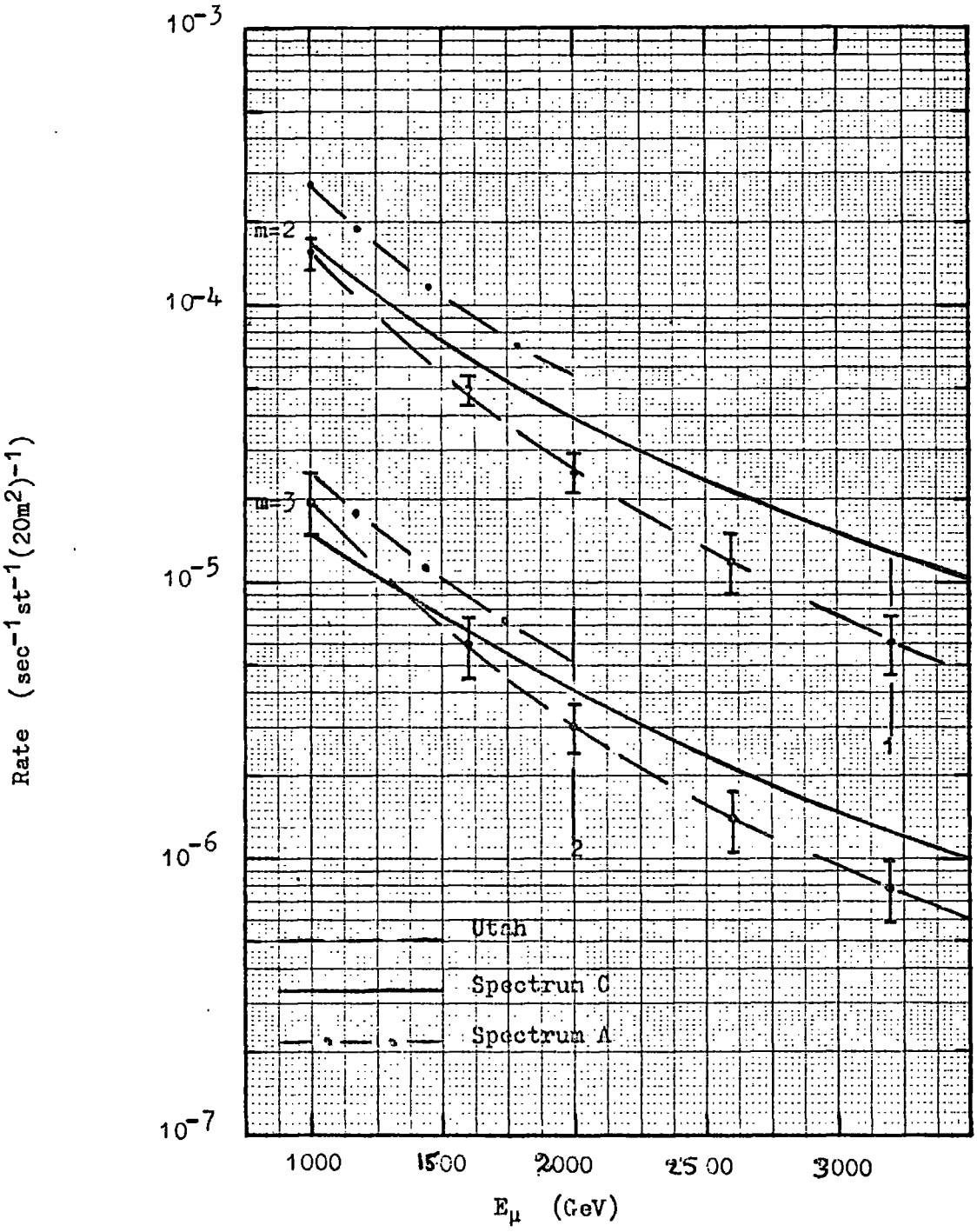

Fig. 5.17. Comparison of the frequency of detecting m muons in the Utah detector (obtained from the empirical density spectra) with the predictions of the "$E^{1/4}$ model" as a function of threshold energy at $\theta=60^{\circ}$. The vertical lines marked 1 and 2 represent the approximate limit of the experimental data.

been used. The same method could not be used for doubles since the curves are normalized to give agreement with the observed number of doubles.

Also shown for comparison are the rates predicted by the "$E^{-\frac{1}{2}}$ model" assuming the primary spectrum consisting purely of protons, Spectrum C, and less accurately calculated rates for the primary spectrum containing only protons above 10^{15}eV, Spectrum A.

From this comparison it is seen that the predicted curves are less steep than the Utah ones for both primary spectra. This is reflected in the density spectra comparison where the ratio of predicted to empirical density spectra is seen to increase with threshold energy for all models considered.

Considering the curves for Spectrum C it is seen that the rates of doubles agree with the experimental rate at a muon threshold energy of 1000 GeV but diverge above this and lie outside the errors. In the case of triples the predicted curve is lower than the Utah one below threshold energies of ~ 1500 GeV but above this it is seen that the curves tend to diverge.

The effect of straggling of the muons has been neglected in the Utah curves and this will tend to increase the discrepancies at higher threshold energies.

5.4.5. Discussion of the Comparison Between the Experimental and Theoretical Density Spectra and Rates.

One must conclude from the above comparisons that none of the models considered is capable of giving good agreement with the Utah results. All the predictions are found to be higher than the

experimental ones and the discrepancies increase with threshold energy.

From the comparison of the density spectra when the modulated primary spectrum is used it is clear that the "$E^{-\frac{1}{4}}$ model" gives a better fit than the "$E^{-\frac{1}{2}}$ model" with experiment but the discrepancy is still serious even when a slow increase in $<p_t>$ with interaction energy is allowed for. The inclusion of kaons makes the discrepancy greater.

When the primary spectrum consisting of protons alone above 10^{15}eV is considered with the "$E^{-\frac{1}{4}}$ model" the density spectra fall sharply above densities $\sim 10^{-2}$ m^{-2} and fall below the preferred Utah curves above these densities. Furthermore the predicted rates of doubles and triples are higher than found experimentally, the disagreement increasing with threshold energy. The density spectra for the "$E^{-\frac{1}{2}}$ model" are higher than for the "$E^{-\frac{1}{4}}$ model" and the fit with the experimental data is worse.

Comparing the predicted rates with the experimental rates using the primary spectrum consisting purely of protons shows that at higher threshold energies one still gets too many events predicted using the "$E^{-\frac{1}{4}}$ model". This indicates that adjustments in the primary composition alone will not be sufficient to bring about agreement between the predicted and observed results.

Assuming that the basic assumptions about the energy distribution of the secondaries is correct, a number of possible modifications to the model can be considered to obtain better agreement between experiment and theory.

(a) Transverse Momentum.

Considering the "$E^{-\frac{1}{4}}$ model" there is some evidence already from the

decoherence curve of Coats et al. (1969) that the value of the mean transverse momentum at an energy of $\sim 2\ 10^5$ GeV is somewhat higher than that assumed in most of these calculations (i.e. 0.4 GeV/c). This is higher than values obtained at lower energies by other experiments and lends support to the suggestion of De Beer et al. (1968b) that there is a slow increase in the mean transverse momentum with increasing interaction energy.

As has been seen already the increase suggested by De Beer et al. is not sufficient to bring about agreement when the "$E^{\frac{1}{4}}$ model" is used with the modulated spectrum and so to obtain agreement one must either postulate a more rapid increase in $< p_t >$ which is not ruled out by the results from the decoherence curve analysis, or postulate a slow increase in $< p_t >$ together with a phasing out of the heavy primaries over a greater energy region than has been considered so far.

Considering the "$E^{\frac{1}{2}}$ model" one could not get agreement, even if there was no heavy component present, with a slow increase in $<p_t>$. The decoherence curve analysis also implies that if the multiplicity law did vary as $E^{\frac{1}{2}}$ then the increase in $<p_t>$ with interaction energy would be less rapid than for the "$E^{\frac{1}{4}}$ model".

(b) Reduction of the Inelasticity of Interaction.

A possible way of reducing the number of muons detected is to decrease the inelasticity of the interactions thereby decreasing the height of origin of the muons. Because the muons would be formed in a region where the atmospheric density was greater their parent pions would have a greater chance of interacting and fewer would decay into

muons. However, there is no evidence from other experiments to support this and difficulties would almost certainly arise in explaining shower absorption characteristics. There is also the fact that a decrease in inelasticity would necessitate a rise in the assumed primary spectrum in order to maintain agreement with extensive air shower measurements, and this would tend to compensate for the loss of muons which would otherwise arise.

(c) Logarithmic Multiplicity Law.

If one were to use a logarithmic multiplicity law the number of pions produced in an interaction would be decreased and so, as in the case of a reduction in the inelasticity, the muons would be formed lower down in the atmosphere leading to a reduction in their number for a given primary energy. It would also lead to a reduction in the assumed primary energy spectrum in order to maintain agreement with extensive air shower measurements. On the other hand the lateral distributions obtained using this type of multiplicity law will be narrower than obtained using the "$E^{\frac{1}{4}}$" and "$E^{\frac{1}{2}}$" models and this will compensate to some extent the decrease in the density spectra due to the other causes.

There is some evidence, however, that a logarithmic increase in the multiplicity is not likely. Machin et al. (1969) have measured the lateral distributions of high energy muons at large distances from the shower core, and Orford and Turver (1969) have made calculations to explain these results. These workers conclude that the experimental results can be explained in terms of an "$E^{\frac{1}{4}}$ model" only if the primary particles are heavy (of mass $\sim$ 56). Thus in order to explain them in terms of a logarithmic multiplicity

law, if indeed this was possible, an even higher mass would be necessary and this seems very unlikely.

There is also evidence that with a multiplicity law varying as $E_p^{\frac{1}{4}}$, assuming the C.K.P. model, the heights of origin of the muons are lower than those determined experimentally (Firkowski et al. 1967; Baxter et al. 1968) and if this is so then the situation will be worse for a logarithmic type multiplicity law.

It is therefore thought that this is probably not an explanation of the discrepancy between the Utah results and theory.

(d) A Change in the Rate of Energy Loss.

The average rate of energy loss by muons in "standard rock" with $\bar{Z} = 11$, $\bar{A} = 22$, $\overline{(Z^2/A)} = 5.5$ and $\rho = 2.65$ g. cm^{-3} is approximately given by

$$-\frac{\partial E}{\partial x} = 1.88 + 0.077 \ln\left\{\frac{E'_m}{mc^2}\right\} + b(E).E \quad \text{MeV g}^{-1}\text{cm}^2. \qquad 5.16.$$

(e.g. Hayman, Palmer and Wolfendale, 1963), where

$$E'_m = E^2 \left\{E + \frac{m^2c^4}{2m_e c^2}\right\}^{-1}$$

is the maximum transferrable energy for a muon of energy E, rest mass m to an electron of rest mass m_e and x is the depth in g.cm^{-2}. There is general agreement as to the values of the first two terms in equation 5.16 which arise from energy losses due to ionization and excitation, while the last term contains losses from bremsstrahlung, pair production and nuclear interactions of muons and its value is not so well known. In fact b should vary slightly with energy, but over the range 500 - 10,000 GeV the variation is small.

If b(E) is replaced by its effective value, b, over the energy range of interest the equation can be solved, following Barrett et al. (1952), as

$$E = \frac{a'}{b} \left(\exp(bh) - 1\right) \qquad 5.17$$

where $a' = 1.88 + 0.077 \ln \left\{ \frac{E^2}{e\, m(E + eA)} \right\}$ MeV g^{-1} cm^2

$A = 11.3$ Gev and $e = 2.7$.

From equation 5.17 the average range-energy curve can be obtained for muons.

Porter and Stenerson have used an effective b value of $3.5\ 10^{-6}$ $g.^{-1}$ cm^2 which was derived by Kobayakawa (1967). However, there is a certain amount of doubt about its true value because of a lack of knowledge about the cross-sections of the three processes involved. Hayman, Palmer and Wolfendale (1963), give $b = (3.95 \pm 0.25) \times 10^{-6}$ $g^{-1}.$ cm^2, while Menon and Ramana Murthy (1967) give a value of $(3.6 \pm 0.6) \times 10^{-6} g^{-1}.$ cm^2. The difference in these values comes mainly from the lower value of the photo-nuclear cross section taken by Menon and Ramana Murthy. However, Erlykin (1966) has made calculations on the bremsstrahlung and pair production cross sections and these indicate that even if the photo-nuclear cross section taken by Menon and Ramana Murthy is used then b is at least equal to 4.0 10^{-6} $g^{-1}.cm^2$. Thus it is possible that the value of b used by Porter and Stenerson to convert their measured depths to energies is too low.

To investigate the effects of this the observed rates of doubles and triples through 20 m^2 have been converted from a function of threshold energy to a function of depth using $b = 3.5\ 10^{-6} g^{-1}.cm^2$.

The theoretical predictions for the "$E^{\frac{1}{2}}$ model" and the primary spectrum consisting only of protons (Spectrum C) have been treated in the same way but an effective value of $b = 4.0\ 10^{-6}$ g.$^{-1}$cm^{2} has been used.

Fluctuations in the energy losses have been neglected in the second case, while in the first one they need not be considered as they were not included in the original conversion from depth to threshold energy. Their effect would be to raise the theoretical points at the larger depths.

It is seen in figure 5.18 that there is much better agreement at larger depths than before, although the agreement is not so good at smaller depths, particularly for triples.

Also shown in figure 5.18 are predicted intensities for the primary spectrum consisting of protons only about 10^{15}eV i.e. Spectrum A. It is seen that the predicted rates of doubles are still higher than observed although the fit for triples is quite good. If slightly higher b values were used or an increase in the mean transverse momentum was postulated agreement could possibly be obtained.

However before definite conclusions can be drawn a better knowledge of the experimental errors is required.

(e) Direct Production

As stated previously in order to explain the angular variation of the single muon spectra Bergeson et al. postulated their direct production process of muons. In order to maintain agreement with the vertical depth intensity curve they also postulated an increase in

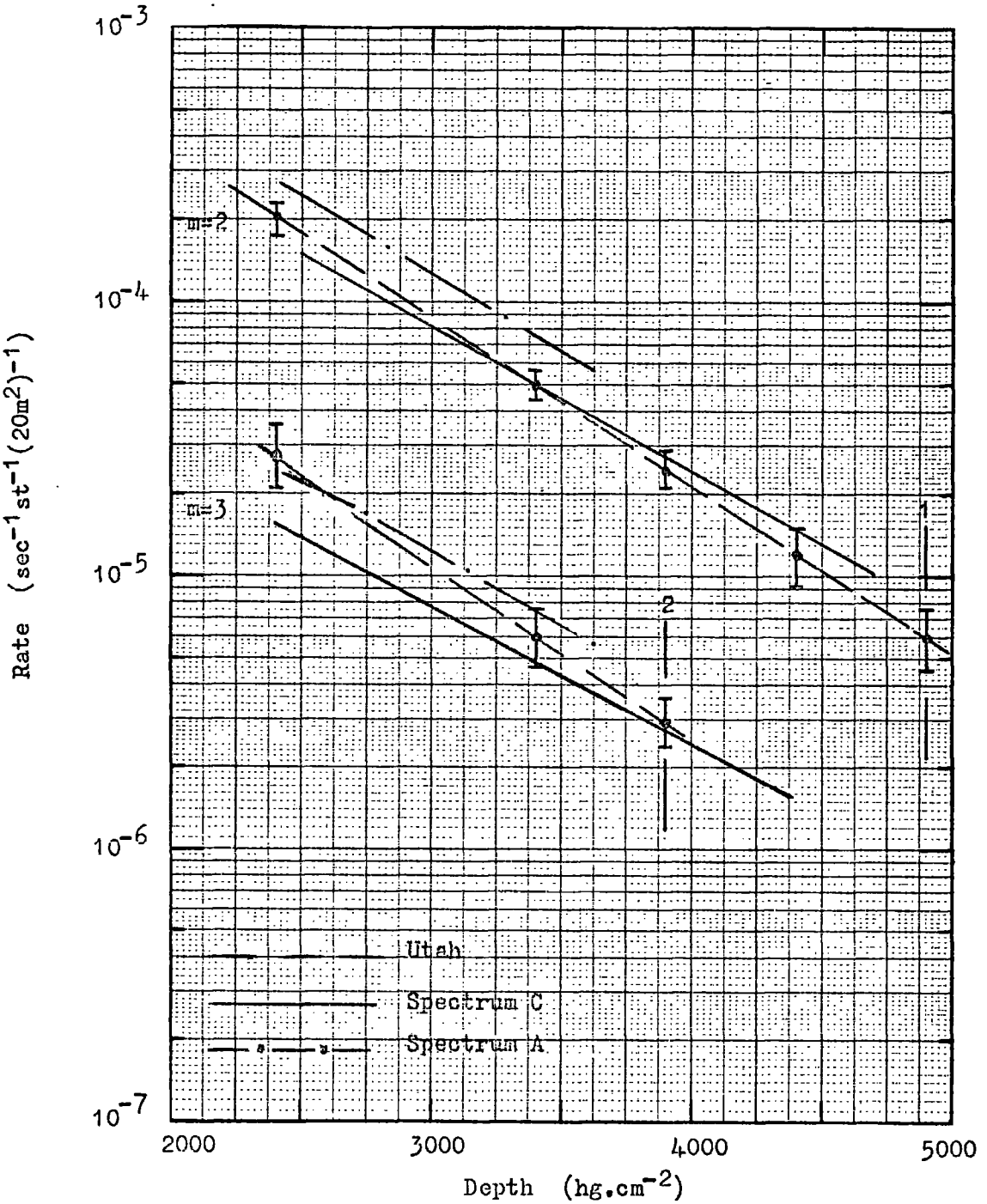

Fig. 5.18. Comparison of the frequency of detecting m muons in the Utah detector (obtained from the empirical density spectra) with the predictions of the "$E^{1/4}$ model" as a function of depth at $\theta=60^{o}$ assuming $b=4.0\ 10^{-6}\ g^{-1}cm^{2}$. The vertical lines marked 1 and 2 represent the approximate limit of the experimental data.

the value of b with increasing muon energy. The actual mechanism of the direct production process is not yet known, in fact it is not even certain that the process exists, and so the effect on multiple muon events is uncertain. However, it is thought that the effect will be small because if it is due to the decay of a massive particle, which is thought to be one possibility, this particle must have a very large mass (> 3 GeV) since it has not been detected at accelerator energies and so the muon produced by its decay will have a very large transverse momentum and the detection probability in the case of multiple events would be expected to be small. Thus it is probable that the main effect of the process on multiples should come from the change in the energy loss coefficient b. An approximate range-energy curve incorporating these values has been constructed from a comparison of the vertical muon energy spectrum given by Bergeson et al. (1968) and the world wide depth intensity curve of Larson. Since these are said to be consistent the range energy curve should also include the effect of fluctuations in the energy loss processes.

Figure 5.19 shows a comparison between the appropriate preferred Utah spectra at 60°, and the different models at threshold energies of 10^3 and $2\ 10^3$ GeV.

Considering the $E^{\frac{1}{2}}$ model folded in with the modulated primary spectrum one sees that at higher densities the theoretical curves are above the preferred Utah ones. For the density spectrum corresponding to a threshold energy of 2000 GeV the predicted one falls below the Utah one at densities less than $\sim 10^{-3}\ m^{-2}$. One could possibly

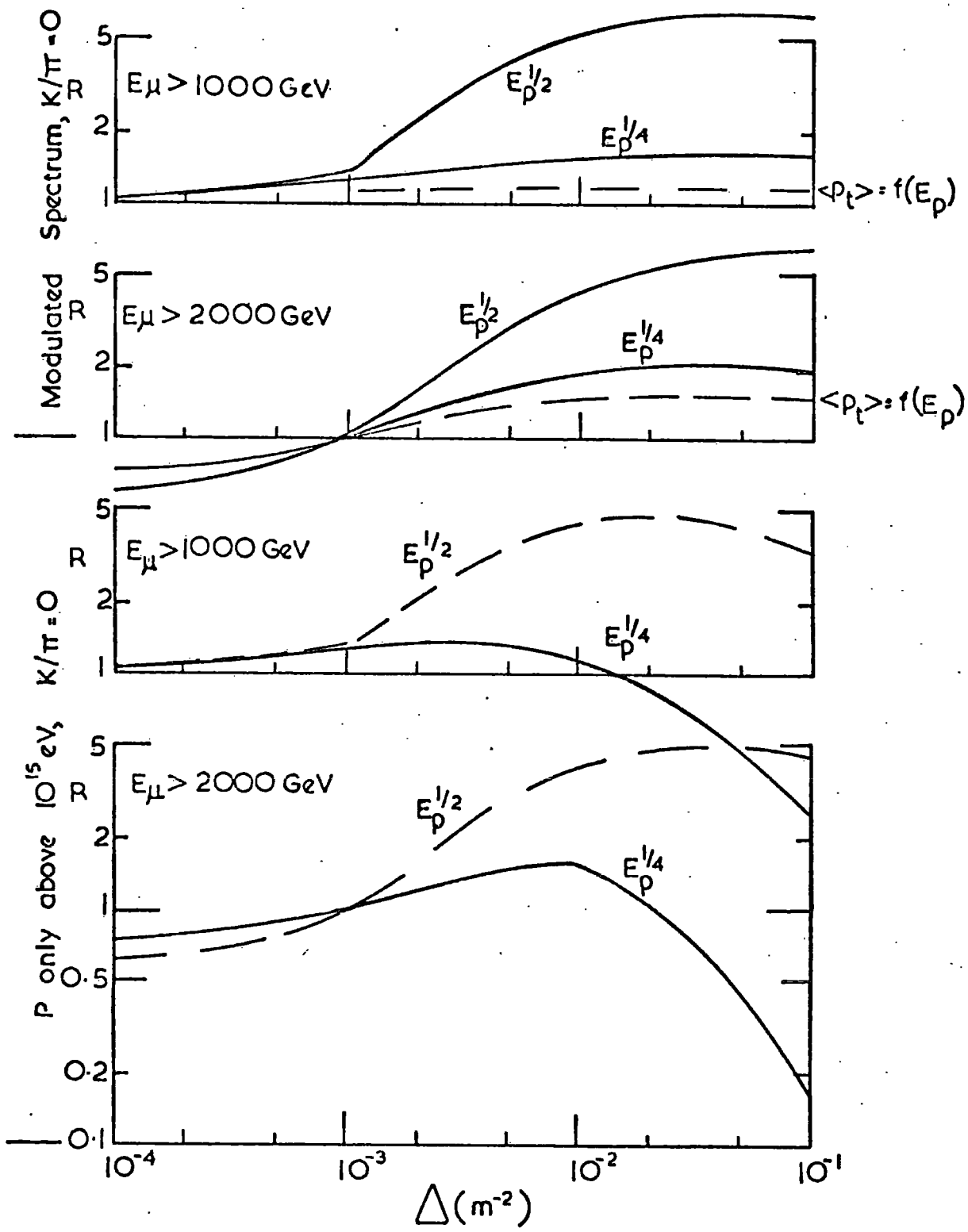

Fig. 5.19. Ratio R of calculated integral density spectrum to Utah empirical spectrum if "direct production" is assumed.

interpret this as due to the Utah spectrum containing singles from the "direct production" process which have not been included in the theoretical curve. The effect of letting the mean transverse momentum rise with increasing interaction energy is to bring the experimental and theoretical curves into better agreement, but in the case of the 2000 GeV threshold curve the fit at high densities is still not good. The addition of kaons will worsen the fit.

When folded in with the primary spectrum containing only protons above 10^{15}eV i.e. Spectrum A, it is seen that the fit is similar to the previous case at densities below $10^{-2}m^{-2}$. However, at higher densities the predicted curves fall below the Utah ones. Comparing the predicted rates for this spectrum with the observed rates (see figure 5.20) it is seen that the predicted rate of doubles is still too high, although the fit for triples is quite good.

Figure 5.20 also shows the variation of rate through 20 m^2 with depth for the "$E^{\frac{1}{4}}$ model" and the spectrum consisting purely of protons i.e. Spectrum C. It is seen that at the lower threshold energies the predicted rates are lower than observed for both doubles and triples and lie outside the estimated errors. However, a better knowledge of the errors is needed before definite conclusions can be drawn.

Considering the fit between the density spectra for the "$E^{\frac{1}{2}}$ model" and the Utah ones it is seen that the fit is still inferior to that of the "$E^{\frac{1}{4}}$ model" and to obtain agreement a large rise in $\langle p_t \rangle$ with interaction energy is required, whichever primary spectrum is used.

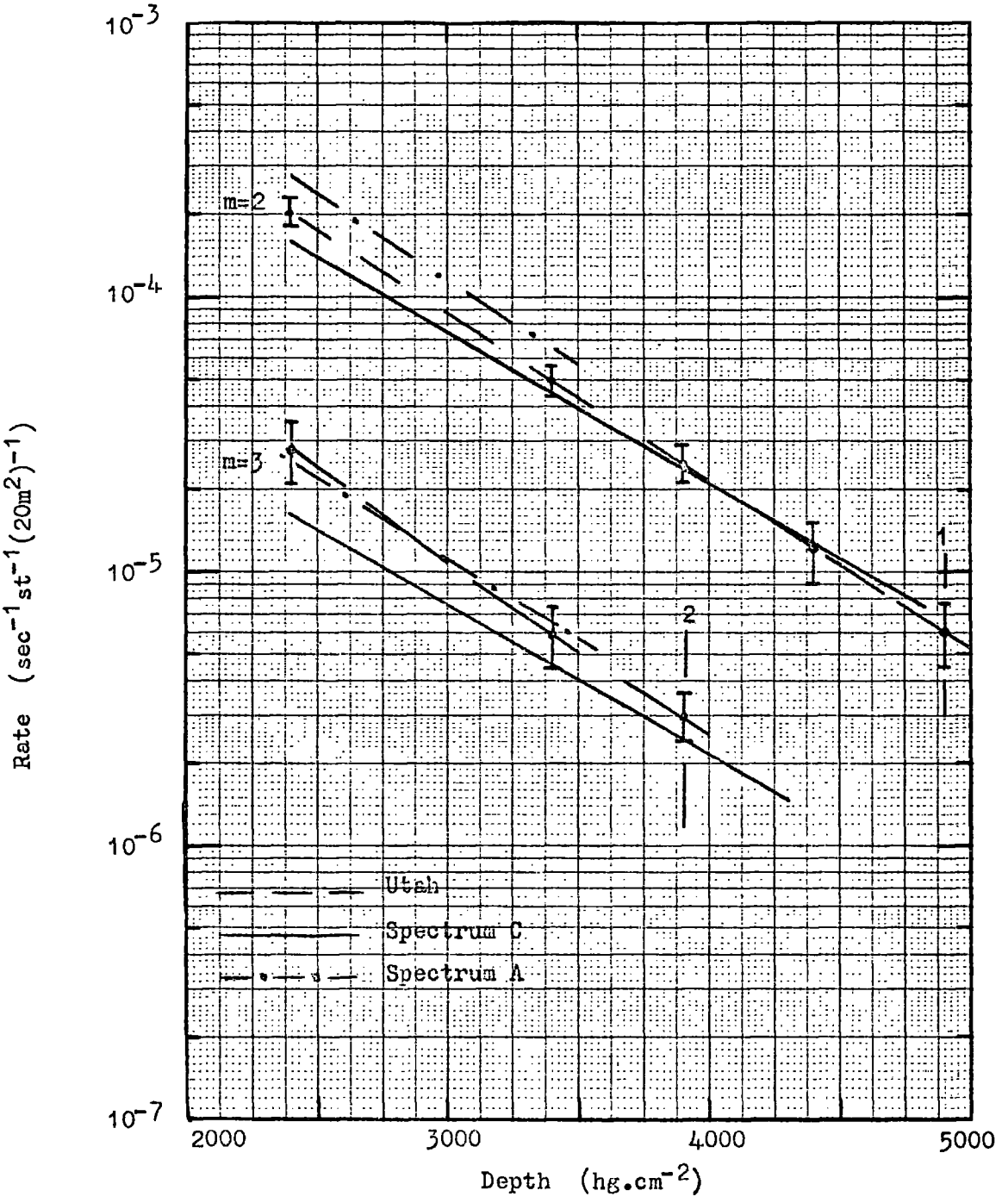

Fig. 5.20. Comparison of the frequency of detecting m muons in the Utah detector (obtained from the empirical density spectra) with the predictions of the "$E^{1/4}$ model" as a function of the depth at $\theta=60^{o}$ assuming "direct production". The vertical lines marked 1 and 2 represent the approximate limit of the experimental data.

However, it should be emphasised that if the so-called "direct production" process does exist, and does contribute significantly to the multiple muon events all the above comparisons will be invalidated since any extra contribution from this process has not been considered in the theoretical predictions.

5.5. Conclusions.

It has been shown in this Chapter that the single muon energy spectrum measured at Utah has a smaller zenith angle dependence than would be expected from either the "$E^{\frac{1}{4}}$" or "$E^{\frac{1}{2}}$" models which are based on muons coming from the decay of pions. If this result is substantiated by further experimental evidence it supports the conclusion of Bergeson et al.(1968) that there are two components contributing to the production of muons, one of which is the normal component due to pion and kaon decay, and the other due to some new process, which becomes important only at very high muon energies. The discrepancy may also be due to some technical cause affecting the experimental results.

The decoherence curve studies of Porter and Stenerson have been shown to be somewhat inconsistent with the theoretical results and also the later ones of Coats et al. (1969). These latter results indicate that the mean transverse momentum of pions in high energy interactions at energies of about 2 10^5GeV is 0.67 $\pm$ 0.1 GeV/c, assuming the C.K.P. transverse momentum distribution for the "$E^{\frac{1}{4}}$ model", and a value $\sim$ 0.5 GeV/c if the "$E^{\frac{1}{2}}$ model" is used. However, more detailed studies may alter these values somewhat. It seems though that a value of 0.4 GeV/c as found at lower energies

will not bring about agreement and so there is evidence for a slow rise in $\langle p_t \rangle$ with interaction energy as suggested by De Beer et al. (1968b). The experimental results are not yet of sufficient accuracy to distinguish between the different forms of transverse momentum distribution that have been proposed by various authors.

The density spectra given by Porter and Stenerson are very difficult to interpret. The basic trouble lies in the fact that the rates of doubles and triples in the experiment seem to have the same dependence on depth as would be predicted by the depth-intensity curve of singles. This is not found to be the case for the theoretical models, which predict a less strong dependence on depth for the doubles and triples. There is also difficulty because of the different zenith angle dependence of the single muon intensity for the theoretical and experimental cases. Thus if some new process is not postulated the number of single muons observed experimentally is less at 60° than is predicted theoretically. If one accepts that the reason for this is due to some new process and that this process is that postulated by Bergeson et al.(1968) then one must make some assumptions as to its effects on the multiple muon events. In any case one cannot expect to get agreement over all zenith angles between the experimental curves and the theoretical curves at low densities where the singles are important.

If the "direct production" process is assumed not to be the cause of the discrepancy in the angular dependence of the single muon intensity and that some other factor is the cause which does not affect the multiple events, then a comparison between the density

spectra and rates at a zenith angle of 60° for each primary spectrum in turn leads one to conclude that:-

i) The modulated primary spectrum predicts too many multiple muons, the discrepancy increasing with threshold energy, for both the "$E^{\frac{1}{2}}$" and "$E^{\frac{1}{2}}$" models. Even if a slow increase in $\langle p_t \rangle$ with interaction energy is allowed and the energy loss coefficient b is raised to $4.0\ 10^{-6}$ g.$^{-1}$cm^2 good agreement cannot be obtained for either model although it is better if the "$E^{\frac{1}{2}}$ model" is used. A faster rise in the mean transverse momentum together with an increase in the value of b could possibly bring about agreement with experiment for the "$E^{\frac{1}{2}}$ model".

ii) The primary spectrum containing only protons above 10^{15}eV also predicts more multiple muons than observed for both theoretical models. Agreement with the Utah rates may be possible if one takes the "$E^{\frac{1}{2}}$ model" and allows a rise in $\langle p_t \rangle$ with interaction energy and/or an increase in the b value. However, agreement with the shape of the preferred Utah density spectra is not possible at high densities.

iii) The "protons only" primary spectrum, which can probably be considered as an extreme case, still predicts too many doubles and triples at higher threshold energies, although the agreement is within the errors at the lower threshold energies for the "$E^{\frac{1}{2}}$ model". If a b value of $4.0\ 10^{-6}$ g^{-1}.cm^2 is used better agreement results at the higher threshold energies, although it deteriorates at the lower threshold energies. Alternatively a rise in $\langle p_t \rangle$ with interaction energy will give a better fit. The shape of the density spectra again do not agree well at high densities with those of Porter and

Stenerson.

If one accepts that the experimentally found angular dependence of single muons is due to the new process proposed by Bergeson et al. (1968) and that its effect on the multiple muon events is small then its main consequence will be the increased energy loss of muons with high energies.

Again considering the primary spectra in turn one can conclude that:-

i) The Modulated primary spectrum still predicts too many multiple events for both the models considered. Good agreement is obtained using the "$E^{\frac{1}{4}}$ model" at a threshold energy of 1000 GeV with the Utah density spectra both in shape and magnitude if a slow rise in $\langle p_t \rangle$ with interaction energy is allowed but the fit at the higher densities for the 2000 GeV threshold is not good.

ii) The primary spectrum containing only protons above 10^{15} eV gives too many doubles although the fit for triples is quite good using the "$E^{\frac{1}{4}}$ model".

A better fit to the doubles could be obtained if the transition to protons took place over a more extended energy region than considered here.

A slow rise in $\langle p_t \rangle$ with interaction energy would give a better fit to the doubles although the fit to the triples would not be so good. However, the experimental errors are uncertain and so a fit may be possible.

The "$E^{\frac{1}{2}}$ model" still predicts too many multiple events.

iii) The 'protons only' primary spectrum gives good agreement with the measured rates of doubles, except at the lower threshold energies, and slightly less good agreement with triples if the "$E^{-\frac{1}{4}}$ model" is used.

The intensities of multiples are higher than measured experimentally, if the "$E^{-\frac{1}{2}}$ model" is used and a large increase in $\langle p_t \rangle$ with interaction energy would be needed to bring about agreement.

It seems then that there are several possible ways of obtaining agreement between experiment and theory and until more definite values of the mean transverse momentum and b are available it is difficult to draw definite conclusions about the primary composition.

It seems that the "$E^{-\frac{1}{4}}$ model" gives better agreement than the "$E^{-\frac{1}{2}}$ model" irrespective of the primary composition above 10^{15}eV. However, the latter model cannot be ruled out completely if one takes into account the uncertainty in the intensity of the primary spectra used with this model and the uncertainties in the value of b and $\langle p_t \rangle$. However, even if the primaries are considered to consist only of protons the primary intensity would have to be reduced by about a factor 3 at $\sim 10^{15}$eV to get agreement with b = $4.0\ 10^{-6}$ g. $^{-1}$ cm^2, although this would be smaller if an increase in $\langle p_t \rangle$ with interaction energy was also assumed.

The fact that the experimental results of Rogers et al. (1969) on the rates of muons at large zenith angles agree with the theoretical predictions of De Beer et al. (1969) in the region corresponding to primary energies below 10^{15}eV gives support to the magnitude of the spectra taken, at least for the "$E^{-\frac{1}{4}}$ model".

The comparison cannot be said to contradict the "direct production" hypothesis. It seems that one of the parameters that can be changed to bring about better agreement is the energy loss coefficient b. If b is changed assuming no "direct production" then the relatively good agreement between the measured vertical depth intensity curve compiled by Larson (1968) and the theoretical curve will be destroyed and it may be necessary to postulate an increase in the primary intensity or the addition of kaons to the secondaries of high energy interactions. On the other hand the "direct production" process enables b to be changed and agreement may still be possible with the measured vertical depth intensity curve. However, if the process has an appreciable effect on multiple muon events the conclusions may have to be changed.

CHAPTER 6.

COMPARISON OF THE PRESENT RESULTS WITH THOSE OF OTHER WORKERS.

6.1. Introduction

The results and conclusions obtained so far are based on the assumption that the C.K.P. energy distribution of secondary particles produced in high energy collisions is valid at energies several orders of magnitude greater than those for which it was originally postulated. This is also true for the majority of the other parameters used in the present work. Thus it is necessary to examine the validity of the model by comparing it with existing experimental data.

A number of workers have proposed different models and their predictions are compared to the present work at high muon energies since the C.K.P. model cannot be considered unique and it is important to know the effects of differing assumptions on the present conclusions.

Finally a comparison of the present work on high energy muons will be made with the existing experimental data in order to test further the validity of the model at high energies and where possible to draw further conclusions about the model parameters.

6.2. Comparison of the General Features of the C.K.P. Model with Experiment.

The general features of the C.K.P. model have been compared with experimental results by De Beer et al. (1966) using a model with similar parameters to those used in the present work. These comparisons related to shower size and the numbers and lateral distributions

of muons having energies less than about 100 GeV.

These workers concluded that the C.K.P. energy distribution predicted with fair accuracy the shape of the muon energy spectrum in showers of size 10^6 particles, although the absolute values tended to be a little lower than found experimentally if protons were assumed to be the primary particles and the multiplicity varied as $E_p^{\frac{1}{4}}$. If a multiplicity law varying as $E_p^{\frac{1}{2}}$ was used, however, the predicted energy spectrum was found to be too high, even if primary protons were assumed. The discrepancy for the $E_p^{\frac{1}{4}}$ multiplicity law could be largely removed if primary particles having a mass ~ 4 were postulated. Thus it seems that the model is capable of predicting the longitudinal development of extensive air showers with reasonable accuracy.

De Beer et al. did not find such good agreement when comparing their predicted muon lateral distributions with experimentally measured ones. For all energy thresholds it was found that the predicted lateral distributions within 10-20 metres of the axis were in excess of the experimental ones. Part of this discrepancy was attributed to experimental errors in core location but this was still not sufficient to bring about agreement and it was found necessary to postulate a cut-off in the transverse momentum distribution for values of p_t less than 0.1 GeV/c to bring about near consistency. The effect of this excess on the density spectra of high energy muons has been considered and found to be small due to the large area of the Utah detector (see Chapter 4).

At large distances from the core the model was found to under-

estimate the number of muons particularly at large muon energies when compared with the results of Barnaveli et al. (1964). This was also found to be the case when De Beer et al. (1968b) compared their predictions with the experimental results of Earnshaw et al. (1967). In both cases a multiplicity law varying as $E_p^{\frac{1}{4}}$ and primary protons were assumed. In order to get agreement the value of $\langle p_t \rangle$ was required to increase with interaction energy. This deficiency could affect the results and conclusions from the analysis of the Utah data but has been allowed for by regarding $\langle p_t \rangle$ as a variable parameter.

De Beer et al. (1968a) have calculated the mean height of origin of muons as a function of primary energy and shower size for the $E_p^{\frac{1}{4}}$ multiplicity law. When these predictions are compared with the experimental results of Firkowski et al. (1967) and Baxter et al. (1968) it is found that the experimental results indicate greater heights of production than predicted theoretically, e.g. Firkowski et al. give the upper limit of the height of production of muons in showers of size $\sim 2\ 10^6$ particles as 10 ± 3 kilometres compared to the predicted height of origin for muons with energies greater than 1 GeV of ~ 4 -5 kilometres.

De Beer et al. (1968a) have also calculated the fluctuations expected in electron and muon numbers for different assumptions about the primary composition and two different models of high energy interactions viz. the so-called C.E. model and the C.K.P. model, both with multiplicity laws varying as $E_p^{\frac{1}{4}}$. The results were found to be quite sensitive to the model adopted. Adcock et al. (1968a) compared

these results with the existing experimental data and found that the C.K.P. model gave good agreement with these.

Thus it seems that the C.K.P. model gives fair agreement with experimental results as far as the longitudinal development of E.A.S. is concerned and can be regarded as a satisfactory first approximation. The situation is not so satisfactory as regards the adopted transverse momentum distribution but tolerable agreement can be obtained with experiment with reasonable modifications.

It is possible that the discrepancy found in the heights of origin of the muons may be linked with the discrepancies found in the lateral distributions but more investigations are obviously needed on this point before definite conclusions can be drawn.

6.3. Comparison with the Theoretical Predictions of Other Workers.

6.3.1. Lal.

Lal (1967) has made one dimensional semi-Monte Carlo calculations on the muon component in the vertical direction for a variety of models based on the C.K.P. energy distribution. His results refer to muon energies above 180 GeV. The different models are described in Table 6.1.

Model A is identical to the "$E^{-\frac{1}{4}}$ model" used in the present work except that the spread in muon energies has been approximated by assuming that $E_{\mu} = 0.79\ E_{\pi}$ and that the decay constant $B \simeq 120$ GeV.

Figure 6.1. shows the integral energy spectra of muons from model A compared to the present calculations (converted to a zenith angle of 0^{o} by assuming that the muon number varies with zenith angle, θ, as sec θ) for primary energies of 2.6×10^{14}eV

TABLE 6.1.

Models and results of Lal (1967)

Different Models	Inelasticity		Multiplicity n_s = total no. of charged and neutral particles		$N_\mu (E_p, \geq E_\mu)$ $E_p = 5.6\ 10^{15}$ eV.	
	N-N	π-N	N - N	π - N	$E_\mu > 640$ GeV	$E_\mu > 216$ GeV
Experimental Values.					28(rel.6.1) 38(rel.6.2) 46(rel.6.3)	146 (rel.6.1) 126 (rel.6.2) 184 (rel.6.3)
A	0.5	1.0	$2.7\ E_p^{0.25}$	$2.7\ E_p^{0.25}$	28	160
B	0.35	1.0	"	"	18	105
C	0.5	0.5	"	"	9	42
D	"	1.0	"	$5.1 \log E_p$	26	140
E	"	"	$7.2 \log E_p$	"	17	100
F	"	"	$4.75+0.25E_p^{0.5}$	"	44	230
G	0.35	"	"	"	27	145
H	0.5	"	"	$2.2+0.7E_p^{0.5}$	32	310
I	0.35	"	"	"	18	170

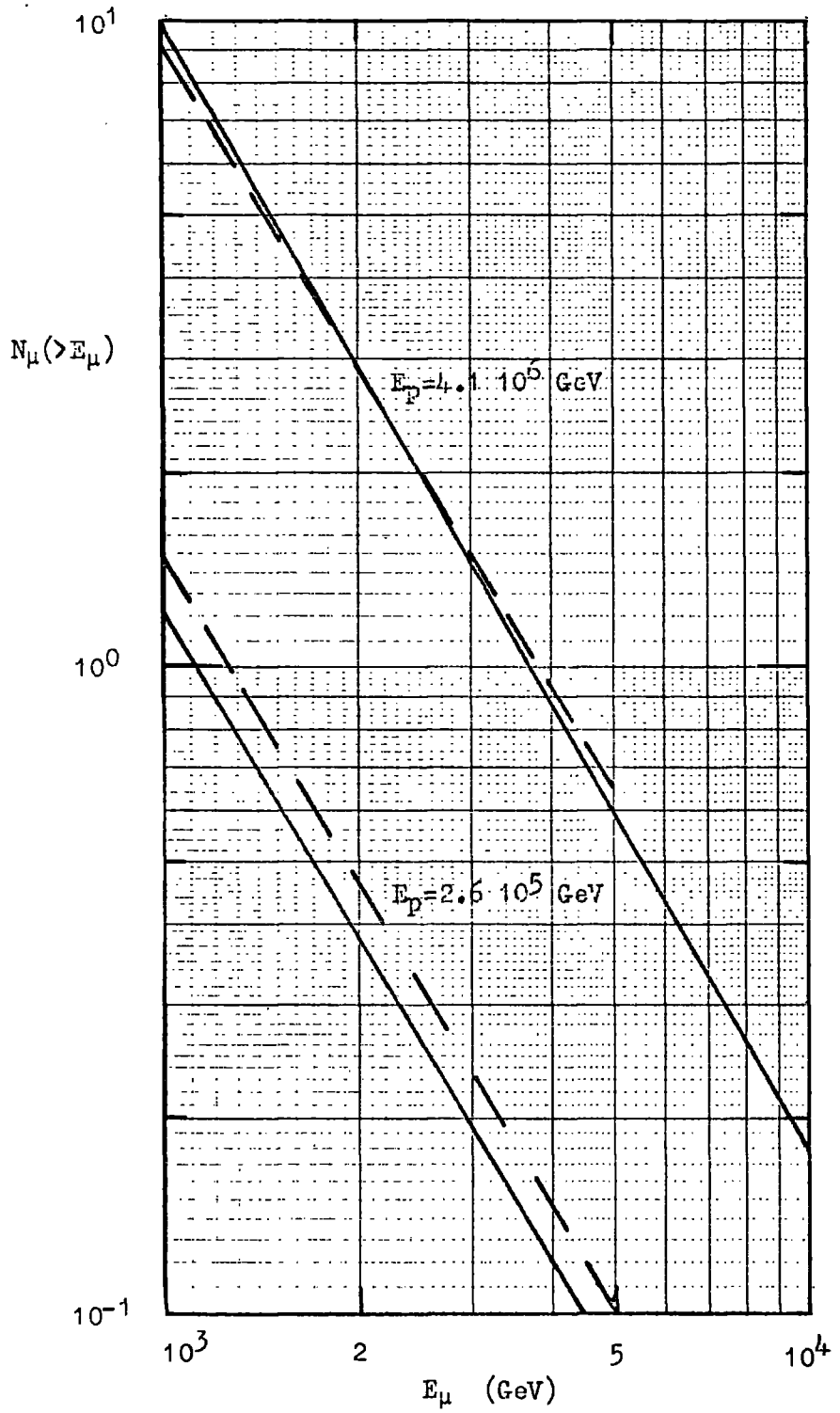

Fig. 6.1. Comparison of the integral energy spectrum of muons calculated by Lal, 1967 (full lines) with the "$E^{1/4}$ model" of the present work (dashed lines) for two primary energies and $\theta=0^o$.

and 4.1 10^{15}eV. It is seen that the agreement is good in both cases considering the different approximations made in both models.

Figure 6.2 shows a comparison between the predictions of model A and the present results for the "$E^{-\frac{1}{2}}$ model" (again reduced by 1/ sec 60°) for the number of muons as a function of primary energy at threshold energies of 600 and 2000 GeV. Again the agreement is quite good and so it seems that the present calculations are accurate as regards the longitudinal development of high energy muon showers.

Lal has compared his results with the experimental ones of Chatterjee et al. (1966), Greisen's expression (1960) for the relation between the number of muons above a given energy in a shower of a given size at sea-level, and Greisen's expression (1960) describing the results of Bennett (1960). These expressions are respectively

$$N_{\mu}(N, \geq E_{\mu}) = 1.6\ 10^{5} \left\{\frac{N}{10^{5}}\right\}^{0.47} E_{\mu}^{-1.5} \qquad 6.1$$

where N_{μ} is the number of muons of energy greater than or equal to E_{μ} in a shower of size N particles in the range 10^{5} - 10^{6} at an atmospheric depth of 920 g.cm^{-2}.

$$N_{\mu}(N, \geq E_{\mu}) = 1.7\ 10^{5} \left\{\frac{2}{E_{\mu}+2}\right\}^{1.37} \left\{\frac{N}{10^{6}}\right\}^{0.75} \qquad 6.2$$

at sea-level and

$$N_{\mu}(N, \geq E_{\mu}) = 1.3\ 10^{5} \left\{\frac{2}{E_{\mu}+2}\right\}^{1.29} \left\{\frac{N}{10^{6}}\right\}^{0.75} \qquad 6.3.$$

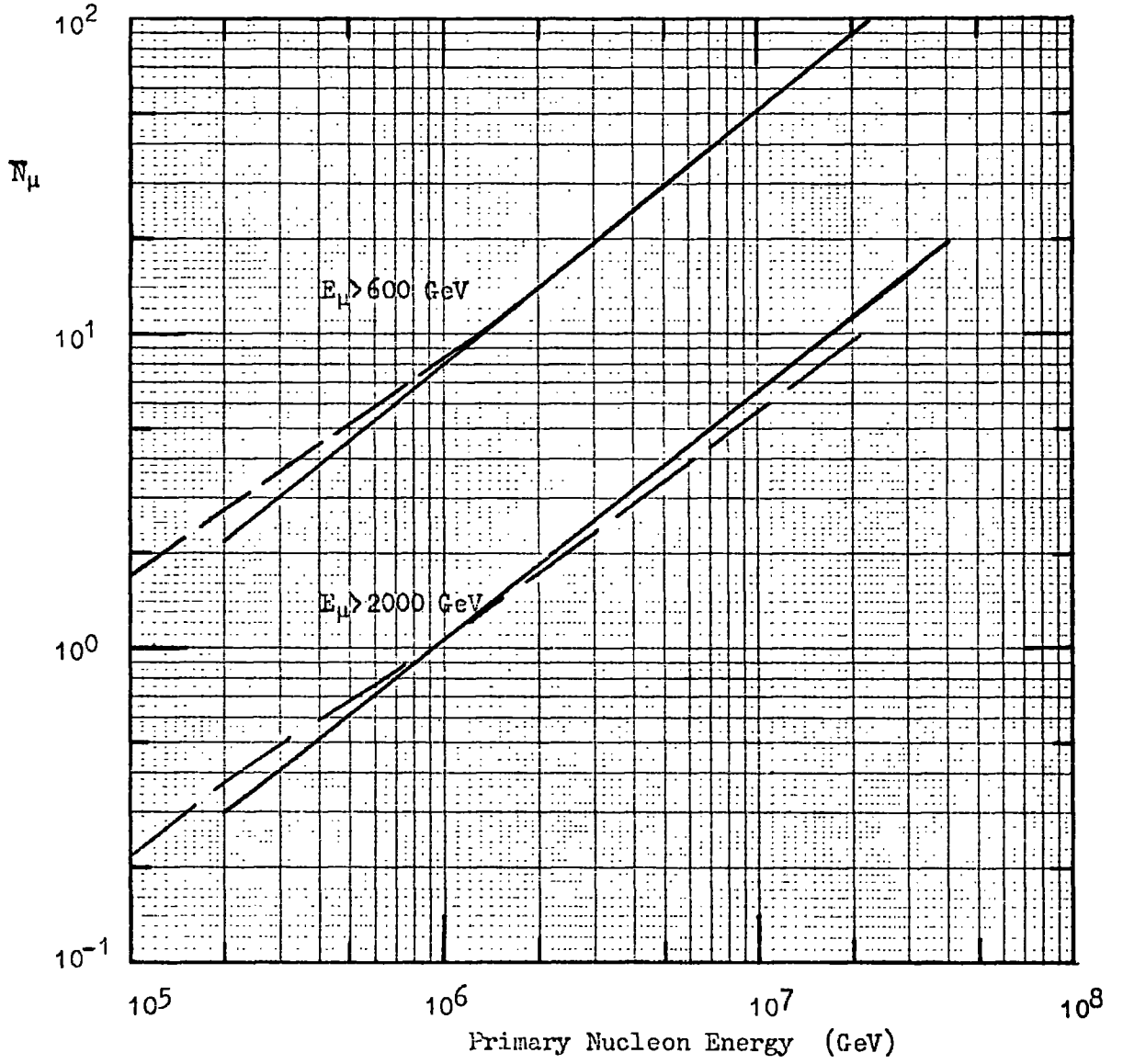

Fig. 6.2. Mean muon number as a function of primary nucleon energy for $\theta=0^\circ$ and pions only as calculated by Lal, 1967 (full lines) and the "$E^{1/4}$ model" of the present work (dashed lines).

He has then used the curves of Bradt et al. (1966) on the shower size versus atmospheric depth versus intensity, and the intensity versus primary energy, E_p, to obtain the relation between E_p and N at 920 g.cm^{-2} atmospheric depth. From this information he has calculated the number of muons with energy above 216 and 640 GeV at an atmospheric depth of 920 g.cm^{-2} corresponding to a shower size of 10^6 particles (according to Lal this corresponds to a shower size of 5.25 10^5 particles at 1030 g.cm^{-2} from the data of Bradt et al. and a primary energy of 5.6 10^6 GeV) and compared the results with the predictions of the three expressions given above. The results are shown in table 6.1. From the comparison he concludes that the models A,D and G give the best fit. However, these conclusions must be treated with a certain amount of caution. The earlier results of Chatterjee et al. have since been modified (Chatterjee et al. 1968a) and expression 6.1. has been superseded by

$$N_\mu(>E_\mu, N) = 6.5\ 10^6 \left\{\frac{N}{10^5}\right\}^{0.62} E_\mu^{-2.2 \pm 0.1} \qquad 6.4.$$

This is a composite result and taking the values from a best fit to the results of Chatterjee et al. (1968a) for muons of energy greater than 640 and 220 GeV for a shower size of 10^6 particles one obtains 25 and 187 muons respectively. This obviously does not affect his conclusions very much.

Another point is that he has assumed that the primary particles responsible for showers of size 10^6 particles at 920 g.cm^{-2} are solely protons in his calculations. This may not in fact be the case, and if heavy primaries are present in the primary flux to a large extent this could affect his conclusions, since the number of high energy muons in

a shower is a function of the mass of the primary particle. Also there is some uncertainty in the figure used by Bradt et al. to determine the primary energy from the shower size and so a better type of analysis would be to work back from a shower size of 10^6 particles and calculate the appropriate primary energy for each model allowing for fluctuations and the assumed primary composition.

6.3.2. Cowsik.

Cowsik (1966) has made calculations on the longitudinal development of the high energy nuclear-active and muonic components in E.A.S. using a model whose essential features are the same as that of Pal and Peters (1964). The main features of the model are as follows:-

A) Nucleon Interactions.

i) The interaction length of nucleons is 75 $g.cm^{-2}$.

ii) There is a very high probability of the nucleon being excited into isobaric states, whose subsequent de-excitation leaves the nucleon with a flat energy spread between 35% and 75% i.e. an elasticity $\sim 0.35 - 0.7$.

iii) The de-excitation proceeds through the emission of pions, numbering about 2.4 per collision on average and which carry off 27% of the incident energy. These are assumed to be emitted isotropically in the isobar rest frame each having a unique energy of 250 MeV.

iv) The remaining 20% is taken up by a fireball which moves slowly in the C.M.S.. This fireball emits nucleon-antinucleon pairs and pions isotropically in the C.M.S.. The nucleons and pions

are assumed to share the energy equally and each nucleon and pion is assumed to have a constant energy in the C.M.S. that of the nucleons being $\simeq 2$ GeV and that of the pions $\simeq 0.6$ GeV. The multiplicity of the nucleons and the pions at high energies becomes $N_{\pi^-} \simeq 0.073\ E^{\frac{1}{4}}$ and $N_{\pi^-} \simeq 0.23\ E^{\frac{1}{4}}$ respectively.

B) Pion Interactions

i) The interaction length of pions ~ 120 g.cm^{-2}.

ii) The interactions are completely inelastic.

iii) A fireball which is almost completely at rest in the π-π system is formed and this radiates pions and nucleons in a manner similar to that in nucleon interactions.

The decay constant B is taken as 128 GeV. The method of calculation is by the solution of appropriate diffusion equations and so fluctuations in the interaction points are included as well as fluctuations in the inelasticity of the interactions.

Figure 6.3 shows the energy spectrum of muons produced in a shower of primary energy 10^6 GeV for Cowsik's model and the "$E^{\frac{1}{4}}$ model" of the present work (reduced by $1/\sec 60^0$). The two spectra are seen to differ quite widely. The shape of the Cowsik one can be understood as follows:- at low muon energies the major contribution comes from the fireball or pionization process. As the threshold energy is raised the mean energy of the pions in the fireball becomes equal to and finally lower than the threshold energy and the contribution from this process drops rapidly. Then the muons arising from the decay of the isobar pions take over. The kink in the spectrum is the point at which this occurs.

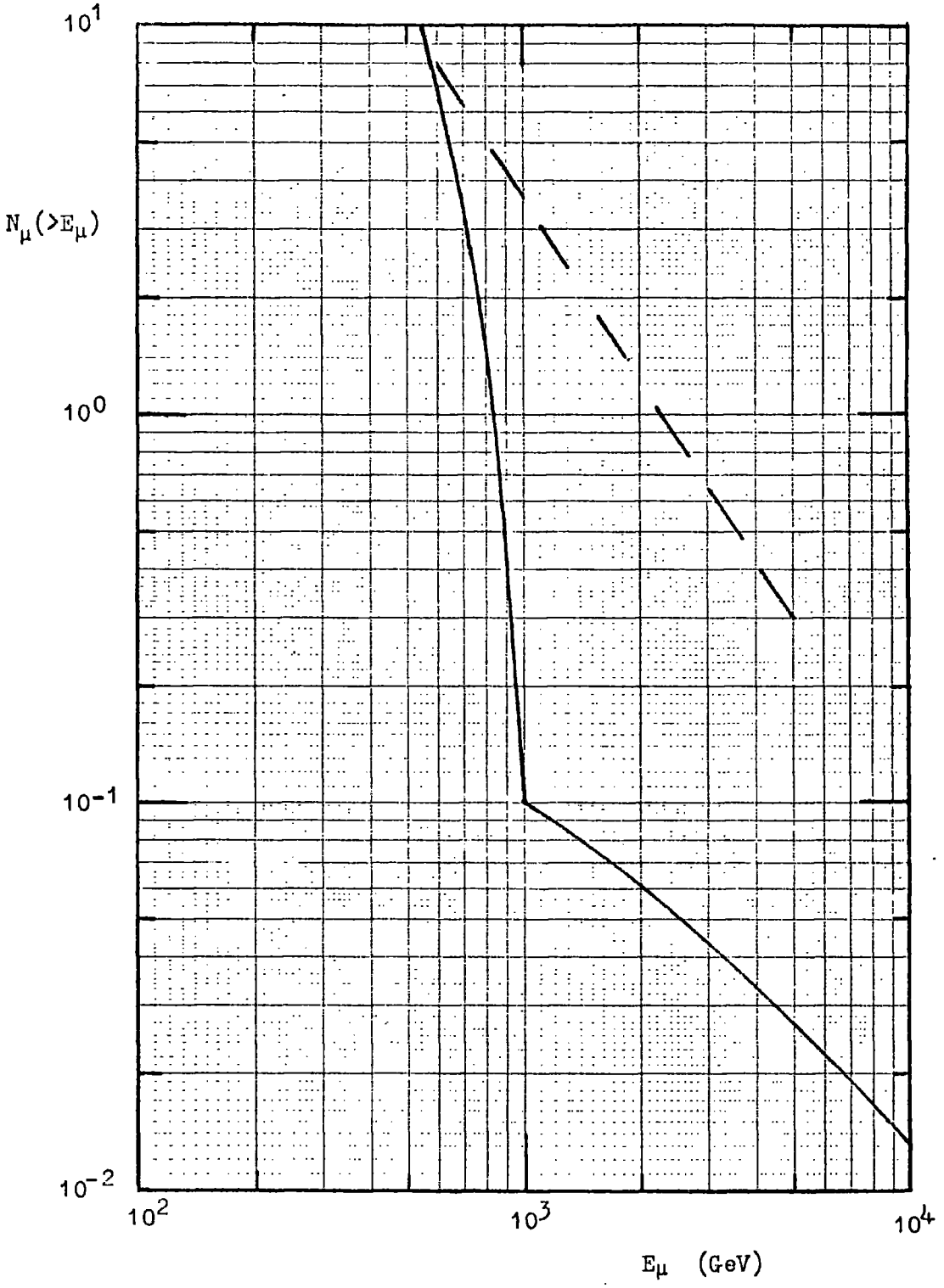

Fig. 6.3. Comparison of the integral energy spectrum of muons predicted by Cowsik,1966 (full line) with the "$E^{1/4}$ model" of the present work (dashed line) for $E_p=10^6$ GeV and $\theta=0^o$.

Figure 6.4 shows the average number of muons plotted as a function of primary energy for the model of Cowsik and the "$E^{\frac{1}{4}}$ model" of the present work. The curves are for threshold energies of 1000 and 2000 GeV and a zenith angle of 0^{o}. As would be expected the results predicted by the two models differ greatly. The initial rise in the curves from the isobar model is due to the muons coming from the isobar pion decay. As the primary energy is increased the energy at which the isobar pion decay takes over from the fireball pion decay increases, being $\sim 10^{15}$eV for a threshold energy of 1000 GeV and so the muon number falls. Above $\sim 10^{15}$eV the muons come mainly from the fireball process and the number increases with increasing primary energy.

Cowsik (1968) has folded his results in with a primary spectrum which has a rigidity cut-off at 10^{5} GeV, the composition of the primaries being the same as that found at low primary energies up to the cut-off. There is a further proton component in this model which has an intensity of about one twentieth that of the first proton component. Using this spectrum he finds good agreement with the experimental results of Chatterjee et al. (1968a, 1968b) on the muon number as a function of shower size up to muon threshold energies of 640 GeV.

He concludes that the necessary value of $\langle p \rangle_{t}$ to explain the results of Chatterjee et al. (1968a) is 0.5 GeV/c.

6.3.3. Murthy et al.

Murthy et al. (1968a,b,c) have made calculations of the average characteristics of E.A.S. and Monte-Carlo calculations to investigate

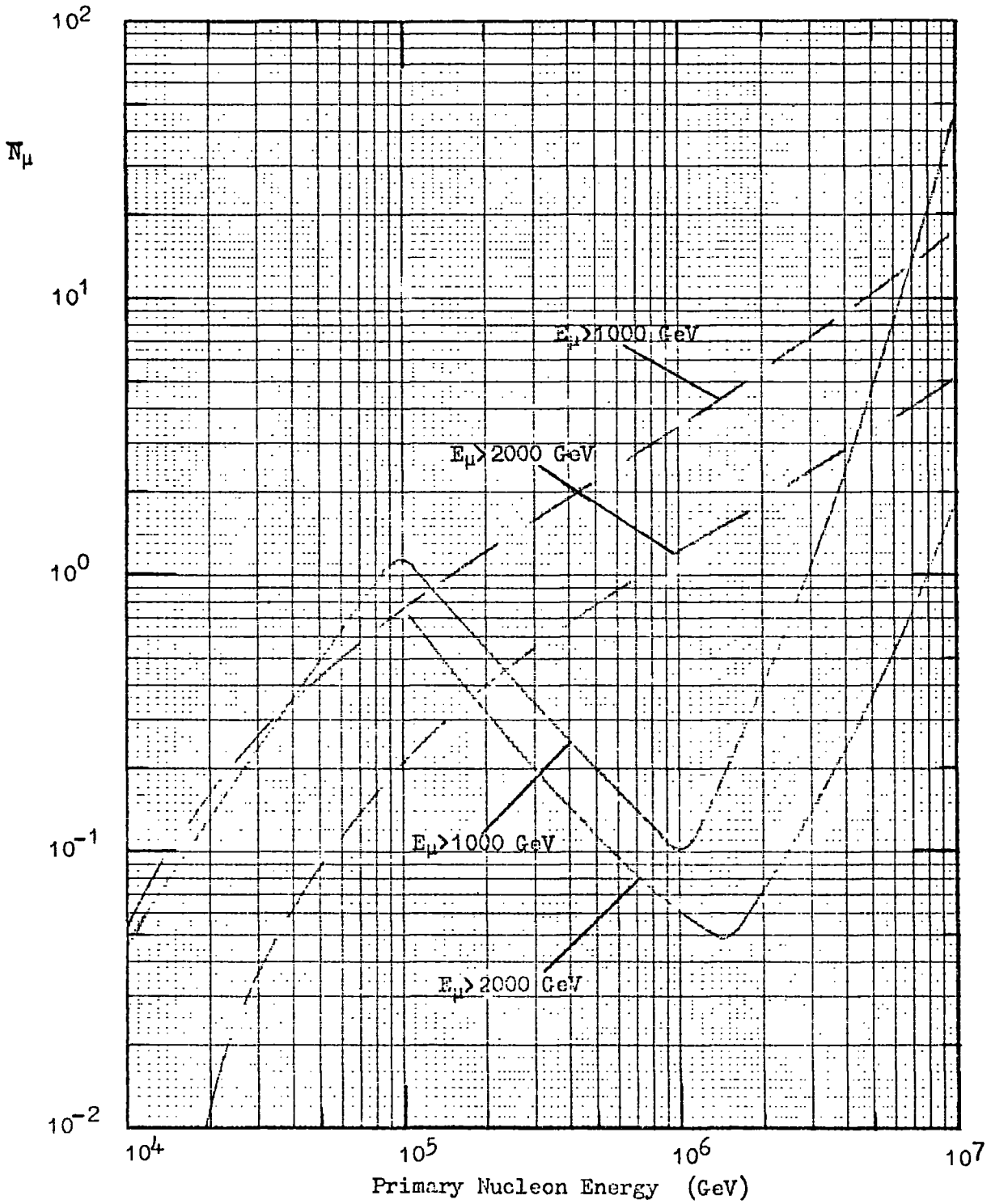

Fig 6.4. Mean muon number as a function of primary nucleon energy for $\theta=0^o$ and pions only as predicted by Cowsik, 1966 (full lines) and the "$E^{1/4}$ model" of the present work (dashed lines).

the effects of fluctuations in E.A.S., using eight different models of nuclear interactions for vertical showers. The eight models are described in table 6.2. The IBN and IB models are akin to those proposed by Pal and Peters (1964). In each interaction, 20% of the primary energy is shared by the constituents of a fireball. The surviving nucleon is excited with a 70% probability into an isobar state of mass 2.4 which decays to the ground state in three successive steps, in each of which a pion of momentum 0.4 GeV/c is emitted isotropically in the rest system of the parent.

Except for isobar decay pions, whose transverse momentum is worked out kinematically, the C.K.P. transverse momentum distribution is used for all created particles and the mean transverse momentum used is 0.36 GeV/c.

The results on high energy muons are not directly comparable to those of the present work but since the QL model is identical to the "$E^{\frac{1}{4}}$ model" an idea of the effects of the different assumptions can be gained from a comparison of the results of this model with those of the other models.

From a comparison of the width of the predicted lateral distributions with those of Chatterjee et al. (1968a) it is found that the former are less wide than the experimentally determined ones. They conclude that this indicates either a higher $< p_t >$ value than used or that the predicted height of production is too low.

Comparing the predicted and experimental energy spectra of high energy muons in a shower of size $5\ 10^5$ particles, the model

TABLE 6.2.

Models of Murthy et al. (1968)

	Model QLN		Model LLN		Model HLN		Model IBN		
							Nucleon		
	Nucleon	Pion	Nucleon	Pion	Nucleon	Pion	Fireball	Isobar	Pion
Multiplicity, M	$2.7\,E'^{\frac{1}{4}}$		$5.26\log(E'/18+1)$		$0.96\,E'^{\frac{1}{2}}$		$0.25E'^{\frac{1}{2}}$	3	$0.96\,E'^{\frac{1}{2}}$
Inelasticity, K	0.5	1	0.5	1	0.5	1	0.2	Distribution with average 0.3	1
Mean free path in g/cm^2	80	120	80	120	80	120	80		120
Fraction of $N\bar{N}$ produced, f	$7(500/E'+1)^{-1}$		$7(500/E'+1)^{-1}$		$7(500/E'+1)^{-1}$		Isobar excitation probability is 0.7 $7(500/E'+1)^{-1}$		$7(500/E'+1)^{-1}$
Energy spectrum of created particles	Exponential		Exponential		Exponential		Distribution decided by kinematics		Experimental

*E' is the projectile energy.

The average energy of created pions and nucleons is assumed to be proportional to their respective masses.

QL, LL, HL, and IB models are identical with QLN, LLN, HLN, and IBN models respectively, except that all the created particle are assumed to be pions, i.e. f = 0. QL, LL, and HL stand for "quarter-law", "log-law", and "half-law" of multiplicity variation,

IB is the only one which agrees with the results of Chatterjee et al. (1968a), all the other models predicting too few muons. All models predict fewer muons and a different slope compared to the expression of Greisen (1960), at muon energies above about 100 GeV, for the above shower size.

Murthy et al. conclude that none of the models give agreement as regards absolute numbers over the whole muon energy range but rule out the HL and HLN models from considerations of the steady state muon spectrum and the variation of the depth of the shower maximum with shower size.

6.3.4. Bradt and Rappaport.

Bradt and Rappaport (1967) have done Monte Carlo calculations on the nuclear-active and muon components of E.A.S. at two different atmospheric depths, 530 and 970 g.cm^{-2}, using different models and two types of primaries - protons and iron nuclei.

In the two models of interest the energy spectrum of the secondary pions, which were assumed to comprise all secondaries, was adapted from the approximations of Tanahashi (1965) for a two centre model, with and without the addition of a few very high energy pions (models 1 and 2 respectively). Thus model 2 is a "two-centre" model and has a multiplicity varying as $E_p^{0.28}$ and model 1 is similar to an isobar model and has a multiplicity varying as $E_p^{0.22}$.

The transverse momentum distribution is of the form given by Aly et al. (1964) (see section 3.4)with a mean of 0.35 GeV/c and a cut-off at values above 1.0 GeV/c. The inelasticity distribution was taken to be uniform from 0.25 to 0.75 for nucleons and 1.0 for

pions. The mean interaction lengths of pions, nucleons and iron nuclei were taken to be 80, 80 and 15 $g.cm^{-2}$ respectively.

The integral energy spectrum of muons in a shower initiated by a primary nucleon of energy 10^{15}eV predicted by the isobar model is compared with the prediction of the "$E^{\frac{1}{4}}$ model" from the present work in figure 6.5. It is seen that the two spectra do not differ greatly as regards total number but the slope of the isobar spectrum is less than the C.K.P. one, viz. $\simeq$ 1.5 compared to -1.7.

In general the "two-centre " model predicts slightly more muons than the isobar model for proton primaries and at high threshold energies has a steeper energy spectrum. The differences between the models are small compared to the differences due to the primary mass. The muon energy spectra for iron nuclei exhibit a sharp cut-off at about $10^{-3}E_p$ due to the fact that in the break-up model no nucleon receives more than 1/56 of the primary energy, E_p.

From a comparison of their results with experiment they conclude that their is a deficiency of muons with large p_t. They also conclude that the fragmentation model for heavy primaries is relatively unimportant and that only the scatter of the final muon parent has a significant effect on the muon lateral distribution.

6.4. Comparison of Experimental Results with the Present Work.

6.4.1. Chatterjee et al. (1966, 1968a).

This group have made measurements on high energy muons ($>$ 220 GeV and >640 GeV) in extensive air showers in the size range 10^5-10^7 particles using a large air shower array on the surface (atmos-

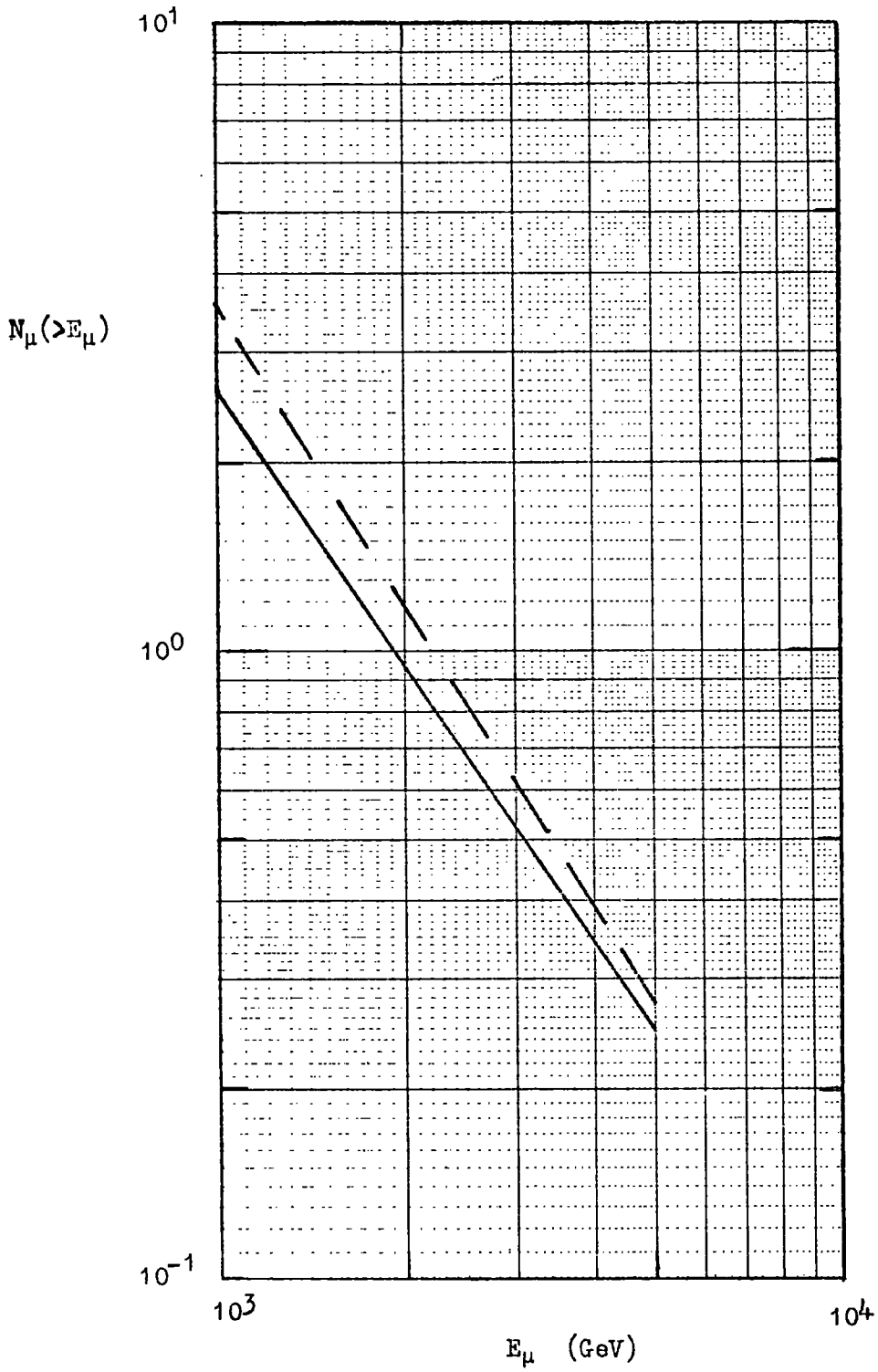

Fig. 6.5. Comparison of the integral energy spectrum of muons predicted by the isobar model of Bradt and Rappaport, 1967 (full line) with the "$E^{1/4}$ model" of the present work (dashed line) for $E_p=10^6$ GeV and $\theta=0^o$.

pheric depth 920 g.cm^{-2}) and muon detectors deep underground in the Kolar Gold Mines, India.

The air shower array (figure 6.6) consists of 20 plastic scintillators, each of area 1 m^2; 19 are laid out in concentric circles up to a maximum radius of 100 m and one is located 200 m from the centre.

The muon detectors are located at two depths, 270 m (U_1) and 600 m(U_2) . The detectors at the U_1 level consist of four plastic scintillators, each of area 1.44 m^2 and at the U_2 level five water Cerenkov detectors each of area 2 m^2. The underground detectors provide only information that at least one muon has passed through them when they are triggered, the number of muons is unknown.

In order to determine the shower size and core position of the E.A.S., the lateral density distribution of charged particles was assumed to have the form given by the Nishimura-Kamata-Greisen relation. In the present analysis only those showers whose cores fell within 50 metres of the centre of the array and whose probability of detection was nearly unity were accepted. The lateral distributions of muons were assumed to be of the form

$$\rho_\mu(r) = \left\{\frac{N_\mu}{2\pi r_o^2}\right\} \exp\left\{-\frac{r}{r_o}\right\} \qquad 6.5$$

Under these assumptions the probabilities of one and two muon detectors being triggered by muons associated with E.A.S. was calculated as a function of N_μ and r_o. From the experimentally measured fluxes these probabilities were known and so N_μ and r_o were obtained in terms of shower size. Figure 6.7 shows the dependence of the total number of muons of energy > 220 GeV and

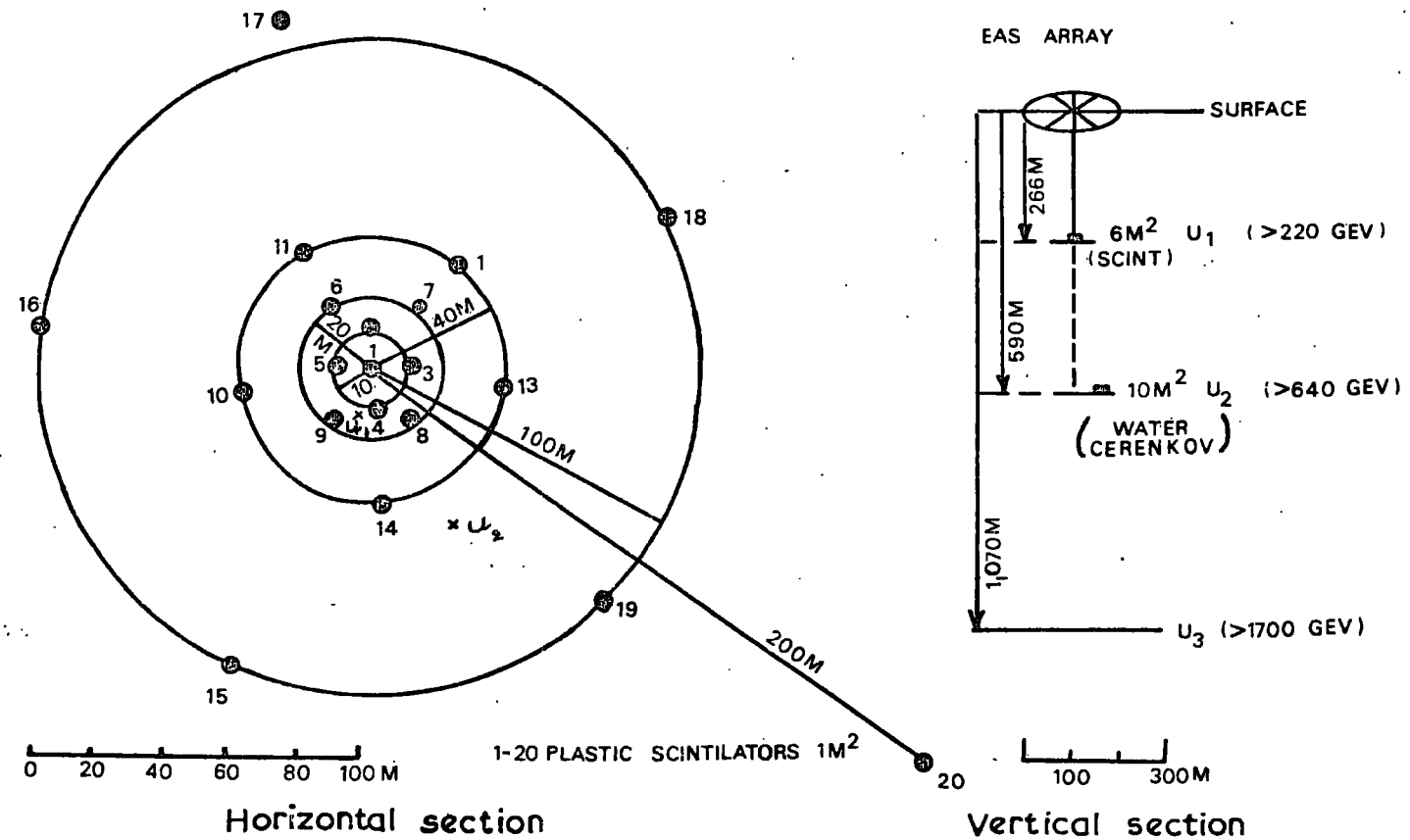

FIG.6.6. THE EXTENSIVE AIR SHOWER ARRAY IN THE KOLAR GOLD MINES

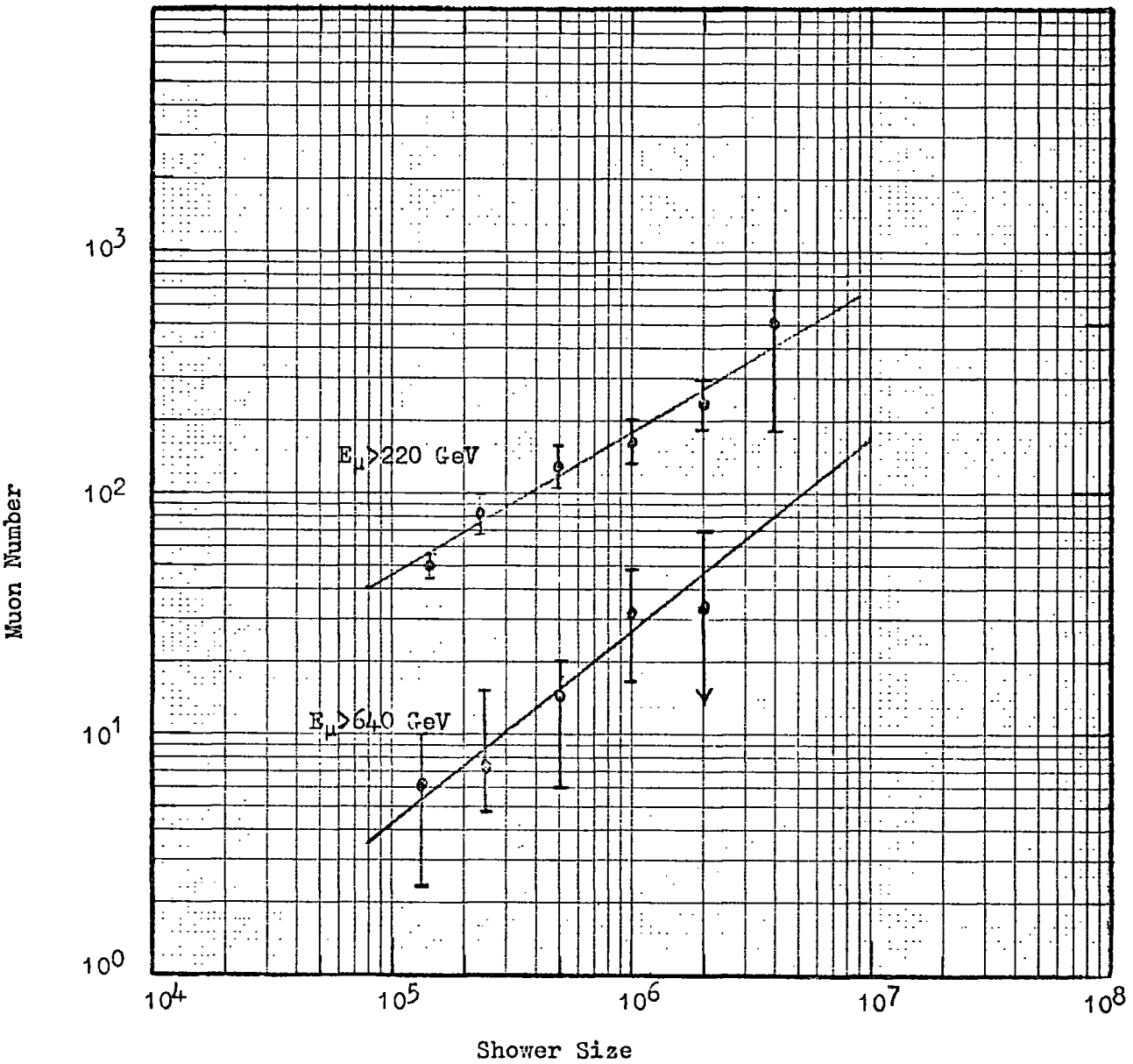

Fig. 6.7. Variation in the number of muons ($E_\mu > 220$ GeV and $E_\mu > 640$ GeV) with shower size at an atmospheric depth of 920 g.cm^{-2} as measured by Chatterjee et al., 1968a.

>640 GeV on the shower size (N) in the range 10^5 - 10^7 particles. The dependence can be expressed by

$$N_\mu(>220\ \text{GeV}) = 47\ (N/10^5)^{0.58 \pm 0.1} \qquad 6.6$$

$$N_\mu(>640\ \text{GeV}) = 4\ (N/10^5)^{0.77 \pm 0.2} \qquad 6.7$$

Only results for the 640 GeV threshold have been obtained in the present calculations (to be precise 600 GeV). In order to compare these with those of Chatterjee et al. (1968a), the latter have been converted to sea-level using the shower size versus atmospheric depth curves of Bradt et al. (1966). This means extrapolating the latter to sea-level but the error should be small compared to the errors on the experimental points. This assumes that the detected showers are almost vertical but this is probably justified since only showers falling within 50 metres of the centre of the array were considered so that the maximum zenith angle of showers detected should be $\sim 10^0$ for muons of energy above 640 GeV.

The predicted values of N_μ (>600 GeV) versus N were obtained assuming primary protons, using the relationship between shower size and primary energy given by De Beer et al. (1966), allowing for fluctuations, in the vertical direction. It is not quite correct to use this since the multiplicity of pions in these calculations is slightly higher than in the present work. However, the effect should be small (see difference in models I and II in De Beer et al.) and should have the effect of raising the predicted points which are shown in figure 6.8.

It is seen that the predicted points are consistently lower than the experimentally derived ones, although they lie within

the experimental errors. It seems though that there is probably a real difference between the two results. The difference, however, would be easily removed by the addition of heavy primaries to the primary spectrum. An average primary mass $\lesssim 2$ should be sufficient to bring about agreement.

Note that this comparison is for the "$E^{\frac{1}{4}}$ model". One would expect the "$E^{\frac{1}{2}}$ model" to predict higher values of N_μ/N_e. The addition of kaons to the secondaries would also increase N_μ/N_e.

6.4.2. Barret et al. (1952)

This group carried out a series of experiments on underground muons at a depth of 1600 hg.cm^{-2} (corresponding to a muon threshold energy of 560 GeV) in a salt mine near Ithaca.

One of the experiments determined the decoherence curve of underground muons and from this it was found that a lateral distribution of the form

$$\rho_\mu(r) = \begin{cases} 1/\pi\sigma^2 & r < \sigma \\ 0 & r > \sigma \end{cases} \qquad 6.8$$

would fit the results, with σ = 13 m. This implied that the mean radius of the showers detected was 8.7m.

Using this lateral distribution, it was possible to predict the expected ratios of doubles to singles and triples to doubles which when compared to the measured ratios gave a muon multiplicity spectrum

$$F(M) \propto M^{-3.4 \pm 0.1} \qquad 6.9.$$

under the assumption that the multiplicity spectrum could be approximated by a power law. Combining this with the number spectrum of electrons over the relevant shower size range they concluded that

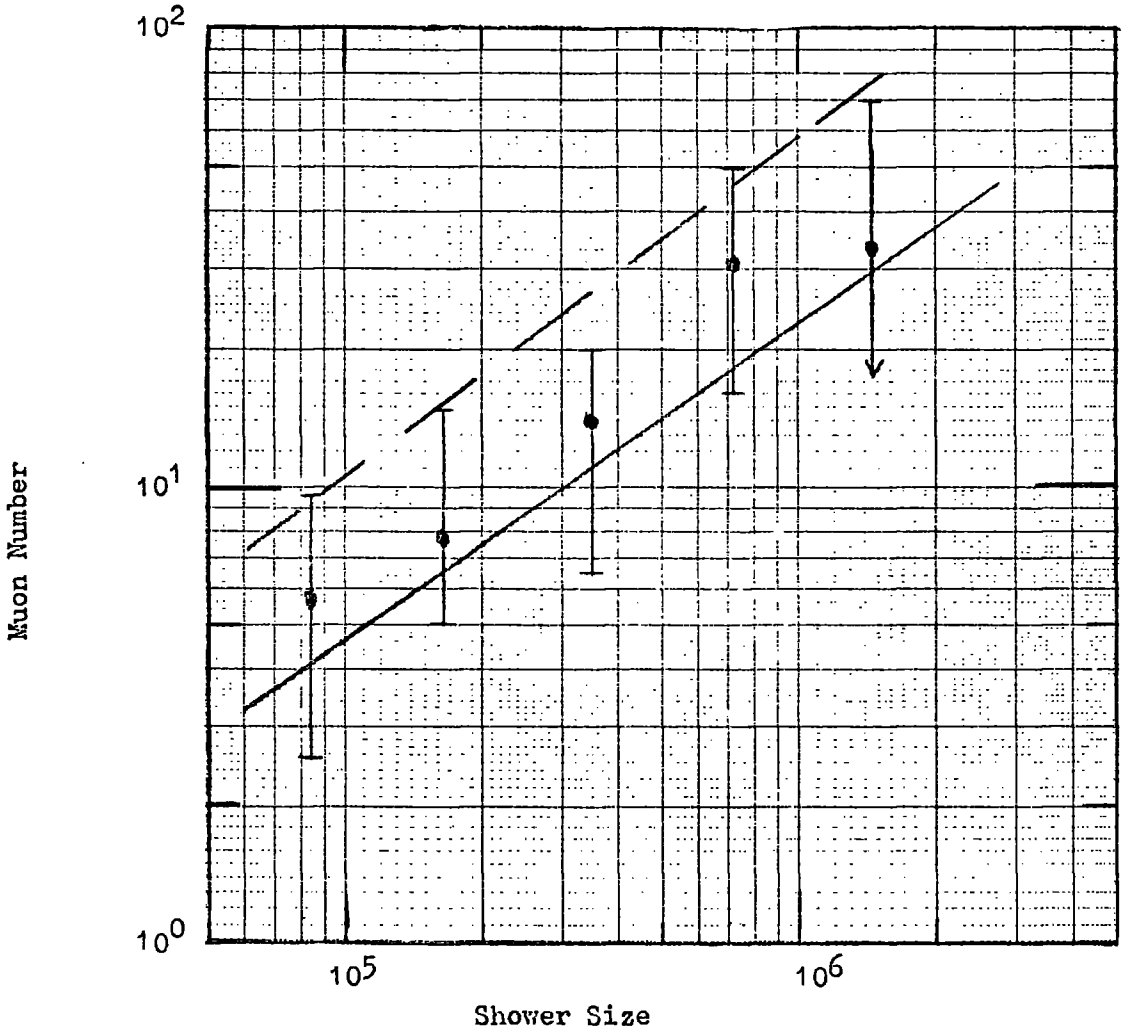

Fig. 6.8. Variation in the number of muons (E_μ>640 GeV) with shower size at sea-level. The dashed line refers to relationship given by Greisen (1960), the full line to the present work assuming the "$E^{1/4}$ model" and the points to the results of Chatterjee et al. (1968a) converted from a depth of 920 g.cm^{-2}.

$$N_\mu (>560) \propto N^{0.58 \pm 0.05} \qquad 6.10$$

Greisen (1960), however, has reanalysed the data and by comparing the measured absolute frequency of showers as a function of the number of muons to the frequency of extensive air showers at sea-level with N charged particles he finds that

$$N_\mu (>560\text{GeV}) = 75 \quad (N/10^6)^{\alpha} \qquad 6.11$$

with $\alpha \simeq 0.7$ for large values of N and N_μ, decreasing towards 0.5 for N_μ in the neighbourhood of one (i.e. showers of 500 to 1000 electons contain on the average one such muon).

With this information and that from other experiments Greisen predicts

$$N_\mu (>E_\mu, N) = 1.7\ 10^5 \left\{ \frac{2}{E_\mu + 2} \right\}^{1.37} \left\{ \frac{N}{10^6} \right\}^{0.75} \qquad 6.12$$

This line is shown in figure 6.8 for $E_\mu > 640$ GeV. It is seen to be higher than that given by Chatterjee et al. (1968a) even after correction for the difference in atmospheric depth of the two experiments. The reason for this is not clear. Greisen does not give any information on his analysis or any error estimation. Two possible explanations are that the mean zenith angle is different in the two cases and also the form of the lateral distributions are different leading to a difference in the estimate of the muon number.

In order to get better agreement with Greisen's result the predicted points could be increased by postulating heavy primaries in the primary spectrum and/or a multiplicity law varying faster than $E_p^{\frac{1}{2}}$.

6.4.3. The Vertical Sea-Level Energy Spectrum of Muons above 1000 GeV.

At these energies the intensities deduced from various experimen-

tal determinations suffer from large statistical and/or systematic errors. However, a comparison of the present models with experiment serves both as a check on the models themselves and also on the magnitude of the primary spectrum used.

At the energies involved there are three main methods used to determine the sea level muon spectrum:- from measurements of γ -ray spectra at various heights in the atmosphere, from intensity measurements underground and from burst spectra measurements. All the methods are indirect and so their accuracy also depends on the theory adopted, which in all cases depends on some unknown parameters.

i) Energy Spectrum from γ-ray Spectra Measurements.

Since muons are genetically related to γ-rays in the atmosphere via their parent particles (pion and kaons) it should be possible in theory to establish relationships between the sea-level muon spectrum and that of γ-rays at various depths in the atmosphere. Several groups of workers have measured the energy spectrum of high energy γ-rays using nuclear emulsion methods at mountain, aeroplane and balloon altitudes. There is some disagreement among the different workers but the later results are in closer agreement.

Duthie et al. (1962) and Mayes, (1964) have used these results to deduce the sea-level energy spectrum of muons via the parent meson production spectrum. The parameters involved in the models are: (a) the absorption mean free path of the high energy nuclear-active component, (b) the assumption of charge independence in the production of the parent mesons, (c) the pion to kaon ratio

among the secondaries of high energy nuclear interactions and (d) the interaction characteristics of the parent pions.

Only the first of these has been measured at the energies involved (Duthie et al. (1962), Fujimoto (1964)) and so the other parameters have to be extrapolated from lower energy measurements.

The sea-level muon spectrum deduced by Mayes (1964) is shown in figure 6.9.

ii) Energy Spectrum from Underground Intensity Measurements.

The sea-level energy spectrum can be derived from measurements of the muon intensity at various depths underground. Muons of energy above 1000 GeV correspond to depths greater than ~ 2500 hg.cm^{-2}.

Menon and Ramana Murthy have given a discussion of underground experiments performed at depths greater than 2000 hg.cm^{-2}. They have also derived a depth intensity curve down to depths of ~ 8000 hg.cm^{-2}.

The sources of the data and the technique used are summarized in Table 6.3.

Table 6.3.

Worker	Technique
Bollinger (1951)	G.c., 4 fold, 30 cm lead
Barton (1961)	G.c., 2 fold and s.c.
Miyake et al. (1962, 1964)	s.c., 2 fold, 5 cm lead.
Castaglioni et al. (1965)	s.c.,2 fold,1 - 6 cm lead

key: G.c. Geiger counters; s.c. scintillation counters.

From this depth intensity curve and the range-energy relation of muons they were able to work back and deduce the energy spectrum of sea-level muons allowing for the variation in the rock over each experiment from standard rock.

The actual energy loss formula used by Menon and Ramana Murthy was

$$-\frac{\partial E}{\partial x} = 1.88 + 0.0766 \ln\left\{\frac{E'max}{m_\mu c^2}\right\} + 3.6\ 10^{-6}E \qquad 6.13$$

where the symbols are as in equation 5.16. They also took into account the effect of fluctuations on the range energy relation. As already mentioned the exact value of the energy loss coefficient is not accurately known due to a lack of knowledge of the photo-nuclear cross-section and they in fact assumed a value of b = (3.6 $\pm$ 0.6) 10^{-6} $g^{-1}.cm.^2$ The results are shown in figure 6.9. Osborne et al. (1964) composed a spectrum using essentially the same method as Menon and Ramana Murthy. This has been slightly modified by Aurela and Wolfendale (1967) and the results are found to agree within the standard deviations estimated by Menon and Ramana Murthy.

Kobayakawa (1968) has also calculated the sea-level muon spectrum from underground measurements. His treatment differs in three ways from earlier works: (a) he derives the average range-energy relation without the assumption that the b value in the energy loss equation is constant, (b) reliable values of the enhancement factor resulting from fluctuations in the energy loss of muons travelling through great thicknesses of material are used, and (c) the differences in the rocks of respective authors are taken into account by directly converting the measured

intensities to the sea-level spectrum by using the appropriate average range-energy curves and correction factors. He finds an exponent of -2.541 ± 0.190 (95% confidence limit) over the energy range 0.4 - 7 TeV having a weighted mean energy of 0.70 TeV.

The results from the Utah detector need not be discussed further as they have already been considered in Chapter 5.

iii) Energy Spectrum from Burst Measurements.

High energy muons produce bursts essentially through electromagnetic processes. From the measured burst spectrum one can deduce the energy spectrum of muons at sea-level (e.g. Krasilinikov (1964), Dimitriev and Khristiansen (1963) and Higashi et al. (1964)).

The results of these workers are shown in figure 6.9. The results of Krasilinikov (1964) and Higashi et al. (1964) agree with each other within the errors, which are rather large, while the results of Dimitriev and Khristainsen seem to be on the high side over the entire range.

The discrepancy that exists between the energy spectrum deduced from burst measurements by Dimitriev and Khristiansen and the energy spectra obtained by various other types of observations, particularly the underground observations, cannot be understood at present. The aspects involved in deducing the high energy muon spectrum from burst spectra measurements are (a) the validity of quantum electrodynamics at short distances, $\sim 10^{-14}$ cms, (b) a knowledge of the non-electromagnetic interactions of muons, and (c) an understanding of the corrections for the effects of fluctuations in burst size for a given energy transfer.

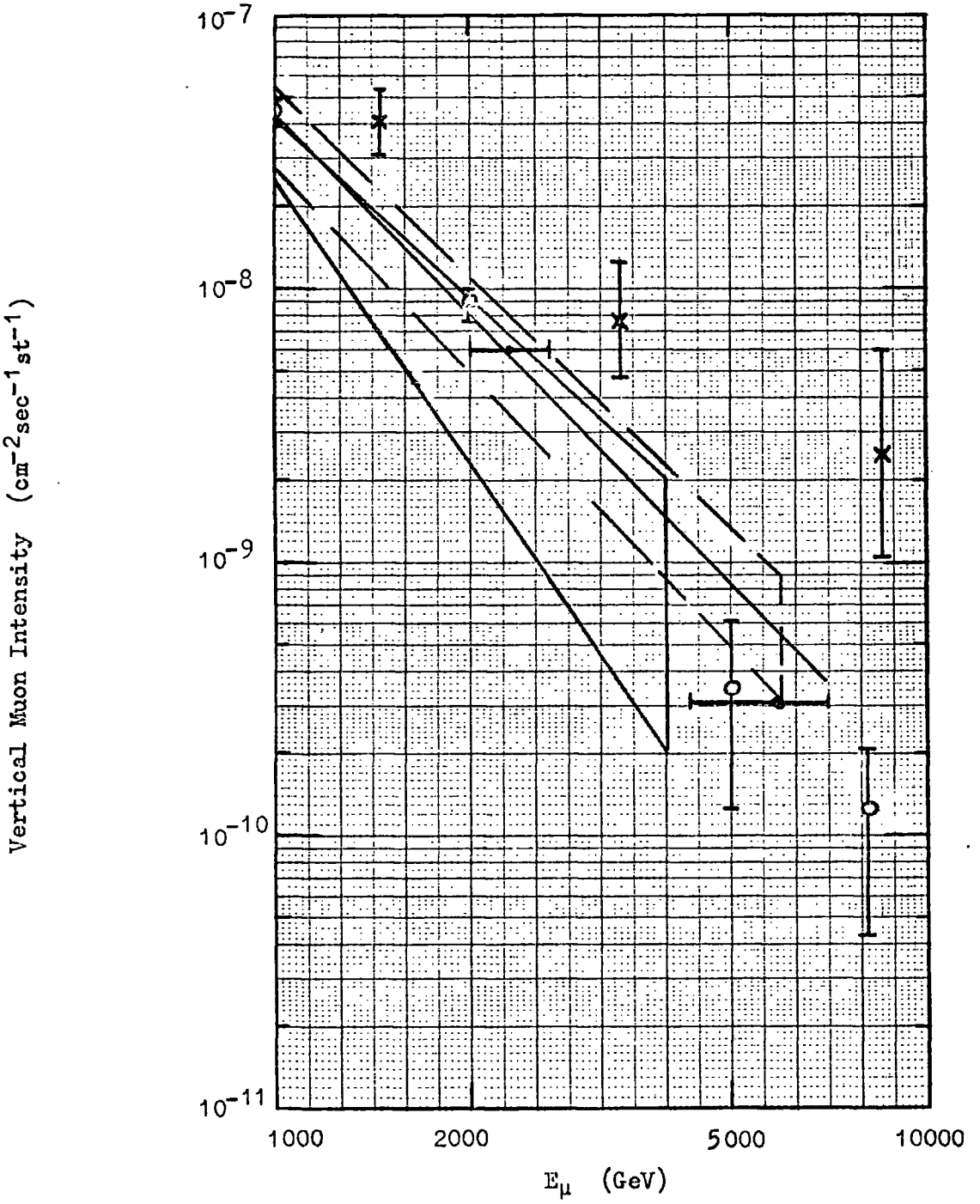

Fig. 6.9. Integral energy spectrum of muons in the vertical direction as reported by various authors. Key: × Dimitriev and Khristiansen (1963), ○ Mayes (1964), • Menon and Ramana Murthy (1967), the continuous line shows the spectrum given by Kobayakawa (1968), the band with continuous line shows the spectrum of Higashi et al. (1964) and the band with broken lines the spectrum of Krasilinikov (1964).

iv) Composite Muon Energy Spectrum

Neglecting the results of Dimitriev and Khristiansen, Menon and Ramana Murthy have drawn a composite sea-level muon energy spectrum from various measurements. This is shown in figure 6.10 where it is compared with the predictions of the "$E^{\frac{1}{4}}$" and "$E^{\frac{1}{2}}$" models, both of which have been obtained from the original calculations for a zenith angle of 60° by multiplying by cos 60°.

It is seen that both of the theoretical spectra lie within the limits of the composite spectrum and so it is not possible to distinguish between the two models on this basis. However, the fit between the theoretical and experimental results means that for the assumptions made in the models the magnitude of the primary intensity adopted is reasonable over the energy range covered by these spectra, although the experimental errors are very large. It would be possible to lower the primary intensity for the "$E^{\frac{1}{4}}$ model" by about a factor 2 at a primary energy of $\sim 2\ 10^{4}$ eV, corresponding to the median primary energy of muons with energy above 5000 GeV, and still maintain agreement. This could bring about better agreement with the Utah results but would also mean changing the slope of the primary spectrum and would probably lead to disagreement with the shower size spectrum. It would also be possible to lower the intensity for the "$E^{\frac{1}{2}}$ model" by $\sim 16\%$ at a primary energy of $\sim 4\ 10^{13}$ eV and by $\sim 25\%$ at $8\ 10^{14}$eV but this would not be sufficient to bring about agreement with the Utah results. If kaons were present to a significant extent among the secondaries of high energy interactions it might be possible to lower the primary intensity and still maintain agreement with the

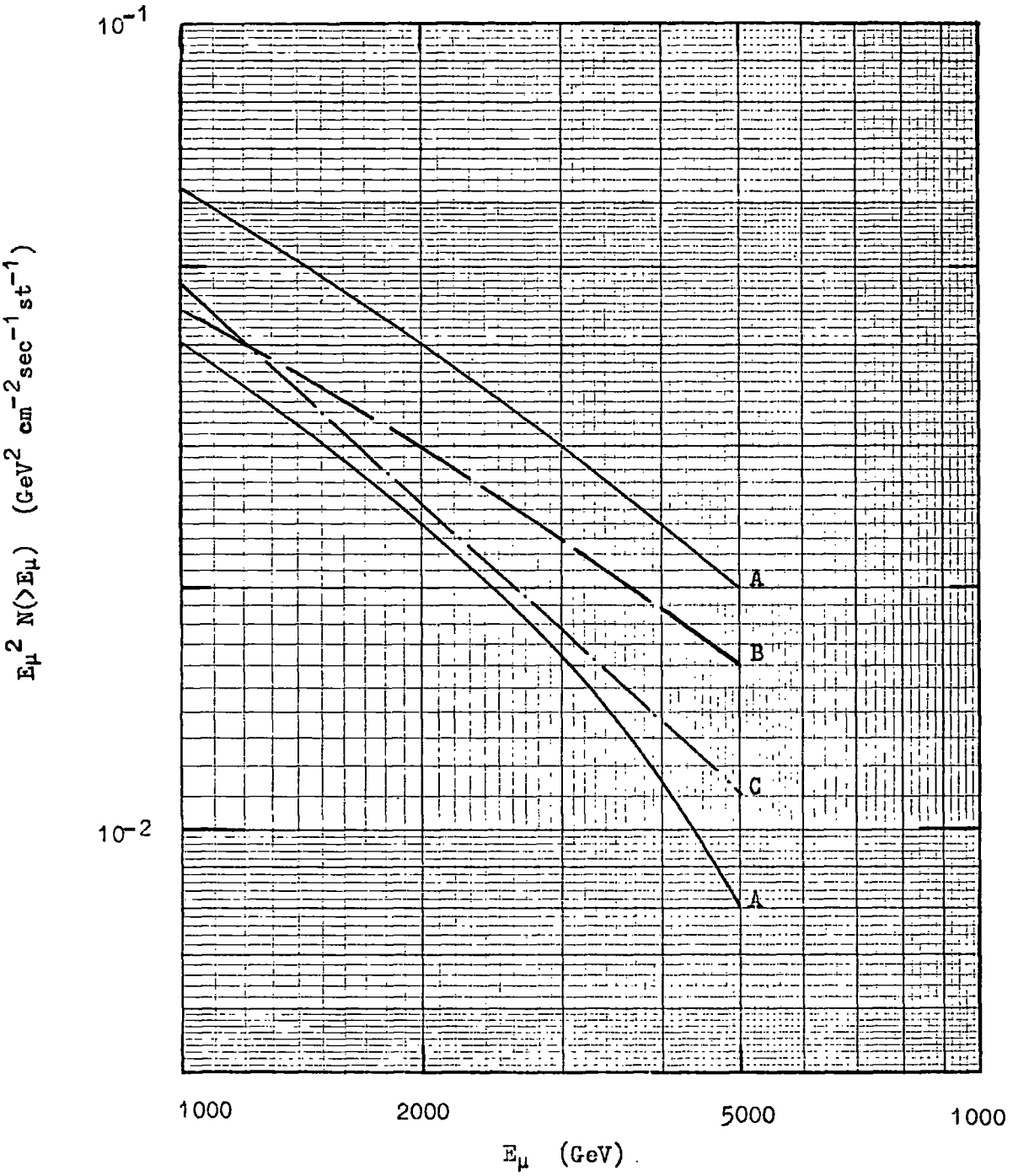

Fig. 6.10. Vertical energy spectra of muons. Key: A, composite energy spectrum given by Menon and Ramana Murthy (1967), B, spectrum predicted by the "$E^{1/4}$ model" of the present work, C, spectrum predicted by the "$E^{1/2}$ model" of the present work.

measured muon spectrum.

It seems then that the primary intensity taken for each model is reasonable considering it gives agreement with experiment for both the electron and muon components.

6.5. Conclusions

It seems that the C.K.P. model is capable of explaining the longitudinal development of E.A.S. reasonably well. The transverse momentum distribution may be in need of modification at low values of p_t and an increase in the mean transverse momentum seems to be needed with increasing interaction energy if the multiplicity law is assumed to vary as $E_p^{\frac{1}{4}}$.

The present calculations seem to be in good agreement with those of Lal (1967) with regard to the longitudinal development of the showers using a similar model and this indicates that the method of calculation is satisfactory although a comparison of lateral distributions has not been possible.

Cowsik's results differ considerably from those of the present work and together with those of Murthy et al. and Bradt and Rappaport indicate that a higher value of $\langle p_t \rangle$ than 0.4 GeV/c is needed to explain the existing experimental results.

A comparison of the present results with the experimental ones of Chatterjee et al. (1968a) indicates a deficiency in the number of predicted muons with energy greater than $\sim$ 640 GeV but the difference is not great and agreement should be possible for a primary composition of mean mass number $\lesssim 2$, or the addition of kaons to the secondary particles produced in high energy interactions. This is for the

"$E^{\frac{1}{4}}$ model".

The expression of Greison (1960) gives higher values of muon numbers as a function of shower size than found by Chatterjee et al. and this possibly indicates a higher proportion of heavy primaries, of kaons among the secondaries of high energy interactions than in the case of Chatterjee et al.. It would seem that the results of Chatterjee et al. should be the more reliable, however, since they have a large E.A.S. array above their muon detectors and assume a more realistic form for the lateral distributions of the muons, but until more results are available it is not possible to decide between the two sets of results with certainty.

The comparison between the measured sea-level spectrum of muons with energy above 1000 GeV with the theoretically predicted ones shows that within the very wide experimental error limits both the "$E^{\frac{1}{4}}$" and "$E^{\frac{1}{2}}$" models give agreement. Thus the primary intensities adopted for each model would seem to be reasonable.

CHAPTER 7.

CONCLUSIONS AND FUTURE WORK

7.1. Introduction

From an analysis of the characteristics of ultra-high energy muons an attempt has been made to draw conclusions about the mass composition of the primary cosmic radiation at energies above those at which direct observations can be made and also to gain information on the characteristics of ultra-high energy nuclear interactions, in particular the multiplicity of the secondary particles produced in these interactions, the form of their transverse momentum distribution and the mean value of their transverse momentum.

However, the conclusions of such an analysis are dependent on the theoretical model used and on various assumptions made in the analysis and so careful consideration must be given to these factors before definite conclusions are drawn.

7.2. The Transverse Momentum.

From the studies of the decoherence curve of high energy muons underground measured by Coats et al. (1969) a value of 0.72 ± 0.08 GeV/c has been obtained for the mean transverse momentum of pions produced in interactions of energy $\sim 2\ 10^{14}$eV assuming the "$E^{\frac{1}{4}}$ model" If the "$E^{\frac{1}{2}}$ model" is used a mean transverse momentum of ~ 0.5 GeV/c is obtained for a primary interaction energy of $\sim 4\ 10^{14}$eV.

These values must be regarded as preliminary because of various factors in the analysis. These factors include the neglect of the effects of geomagnetic deflection, Coulomb scattering, the assumption that all the muons detected come from pions and the

neglect of possible correlations between the transverse momentum and the multiplicity. Also it was assumed that the primary particles consist only of protons.

Approximate calculations for the effect of heavy primaries present to the extent found at low primary energies indicate that their effect is to reduce the mean transverse momentum to 0.67 ± 0.1 GeV/c at primary energies ~2 10^5GeV if the "$E^{\frac{1}{4}}$ model" is assumed.

Evidence for a value of the mean transverse momentum higher than 0.4 GeV/c comes from the results of several groups of workers. From a comparison of the width of showers of muons with energy above 220 GeV with the theoretical calculations of Murthy et al. (1968a), Chatterjee et al. (1968a) conclude that a mean transverse momentum of 0.6 - 0.7 GeV/c would be needed to fit their experimental results. De Beer et al. (1968b) using a model similar to the "$E^{\frac{1}{4}}$ model" of the present work find that if the results of Earnshaw et al. (1967) are interpreted in terms of an increase in the mean transverse momentum of secondary pions produced in high energy interactions then, even allowing for a possible selection bias in the experimental results, a mean transverse momentum rising from ~0.4 GeV/c for pion interactions of mean energy ~ 40 GeV through ~ 0.6 GeV/c for interactions of 200 GeV to 1.0 ± 0.3 GeV/c for interactions of mean energy ~ 4 10^3 GeV is needed. However, it should be noted that Orford and Turver (1968) have put forward an alternative explanation of the results of Earnshaw et al. in terms of a multiplicity law varying as the square root of the interaction energy above 3.10^{12}eV and primary particles having a mass greater than 10 at primary energies ~2 10^7eV,

although even in this work a mean transverse momentum of 0.5 GeV/c was used.

It has not been possible to distinguish between different forms of the transverse momentum distribution. However, it seems that the C.K.P. distribution represents the present data adequately.

7.3. Multiplicity Law of Secondary Particles in High Energy Interactions.

Two multiplicity laws of secondary charged particles produced in high energy interactions have been considered in the present calculations which are denoted by the "$E^{\frac{1}{4}}$ model" and the "$E^{\frac{1}{2}}$ model".

The main information on the relative merits of the two models comes from a comparison of the predicted and empirically derived density spectra and rates of high energy muons.

This comparison indicates that whichever model is considered then the predicted rates of doubles and triples is too high when the preferred primary spectra, i.e. Spectrum A and Spectrum B are folded in.

The various possibilities of explaining this discrepancy have already been discussed in Chapter 5.

The comparison also indicates that whichever of the two preferred primary spectra is used then the "$E^{\frac{1}{4}}$ model" seems to give the better fit.

However, before definite conclusions are drawn a closer examination of the intensity of the primary spectra used must be made.

The intensity of the primary spectra used for the "$E^{\frac{1}{4}}$ model" has been derived by De Beer et al. (1969) from a survey of sea-

level shower size spectrum measurements, and working back from these measurements to the primary spectrum using a theoretical model similar to the one used in the present work. Obviously such a procedure depends on the contents of such a survey. However, a comparison with the results of other workers indicates that the intensities assumed for each spectrum are reasonable.

The other relevant factor is the amount by which the intensity of the primary spectra must be raised to allow for the decrease in the shower size for a given primary energy when using the "$E^{\frac{1}{2}}$ model". The increase used in the present work is based on calculations by De Beer et al.(1966). This enhancement factor must be regarded as very approximate because De Beer et al. used a slightly different multiplicity law than adopted in the present work for the "$E^{\frac{1}{2}}$ model" and did not consider the effects of fluctuations in the shower size for their model with the multiplicity varying as the square root of the interaction energy. It is thought that the present enhancement factor is probably an overestimate and so will lead to the intensity of the primary spectra used for the "$E^{\frac{1}{2}}$ model" being overestimated. Some increase in the assumed primary spectra must be made for the "$E^{\frac{1}{2}}$ model" but it is not possible to know the exact amount until more accurate calculations have been carried out to allow for this. Therefore, although the present calculations favour the "$E^{\frac{1}{4}}$ model" the "$E^{\frac{1}{2}}$ model" cannot be ruled out.

7.4. Mass Composition of the Primary Cosmic Radiation.

It has been seen in Chapter 5 that it is not possible at present to draw conclusions about the mass composition of the primary cosmic

radiation from a comparison of the predicted and empirically derived density spectra.

If the conservative values of the model parameters are used then both of the preferred primary spectra predict rates which are higher than observed experimentally for both of the multiplicity laws considered.

Since this discrepancy increases with muon threshold energy it seems to be due not simply to an overestimate of the primary intensity. From the possible causes of this overestimate which have been considered the most likely parameters to change to bring about better agreement seem to be the value of the mean transverse momentum and/or the value of the energy loss coefficient b (with or without direct production) both of which have some justification (see Chapter 5).

The only experimental results which seem to be in contradiction with the present work are those of Grigorov et al. (1967), from observations with the 'Proton' satellites, who have concluded that the proportion of heavy nuclei in the primary cosmic radiation begins to increase at primary energies of 10^{12}eV. Using the present models too few high energy muons would probably be observed if this composition was adopted.

7.5. Future Work.

7.5.1. Introduction.

It has been seen that the conclusions from the present work are limited to a certain extent by the statistical accuracy of the Utah results. It also seems that the method of deriving empirical density spectra is not very satisfactory because it is difficult

to estimate the experimental errors from these and also to allow for the fact that the sensitive area of the detector changes with angular and detected multiplicity variations.

Recently the completed Utah detector has been run and results of much greater statistical accuracy should be available shortly thus enabling a more thorough analysis to be made.

A possible method of analysing these results to obtain information on the multiplicity law of high energy interactions, on the transverse momentum of the secondary particles in such interactions and the properties of the primary cosmic radiation is described below.

The following parameters are considered as variables:-

i) The mean transverse momentum $\langle p_t \rangle$, the C.K.P. transverse momentum distribution being assumed.

ii) The exponent α in the multiplicity variation $n_s = A\, E_p^{\alpha}$ above $E_p = 3000$ GeV; below a primary nucleon energy of 3000 GeV the relation $n_s = 2.7\, E_p^{\frac{1}{4}}$ appears to fit the available experimental data rather well and this expression is used.

iii) The magnitude of the primary spectrum, although when it is necessary to use the form of the spectrum for specific predictions the relation given by equation 4.23 is used i.e. Spectrum C.

7.5.2. Derivation of the Mean Transverse Momentum.

From studies of the decoherence curves of high energy muons it should be possible to obtain fairly accurate values of the mean transverse momentum of the secondary particles produced in high energy interactions assuming different values of α .

If sufficient data are available it should also be possible to obtain estimates of the mean transverse momentum for different threshold and therefore different primary energies.

It may also be possible to obtain decoherence curves for triples and this would give information on the values of the transverse momentum at even higher primary energies for different values of α.

Thus if the value of α was known accurate values of the mean transverse momentum could be obtained.

The derivation of α is described in the next section.

7.5.3. Derivation of α.

Having obtained values of the mean transverse momentum in the relevant energy range for appropriate values of α the rates of multiple muon events of different multiplicities can be calculated for different values of α.

To illustrate the method it will be assumed that the mean transverse momentum obtained from the decoherence curve analysis is 0.4 GeV/c for all values of α. In practice the appropriate values of $\langle p_t \rangle$ should be used and similar curves calculated.

Figure 7.1. shows the calculated frequencies of detection of multiplicities 1 - 4 inclusive for a detector of area 20 m^2 (the approximate area of the Utah detector) at a zenith angle of 60° for $\alpha = \frac{1}{2}$ and $\alpha = \frac{1}{4}$.

Figure 7.2. shows the appropriate median energy versus muon threshold energy for the two values of α, $\frac{1}{4}$ and $\frac{1}{2}$, for a detector of area 20 m^2 and a zenith angle of 60°.

The practical significance of such a figure is that the data

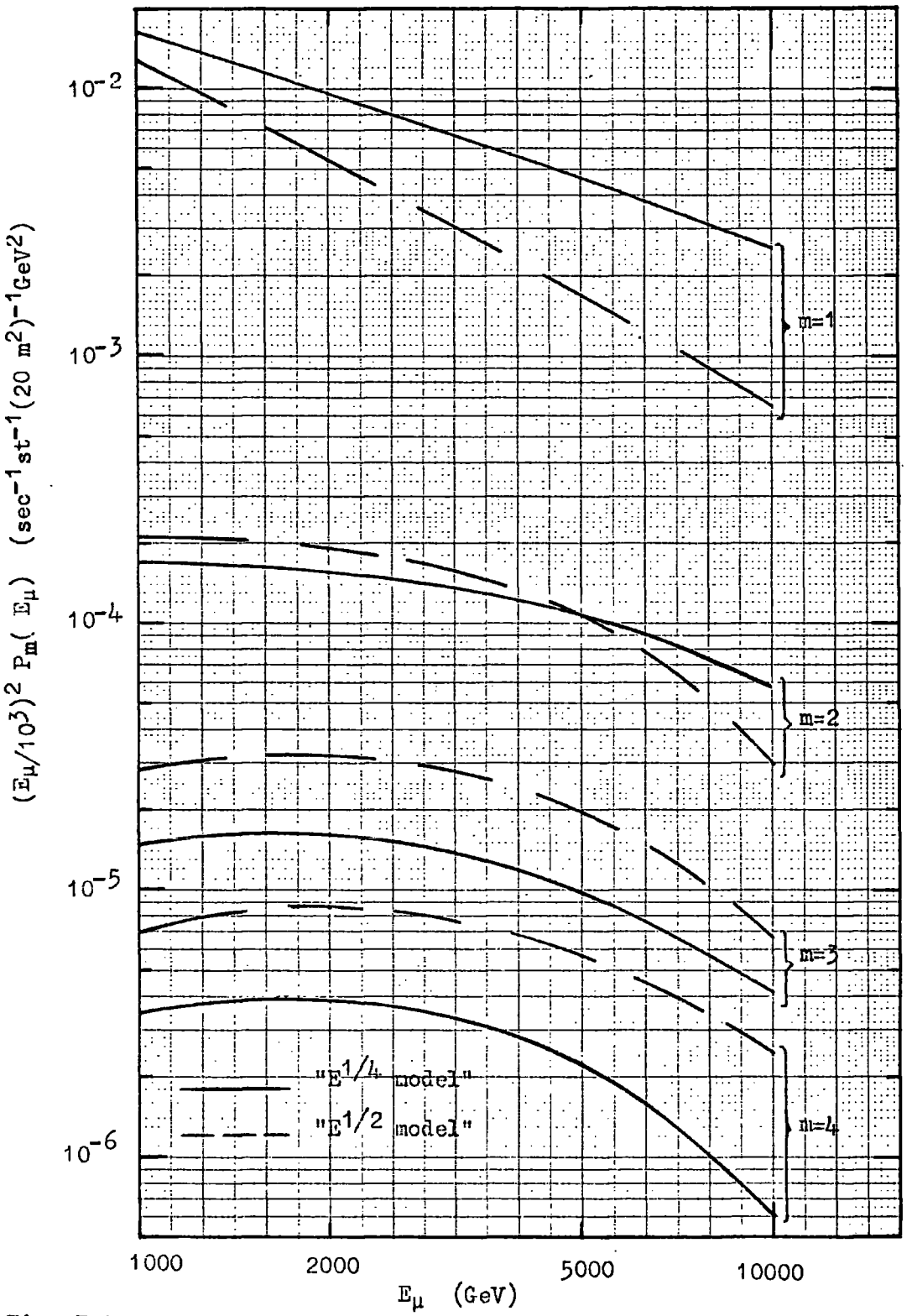

Fig. 7.1. The expected frequency of detecting m muons in a detector of area 20 m^2 at $\theta=60^o$ as a function of threshold energy. assuming proton primaries and $\langle p_t \rangle = 0.4$ GeV/c.

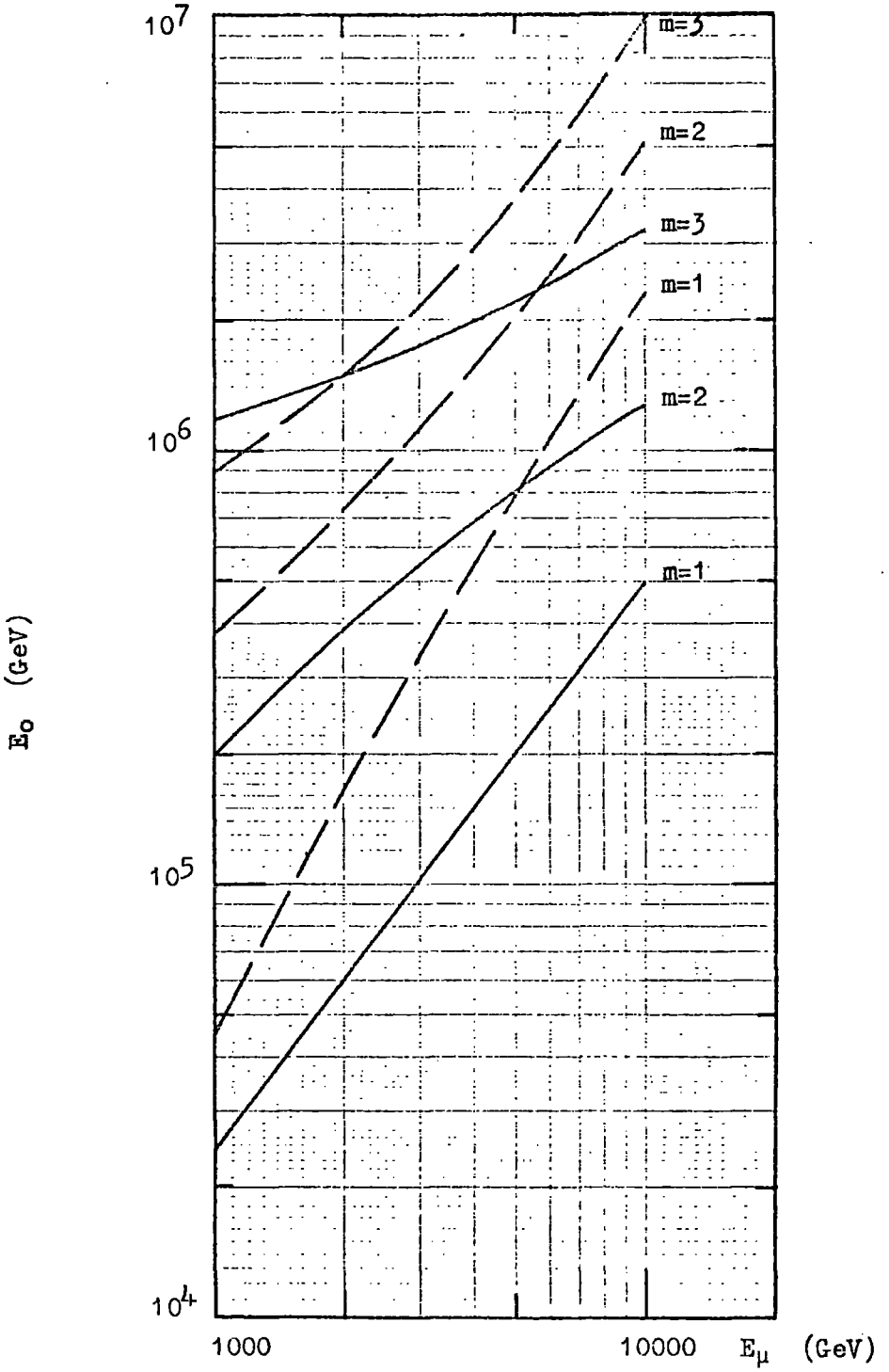

Fig. 7.2. Median primary energy, E_o, as a function of muon threshold energy for various multiplicities, m, of detected muons at $\theta=60^o$ assuming primary protons and $\langle p_t \rangle = 0.4$ GeV/c.

from different threshold energies and different multiplicities can be selected in such a way that they refer to the same primary energy. For example in this case for $\alpha = \frac{1}{4}$ the same primary energy, 2 10^5GeV, results if single muons of energy above 5000 GeV and doubles with energy above 1000 GeV are studied. Similarly primary nucleons of median energy 5.5 10^5 GeV give rise to singles with energy greater than 11000 GeV and doubles with energy greater than 3000 GeV.

Using the data of figures 7.1 and 7.2 it is possible to construct curves of the type shown in figure 7.3. This gives the ratio of the predicted frequency of doubles (above a given threshold energy) to that of singles with an energy above that threshold energy which corresponds to the same median primary energy, as a function of the single muon threshold energy. Along each of these (full line) curves α varies and any point on a line corresponds to a fixed α and a fixed primary energy. For example the curve for n = 2 at E_μ = 8500 GeV corresponds to $\alpha = \frac{1}{4}$, and the ratio of $P_2 (E_\mu > 2000 \text{ GeV}) / P_1 (E_\mu > 8300 \text{ GeV})$, is 0.95. From figure 7.2. we see that the median primary energy for both these multiplicities is $\sim 4\ 10^5$ GeV.

The manner in which such a plot can be used is illustrated by the straight line drawn through the hypothetical experimental points. This refers to n = 2 i.e. doubles with energy above 2000 GeV. The circles refer to singles at threshold energies below that responsible for doubles but extrapolation to meet the line n = 2 gives the condition that the median primary energies are the same. The value of α at this intersection point is then the experimentally

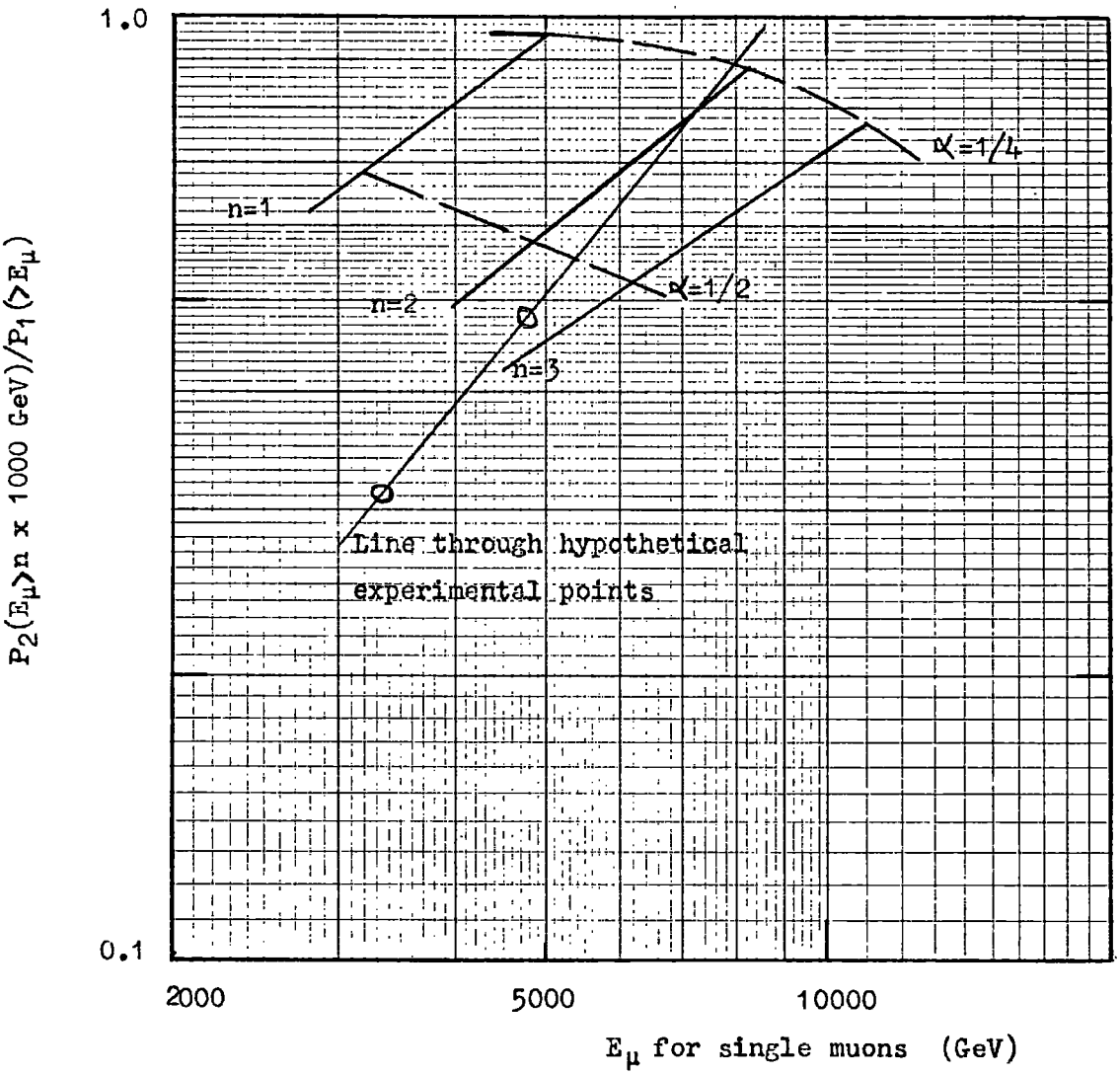

Fig. 7.3. Ratio of the frequency of doubles to singles as a function of threshold energy for singles for a detector area of 20 m^2, $\theta=60^o$, $<p_t>=0.4$ GeV/c and primary protons (see text for explanation).

derived value independent of the primary intensity.

Similar curves can be plotted which relate to the ratios P_3 to P_2, P_4 to P_3 etc. and so α values pertaining to higher primary energies can be determined (if in fact α does vary with the primary energy) by plotting the experimental data in a similar manner.

The values of α obtained are in fact effective values since it is assumed that the primary particles are all single nucleons.

In fact one may be able to draw conclusions about the primary mass and the multiplicity law from such a comparison. Thus if the value of α obtained is higher than permitted by the kinematics of high energy interactions it indicates that some heavy nuclei are present in the primary cosmic radiation. If α turns out to be less than $\frac{1}{4}$ then it indicates that the primary particles are mainly protons in the relevant energy region.

Furthermore trends in α could be useful. Thus an increase in α at primary energies $\sim 10^{15}$ could possibily be interpreted as evidence for an increase in the primary mass at these energies, or alternatively a decrease would give support to the theory that the primary particles above $\sim 10^{15}$eV were becoming lighter.

In theory it may also be possible to draw conclusions about the existence of the "direct production" process . Thus if at a given primary energy it was possible to compare the value of α obtained from the ratio P_2 to P_1 with that of P_3 to P_2 and the former turned out to be bigger than the latter then this would support the existence of the "direct production" process. However, it may not be possible experimentally to detect enough events to obtain values of the P_2/P_1 ratio corresponding to the required primary energy,

since the threshold energy would need to be very high, unless α was very large.

Having obtained values of α in this fashion then values of the mean transverse momentum could be obtained from the results of section 7.4.2.

7.5.4. Derivation of the Primary Intensity.

Having derived α and $\langle p_t \rangle$ as a function of the primary energy the experimental results can be taken together with the theoretical predictions to determine the primary intensity for various primary energies. The determination is by way of finding the relationship of the observed number of events of a given multiplicity to that given in figure 7.1. (in this example where the $\langle p_t \rangle$ found from the decoherence curves is assumed to be 0.4 GeV/c for all values of α) and by scaling the primary intensities given by equation 4.23 accordingly.

Performed in this way the calculations give the primary spectrum that would apply if all the primary particles were single nucleons.

7.5.5. Effect of Detector Area.

The effects of small changes in the detector area on the predicted rate can be allowed for using curves of the form shown in figures 4.24 and 4.25. Also changes in the predicted rates due to variations in the radii of the showers caused by mean transverse momenta different from 0.4 GeV/c can be allowed for using these curves. Figure 7.4. shows the mean radius of showers of different threshold energies for the "$E^{\frac{1}{2}}$" and "$E^{\frac{1}{4}}$" models as a

Fig. 7.4. Mean radial distances of EAS muons from shower core at $\theta=60^{\circ}$ for $\langle p_t \rangle = 0.4$ GeV/c and primary protons.

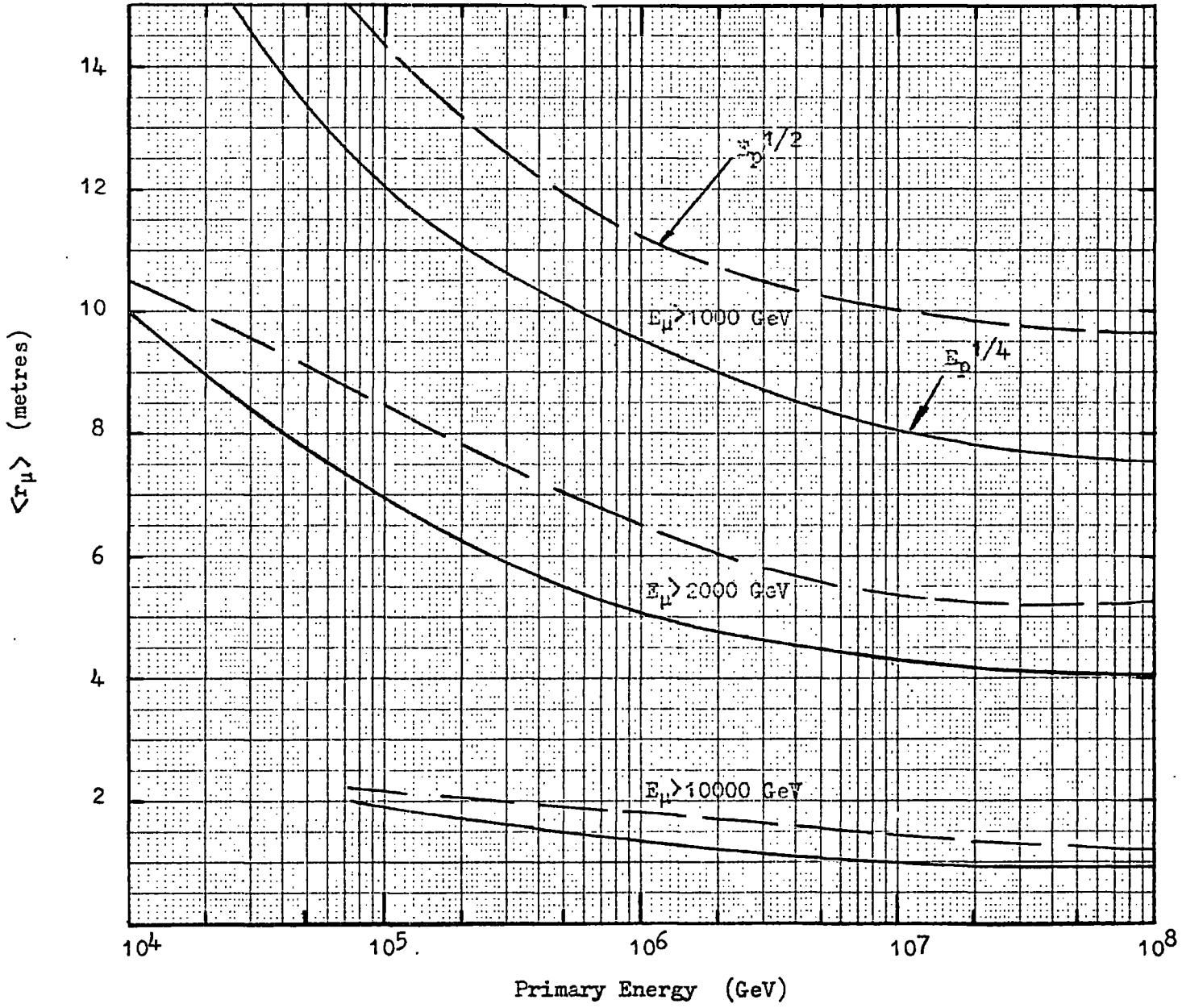

function of primary energy. These curves are for $< p_t >$ = 0.4 GeV/c and a zenith angle of 60^0. If for $<p_t>$ = 0.4 GeV/c the radius of a shower is r than for $<p_t>$ = 0.4 f GeV/c the mean radius of the shower is f.r. If we wish to find the predicted rate of doubles through an area A for $<p_t>$ = 0.4 f GeV/c then assuming the rate is a function of the relative area of the shower to the detector

$$A' = f^2 A$$

where A' is the area that must be looked up in figure 4.24 to find the new predicted rate of doubles through the area A at a zenith angle of 60^0. This is not exactly true because the median primary energy responsible for the doubles will vary for different values of the mean transverse momentum but for small changes in $<p_t>$ it should be a good approximation.

This procedure could also be carried out for different zenith angles and threshold energies if the values of the mean radius of the showers were known.

7.5.6. Angular Variation.

The bulk of the angular variation in the predicted frequencies of various multiplicities comes from geometrical factors, notably the increase in mean distance to the generation layer as the zenith angle increases. This is only true of course if the basic interaction mechanism is as assumed here and that no other process contributes to muon production e.g. the "direct production" process postulated by Bergeson et al. (1968).

Despite the probable lack of fundamental character of the angular variation there is the practical point that the data from

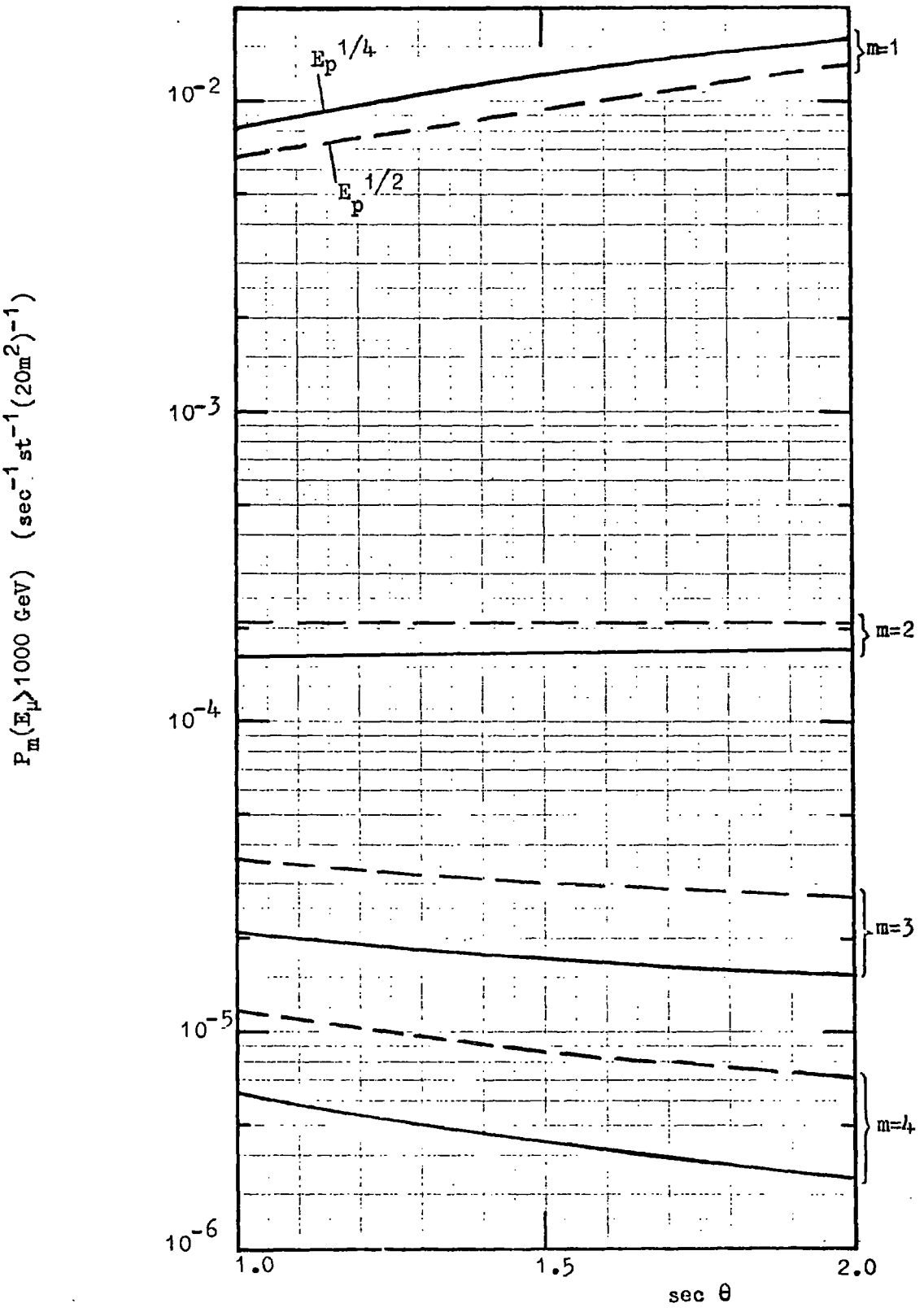

Fig. 7.5. The frequency of detecting m muons in a detector of area 20 m^2 as a function of sec θ for $\langle p_t \rangle$=0.4 GeV/c E_μ>1000 GeV and the "Protons only" primary spectrum.

different zenith angles must be combined in some way and extrapolation from one angle to another is necessary.

Examples of the variation of predicted rates with angle are given in figure 7.5. for a muon threshold of 1000 GeV and a detector area of 20 m^2. It will be noted that over a wide range of angles the variation of the logarithm of the rate with angle is almost proportional to $\sec^{\beta}\theta$ where β is a function of the detected multiplicity.

These calculations were performed using a different method to that described in Section 4.2, but the model parameters were the same.

APPENDIX A

Method of Calculation

The following diffusion equation is taken as the starting point of the calculations

$$\frac{\partial \pi(E,x)}{\partial x} = -\left\{1+\frac{B}{E(x+x_o)}\right\}\pi(E,x)+\int_E^\infty S(E',E)\pi(E',x)dE' \qquad A.1.$$

which is described in Chapter 4. This equation describes the propagation of the pion cascades in the atmosphere due to the interaction of a primary at a depth x_o, where x_o is measured in units of pion interaction lengths. It is solved by the method of successive generations.

The equations for successive generations from A.1. are:-

$$\frac{\partial \pi_1(E,x)}{\partial x} = -\left\{1+\frac{B}{E(x+x_o)}\right\}\pi_1(E,x) \qquad A.2.$$

$$\frac{\partial \pi_n(E,x)}{\partial x} = -\left\{1+\frac{B}{E(x+x_o)}\right\}\pi_n(E,x)+\int_E^\infty S(E',E)\,\pi_{n-1}(E',x)\,dE' \qquad A.3.$$

for $n = 2,3,4, \ldots\ldots$

Equation A.2. is solved simply as

$$\pi_1(E,x) = \pi(E,0)\left\{\frac{x+x_o}{x_o}\right\}^{-B/E} e^{-x} \qquad A.4.$$

Under the assumption that pion decay is neglected, A3 is solved as

$$\pi_n(E,x) = \pi_n(E)\frac{x^{n-1}}{(n-1)!}e^{-x} \qquad A.5.$$

where $$\pi_n(E) = \int_E^\infty S(E',E)\,\pi_{n-1}(E')\,dE' \qquad A.6.$$

Thus we have $\pi_n(E,x)$ in terms of two independent variables, E and x. The value of $\pi_n(E)$ is calculated numerically in the steps

of 0.1. logarithmic intervals.

From the muon energy distribution given by equation 4.5., the fraction of muons having an energy above the threshold energy, E_T, resulting from the decay of pions of energy E_π is

$$F_\mu(>E_T) = \frac{E_\pi - E_T}{E_\pi (1-r^2)} \qquad \text{for } E_T \geq r^2 E$$

$$= 1 \qquad \text{for } E_T \leq r^2 E \qquad \text{A.7.}$$

Thus the number of charged muons coming from the first pion generation, with an energy above E_T is

$$N_\mu(1) = \frac{2}{3} \int_0^\infty \int_{E_T}^\infty \frac{B}{E(x+x_\circ)} \pi_1(E) \left\{ \frac{x+x_\circ}{x_\circ} \right\}^{-B/E} e^{-x} F_\mu(>E_T)\, dx dE \qquad \text{A.8.}$$

The decay probability of a pion of energy E, produced at an atmospheric depth x is

$$DP(E,x) = \int_0^\infty \frac{B}{E(x+t)} \left\{ \frac{x}{x+t} \right\}^{B/E} e^{-t}\, dt \qquad \text{A.9.}$$

therefore the number of charged muons above a threshold energy E_T coming from the n'th pion generation is (for n> 1)

$$N_\mu(n) = \int_0^\infty \int_{E_T}^\infty \int_E^\infty \frac{2}{3} \pi_{n-1}(E',x) S(E',E) DP(E,x) F_\mu(>E_T)\, dx\, dE\, dE' \qquad \text{A.10.}$$

So the total number of muons with an energy above E_T is, from a single nucleon interaction

$$N_\mu(>E_T) = \sum_{n=1}^{\infty} N_\mu(n) \qquad \text{A.11.}$$

In calculating the lateral distributions the first five moments are calculated for a fixed pion transverse momentum of 0.2 GeV/c. The value 0.2 GeV/c is chosen because if the mean value of the transverse momentum is 0.4 GeV/c and the C.K.P. transverse momentum

distribution is assumed then the lateral distributions are easily reconstructed from the moments using equation 4.11.

The k'th moment for the first pion generation is given by

$$r_1^k = \frac{2}{3N_\mu(1)} \int_{E_T}^{\infty} \pi_1(E) DP(E,x_o) \left\{ \frac{0.2\, h(x_o)}{E} \right\}^k F_\mu(>E_T)\, dE \qquad \text{A.12.}$$

where $h(x_o)$ is the height corresponding to an atmospheric depth x_o and is obtained from the properties of the atmosphere.

For the n'th pion generation

$$r_n^k = \frac{2}{3N_\mu(n)} \int_0^{\infty}\int_{E_T}^{\infty}\int_{E}^{\infty} \pi_{n-1}(E',x) S(E',E) DP(E,x) F_\mu(>E_T) \left\{ \frac{0.2h(x)}{E} \right\}^k dx\, dE\, dE' \qquad \text{A.13.}$$

Therefore the total k'th moment for all generations is

$$r^k = \frac{1}{N_\mu} \sum_{n=1}^{\infty} r_n^k N_\mu(n) \qquad \text{A.14.}$$

APPENDIX B

Fixed Height Approximation for the Muon Lateral Distribution.

For the C.K.P. energy distribution

$$N(E_\pi)\, dE_\pi = \frac{A}{T} \exp\left\{-\frac{E_\pi}{T}\right\} dE_\pi \qquad \text{B.1.}$$

where $N(E_\pi)$ is the average number of pions produced with an energy between E_π and $E_\pi + dE_\pi$, A is the charged pion multiplicity in the forward cone and T is the mean energy of the pions in the forward cone produced by the interaction of a primary particle.

For high energy pions originating at a fixed height their decay probability is approximately K/E_π, where K is a constant depending on the height of pion formation. Therefore

$$N_\mu(r, > E_\mu)\, dr = \frac{KA}{T} \int_E^\infty \frac{E_\pi r}{h^2 p_o^2} \exp\left\{-\frac{E_\pi r}{hp_o} - \frac{E_\pi}{T}\right\} dE_\pi\, dr \qquad \text{B.2.}$$

where $N_\mu(r, > E_\mu)$ is the number of muons with an energy greater than E_μ falling at a distance between r and r + dr from the shower axis, h is the height of pion formation, $E \simeq 1.3E_\mu$ (i.e. the energy spread of muons produced in π–μ decay has been neglected) and a C.K.P. type of transverse momentum distribution has been assumed with a mean of $2p_o$.

Thus the muon density at r for muons of energy above E_μ is

$$\rho_\mu(r, > E_\mu) = \frac{KA}{2\pi h^2 p_o^2 T} \left\{\frac{E}{\alpha} + \frac{1}{\alpha^2}\right\} \exp(-\alpha E) \qquad \text{B.3.}$$

where $\alpha = \frac{r}{hp_o} + \frac{1}{T}$

For $r/hp_o \gg T^{-1}$ the expression becomes

$$\rho_\mu(r, > E_\mu) \propto \frac{1}{r} \exp(-r/r_o) \qquad \text{B.4.}$$

where $r_o = hp_o/E$.

APPENDIX C.

THE ATMOSPHERE.

The atmosphere may be divided into two layers, the trophosphere and the stratosphere, these being separated by the tropopause. The trophosphere extends from sea-level to the tropopause and in this region the temperature decreases with increasing altitude. The stratosphere comprises the region above the tropopause and the temperature is independent of altitude.

Osborne (1966) has shown that for the latitude of Durham (55°N) the relationship between the vertical height h_v (in kilometres) and the atmospheric depth x_v (in $g.cm^{-2}$) is given by

$$h_v(x_v) = 46.380 - 13.398\, x_v^{0.179} \qquad \text{for } x_v \geq 253.3 \text{ g.cm}^{-2}$$

$$h_v(x_v) = 46.040 - 6.4576\, \ln(x_v) \qquad \text{for } x_v \leq 253.3 \text{ g.cm}^{-2} \qquad \text{C.1.}$$

Assuming the "flat earth" approximation then for a zenith angle θ equation C.1. becomes.

$$h_\theta(x_\theta) = \left\{ 46.380 - 13.398\, (x_\theta \cos\theta)^{0.179} \right\} \sec\theta$$

$$\text{for } x_\theta \geq 253.3 \sec\theta \text{ g.cm}^{-2}.$$

$$h_\theta(x_\theta) = \left\{ 46.040 - 6.4576 \ln (x_\theta \cos\theta) \right\} \sec\theta$$

$$\text{for } x_\theta \leq 253.3 \sec\theta \text{ g.cm}^{-2} \qquad \text{C.2.}$$

where $h_\theta(x_\theta)$ is the inclined height (in kilometres) corresponding to an atmospheric depth x_θ (in $g.cm^{-2}$) at a zenith angle θ.

REFERENCES

P.I.C.C.R.s= Proceedings of the International Conference on Cosmic Rays.

ABRAHAM, F., KIDD, J., KOSHIBA, M., LEVI-SETTI, R., TSAO, C.H., and WOLTER, W., 1963, Nuovo Cimento, 28, 221.

ABRAHAM, F., GIERULA, J., LEVI-SETTI, R., RYBICKI, K., TSAO, C.H., WOLTER, W., FRICKEN, R.L., and HUGGETT, R.W., 1965, EFINS, 65-44, Chicago University, 844.

ABRAHAM, F., GIERULA, J., LEVI-SETTI, R., RYBICKI, K., TSAO, C.H., WOLTER, W., and HUGGETT, R.W., 1967, Phys. Rev., 159, 1110.

ADCOCK, C., DE BEER, J.F., ODA, H., WDOWCZYK, J., and WOLFENDALE, A.W., J. Phys. A. (Proc. Phys. Soc.), 1968a, (2), 1, 82.

ADCOCK, C., ODA, H., WDOWCZYK, J., and WOLFENDALE, A.W., 1968b, P.I.C.C.R., Calgary, 2, S 181.

ADCOCK, C., WDOWCZYK, J., and WOLFENDALE, A.W., 1969a, J. Phys. A (Gen. Phys.),(2), 2, 574.

ADCOCK, C., WDOWCZYK, J., and WOLFENDALE, A.W., 1969b, P.I.C.C.R., Budapest, (in the press).

AKASHI, M., et al., 1962, P.I.C.C.R., Kyoto, 3, 427.

AKASHI, M., et al., 1963, P.I.C.C.R., Jaipur, 5, 326.

ALAKOZ, A.V., BOLOTOV, V.N., DEVISHEV, M.I., KLIMANOVA, L.F., and SHMELEVA, A.P., 1968, P.I.C.C.R., Calgary, 3, S694.

ALY, H.H., DUTHIE, J.G.M., KADDOURA, A., PERKINS, D.H., and FOWLER, P.H., 1960, Proc. Rochester Conf. on High Energy Physics, 829.

ALY, H.H., KAPLON, M.F., and SHEN, M.L., 1964, Nuovo Cimento, 32, 905.

ANAND, K.C., DANIEL, R.R., STEPHENS, S.A., BHOWMIK, B., KRISHNA, C.S., ADITYA, P.K., PURI, R.K., 1968, P.I.C.C.R., Calgary, 3, 652.

ANDREWS, D., EVANS, A.C., REID, R.J.O., TENNENT, R.M., WATSON, A.A., and WILSON, J.G., 1969, P.I.C.C.R., Budapest, (in the press).

ASHTON, F., and WOLFENDALE, A.W., 1963, Proc. Phys. Soc., 81, 593.

AURELA, A.M., and WOLFENDALE, A.W., 1967, Ann. Sci. Fenn. A, (VI), 227, 1.

BAKICH, A.M., MELLEY, D., McCUSKER, C.B.A., NELSON, D., PEAK, L.S., RATHGEBER, M.H., and WINN, M.M., 1968, P.I.C.C.R, Calgary, 2, S 30.

BARADZEI, L.T., RUBTSOV, V.I., SMORODIN, Y.A., SOLOVYOV, M.V., and TOLKACHEV, B.V., 1962, P.I.C.C.R., Kyoto, 3, 433.

BARNAVELI, T.T., et al. 1964, Izv. Akad. Nauk. SSSR Ser. Fiz., 28, 1782.

BARRETT, P.H., BOLLINGER, L.M., COCCONI, G., EISENBERG, Y., and GREISEN, K., 1952, Rev. Mod. Phys., 24, 133.

BARTON, J.C., 1961, Phil. Mag., 6, 1271.

BAXTER, A.J., WATSON, A.A., and WILSON, J.G., 1968, P.I.C.C.R., Calgary, 2, S 9.

DE BEER, J.F., HOLYOAK, B., WDOWCZYK, J., and WOLFENDALE, A.W., 1966, Proc. Phys. Soc., 89, 567.

DE BEER, J.F., HOLYOAK, B., ODA, H., WDOWCZYK, J., and WOLFENDALE, A.W., 1968a, J. Phys. A(Proc. Phys. Soc.), (2), 1, 72.

DE BEER, J.F., HOLYOAK, B., ODA, H., WDOWCZYK, J., and WOLFENDALE, A.W., 1968b, P.I.C.C.R., Calgary, 3, S737.

DE BEER, J.F., HOLYOAK, B., TURNER, M.J.L., WDOWCZYK, J., and WOLFENDALE, A.W., 1969, J. Phys. A, 2, 354.

BENNETT, S., 1960, as quoted by GREISEN, 1960.

BENNETT, S., DELVAILLE, J., GREISEN, K., and KENDZIORSKI, F., 1962, P.I.C.C.R., Kyoto, 3, 196.

BERGESON, H.E., and WOLFSON, C.J., 1967, Nucl. Instr. and Meth., 51, 47.

BERGESON, H.E., KEUFFEL, J.W., LARSON, M.O., MARTIN, E.R., and MASON, G. W., 1967, Phys. Rev. Letters, 19, 1487.

BERGESON, H.E., KEUFFEL, J.W., LARSON, M.O., MASON, G.W., and OSBORNE, J.L., 1968, Phys. Rev. Letters, 21, 1089.

BHABHA, H.T., 1953, Proc. Roy. Soc., A152, 559.

BIGI, A., et al., 1962, Proc. C.E.R.N. High Energy Conf. (Geneva: C.E.R.N), 247.

BOHM, E., BUSCHER, W., FRITZE, R., ROOSE, U.J., SAMORSKI, M., STAUBERT, R., and TRUMPER, J., 1968, P.I.C.C.R., Calgary, 2, S 41.

BOLLINGER, L.M., Ph.D. Thesis, Cornell University.

BOWLER, M.G., FOWLER, P.H., and PERKINS, D.H., 1962, Nuovo Cimento, 26, 1183.

BOZOKI, G., FENYVES, E., CHRISTOV, C., AHABABIAN, N., BELEV, B., and KAVLAKOV, S., 1968, P.I.C.C.R., Calgary, 3, S 753.

BRADT, H., CLARK, G., LA POINTE, M., DOMINGO, V., ESCOBAR, I., KAMATA, K., MURAKAMI, K., SUGA, K., and TOYODA, Y., 1966, P.I.C.C.R., London, 2, 715.

BRADT, H., and RAPPAPORT, S., 1967, Phys. Rev., 164, 1567.

BRAY, A.D., et al., 1964, Nuovo Cimento, 32, 827.

BRAY, A.D., CRAWFORD, D.F., JAUNCEY, D.L., McCUSKER, C.B.A., MELLEY, D., NELSON, D., POOLE, P.C., RATHGEBER, M.H., SEET, S.H., ULRICHS, J., WAND, R.H., and WINN, M.M., 1966, P.I.C.C.R., London, 2, 668.

BROOKE, G., and WOLFENDALE, A.W., 1964, Proc. Phys. Soc., 83, 843.

BROOKE, G., HAYMAN, P.J., KAMIYA, Y., and WOLFENDALE, A.W., 1964, Proc. Phys. Soc., 83, 853.

CASTAGNOLI, C., DE MARCO, A., LONGETTO, A., PENENGO, P., 1965, Nuovo Cimento, 35, 969.

CHATTERJEE, B.K., et al., 1966, P.I.C.C.R., London, 2, 627.

CHATTERJEE, B.K., MURTHY, G.T., NARANAN, S., SIVAPRASAD, K., SREEKANTAN, B.V., SURI, A., and VISWANATH, P.R., 1968a, P.I.C.C.R., Calgary, 2, S 13.

CHATTERJEE, B.K., et al., 1968b, P.I.C.C.R., Calgary, 2, S 131.

CIOK, P., COGHEN, T., GIERULA, J., HOLYNSKI, R., JURAK, A., MIESOWICZ, M., SANIEWSKA, T., STANISZ, O., and PERNEGR, J., 1958, Nuovo Cimento, 8, 166.

COATS, R.B., OZAKI, S., STENERSON, R.O., BERGESON, H.E., KEUFFEL, J.W., LARSON, M.O., LOWE, G.H., OSBORNE, J.L., and PARKER, J.H., 1969, P.I.C.C.R., Budapest, (in the press).

COCCONI, G., 1961, Int. Conf. on Theor. Aspects of Very High Energy Phenomena, (GENEVA-CERN), 128.

COCCONI, G., KOESTER, L.G., and PERKINS, D.H., 1961, Lawrence Radiation Laboratory High Energy Physics, Study Seminars, No. 28, part 2, UCID - 1444, pp. 1-36.

COCCONI, G., 1966, P.I.C.C.R., London, 2, 616.

COLGATE, S.A., and WHITE, R.H., 1966, Ap.J., 143, 626.

COWSIK, R., 1966, P.I.C.C.R., London, 2, 656.

COWSIK, R., 1968, P.I.C.C.R. Calgary, 2, S142.

DANIELSON, R.E., 1959, Phys. Rev., 113, 1311.

DICKE, R.H., PEEBLES, P.J.E., ROLL, P.G., and WILKINSON, D.J., 1965, Ap. J., 142, 414.

DIMITRIEV, V.A., and KHRISTIANSEN, G.B., 1963, Zh. Eksp. Teor. Fiz., 44, 405.

DOBROTIN, N.A., GUSEVA, V.V., KOTELNIKOV, K.A., LEBEDEV, A.M., RYABIKOV, S.V., SLAVATINSKY, S.A., and ZELEVINSKAYA, N.G., 1962, P.I.C.C.R., Kyoto, 3, 395.

DOBROTIN, N.A., and SLAVATINSKY, S.A., 1960, Proc. Rochester Conference on High Energy Physics, 819.

DOBROTIN, N.A., and SLAVATINSKY, S.A., 1967, P.I.C.C.R., Calgary, A, 416.

DODD, P., JOBES, M., KINSON, J., TALLINI, B., FRENCH, B.R., SHERMAN, H. J., SKILLICORN, I.O., DAVIES, W.T., DERRICK, M., and RODOJICIC, D., 1961, Int. Conf. on Elem. Particles, Aix-en-Provence, 1, 433, (Saclay, C.E.N).

DURGAPRASAD, N., FICHTEL, C.E., GUSS, D.E., REAMES, D.V., O'DELL, F.W., SHAPIRO, M.M., SILBERBERG, R., STILLER, B., TSAO, C.H., 1969, GSFC Preprint, No X-611-69-427.

DUTHIE, J., FOWLER, P.H., KADDOURA, A., PERKINS, D.H., and PINKAU, K., 1962, Nuovo Cimento, 24, 122.

EARNSHAW, J., 1968, Ph.D. Thesis, University of Durham.

EARNSHAW, J.C., ORFORD, K.J.,ROCHESTER, G.D., SOMOGYI, A.J.,TURVER, K.E., and WALTON, A.B., 1967, Proc. Phys. Soc., 90, 91.

EDWARDS, B., LOSTY, J., PERKINS, D.H., PINKAU, K., and REYNOLDS, J., 1958, Phil. Mag., 3, 237.

ELBERT, J.W., ERWIN, A.R., MIKAMO, S., REEDER, D., CHEN,Y.Y., WALKER, W.D., and WEINBERG, A., 1968, Phys. Rev. Letters, 20, 124.

EREMENKO, YU. A., LUKIN, YU.T., and TAKIBAEV, ZH.S., 1968, P.I.C.C.R., Calgary, 3 S697.

ERLYKIN, A.D., 1966, P.I.C.C.R., London, 2, 999.

FAN, C.Y., GLOECKLER, G., and SIMPSON, J.A., 1968, P.I.C.C.R., Calgary, 3, S 548.

FERMI, E., 1950, Prog. Theor. Physics, 5, 570.

FIRKOWSKI, R., WDOWCZYK, J., and ZAWADZKI, A., 1967, Institute of Nuclear Research, Lodz, Report "P" No. 803/VI/PH.

FOWLER, P.H., and PERKINS, D.H., Proc. Roy. Soc., A278, 401.

FRAUTSCHI, S.C., 1963, Nuovo Cimento, 28, 409.

FUJIMOTO, Y., 1964, P.I.C.C.R., Jaipur, 5, 326.

GINZBURG, V.L., and SYROVATSKII, S.I., 1964, 'The Origin of Cosmic Rays', Oxford: Pergamon Press.

GOLDSACK, S.J., RIDDIFORD, L., TALLINI, B., FRENCH, B.R., NEALE, W.W., NORBURY, J.R., SKILLICORN, I.O., DAVIES, W.T., DERRICK, M., MULVEY, J.H., and RADOJICIC, D., 1962, Nuovo Cimento, 23, 941.

GREISEN, K., 1960, Ann. Rev. Nucl. Sci., 10, 63.

GREISEN, K., 1966a, P.I.C.C.R., London, 2, 609.

GREISON, K., 1966b, Phys. Rev. Letters, 16, 405.

GRIGOROV, N.L., SHESTEPEROV, V.Yu., BRIKKER, S.I., PODGURSKAYA, A.V., POPERYEKOVA, L.M., PLEKHOVA, A.I., SAVELYEVA, A.I., SOBINYAKOV, V.A., 1966, P.I.C.C.R., London, 2, 851.

GRIGOROV, N.L., NESTEROV, V.E., RAPOPORT, I.D., SAVENKO, I.A., and SKURIDIN, G.A., 1967, P.I.C.C.R., Calgary, A, 512.

GUSEVA, V.V., DOBROTIN, N.A., ZELEVINSKAYA, N.G., KOTELNIKOV, K.A., LEBEDEV, A.M. SIAVATINSKY, S.A., P.I.C.C.R., Kyoto, 3, 375.

HANSEN, L., and FRETTER, W., 1960, Phys. Rev., 118, 812.

HASEGAWA, H., et al. 1962, P.I.C.C.R., Kyoto, 3, 189.

HAYMAN, P.J., PALMER, N.S., and WOLFENDALE, A.W., 1963, Proc. Roy. Soc., A275, 391.

HEISENBERG, W., 1952, Z. Phys., 133, 65.

HIGASHI, S., KITAMURA, T., WATASE, Y., ODA, M., and TANAKA, Y., 1964, Nuovo Cimento, 32, 1.

HILLAS, A.M., 1966, P.I.C.C.R., London, 2, 758.

HILLAS, A.M., 1967, Phys. Letters, 24A, 677.

HILLAS, A.M., 1968, P.I.C.C.R., Calgary, 3, S625.

HILLAS, A.M., 1969, P.I.C.C.R., Budapest, (in the press).

HILTON, L.K., MORRIS. M.L., and STENERSON, R.O., 1967, Nucl. Instr. and Meth., 51, 43.

HUGGETT, R.W., 1966, P.I.C.C.R., London, 2, 898.

I.C.E.F., 1963, Nuovo Cimento (Suppl. 1), 1, 1039.

IMAEDA, K., 1962, Nuovo Cimento, 26, 417.

IMAEDA, K., 1968, P.I.C.C.R., Calgary, 3, S 722.

KEUFFEL, J.W., and PARKER, J.L., 1967, Nucl. Inst. and Meth., 51, 29.

KINSEY, J.H., 1968, GSFC Preprint, X-611-68-352.

KOBAYAKAWA, K., 1967, Nuovo Cimento, 47, 156.

KOBAYAKAWA, K., 1968, P.I.C.C.R., Calgary, 2, S 395.

KOSHIBA, M., and YAMADA, S., 1967, Phys. Rev., 157, 1279.

KOSHIBA, M., NOZAKI, T., TOTSUKA, Y., and YAMADA, S., 1968, P.I.C.C.R., Calgary, 3, S671.

KRASILINIKOV, D., 1964, P.I.C.C.R., Jaipur, 6, 124.

KRAUSHAAR, W.L., and MARKS, L.J., 1954, Phys. Rev., 93, 326.

KUZMIN, V.A., and ZATSEPIN, G.T., 1966, JETP Letters, 4, 144.

LAL, S., 1967, Nuovo Cimento, 48, 466.

LAL, S., PAL, Y., RAGHAVEN, R., SREEKANTAN, B.V., SUBRAMANIAN, A., and VERMA, S.D., 1962, P.I.C.C.R., Kyoto, 3, 390.

LANDAU, L.D., 1953, Izv. Akad. Nauk., Fiz. Ser., 17, 51.

LARSON, M.O., 1968, Ph.D. Thesis, University of Utah.

LEWIS, H., OPPENHEIMER, J., and WOUTHUYSEN, A., 1948, Phys. Rev., 93, 326.

LINDENBAUM, S.J., and STERNHEIMER, R.M., 1962, Brookhaven Rep. BNL772 (T-290), 32.

VON LINDERN, 1961, Ph.D. Thesis, Ludwigs Maximilians University.

LINSLEY, J., 1962, Phys. Rev. Letters, 9, 126.

LINSLEY, J., and SCARSI, L., 1962, Phys. Rev. Letters, 9, 123.

LINSLEY, J., SCARSI, L., and ROSSI, B., 1962, P.I.C.C.R., Kyoto, 3, 91.

LINSLEY, J., 1963a, Phys. Rev. Letters, 10, 143.

LINSLEY, J., 1963b, P.I.C.C.R., Jaipur, 4, 77.

LOHRMAN, E., TEUCHER, H.W., and SCHEIN, H., 1961, Phys. Rev., 122, 672.

McCAUGHAN, J.B.T., McCUSKER, C.B.A., SEET, S.H., WAND, R.H., O'DONNELL, B., PRESCOTT, J.R., and WILSON, B.G., 1966, P.I.C.C.R., London, 2, 720.

McCUSKER, C.B.A., 1967, P.I.C.C.R., Calgary, A, 397.

McCUSKER, C.B.A., and PEAK, L.S., 1963, P.I.C.C.R., Jaipur, 5, 35.

MCCUSKER, C.B.A., PEAK, L.S., and RATHGEBER, M.H., 1968a, P.I.C.C.R., Calgary, 2, S32.

McCUSKER, C.B.A., PEAK. L.S., and WOOLCOTT, R.L.S. 1968b, P.I.C.C.R., Calgary, 3, S694. 655

McCUSKER, C.B.A., and CAIRNS, I., 1969, Phys. Rev. Letters, 23, 658.

MACHIN, A.C., ORFORD, K.J., PICKERSGILL, D.R., and TURVER, K.E., 1969, P.I.C.C.R., Budapest, (in the press).

MALHOLTRA, P.K., 1964, Nucl. Phys. (Netherlands), 59, 551.

MALHOLTRA, P.K., SHUKLA, P.G., STEPHENS, S.A., VIJAYALAKSHMI, B., BOULT, J., BOWLER, M.G., FOWLER, P.H., HACKFORTH, H.L., KEEREETAVEEP, J., MAYES, V.M., and TOVEY, S.N., 1965, Nuovo Cimento, 40, 385.

MALHOLTRA, P.K., et al.,1966a, P.I.C.C.R., London, 2, 875.

MALHOLTRA, P.K., et al., 1966b, P.I.C.C.R., London, 2, 840.

MATANO, T., MIURA, I., NAGANO, M., ODA, M., SHIBATA, S., TANAKA, Y., TANAHASI, G., and HASEGAWA, H., 1963, P.I.C.C.R., Jaipur, 4, 129.

MATANO. T., NAGANO. M., SHIBATA, S., SUGA, K., TANAHASHI, G., and HASEGAWA, H., 1968, P.I.C.C.R., Calgary, 2, S56.

MAYES, V.M., 1964, as quoted by Menon and Ramana Murthy, 1967.

MENON, M.G.K., and RAMANA MURTHY, P.V., 1967, Prog. in Elem. Particle and Cosmic Ray Physics, IX, 163.

MINAKAWA, O., et al., 1959, Nuovo Cimento (Suppl. 1), 11, 125.

MIYAKE, S., NARASIMHAM, V.S., and RAMANA MURTHY, P.V., 1962, P.I.C.C.R., Kyoto, 3, 318.

MIYAKE, S., NARASIMHAM, V.S., and RAMANA MURTHY, P.V., 1964, Nuovo Cimento, 32, 1505.

MIYAKE, S., HINOTANI, K., ITO, N., KINO, S., SASAKI, H., YOSHII, H., SAKUYAMA, H., and KATO, E., 1968, P.I.C.C.R., Calgary, 2, S 25.

MURTHY, G.T., SIVAPRASAD, K., SRINIVASA RAO, M.V., TONWAR, S.C., WATCHA, R.H., and WISWANATH, P.R., 1968a, P.I.C.C.R, Calgary, 2, S147.

MURTHY, G.T., et al., 1968b, P.I.C.C.R., Calgary, 2, S153.

MURTHY, G.T., et al.,1968c, P.I.C.C.R., Calgary, 2, S159.

MURZIN, V.S., 1966, P.I.C.C.R., London, 2, 872.

NIKOLSKII, S.I., 1963, Soviet Physics - Uspecki, 5, 849.

NIKOLSKII, S.I., 1967, Soviet Physics - JETP, 24, 535.

OGITA, N., 1962, Prog. Theor. Phys., Japan, 27, 105.

OGITA, N., RATHGEBER, M., TAKAGI, S., UEDA, A., 1968, P.I.C.C.R., Calgary, 2, S 164.

ORFORD, K.J., 1968, Ph.D. Thesis, University of Durham.

ORFORD, K.J., and TURVER, K.E., 1968, Nature, 219, 706.

ORFORD, K.J., TURVER, K.E., and WALTON, A.N., 1968, P.I.C.C.R., Calgary, 2, S119.

ORFORD, K.J. and TURVER, K.E., 1969, P.I.C.C.R., Budapest, (in the press).

ORMES, J.F., and WEBBER, W.R., 1966, P.I.C.C.R., London, 1, 349.

OSBORNE, J.L., and WOLFENDALE, A.W., 1964, Proc. Phys. Soc., 84, 901.

OSBORNE, J.L., WOLFENDALE, A.W., and PALMER, N.S., 1964, Proc. Phys. Soc., 84, 911.

OSBORNE, J.L., 1966, Ph.D. Thesis, University of Durham.

PAL, Y., and PETERS, B., 1964, K. Danske Vidensk Selsk Mat.-Fys. Medd. (Denmark), 33, No. 15, 54.

PARKER, J.L., 1967, Ph.D. Thesis, University of Utah.

PEAK, L.S., and WOOLCOTT, R.L.S., 1966, P.I.C.C.R., London, 2, 905.

PERKINS, D.H., 1960., Prog. in Elem. Particle and Cosmic Ray Physics, V, 259.

PETERS, B., 1952, Prog. in Cosmic Ray Physics, I, 191.

PETERS, B., 1961, Nuovo Cimento, 22, 800.

PETERS, B., 1962, Proc. Conf. on High Energy Phys. (CERN), 623.

PETERS, B., 1966, Seminar for an Intersecting Storage Rings Study Group held at CERN, 10th March, 1966.

PINKAU, K., 1966, P.I.C.C.R., London 2, 895.

La POINTE, M., KAMATA, K., GAEBLER, J., ESCOBAR, I., DOMINGO, V., SUGA, K., MURAKAMI, K., TOYODA, Y., and SHIBATA, S., 1968, P.I.C.C.R., Calgary, 2, S68.

PORTER, L.G., and STENERSON, R.O., 1969, J. Phys. A, 2, 374.

PRESCOTT, J.R., 1956, Proc. Phys. Soc. A, 69, 870.

RATNER, L.G., EDWARDS, K.W., AKERLOF, C.W., CRABB, D.G., DAY, J.L., KRISH, A.D., and LIN, M.T., Phys. Rev. Letters, 1967, 18, 1218.

ROGERS, I.W., THOMPSON, M.G., TURNER, M.J.L., and WOLFENDALE, A.W., 1969, J. Phys. A, 2, 365.

ROLL, P.G., and WILKINSON, D.T., 1967, Annals of Physics, 44, 289.

SAMORSKI, M., STAUBERT, R., TRUMPER, J., BOHM, E., BUSCHER, W., and FRITZE, R., 1970, Z. Phys., 230, 1.

SEKIDO, Y., KONDO, I., MURYAMA, T., OKUDA, H., SAKAKIBARA, S., and FUJIMOTO, K., 1966, P.I.C.C.R., London, 2, 632.

SREEKANTAN, B.V., 1968, Colloq. on Cosmic Ray Studies, Nov. 11-16, Tata Inst. of Fundemental Research, 151, 1969.

SWINSON, D.B., and PRESCOTT, J.R., 1966, P.I.C.C.R., London, 2, 721.

SWINSON, D.B., and PRESCOTT, J.R., 1968, P.I.C.C.R., Calgary, 2, S292.

TAKAGI, G., 1952, Prog. Theor. Phys., 7, 123.

TAMAI, E., TSUBOMATSU, M., and OGURA, K., 1968, P.I.C.C.R., Calgary, 3, S598.

TANAHASHI, G., 1965, Jour. Phys. Soc. Japan, 20, 883.

THIELHEIM, K.O., and BEIERSDORF, R., 1970, J. Phys. A, 3, 79.

TOMASZEWSKI, A., MICHALAK, W., and SROKA, J., 1966, Nuovo Cimento, 32, 905.

TRUMPER, J., 1969, P.I.C.C.R., Budapest, (in the press).

VERNOV, S.A., and KHRISTIANSEN, G.B., 1967, P.I.C.C.R., Calgary, A, 345.

VERNOV, S.N., KHRISTIANSEN, G.N., ABROSIMOV, A.T., ATRASHKEVITCH, V.B., BELJAEVA, I.F., KULIKOV, G.V., MANDRITSHKAYA, K.V., SOLOVJEVA, V.I., and KHRENOV, B.A., 1968, P.I.C.C.R., Calgary, 2, S197.

WADDINGTON, C.J., 1960, Progress in Nuclear Physics, 8, 1.

WEBBER, W.R., 1966, P.I.C.C.R., London, 1, 345.

WEBBER, W.R., ORMES, J.F., and VON ROSENVINGE, T., 1966, P.I.C.C.R., London, 1, 407.

WEBBER, W.R., 1967, Handbuch der Physik, XLVI/2, 181.

WDOWCZYK, J., 1966, P.I.C.C.R., London, 2, 691.

WILLIAMS, R.W., 1960, Nuovo Cimento, 16, 762.

YASH PAL, and TANDON, S.N., 1966, Phys. Rev., 151, 1071.

ZATSEPIN, G.T., NIKOLSKII, S.I., and KHRISTIANSEN, G.B., 1963, P.I.C.C.R., Jaipur, 4, 100.

ZATSEPIN, G.T., and KUZMIN, V.A., 1968, P.I.C.C.R., Calgary, 3, S617.

ACKNOWLEDGEMENTS.

The author wishes to thank Professor G.D. Rochester, F.R.S., for the provision of facilities to carry out this work and for his continued support.

He is indebted to his supervisor Professor A.W. Wolfendale for his advice and guidance at all stages of this work. The author would also like to thank Dr. J. Wdowczyk for his invaluable help and co-operation throughout the work.

The valuable discussions with the members of the Durham and Lodz Cosmic Ray Research Groups are acknowledged with gratitude.

The Institute of Nuclear Physics and the University of Lodz, Poland are thanked for their hospitality.

Professors J.W. Keuffel and R.O. Stenerson of the University of Utah are thanked for communicating their results prior to publication and for much helpful correspondence.

The assistance of the staff of the Durham University Computing Unit, the Institute of Nuclear Physics, Lodz, Computer Unit and the Atlas Computer Laboratory, Chilton and the use of their facilities is gratefully acknowledged.

Miss P.A. Wallace and Miss M. Brawn are thanked for their help in preparing the diagrams for this thesis.

Mrs. D.A. Anson is thanked for her typing of this thesis.

Finally the Science Research Council is thanked for the provision of a Research Studentship during the period of this work.